SIMULATION OF THE SEISMIC PERFORMANCE OF NONSTRUCTURAL SYSTEMS

NEES Nonstructural

MODELING AND SEISMIC EVALUATION OF NONSTRUCTURAL COMPONENTS: TESTING FRAME FOR EXPERIMENTAL EVALUATION OF SUSPENDED CEILING SYSTEMS

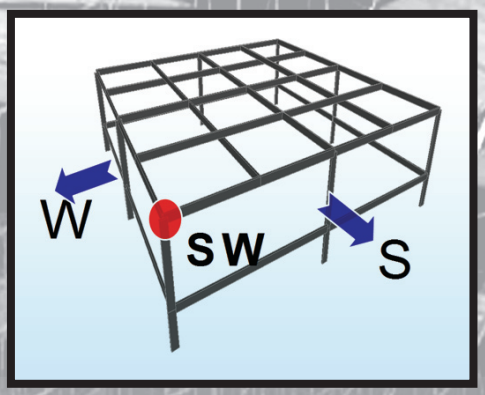

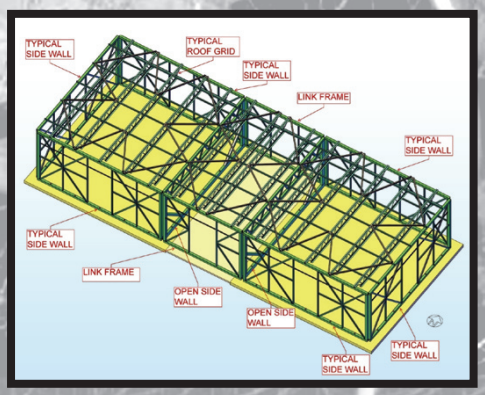

By
Andrei M. Reinhorn, Ki-Pung Ryu and
Giuseppe Maddaloni

Technical Report MCEER-10-0004 ■ June 30, 2010

This research was conducted at the University at Buffalo, State University of New York and was supported by the National Science Foundation under Grant No. CMMI-0721399.

Sponsored by the
National Science Foundation
NSF Grant Number CMMI-0721399

Project Title
Simulation of the Seismic Performance of
Nonstructural Systems

Project Team
University of Nevada Reno
University at Buffalo, State University of New York
Georgia Institute of Technology
Rutherford & Chekene
University of California, San Diego
Consortium of Universities for Research in Earthquake Engineering (CUREE)

Web Site
http://www.nees-nonstructural.org

DISCLAIMER

This report is based upon work supported by the National Science Foundation under Grant No. CMMI-0721399. Any opinions, findings, and conclusions or recommendations expressed in this material are those of the investigators and do not necessarily reflect the views of MCEER, the National Science Foundation, or other sponsors.

Modeling and Seismic Evaluation of Nonstructural Components: Testing Frame for Experimental Evaluation of Suspended Ceiling Systems

by

Andrei M. Reinhorn,[1] Ki-Pung Ryu[2] and Giuseppe Maddaloni[3]

Publication Date: June 30, 2010;
Revised May 27, 2011
Submittal Date: January 28, 2010

Technical Report MCEER-10-0004

NSF Grant Number CMMI-0721399

1 Clifford C. Furnas Eminent Professor, Department of Civil, Structural and Environmental Engineering, University at Buffalo, State University of New York
2 Research Scientist, Department of Civil, Structural and Environmental Engineering, University at Buffalo, State University of New York
3 Assistant Professor, Department of Technology, University of Naples "Parthenope," Italy

MCEER
University at Buffalo, State University of New York
Red Jacket Quadrangle, Buffalo, NY 14261
Phone: (716) 645-3391; Fax (716) 645-3399
E-mail: *mceer@buffalo.edu*; WWW Site: *http://mceer.buffalo.edu*

Project Overview

NEES Nonstructural: Simulation of the Seismic Performance of Nonstructural Systems

Nonstructural systems represent 75% of the loss exposure of U.S. buildings to earthquakes, and account for over 78% of the total estimated national annualized earthquake loss. A very widely used nonstructural system, which represents a significant investment, is the ceiling-piping-partition system. Past earthquakes and numerical modeling considering potential earthquake scenarios show that the damage to this system causes the preponderance of U.S. earthquake losses. Nevertheless, due to the lack of system-level research studies, its seismic response is poorly understood. Consequently, its seismic performance contributes to increased failure probabilities and damage consequences, loss of function, and potential for injuries. All these factors contribute to decreased seismic resilience of both individual buildings and entire communities.

Ceiling-piping-partition systems consist of several components and subsystems, have complex three-dimensional geometries and complicated boundary conditions because of their multiple attachment points to the main structure, and are spread over large areas in all directions. Their seismic response, their interaction with the structural system they are suspended from or attached to, and their failure mechanisms are not well understood. Moreover, their damage levels and fragilities are poorly defined due to the lack of system-level experimental studies and modeling capability. Their seismic behavior cannot be dependably analyzed and predicted due to a lack of numerical simulation tools. In addition, modern protective technologies, which are readily used in structural systems, have never been applied to these systems.

This project sought to integrate multidisciplinary system-level studies to develop, for the first time, a simulation capability and implementation process to enhance the seismic performance of the ceiling piping-partition nonstructural system. A comprehensive experimental program using both the University of Nevada, Reno (UNR) and University at Buffalo (UB) NEES Equipment Sites was developed to carry out subsystem and system-level full-scale experiments. The E-Defense facility in Japan was used to carry out a payload project in coordination with Japanese researchers. Integrated with this experimental effort was a numerical simulation program that developed experimentally verified analytical models; established system and subsystem fragility functions; and created visualization tools to provide engineering educators and practitioners with sketch-based modeling capabilities. Public policy investigations were designed to support implementation of the research results.

The systems engineering research carried out in this project will help to move the field to a new level of experimentally validated computer simulation of nonstructural systems and establish a model methodology for future systems engineering studies. A system-level multi-site experimental research plan has resulted in a large-scale tunable test-bed with adjustable dynamic properties, which is useful for future experiments. Subsystem and system level experimental results have produced unique fragility data useful for practitioners.

This report describes the development of a new testing facility for the evaluation of suspended ceilings and other nonstructural components that can be used with single or tandem shake tables. The 20 × 50 ft test frame was designed to simulate realistic ceiling performance correlated with the response observed during real earthquakes. The frame has dynamic characteristics with variable frequencies to match those typically

found in floors (or roofs) with suspended ceilings. It was also designed to accommodate various structural materials and different framing layouts. Analytical models were developed using SAP2000 to estimate the dynamic properties and complete the design of the test frame. The combined designs of the physical frame and the shake table motion allow for testing a variety of suspended systems while simulating realistic floor motions and eliminating side effects due to wall distortions. Finally, procedures for motion design that can be implemented in other experimental facilities are introduced.

Project Management Committee

Manos Maragakis, Principal Investigator, University of Nevada Reno, Department of Civil Engineering, Reno, NV 89557; *maragaki@unr.edu.*

André Filiatrault, Co-Principal Investigator, University at Buffalo, State University of New York, Department of Civil, Structural and Environmental Engineering, Buffalo, NY 14260; *af36@buffalo.edu.*

Steven French, Co-Principal Investigator, Georgia Institute of Technology, College of Architecture, P.O. Box 0695, Atlanta, GA 30332; *Steve.French@ arch.gatech.edu*.

William Holmes, Rutherford & Chekene, 55 Second Street, Suite 600, San Francisco, CA 94105; *wholmes@ruthchek.com.*

Tara Hutchinson, Co-Principal Investigator, University of California, San Diego, Department of Structural Engineering, 9500 Gilman Drive, #0085, La Jolla, CA 92093; *tara@ucsd.edu*.

Robert Reitherman, Co-Principal Investigator, CUREE, 1301 S. 46th Street, Bldg. 420, Richmond, CA 94804; *reitherman@curee.org*.

ABSTRACT

In the last few decades, it has become clear that failure of suspended ceiling systems in earthquakes endangers safety and impedes continuous operation of a building. In order to evaluate the seismic performance of suspended ceiling systems and provide a better understanding of their seismic design, many shaking table tests have been conducted. However, there were many limitations in these tests, due to the size, frequency limits and work limitations of currently used testing frames.

The purpose of this report is to describe the development of a new testing facility for use with single or tandem shake tables to evaluate suspended ceilings and other nonstructural components. A large reconfigurable frame of 20 ft. by 50 ft. was developed to test a continuous suspended ceiling of up to 1,000 ft^2. The frame has dynamic characteristics with variable frequencies to match those typical of floors and roofs with suspended ceilings. Analytical models were developed using the structural analysis program SAP2000 to estimate the dynamic properties and complete the design of the frame.

Since a test frame has flexibilities and a test system is not perfect, the frame as built cannot accurately deliver a desired "floor motion" at a specific location in a structure. A special open loop procedure, which provides a compensated command "drive" signal to a shake table to obtain a "target floor motion spectrum" at the roof level of the test frame, was proposed and verified experimentally.

The combined designs of the physical frame and the shake table motion allow for testing of a variety of suspended systems while simulating more realistic floor motions and eliminating side effects caused by wall distortions. This study describes the design of the frame and introduces the procedure for motion design which can also be implemented in other experimental facilities.

ACKNOWLEDGEMENTS

Financial support for the work described in this report was provided by the National Science Foundation through the George E. Brown, Jr. Network for Earthquake Engineering Simulation Research (NEESR-GC) for Grand Challenge on Simulation of Seismic Performance of Nonstructural Components, Award #CMMI 0721399 and by the Multidisciplinary Center for Earthquake Engineering Research through grants from New York State. This support is gratefully acknowledged. The support of Prof. G. Maddaloni by the University of Naples, "Parthenope" (Italy), for the development of the compensation procedures, is also acknowledged.

The authors also acknowledge the advice received from industry and academic representatives active in the specific professional areas (alphabetically): Dennis Alvarez, Bob Bachman, Amir Gilani, Paul A Hough, Tony Ingratta, and Shakhzod Takhirov, who reviewed the main parts of this study and made valuable suggestions.

The authors also acknowledge the dedicated assistance of the Structural Engineering and Earthquake Simulation Laboratory (SEESL) staff Mark Pitman, Scot Weinreber and Chris Zimmerman, in performing the experimental work.

TABLE OF CONTENTS

TABLE OF CONTENTS (CONT'D)

LIST OF FIGURES

LIST OF FIGURES (CONT'D)

LIST OF FIGURES (CONT'D)

LIST OF TABLES

CHAPTER 1
INTRODUCTION

The importance of nonstructural components has been demonstrated during past earthquakes since damage to such components can result not only in a substantial reduction of functionality of buildings, but can also be a critical threat to life safety in extreme cases.

In the last few decades, it was clear that suspended ceilings failing in earthquakes endanger safety and impede continuous operation of buildings, many servicing critical health care or business functions. Current standards do not explicitly provide guidance for the seismic design of such suspended "structures" due to their heterogeneous and complex construction. As a result, manufacturers of ceiling products started a campaign, which was motivated by the seismic qualification requirements for nonstructural components introduced in the ASCE 7-05 standard, to experimentally qualify such suspended ceilings. In the past decades, experimental earthquake simulator (shaking tables) tests for suspended ceilings were conducted to evaluate the seismic performance of the systems and provide a better understanding of their seismic design.

Suspended ceiling systems have been examined experimentally in order to evaluate the seismic performance and the fragility of the systems at the University at Buffalo and other experimental facilities. A 16 ft. by 16 ft. square steel space frame designed to install and test suspended ceiling systems has been used for more than a decade for this purpose.

Realizing the shortcomings of the currently used frame, such as size, frequency limits and work limitations, a larger frame was proposed to simulate more realistic ceiling performance, correlated with the response observed in the field. The proposed frame is expected to accommodate various construction conditions in terms of materials and different framing layouts.

1.1 Procedures for Seismic Evaluation of Suspended Ceilings

A summary of testing procedures using testing frames and the main findings of some of the experiments are introduced in this chapter. In addition, information about the dynamic characteristics of generic floors supporting the suspended ceilings are surveyed and presented in order to define the required design characteristics of a testing frame. Table 1-1 summarizes the previous tests which are discussed in more detail below.

Table 1-1 Summary of Previous Seismic Experiments of Suspended Ceiling Systems

Researcher	Test Frame Description	Character. Freq.	Ceiling System Size	Shake Table Description	Test Excitation
(1)	(2)	(3)	(4)	(5)	(6)
ANCO Engineers (1983)	Steel Truss	Unknown	12 × 28 ft.	2-DOF* (ANCO Planar Tri-axial system)	Tri-axial Hor. & Vert. Time History Input *from Taft Earthquake* (1952)
Rihal & Granneman (1984)	Steel Grid (Horizontal Diaphragm)	Unknown	12 × 16 ft.	1-DOF Shaking System	Uni-axial Horizontal Sinusoidal Input
Yao (2000)	Rigid Frame	~ 25 Hz	4 × 13.4 ft.	1-DOF Shaking System	Uni-axial Horizontal Time History Input *from Taiwanese Design Code Spectrum*
Badillo et al.** (2006)	Steel Grid	~17 Hz (h) ~ 9 Hz (v)	16 × 16 ft.	6-DOF Shaking System	Tri-axial Hor. & Vert. Time History Input *from AC 156 RRS*

*: Degrees-Of-Freedom
**: and other researchers at UB-SEESL

1.1.1 Previous Tests of Suspended Ceiling Systems

ANCO Engineers Inc. (1983) performed experimental tests for suspended ceilings using an earthquake simulator in the ANCO Seismic Laboratory. The steel truss R-4 frame, shown in Figure 1-1, was constructed for the tests. The dynamic characteristics of the testing frame were not clearly presented in the test report. A 12 ft. by 28 ft. ceiling using a 2 ft. by 4 ft. installation module was installed in the frame. 1952 Taft earthquake ground motion was used to excite the frame mounted on an earthquake simulator. The test program demonstrated the feasibility of

using shaking table tests to evaluate seismic restraints of nonstructural ceiling components in terms of the use of shaking tables to access component dynamic behaviors and evaluate the effectiveness of building code requirements. The test report observed that the use of the vertical strut (a code requirement) did not decrease the dynamic interaction effects. Pop rivets at wall parameters and safety wires on drop-in light fixtures played a much more important role in seismic hazard mitigation.

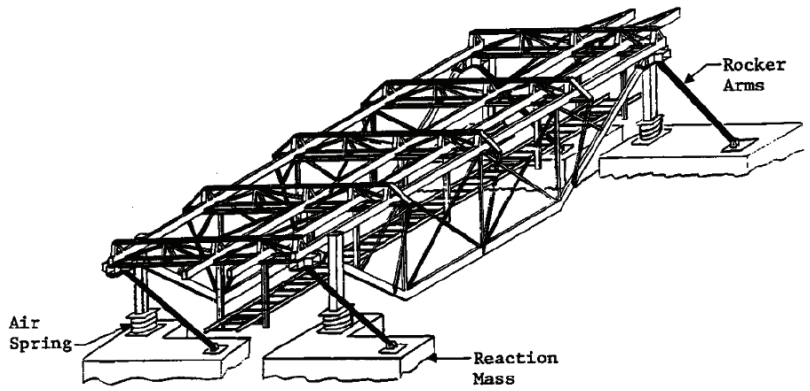

Figure 1-1 Isometric Drawing of R-4 Frame (reproduced from ANCO, 1983)

Rihal and Granneman (1984) conducted an experimental investigation of the dynamic behavior of suspended ceiling systems during earthquakes (see Figure 1-2). The dynamic testing scheme consisted of a structural steel grid simulating a structural horizontal diaphragm, allowed to roll freely on a wheel/bearing assembly. A 12 ft. by 16 ft. suspended ceiling was installed to the grid at the top. A sinusoidal excitation was used as input motions. The main findings were that splayed wire ceiling bracing and vertical struts were effective in reduction of the dynamic response of the suspended ceiling systems.

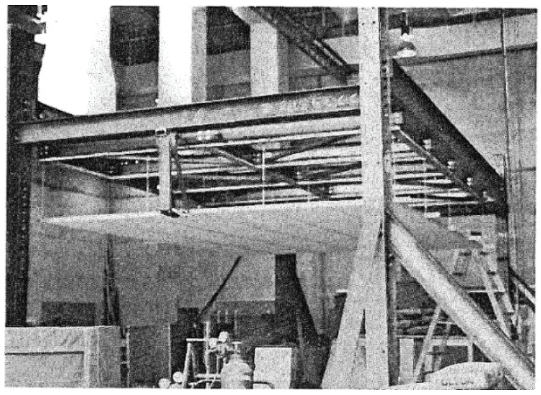

Figure 1-2 Test Frame and Suspended Ceiling (after Rihal and Granneman, 1984)

In 2000, Yao studied seismic performance of direct-hung suspended ceiling systems by analytical modeling, experimental tests, and field survey. A test frame of 48 in. x 161 in. (4 ft. x 13.4 ft.), presented in Figure 1-3, was designed to be very rigid so that its fundamental frequency was 24.8 Hz in order to avoid resonance in the test frame and earthquake motions. The input excitation was a series of uni-axial horizontal sine waves. The main findings were the ineffectiveness of sway wires and that the pop rivet and edge hanger wires provided significant seismic capacity. The study concluded that installing transverse constraint supports could prevent the lateral spread of the ceiling runners (Yao, 2000).

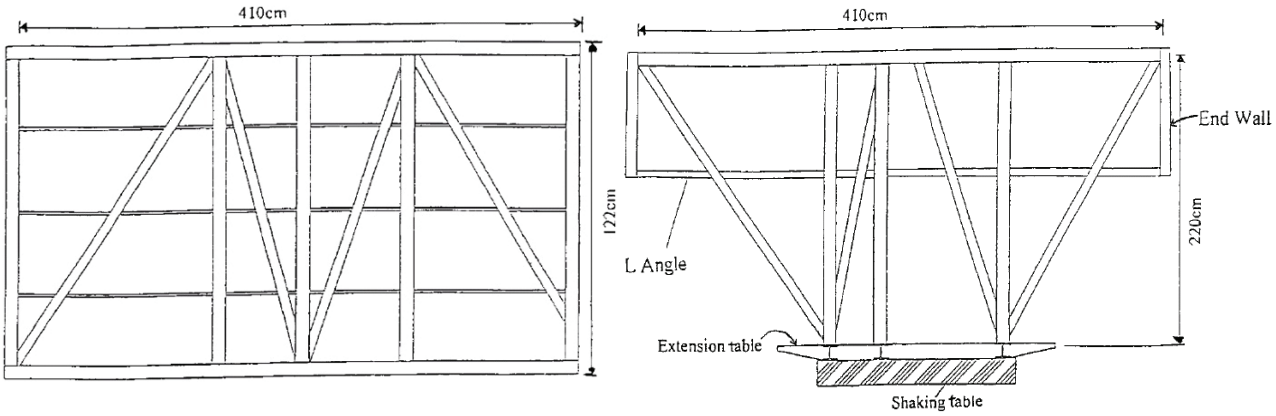

Figure 1-3 Views of Plan and Elevation of Test Frame (reproduced from Yao, 2000)

From 2001 through 2009, ceiling manufacturers performed an extensive series of seismic experiments on suspended ceiling systems at the Structural Engineering and Earthquake Simulation Laboratory (SEESL) of University at Buffalo, the State University of New York (UB) (e.g., Badillo et al., 2002, Kusumastuti et al., 2002, Badillo et al., 2003a-d, Repp et al., 2003, Lavan et al., 2006a-b, and Roh et al., 2008). A test frame of 16 ft. by 16 ft. was designed (Reinhorn, 2000) to represent a typical story on which suspended ceiling systems were installed in practice (see Figure 1-4). In order to simulate the worst-case scenario for actual conditions in earthquake events, the roof of the test frame was designed to have the frequency of a typical slab in the vertical direction (this concept is addressed in the following subchapter 1.1.2). The dynamic characteristics of the frame were 17 Hz and 9 Hz in horizontal and vertical directions, respectively.

(a) Badillo et al., 2006 (b) Maddaloni et al (2009b)

Figure 1-4 Test Frame Mounted on a Shake Table

In order to qualify suspended ceiling systems, the recommendations of ICC-AC-156 "Acceptance Criteria for Seismic Qualification Testing of Nonstructural Components" (ICC, 2007) were used. Although the standard addresses only single point connected nonstructural components, in absence of other standards, the main dynamic characteristics and requirements were adopted for the testing of multiple connection suspended ceilings.

Among the findings based on the series of experiments were that the use of retainer clips substantially improved the seismic capacity of ceiling systems in terms of reducing loss of tiles. However, by retaining the ceiling tiles, the inertial loads on the grid increased. The rivets, attaching main runners and cross tees to wall molding, were also effective to reduce loss of tiles. Performance levels and fragility curves were established for suspended ceilings. The fragility curves showed that including a compression post in suspended ceiling systems improved the seismic performance of the system in terms of reducing damage to the tiles and grid (Badillo et al, 2007). However, more intense testing of various ceilings without the post in the 16 ft. x 16 ft. configuration did not show conclusive reduction of damage. The issue will need further evaluations with a larger frame and relocation of posts.

Based on recent tests conducted at the Structural Engineering and Earthquake Simulation Laboratory (SEESL) at the University at Buffalo (UB), it was proposed to construct a larger test frame approximately 20 ft. by 50 ft. (Maragakis et al., 2007). The frame was proposed to

accomplish two main objectives: (i) represent actual construction practice and (ii) have variable vertical dynamic characteristics to replicate various construction conditions in real life. The following subchapter presents the required design characteristics of the testing frame.

1.1.2 Characteristics of Generic Floor Systems

The ceiling and other nonstructural components such as piping, electrical conduits and fixtures, are suspended from floors or roofs in structures. The characteristics of the testing frame are determined based on the demands of floor (roof) motion as it occurs in the structures. The floor motions are in turn a result of the base (ground) motion and amplifications due to the frame structure and floor diaphragms.

1.1.2.1 Amplifications in Corner of Floors

The ground motion is amplified by the structure at each floor by the modal amplification factors and structure mode shapes (Chopra, 2007). Figure 1-5 presents amplified relative accelerations ($\ddot{y}(t)$) in a corner of the floors, supported by columns and strong beams and excited by ground excitations ($\ddot{x}(t)$) in horizontal (a) and vertical directions (b), respectively.

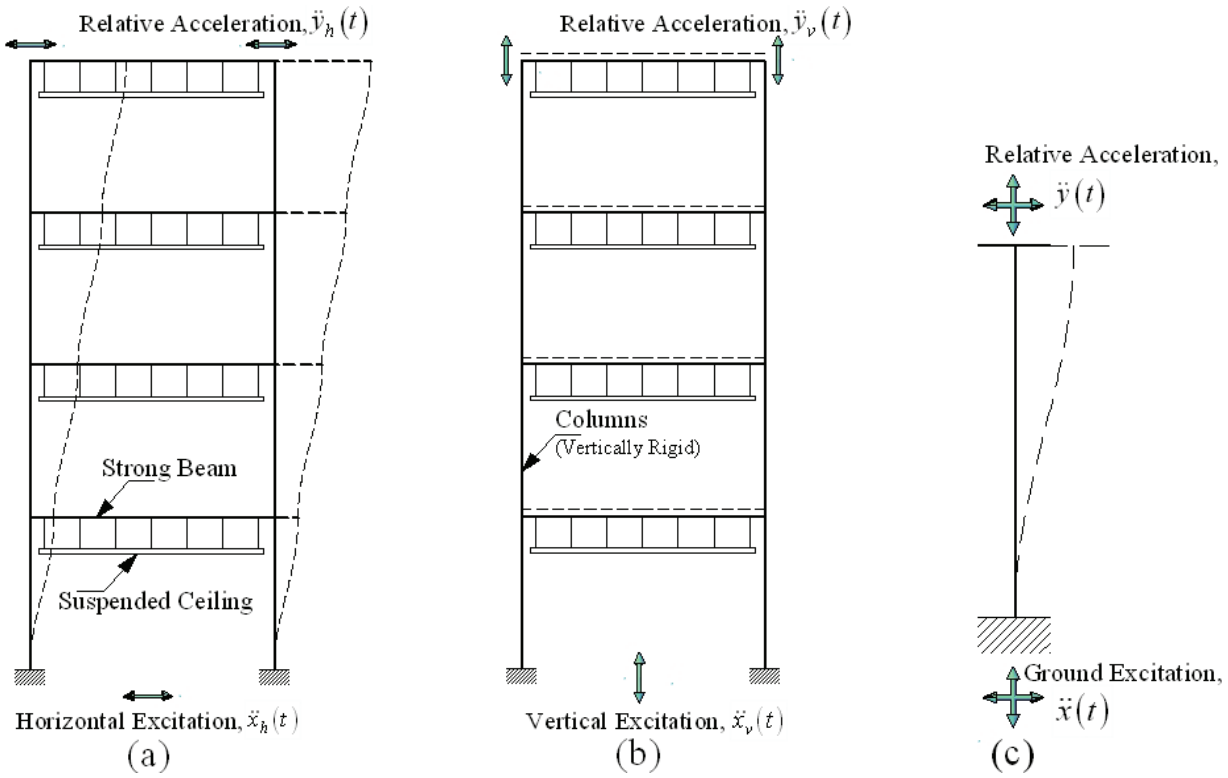

Figure 1-5 Amplification of Motions in Corner of Floors

A simplified model is shown in Figure 1-5(c). Equation (1-1) below presents the floor (absolute) acceleration $\ddot{a}(t)$ with respect to the ground and it can be calculated as the sum of two accelerations:

$$\ddot{a}(t) = \ddot{x}(t) + \ddot{y}(t) \tag{1-1}$$

The relative acceleration $\ddot{y}(t)$ can be expressed in a modal analysis formulation by the product of the modal participation factor Γ and structure mode shape ϕ as follows:

$$\ddot{a}(t) = \ddot{x}(t) + \Gamma\phi\ddot{D}(t) \tag{1-2}$$

where $\ddot{D}(t)$, the modal response, is obtained by solving:

$$\ddot{D}(t) + 2\xi\omega\dot{D}(t) + \omega^2 D(t) = -\ddot{x}(t) \tag{1-3}$$

Converting Equation (1-2) in the frequency domain, results in:

$$\ddot{a}(\omega) = \ddot{x}(\omega) + \Gamma\phi\ddot{D}(\omega) \tag{1-4}$$

In order to explain the "amplification" of floor accelerations $\ddot{D}(\omega)$ is assumed to be the product of the amplification factor α and the ground excitation $\ddot{x}(\omega)$ as follows:

$$\ddot{D}(\omega) = \alpha \cdot \ddot{x}(\omega) \tag{1-5}$$

It is indicated that in the frequency domain the acceleration input and response are related by the specific amplifications applying to both amplitude and phase.

Inserting Equation (1-5) in Equation (1-4) the absolute acceleration is obtained:

$$\ddot{a}(\omega) = \ddot{x}(\omega) + \Gamma \cdot \phi \cdot \alpha \cdot \ddot{x}(\omega) = (1 + \Gamma \cdot \phi \cdot \alpha) \cdot \ddot{x}(\omega) \tag{1-6}$$

where the term of $(1+\Gamma \cdot \phi \cdot \alpha)$ is the amplitude of the amplification. For the horizontal floor acceleration, shown in Figure 1-5 (a), this $(1+\Gamma \cdot \phi \cdot \alpha)$ term is being approximated as $(1 + 2\frac{z}{h})$ in the ICC ES-AC 156 (ICC, 2007), assumed constant for the entire frequency spectrum range:

$$A_{FLX} = S_{DS}\ (1 + 2\frac{z}{h}) \le 1.6\ S_{DS} \tag{1-7}$$

$$A_{RIG} = 0.4\ S_{DS}\ (1 + 2\frac{z}{h}) \le 1.2\ S_{DS} \tag{1-8}$$

where "z/h" approximates the mode shape ϕ and "2" represents the product of the amplification α and the modal participation factor Γ. A_{FLX} and A_{RIG} are spectral accelerations of a flexible component and a rigid component, respectively. The $(1 + 2\frac{z}{h})$ term was formulated in the 1997 NEHRP provisions, based on the examination of building motion records associated to strong motions with peak ground accelerations greater than 0.1g (BSSC, 1997).

For the vertical floor acceleration, shown in Figure 1-5 (b), the amplification effect (α) in the Equation (1-6) is negligible ($\alpha \to 0$) in a corner of the floor since columns are typically rigid in the vertical direction, so that floor amplification is never substantial. Therefore this study recommends a proposed vertical required response spectrum (vRRS) without amplification in vertical direction in the Equation (1-7) and (1-8), as reformulated in Chapter 4.

1.1.2.2 Amplifications in Floors or Roofs Plates

The roof of the testing frame should accommodate the vertical flexibility of floors, or roofs, in typical structures to simulate actual response during seismic events. Niousha (1999) investigated the dynamic response of an actual building with records obtained during a real earthquake. The vertical motion behavior of the nine story reinforced concrete building was studied. The vertical motion was recorded at the center of the first floor and ninth floor plates. The results showed that the vertical acceleration history at the ninth floor was amplified three (x3) times compared with one at the first floor. The amplification of vertical floor motions was caused by the floor dynamics, having the fundamental frequency of 6.0 Hz.

As shown in Figure 1-6, if the roof is rigid the same motions occur at all points on the suspending ceiling system. However, with a flexible roof, every suspension point on the ceiling has different excitations. A flexible roof is more adequate for the testing frame, challenging the grid and its components by imposing differential movements and rotations as long as the roof is representative of an actual structure.

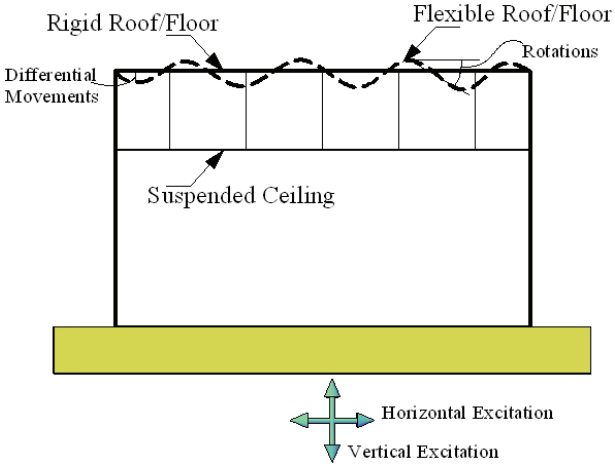

Figure 1-6 Schematic Model for Describing the Flexibility of Roof/Floor

The 2009 NEHRP Provisions update (PROPOSAL 8-13R1) for CHAPTER 13 *Seismic Design Requirements for Nonstructural Components* also indicates that dynamic amplification to a nonstructural component (for example, suspended ceiling systems in this study) occurs where the period of the component matches that of any mode of the supporting structure (ex. roof/floor systems for our study) (NEHRP, 2008). This concept accommodates the new design requirements that a testing frame must represent realistic structure characteristics to simulate reasonable response during earthquake tests.

1.1.2.3 Requirements for a Frame Simulating One Story in Buildings

Suspended ceiling systems are installed at different levels of buildings with different numbers of stories (Figure 1-7a). In order to test the seismic performance of the ceiling systems, a single-story test frame is used (Figure 1-7b) representing a typical story, on which the system is to be installed in practice.

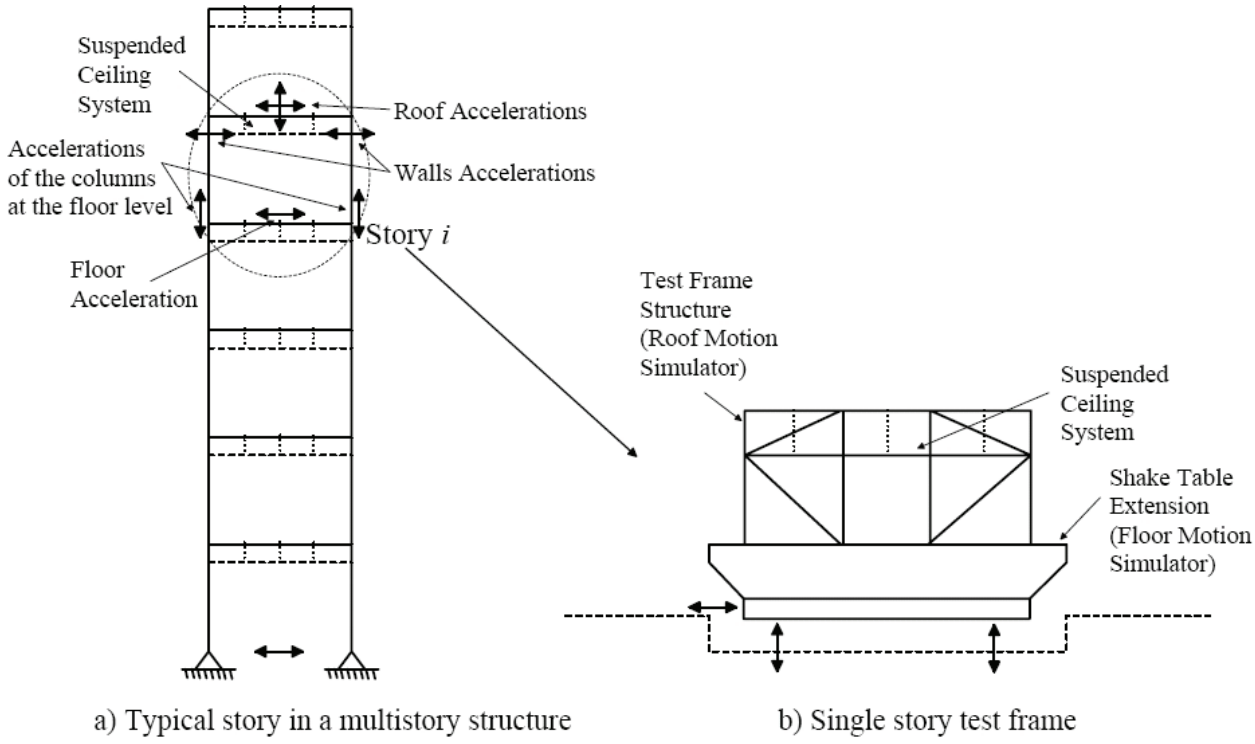

Figure 1-7 Floor and Roof Accelerations of Typical Story Structure (after Roh et al., 2008)

In order to simulate the worst-case scenario for realistic conditions in seismic events, the single-story test frame is designed to accommodate the following concepts: (i) the roof of the frame must have a "typical floor" dynamic characteristic (frequency) in the vertical direction to simulate actual vertical acceleration history of the floor; and (ii) the walls of the frame are designed to be rigid in comparison to the roof system. In order to simulate the desired roof accelerations (i.e. worst-cases), the flexibility of the walls are compensated through the shake table with a special procedure (See Chapter 5).

1.1.2.4 Fundamental Frequencies of Typical Floors

The selection of dynamic characteristics (frequencies) of a roof or floor system must be based on actual roof/floor conditions that can challenge the suspended system in its realistic conditions. Roof/floor dynamic characteristics (frequencies) were mainly investigated for floor vibration studies. A survey of fundamental frequencies of typical floor systems is further presented in the following paragraphs.

AISC Design Guide Series 11 *Floor Vibration due to Human Activity* was written by Murray, Allen, and Ungar (1997), and it has provided the most common criteria for floor vibrations used by engineers in North America. This guide indicates that "most steel framed floor systems in North American office buildings have first natural frequencies in the 5 – 9 Hz range."

In 1998, Allen and Pernica introduced the problems associated with floor vibration and control methods of floor vibration. The study showed that "a steel floor with a concrete deck usually has a natural frequency of between 3 Hz to 10 Hz" (Allen and Pernica, 1998).

Boice in 2003 studied how to improve the predicted response of steel floor systems due to walking. Natural frequency prediction of floor systems was studied by examining 103 case studies currently occupied or under construction in the United States and Europe. Floor systems of various framing were examined. The classifications for framing were hot-rolled beams, hot-rolled girders with joists, hot-rolled girders with castellated beams, and joist girders with joists. A Fast Fourier Transform (FFT) analyzer was primarily used to measure fundamental frequencies and was accurate to within 0.25 Hz. The measured fundamental frequencies of floor systems from 103 case studies were in the range of 3 Hz to 13.5 Hz (Boice, 2003).

Williams and Waldron (1994) investigated vibrations in concrete floors. The study suggested a method to calculate the fundamental frequency of concrete floors. The study presented fundamental frequencies of post-tensioned and reinforced concrete floor slabs measured in field testing. The fundamental frequencies were determined using impact hammer testing and measured in the range of 5.0 Hz to 18.4 Hz. The highest frequency of 18.4 Hz was achieved for a concrete floor slab of a laboratory having a 20 ft. by 23 ft. module (Williams and Waldron, 1994).

Allen and Rainer (1976) also studied vibration for long-span concrete floors. This study recommended vibration criteria for long-span concrete floors and presented field test data. Seven different floor conditions in three buildings were studied. The measured fundamental frequencies were in the 2.6 Hz to 7.7 Hz range.

In addition to the information found in the above publications, fundamental frequencies of typical concrete floor systems were calculated based on the formulation introduced by Blevins (1983). Fundamental frequencies of generic simply supported floors of 20 ft. by 20 ft. with slab thickness of 5 in. to 7 in. without any additional flooring or partition are in the range of 21 Hz to 35 Hz. A summary list of fundamental frequencies of floors, or roofs, is presented in Table 1-2.

Table 1-2 List of Fundamental Frequencies of Typical Floors or Roofs

Structure Materials and System	Fundamental Frequency (Hz)	Method of Estimation	Reference
(1)	(2)	(3)	(4)
Steel	5.0 – 7.0	Author's Comment	Murray et al., 1997
Steel	3.0 – 10.0	Author's Comment	Allen and Pernica, 1998
Steel	3.0 – 13.5	Field Measurement (103 case studies)	Boice, 2003
Concrete	5.0 – 18.4	Field Measurement (13 case studies)	Williams and Waldron, 1994
Concrete	2.6 – 7.7	Field Measurement (7 case studies)	Allen and Rainer, 1976
Concrete	21.0 – 35.0	Prediction by Formulation	Blevins, 1983

It can be concluded that most constructed floors have frequencies in the range of 2.6 Hz to 18.4 Hz with exceptional cases in the range higher than 19 Hz. To challenge the suspended ceilings to maximum response for all possible cases, it is recommended to develop a frame with a roof frequency in the range of 2.6 Hz to 8.0 Hz, which will be in the range of the flat portion of the demand floor spectrum (see ICC-AC-156 standard for example).

1.2 Scope and Outline of this Report

The main goal of this study is to design an extended testing frame for seismic qualification tests of nonstructural "ceiling" components – such as suspended ceilings, electrical systems and piping, among others. The design objectives were as follows: (i) to provide extended space for a continuous ceiling surface up to 1,000 $ft.^2$ to achieve a better correlation between ceiling system performances in experiments and in actual seismic events, and (ii) to provide a roof grid of changeable vertical dynamic characteristics to accommodate various construction practices related to material and framing. In addition, in order to simulate realistic "ceiling" system performance using the designed frame, testing floor motions and test compensation procedures were studied and presented.

Chapter 2 presents the design of a test frame including its overall geometry, dynamic characteristics, and capabilities. Chapter 3 presents the development of an analytical model of the test frame to estimate its characteristics and performance using dynamic analysis. Chapter 4 provides the design and evaluation of the frame's floor/roof motions. A proposed modification to the AC-156 standard for vertical Required Response Spectrum (RRS) and an alternative test motion were introduced. Chapter 5 describes the formulation and evaluation of a compensation procedure for shake table simulation tests that allows correcting imperfections in the frame design. Chapter 6 presents concluding remarks for this study and recommendations for future development. References are listed in Chapter 7. The comments from advisory groups to the design and modeling draft 1 and draft 2 are presented in Appendix A and B.

CHAPTER 2
TEST FRAME DESIGN

2.1 Design Criteria

The new test frame is designed to be used for seismic testing of large nonstructural ceiling-related components – such as suspended ceilings, ducts, electrical conduit and fixtures, and piping, among others, using simulated roof motion. The design objectives are as follows:

- Provide space for a continuous ceiling surface up to 1,000 ft^2 (20 ft.× 50 ft.).
- Produce a modular frame to enable testing of smaller sizes of ceilings, 20 ft. by 20 ft., etc.
- Provide a roof grid of changeable vertical frequencies in the range of 8 to 10 Hz.
- Provide in-plane-stiff walls, having frequencies in excess of 20 Hz.
- Provide out-of-plane frequencies of walls in excess of 10 Hz.

2.2 Overall Geometry

A frame is designed to represent a full-scale typical story in which a ceiling system is to be installed (see Figure 2-1). The suggested frame is designed using ASTM Grade 50 steel (ASTM, 2005). The overall size of the frame is a 20 ft.-2 in. (6.1 m) by 53 ft.-8 in. (16.4 m) (nominal 20 × 50 ft.). Its height is designed as 10 ft. to accommodate a typical slab to slab height and allow effective assemblies during testing. The frame is composed of three modular segments: two 20 ft.-2 in. (6.1 m) by 20 ft.-2 in. (6.1 m) square "typical side wall" frames, and a 13 ft.-4 in. (4.1 m) by 20 ft.-2 in. (6.1 m) "link" frame. The two 20 ft.-2 in. by 20 ft.-2 in. (nominal 20 × 20 ft.) frames could be used independently. The "link frame" will be used only in the full size assembly. The two square frames will be attached to two 23 ft. by 23 ft. square shake tables, respectively. A 10 ft.-6 in. by 23 ft. "bridge" will be installed as a work surface between the two tables. The bridge is made of two identical sub-segments, one previously used in the NEES-Wood project (Christovasilis et al., 1997) at the Structural Engineering and Earthquake Simulation Laboratory (SEESL) at the University at Buffalo, the State University of New York (UB). Commercial "open web steel joists (18K4)" are used for the roof grid system in combination with HSS 2½ x 1½ x 3/16 bars to form 4 ft. by 4 ft. modules. The detailed geometric properties of the extended frame are presented in Figure 2-2 through Figure 2-6.

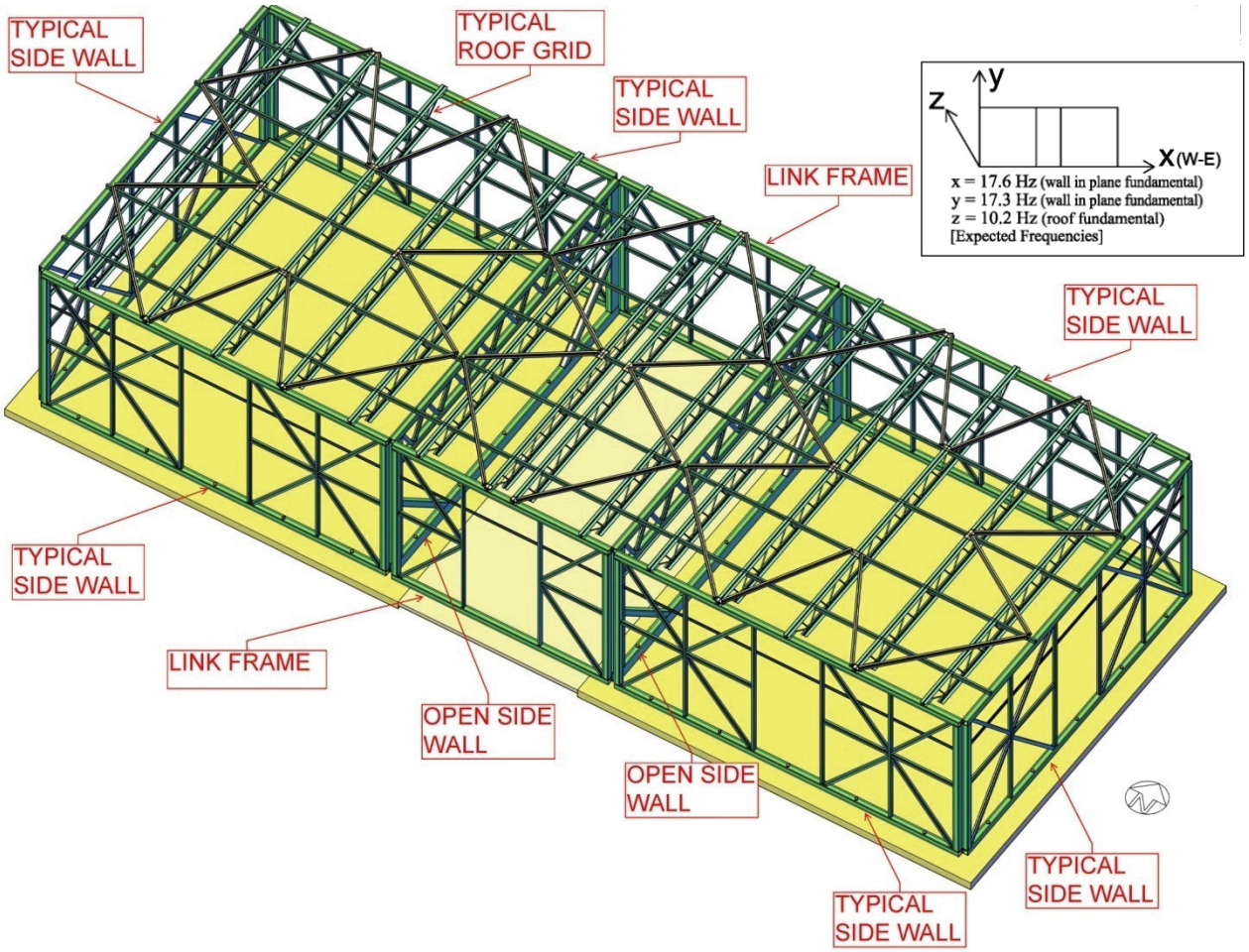

Figure 2-1 CAD 3D Model of the New Test Frame (20 × 50 ft.)

As shown in Figure 2-1 above, the large test frame consists of typical side walls (see Figure 2-5), which are having rigid dynamic characteristics (17.4 Hz in plane) to represent typical wall systems. In order to install the 1,000 ft^2 (20 × 50 ft.) continuous ceiling system, two special open side walls are designed in the middle of the frame (see Figure 2-6). The inside columns and braces, which are shown in the typical side walls, should be removed for openings in the frame. However, the frame becomes flexible without the columns and braces. Therefore, in order to avoid out-of-plane vibration in the transverse direction, stiffer elements (i.e., bigger section trusses, columns and braces) are selected to design open side walls to have the same stiffness as other typical side walls.

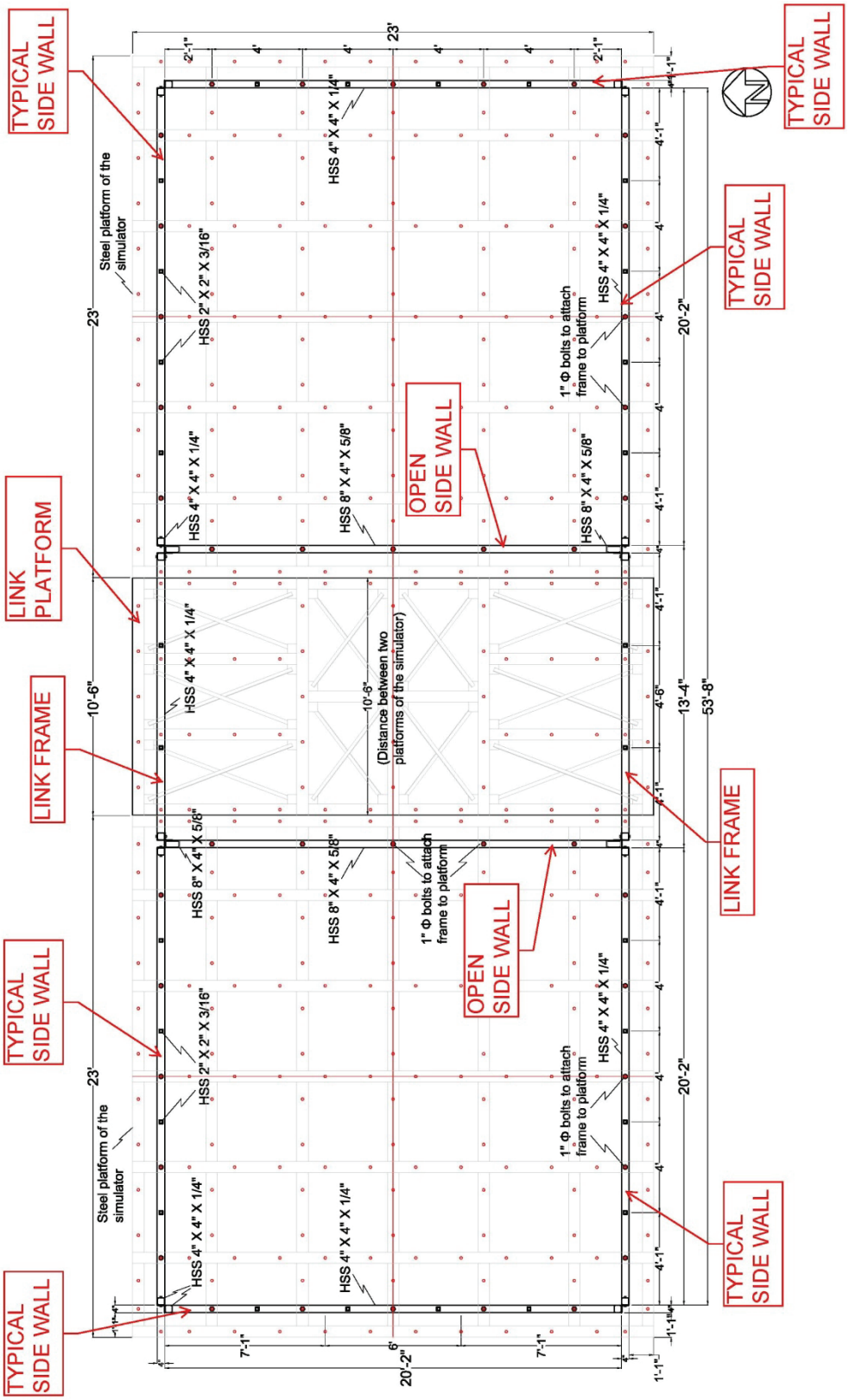

Figure 2-2 Plan View of the Base of the Frame (20 × 50 ft.)

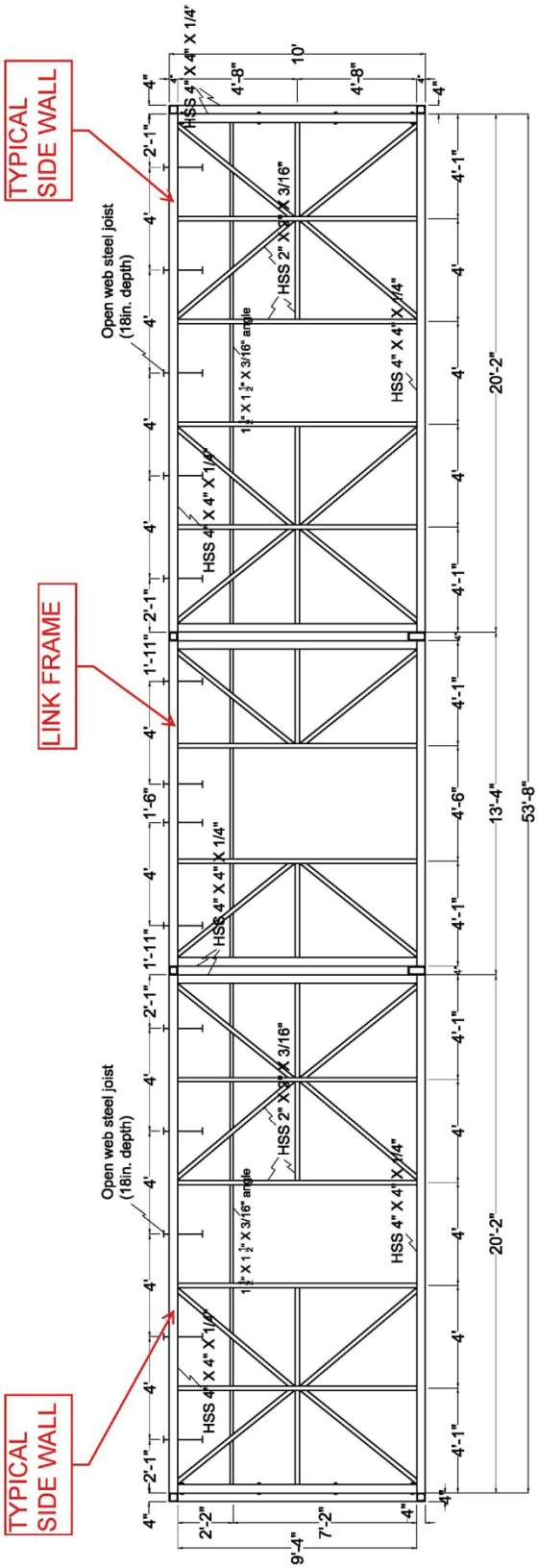

Figure 2-3 Elevation of the South (North) Side of the Frame (20 × 50 ft.)

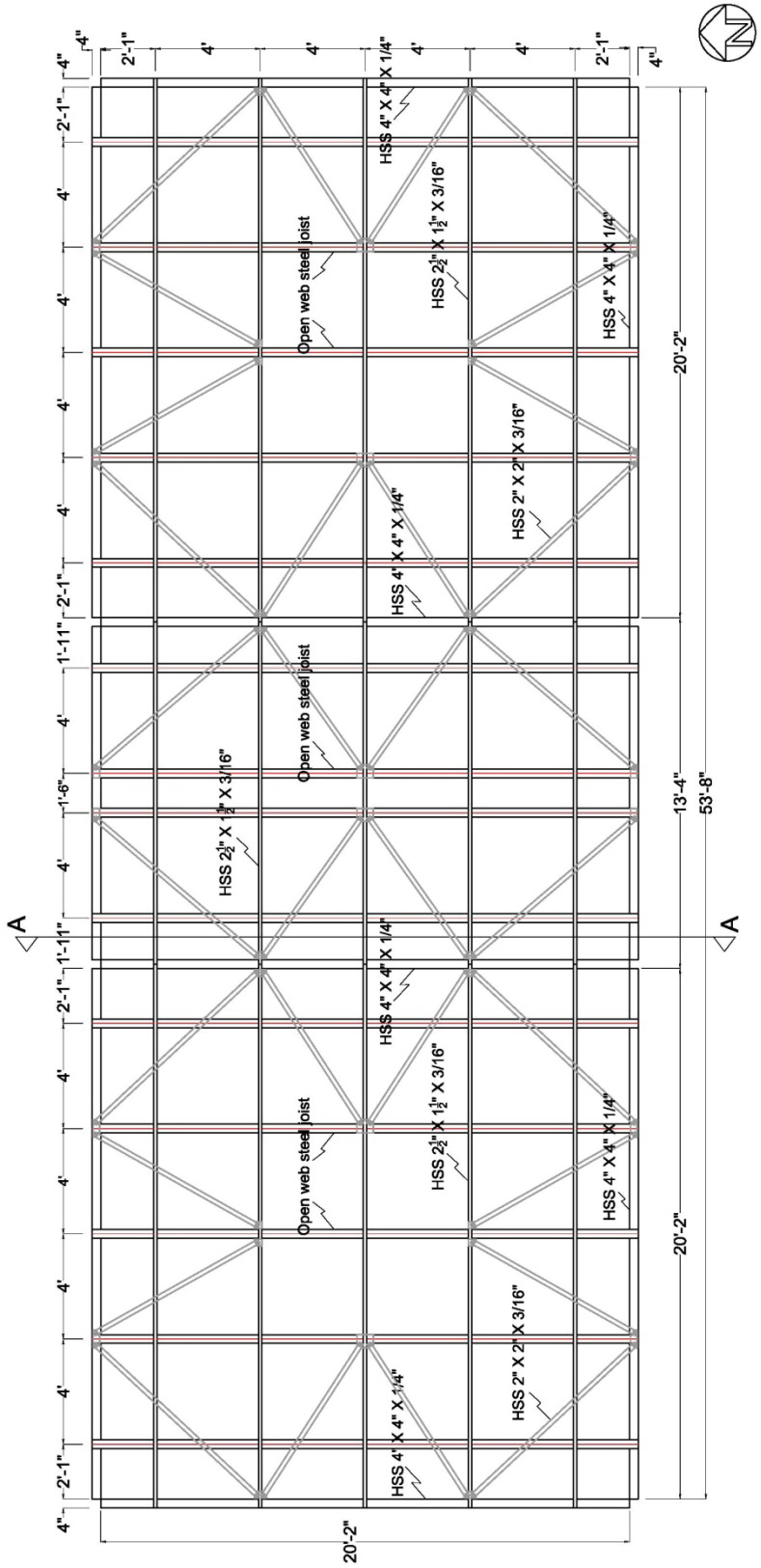

Figure 2-4 Plan View of the Top of the Frame (20 × 50 ft.) Roof Grid

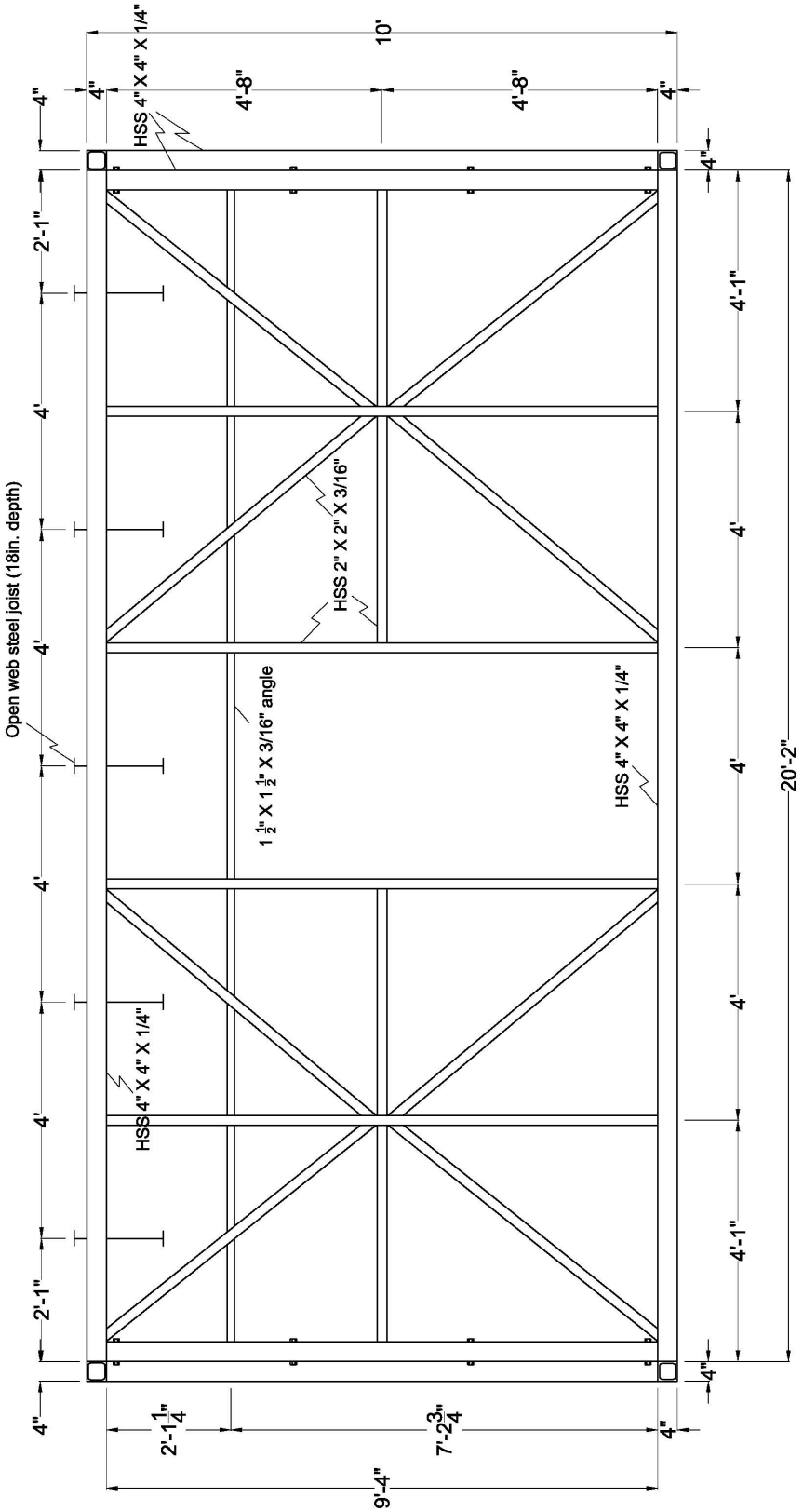

Figure 2-5 Elevation of the Typical Side of the Frame (20 × 50 ft.) - Typical "Side" Frame

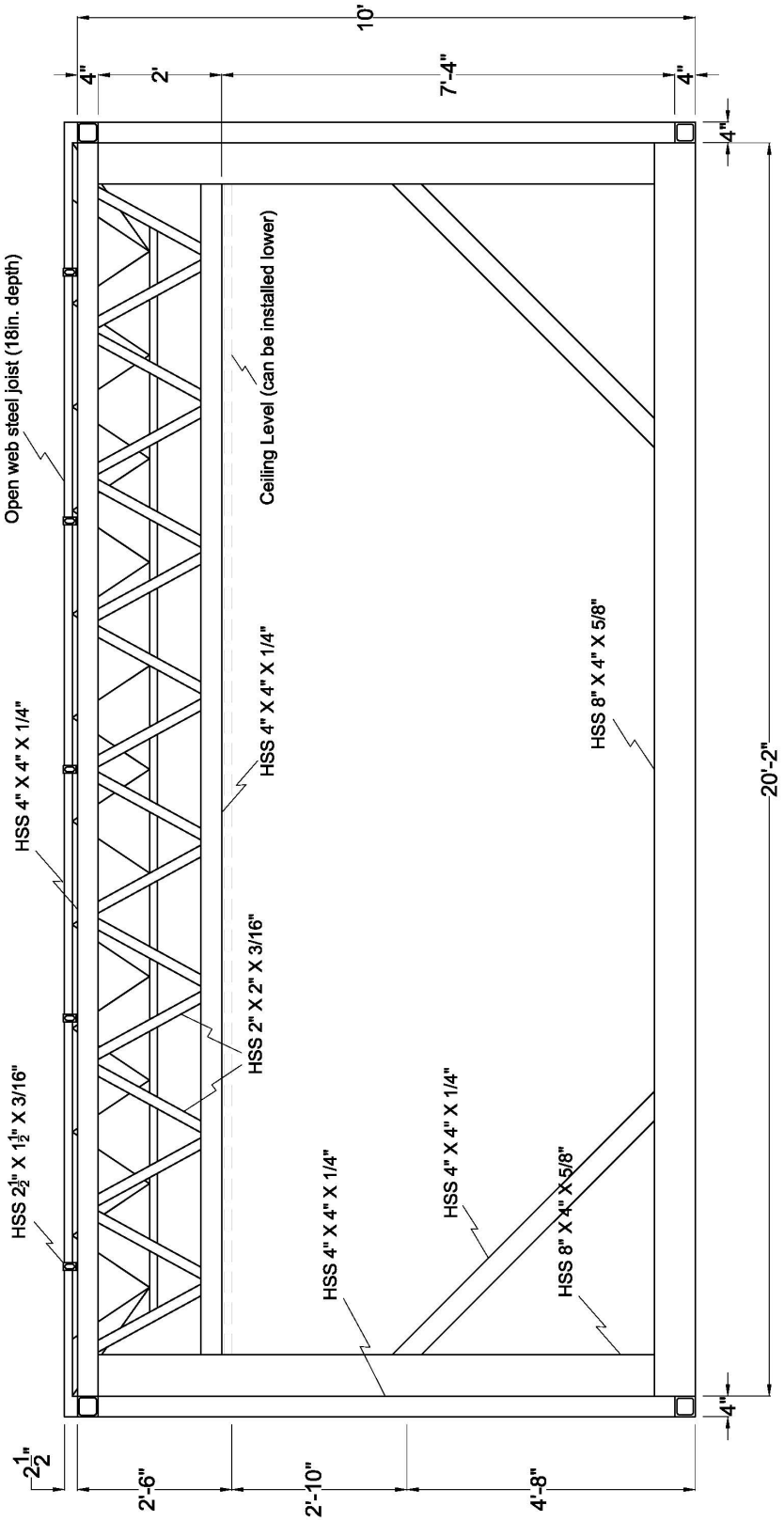

Figure 2-6 Section A-A of the Frame (20 × 50 ft.) - Open "Side" Frame

2.3 Dynamic Characteristics

2.3.1 Proposed Dynamic Characteristics of Test Frame

The dynamic characteristics of the roof of the test frame are designed to represent a typical floor of buildings in order to simulate realistic dynamic responses with floor excitations using a shake table. The range of proposed frequencies is 8 Hz to 10 Hz, chosen based on the literature survey (see Chapter 1), so that the frame is able to simulate an actual amplification in the vertical direction, caused by the flexibility of floors or roofs.

The "wall" of the test frame is designed to represent a "stiffer" wall frame, whose fundamental frequency is around 20 Hz. The horizontal amplification, caused by the flexibility of walls, is simulated by designing floor motions through a compensation procedure introduced in this study (see Chapter 5).

2.3.2 Estimate of Dynamic Properties of Test Frame

Analytical models were made using SAP2000 in order to estimate the dynamic properties of the designed frames, 20 × 50 ft. and 20 × 20 ft. The "Basic Frame Configuration" includes a "floor weight (4 psf)" made of four concrete planks on the roof. The identified natural fundamental frequencies from SAP2000 are shown in Table 2-1 in the vertical and horizontal directions. The analytical model images of the designed frames are presented in Figure 2-7 through Figure 2-10.

Table 2-1 Estimated Fundamental Frequencies of the Test Frame Using SAP2000

	20 × 50 ft. test frame	20 × 20 ft. test frame
Vertical (z)	10.2 Hz	10.2 Hz
Longitudinal (x)	17.7 Hz	17.4 Hz
Transversal (y)	17.7 Hz	17.4 Hz

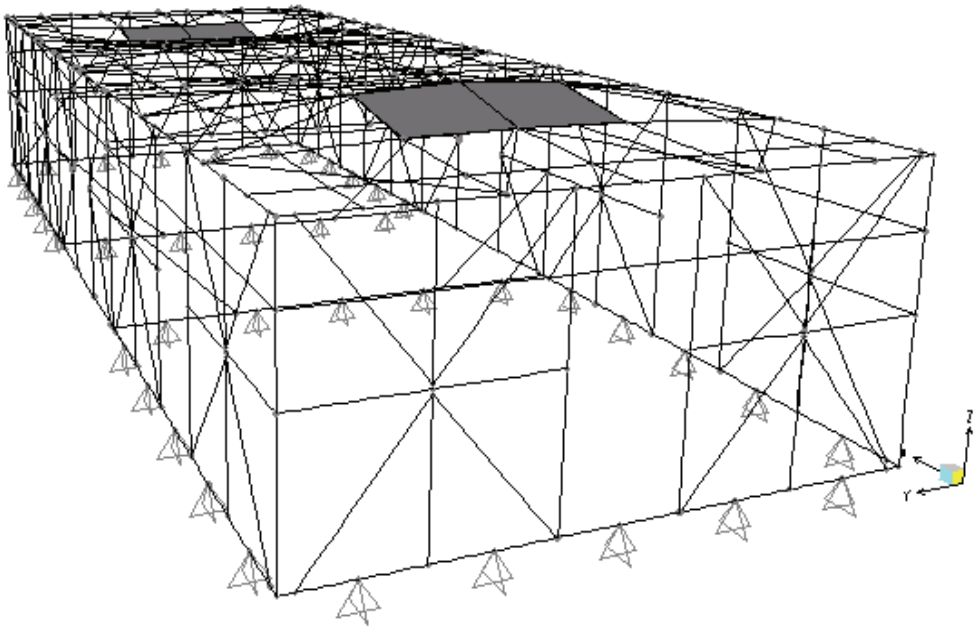

Figure 2-7 Analytical Model (20 × 50 ft.) with Vertical Fundamental Frequency of 10.2 Hz

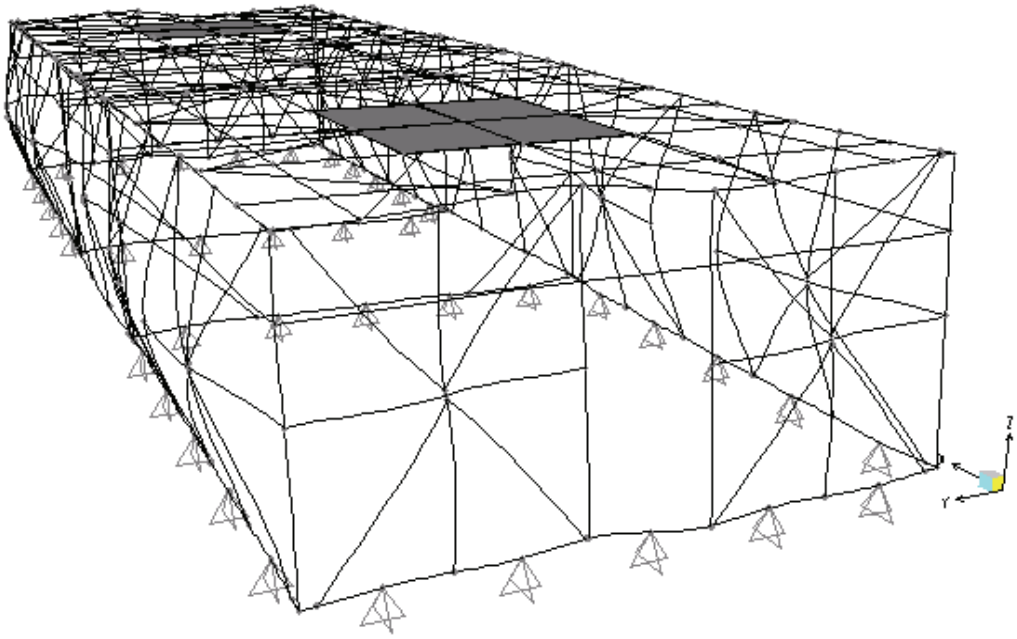

Figure 2-8 Analytical Model (20 × 50 ft.) with Horizontal Fundamental Frequency of 17.7 Hz

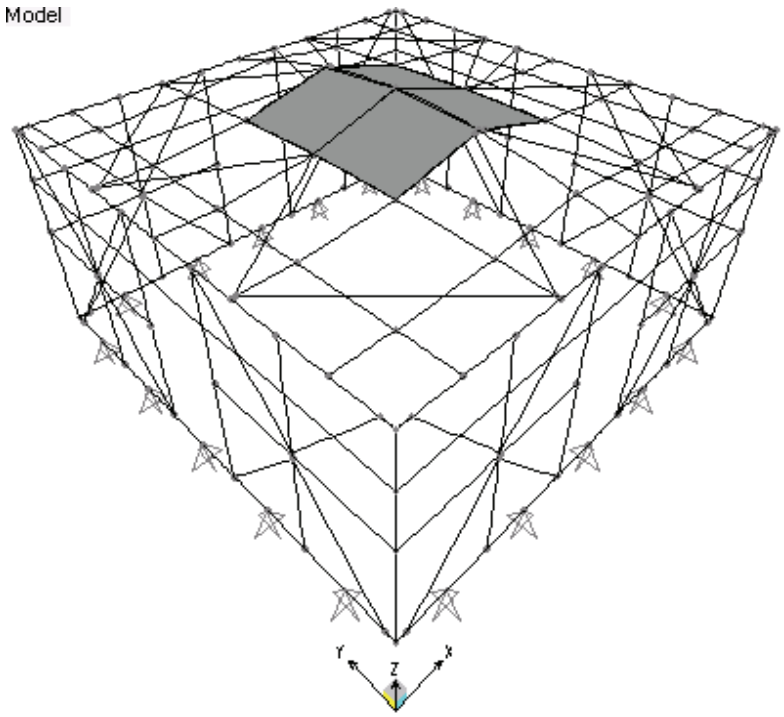

Figure 2-9 Analytical Model (20 × 20 ft.) with Vert. Fundamental Frequency of 10.2 Hz

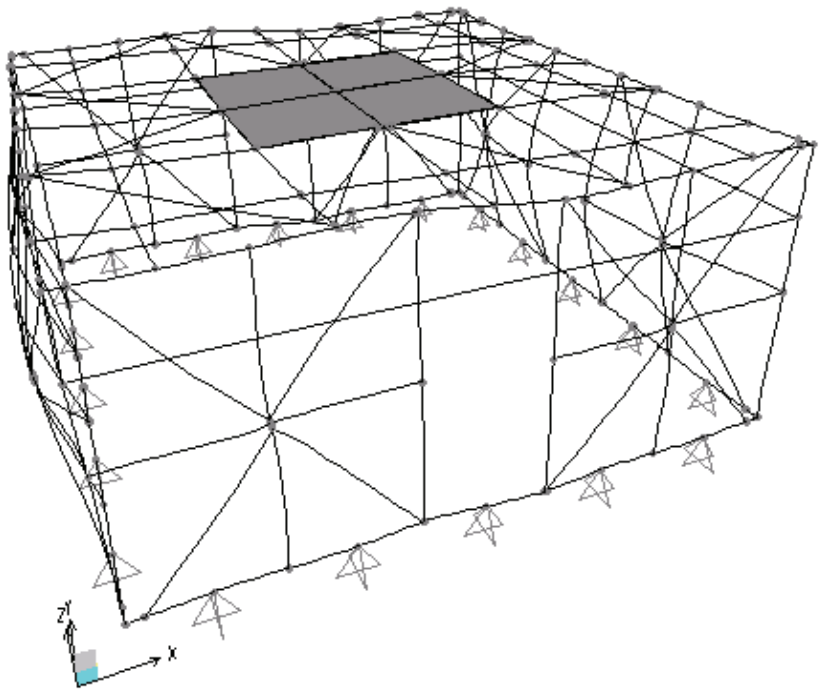

Figure 2-10 Analytical Model (20 × 20 ft.) with Hor. Fundamental Frequency of 17.4 Hz

2.4 Frame Capabilities

2.4.1 Frequency Range of Frame

The addition of ceiling weights affects the reduction of roof frequency, since the frequency is proportional to the inverse of the square root of the mass as in Equation (2-1):

$$f_{zi} = \frac{1}{2\pi}\sqrt{\frac{K}{m_i}} \qquad (2-1)$$

where f_{zi}, m_i, K are the frequency, mass, and stiffness of the basic frame, respectively. The effect of additional ceiling weights on the frequency is indicated as the ratio of the changed frequency (f_{zf}) by additional ceiling weights to the initial frequency (f_{zi}):

$$\frac{f_{zf}}{f_{zi}} = \frac{\frac{1}{2\pi}\sqrt{\frac{K}{m_f}}}{\frac{1}{2\pi}\sqrt{\frac{K}{m_i}}} = \frac{\sqrt{m_i}}{\sqrt{m_f}}, \qquad (2-2)$$

where m_f is the sum of the mass of the basic frame m_i and an additional ceiling mass. As Equation (2-2) shows, if the mass of the initial roof frame is small, the effect of additional ceiling weights on the frequency is relatively large. In order to reduce the variation and make the roof system more practical, reducing the dynamic interaction between ceiling and roof systems, additional mass is installed to the roof grid.

The roof was designed to have a vertical frequency above 20 Hz without additional mass (bare frame) – weight of roof ≤ 1 psf. The roof will support the "floor weight" made of four concrete planks of 4 ft. x 4 ft. x 2 in. placed above the center bays. This accounts for a distributed weight of 4 psf. This is the basic configuration having a vertical frequency of approximately 10 Hz.

When the extremely heavy ceiling tiles are added (having a weight of up to 3 psf), the frequency is lowered to approximately 8 Hz, where further addition of tiles will create the same effect as the original. The change in frequency due to addition of the mass is presented in Figure 2-11. The vertical frequency of the designed frame is scaled to be at the right edge of the "plateau" of the Required Response Spectrum (RRS). Thus, the changed frequency due to the additional mass of the ceiling system will still be within the range of the "plateau" i.e. at maximum.

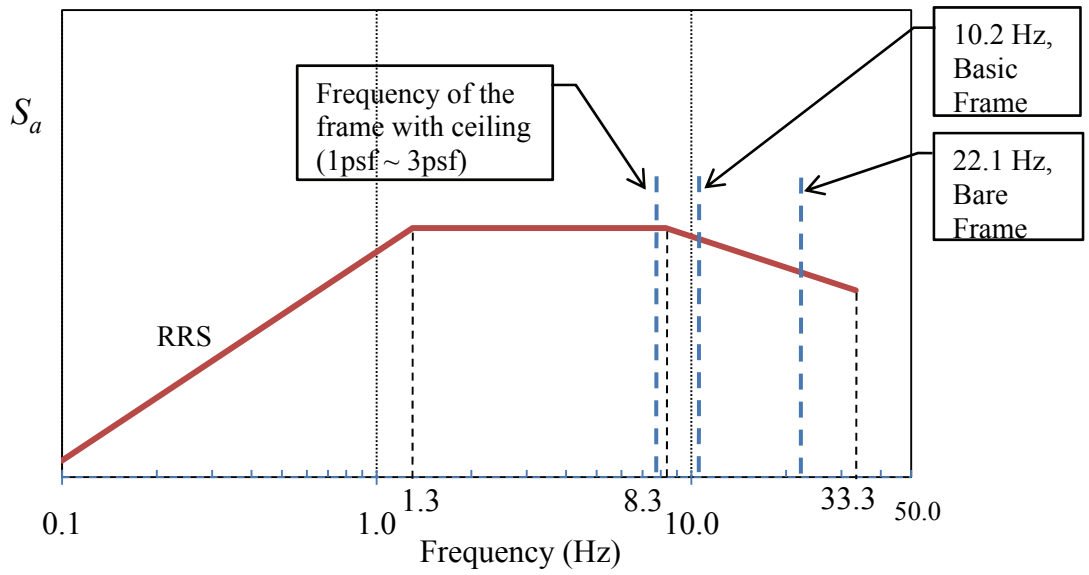

Figure 2-11 Location of the Vertical Frequency of the Frame on the RRS

The effects of additional mass on dynamic properties of the structure are also shown in Table 2-2. The fundamental frequencies of the frame in the longitudinal, transversal, and vertical directions are estimated using an analytical model developed in SAP2000. The additional mass effects are calculated using Equation (2-2). As expected, the ratio of the frequencies obtained from SAP2000 is well matched to the ratio of an initial mass to a changed mass of the roof.

Table 2-2 Effect of Additional Ceiling Weights on Dynamic Properties of the Structure

Description	Long.	Trans.	Vert.	Equivalent Mass			Additional Mass Effects	
20ft. By 20ft. Frame with 18K4 (open web joist)	f_x (Hz)	f_y (Hz)	f_z (Hz)	Add. Mass (lbs·sec^2/ft)	Total Mass $m_i + m_f$ (lbs·sec^2/ft)	Total Weight $W_i + W_f$ (lbs)	$\frac{f_{z_f}}{f_{z_i}}$	$\sqrt{\frac{m_i}{m_f}}$
(1)	(2)	(3)	**(4)**	(5)	(6)	(7)	(8)	(9)
1.0 psf Bare Frame (0 psf – Add. Ceiling Mass)	18.9	19.1	**22.1**	0.0	11.9	382	2.16	2.28
5.0 psf "Basic Model" (4.0 psf - 4 Conc. Planks)	17.4	17.4	**10.2**	49.7	61.7	1,981	1.00	1.00
6.0 psf Floor Weight / Area (1 psf – Add. Ceiling Mass)	16.8	16.9	**9.3**	62.7	74.6	2,400	0.91	0.91
7.0 psf Floor Weight / Area (2 psf – Add. Ceiling Mass)	16.3	16.4	**8.6**	75.2	87.0	2,800	0.84	0.84
8.0 psf Floor Weight / Area (3 psf – Add. Ceiling Mass)	15.8	15.9	**8.1**	87.6	99.5	3,200	0.79	0.79

* The roof area of the frame is 400 ft^2

2.4.2 Adjustable Plenum Height

The height of frame (10 ft.) was selected such that it could allow rapid assembly and disassembly of components, therefore allowing a greater utilization of shake tables. The plenum of different heights can be built by placing "perimeter angles" at various elevations, in increments of 4 in., therefore allowing possible plenum heights of 6 in. to 66 in. (see Figure 2-12).

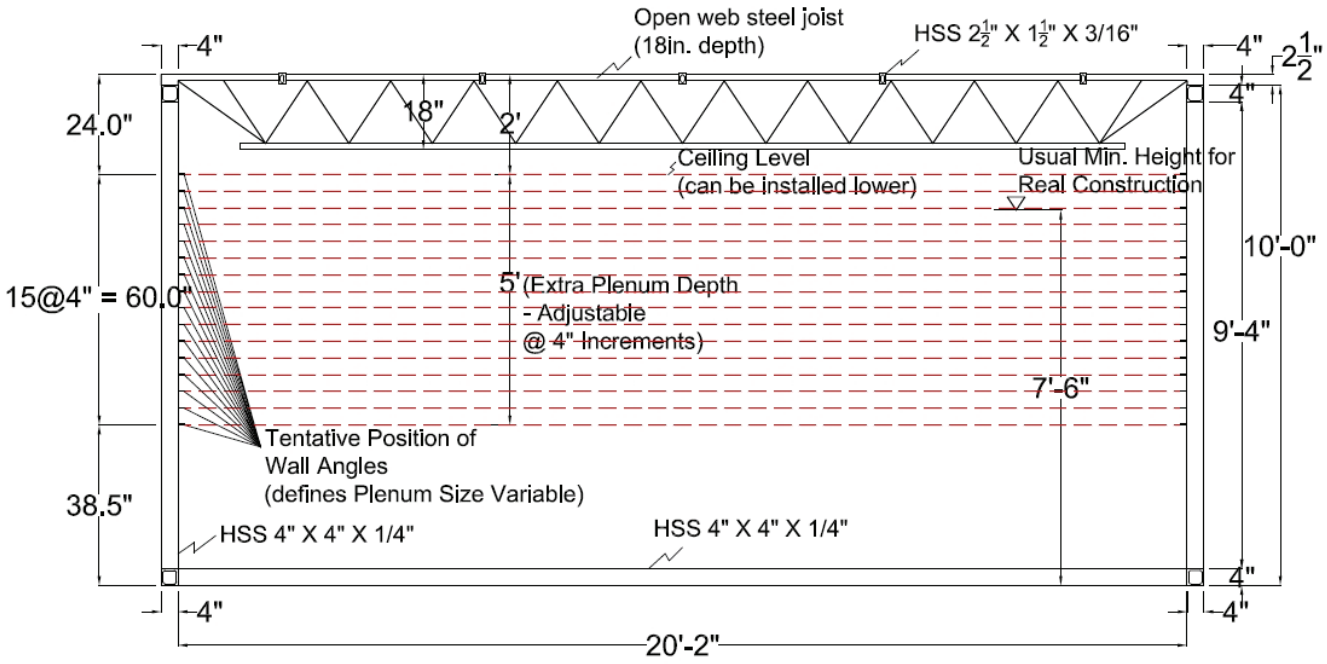

Figure 2-12 Section of the Frame (Adjustable Plenum Heights)

Adverse effects for extreme plenum heights can be eliminated by a special design of the control commands represented by the "table drive" (see Chapter 4).

2.5 Synchronization of Shake Tables

The system is designed with a central link component, built to accomplish synchronization while protecting the shake tables and the specimens in case of malfunctions:

(i) allow a synchronized motion and suppress "minor discrepancies" between shake tables. Differential movement of up to 0.10 in. could be suppressed.

(ii) provide larger differential motions, larger than 0.60 in., breaking a "fuse" that will allow independent motion of shake tables without damaging any of the tables.

(iii) allow some slip between frame and tables, between 0.10 in. and 0.60 in., that will be accommodated and while a 0.30 in. will interrupt experiment.

2.6 Applicability of the Design to Other Installations

The system is custom designed for the shake tables at the SEESL at the University at Buffalo. However, the basic design of smaller components of 20 ft. × 20 ft. can be used in other large installations (UC Berkeley, US Army Corps of Engineers Construction Engineering Laboratory, etc.). Moreover, the design of the procedure for roof motion generation was made to be used at other installations with proper adjustment for local dynamics. The design team can provide training to users and lab operators for similar developments.

CHAPTER 3
ANALYTICAL MODELING

This Chapter describes the modeling and response history analysis of the new (designed) test frame using the structural analysis program, SAP2000. The intent of this part of the study is to anticipate dynamic characteristics of the frame and to evaluate capabilities of the frame, while providing a model for simulation of future experiments.

3.1 Modeling of Existing Test Frame (16 x 16 ft.)

The existing test frame of 16 ft. by 16 ft. designed more than ten years ago (Reinhorn, 2000) to test suspended ceiling systems (see Figure 3-1), was made of Hollow Structural Sections bars: HSS 4×4×1/4 for main frames and HSS 2×2×3/16 for internal columns and roof grids. A list of properties assigned to the frame members is presented in Table 3-1.

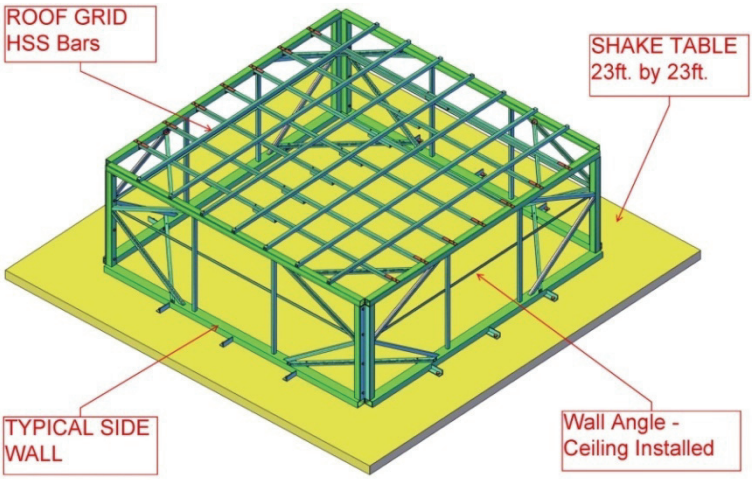

Figure 3-1 AutoCAD 3D Model of the Existing Test Frame (16 × 16 ft.) on a Shake Table

The three-dimensional analytical model shown in Figure 3-2 (a) is created using SAP2000, based on the members, dimensions, and connection details of the actual model. Welded connections (e.g., intersections of roof grids and columns to perimeter bars) are modeled as fixed connections, and bolted connections (e.g., a roof grid to side walls) are modeled as pinned connections. The boundary condition of the frame to a shake table is modeled as a hinge base since the frame is bolted to the table.

Table 3-1 Section Properties of the Test Frame Elements (16 × 16 ft.)

	HSS 6×4×1/4	HSS 4×4×1/4	HSS 2×2×3/16
Installed Location	Bottom Perimeters	Top Perimeters and Edge Columns	Interior Columns, Roof Grid and Braces
(1)	(2)	(3)	(4)
Width (in)	6.0	4.0	2.0
Depth (in)	4.0	4.0	2.0
Thickness (in)	0.233	0.233	0.174
Cross Section Area (in.^{2})	4.300	3.370	1.190
Moment of Inertia 3-3 (in.^{3})	20.900	7.800	0.641
Moment of Inertia 2-2 (in.^{3})	11.100	7.800	0.641
Shear Area 2 (in.^{2})	2.796	1.864	0.696
Shear Area 3 (in.^{2})	1.874	1.864	0.696

Two edge columns at the corners of the frame are modeled as one column, whose property is multiplied by a modification factor of two for a simplified model as shown in Figure 3-2(a). A detailed model, having two edge columns at each corner of the frame, is developed as shown in Figure 3-2(b), and its estimated dynamic characteristics are compared with that of the simplified model in Table 3-2. The difference is approximately 5%, and the simplified modeling scheme is used for this study.

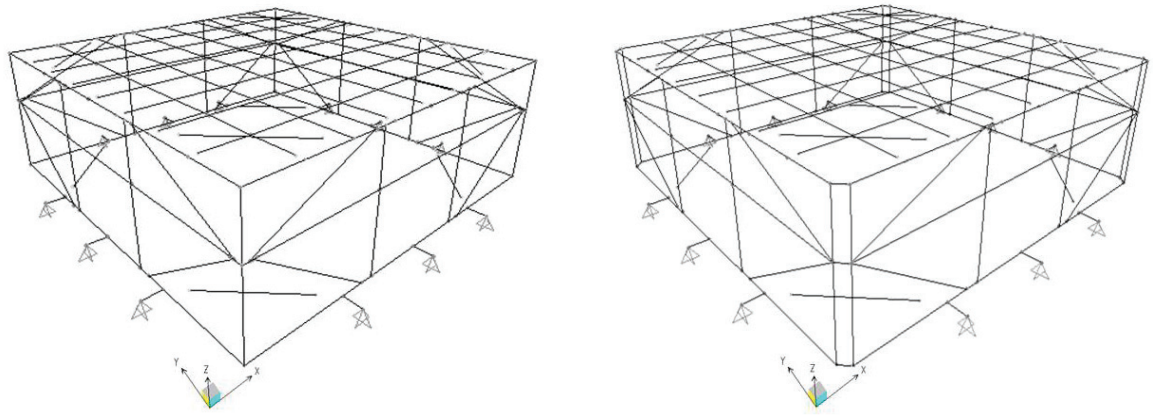

(a) Simplified Model (b) Detailed Model

Figure 3-2 Analytical Model of the Existing Test Frame (16 × 16 ft.) in SAP2000

In order to verify the accuracy of the modeling scheme (simplified), the dynamic characteristics of the existing frame estimated from the analytical model and experiment results are compared and presented in Table 3-2. The results show that there is approximately 20% difference between the characteristics. These errors are assumed as the results of unknown connection conditions (e.g., between fixed and pinned connections) of the frame based on parameter sensitivity studies, conducted during design in order to determine the effects of connection and boundary conditions on the dynamic characteristics of the frame. For example, the vertical frequency of the frame was 11.9 Hz if the connections between the roof grid and the side walls were modeled as fixed instead of pinned connections (bolted connections in the actual frame). The measured frequency 9.4 Hz is the value between the results (7.5 Hz and 11.9 Hz) of the two connection conditions. Although closer results can be obtained by adjusting the "unknown" boundary conditions and connectivity, as shown by the sensitivity study, the model presented above is the one obtained from idealized connectivity and boundary conditions as would be modeled by a regular user without knowing the experimental results. In the new design, the boundary conditions and the connectivity will be chosen and constructed to minimize modeling errors.

Table 3-2 Comparison of Fundamental Frequencies of the Existing Frame (16 × 16 ft.)

	Experiment (Hz)	Simplified Model SAP2000 (Hz)	Detailed Model SAP2000 (Hz)	Difference (%)
(1)	(2)	(3)	(4)	$\lvert\{(3)-(2)\}/(2)\rvert\times 100$
Vertical (z)	9.4	7.5	7.1	20
Longitudinal (x)	17.2	20.5	21.2	19
Transversal (y)	17.2	20.3	21.5	19

3.2 Modeling of New Test Frames (20 × 20 ft. and 20 × 50 ft.)

A new test frame of 20 ft.-2 in. by 20 ft.-2 in. (a square modular frame nominal 20 × 20 ft.) is created as shown in Figure 3-3. A roof grid system is created of open web joists and hollow structural sections (HSS) bars. The open web steel joists make the roof frame stiffer and lighter than that of only HSS. The height of the frame is 10ft. to represent typical building heights.

Additional diagonal braces are planned at the roof level to avoid twisting of the frame. The roof grid is designed to be able to accommodate various floor vertical frequencies with additional weights. The basic configuration is designed to have four concrete blocks of 4 ft. by 4 ft. each, whose weight is equivalent to 4 psf, so that the weight of a roof is 5 psf. A list of properties assigned to the new frame members is presented in Table 3-3.

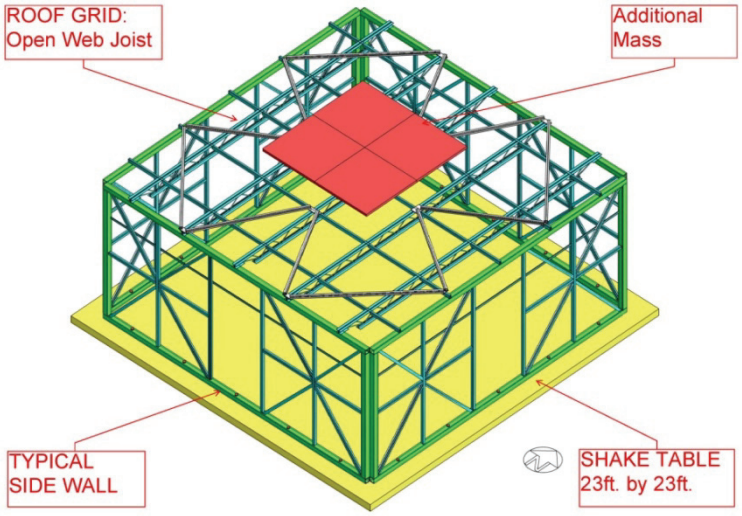

Figure 3-3 AutoCAD 3D Model of a New Test Frame (20 × 20 ft.) on a Shake Table

Table 3-3 Section Properties of the Test Frame Elements (20 × 20 ft. and 20 × 50 ft.)

	Joist 18K4	HSS2.5×1.5×3/16	HSS 4×4×1/4	HSS 2×2×1/4	HSS 8×4×1/4
Element Description	Roof Grid (N-S)	Roof Grid (E-S)	Top and Bottom Perimeters, Edge Columns	Interior Columns, Diagonal Braces (Roof and Walls)	Link Frame 20'-2"by53'-8"
Width (in)	-	1.5	4.0	2.0	8.0
Depth (in)	18.0	2.5	4.0	2.0	4.0
Thickness (in)	-	0.174	0.233	0.174	0.581
Cross Section Area (in.^{2})	-	1.19	3.37	1.19	11.70
Moment of Inertia 3-3 (in.^{3})	81.200	0.882	7.800	0.641	82.000
Moment of Inertia 2-2 (in.^{3})	-	0.390	7.800	0.641	26.600
Shear Area 2 (in.^{2})	-	8.870	1.864	0.696	9.296
Shear Area 3 (in.^{2})	-	0.522	1.864	0.696	4.648

The three-dimensional analytical model is created using SAP2000 as shown in Figure 3-4 based on the members, dimensions, and connection details of the design.

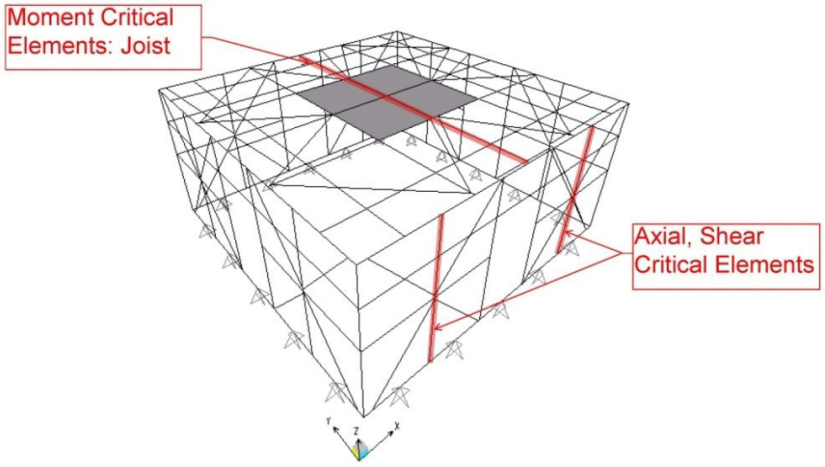

Figure 3-4 Analytical Model of the New Test Frame (20 × 20 ft.) from SAP2000

Using the two 20 × 20 ft. square modular frames mounted on two shake table platforms, an extended test frame of 20 ft.-2 in. by 53 ft.-8 in. is designed (nominal 20 × 50 ft.). A link frame of 13 ft. length is planned to connect the two frames (see Chapter 2.2). Dynamic characteristics are estimated using the analytical model developed in SAP2000 and compared to the desired properties (design criteria) in Table 3-4. The results show the frame has the desired dynamic properties of 2% difference in the vertical direction and approximately 13% difference in the horizontal direction. These differences are managed by adequate compensation procedure (see Chapter 5).

Table 3-4 Comparison of Desired and Estimated Dynamic Characteristics of the New Testing Frames

	Desired (Hz)	20 × 20 ft. Frame SAP2000(Hz)	20 × 50 ft. Frame SAP2000 (Hz)	Difference (%)
(1)	(2)	(3)	(4)	|{(4)-(2)}/(2)|×100
Vertical (z)	8.0 – 10.0	10.2	10.2	2
Longitudinal (x)	20.0	17.4	17.6	12
Transversal (y)	20.0	17.4	17.3	13

3.3 Estimate of Frame Capabilities by Incremental Dynamic Analysis

In order to estimate capabilities of the new test frame, a response history analysis is performed using analytical models developed in SAP2000. Various shaking intensities and various roof weights are chosen as parameters. A set of horizontal and vertical earthquake excitations are obtained from previous experimental tests. The motions were created to generate an AC-156 compatible RRS using a spectrum-matching procedure from the MTS program STEX (MTS, 2004). The vertical motion is calculated as the 2/3 horizontal motion.

First, a model with a roof weight of 8 psf (basic configuration weights of 5 psf and additional weights of 3 psf), is subjected to various shaking levels in order to identify the capabilities of the test frame. The parameter selected to characterize the ground motion is the spectral acceleration mapped at short periods, S_s. The target of shaking levels are S_s = 3.0g, S_s = 4.5g, and S_s = 6.0g by the increment of 1.5g.

The required axial, shear and moment strengths (demands) are calculated and compared with the design (available) strength of each element of the frame according to the *Load and Resistance Factor Design* (AISC, 2007). The design strength must equal or exceed the required strength R_a by Equation (3-1). The design strength is calculated as the product of the resistance factor ϕ and the nominal strength R_n ($\phi_c P_n$, $\phi_v V_n$ and $\phi_b M_n$). Since SAP2000 ver.11.0.8 does not support calculation of the nominal moment strength M_n of joists, the M_n is estimated by Equation (3-2). The critical elements and stresses are presented in Table 3-5 for the 20 × 20 ft. frame and in Table 3-6 for the 20 × 50 ft. frame. The result indicates that the frame is safe when it is subjected up to the shaking intensity of S_s = 4.5g.

$$R_a \leq \phi R_n \qquad (3-1)$$

$$M_n = \sigma_y \times \mathrm{I}/\mathrm{c} \qquad (3-2)$$

for a single joist, where σ_y, I, and c are the yield strength, moment of inertia, and distance between the neutral axis and the bottom of a joist, respectively. The results also show that a joist

located in the middle of a roof grid is a critical element for the required moment strength, and interior columns in the typical walls are critical for the required axial and shear strength. Figure 3-4 above presents the critical elements on a captured image of an analytical model from SAP2000.

Table 3-5 Analysis Results of Required and Available Strength of Elements (20 × 20 ft.)

	Axial, P (kips)		Shear, V (kips)		Moment, M (kips-in)	
Critical Frame Description	Wall-Interior Column, HSS 2*2*3/16		Wall-Interior Column, HSS 2*2*3/16		Open Web Joist, 18K4	
Available Strength (Design Capacity)	$\emptyset_c P_n = 7.1$		$\emptyset_v V_n = 10.5$		$\emptyset_b M_n = 406.0$	
	P_u	Required/ Available (%)	V_u	Required/ Available (%)	M_u	Required/ Available (%)
S_s = 3.0g Max. Required Strength	3.1	44	5.9	56	254.0	63
S_s = 4.5g Max. Required Strength	4.6	64	8.8	83	344.2	85
S_s = 6.0g Max. Required Strength	6.0	84	11.6	111	434.3	107

* LRFD $\emptyset_c = 0.9$, $\emptyset_v = 0.7$, $\emptyset_b = 0.9$

Table 3-6 Analysis Results of Required and Available Strength of Elements (20 × 50 ft.)

	Axial, P (kips)		Shear, V (kips)		Moment, M (kips-in)	
Critical Frame Description	Wall-Interior Column, HSS 2*2*3/16		Wall-Interior Column, HSS 2*2*3/16		Open Web Joist, 18K4	
Available Strength (Design Capacity)	$\emptyset_c P_n = 7.1$		$\emptyset_v V_n = 10.5$		$\emptyset_b M_n = 406.0$	
	P_u	Required/ Available (%)	V_u	Required/ Available (%)	M_u	Required/ Available (%)
S_s = 3.0g Max. Required Strength	4.0	57	6.6	63	254.5	63
S_s = 4.5g Max. Required Strength	5.9	88	9.8	93	344.9	85
S_s = 6.0g Max. Required Strength	7.8	116	13.0	124	435.2	107

* LRFD $\emptyset_c = 0.9$, $\emptyset_v = 0.7$, $\emptyset_b = 0.9$

Second, a limitation of the amounts of additional mass of ceiling systems is estimated. The roof of a new test frame is designed to have changeable frequencies by additional mass (see Chapter 2.4.1). A Basic Configuration model, whose weight of a roof is 5 psf, is subjected to earthquake excitations for AC-156, shaking intensity of S_s = 3.0g, with various additional weight (3.0 psf to 12.0 psf). The analysis results are presented in Table 3-7 for the 20 × 20 ft. frame and in Table 3-8 for the 20 × 50 ft. frame. The first excess of the required strength of moment over the design strength occurs when the weight of a roof is 17.0 psf with 12.0 psf of additional weights for both test frames.

Table 3-7 Analysis Results of Required and Available Strength of Elements (20 × 20 ft.)

	Axial, P (kips)		Shear, V (kips)		Moment, M (kips-in)	
Critical Frame Description	Wall-Interior Column, HSS 2*2*3/16		Wall-Interior Column, HSS 2*2*3/16		Open Web Joist, 18K4	
Available Strength (Design Capacity)	$\emptyset_c P_n = 7.1$		$\emptyset_v V_n = 10.5$		$\emptyset_b M_n = 406.0$	
	P_u	Required/ Available (%)	V_u	Required/ Available (%)	M_u	Required/ Available (%)
Roof Weight: 5.0 psf (Basic Model) Max. Required Strength	2.5	36	4.3	41	141.5	35
Roof Weight: 8.0 psf (Add. Weight: 3.0 psf) Max. Required Strength	3.1	44	5.9	56	254.0	63
Roof Weight: 11.0 psf (Add. Weight: 6.0 psf) Max. Required Strength	4.0	56	6.8	65	357.6	88
Roof Weight: 14.0 psf (Add. Weight: 9.0 psf) Max. Required Strength	4.6	66	8.0	76	387.8	96
Roof Weight: 17.0 psf (Add. Weight: 12.0 psf) Max. Required Strength	5.1	71	10.0	95	487.6	120

* LRFD $\emptyset_c = 0.9$, $\emptyset_v = 0.7$, $\emptyset_b = 0.9$

Table 3-8 Analysis Results of Required and Available Strength of Elements (20 × 50 ft.)

	Axial, P (kips)		Shear, V (kips)		Moment, M (kips-in)	
Critical Frame Description	Wall-Interior Column, HSS 2*2*3/16		Wall-Interior Column, HSS 2*2*3/16		Open Web Joist, 18K4	
Available Strength (Design Capacity)	$\emptyset_c P_n = 7.1$		$\emptyset_v V_n = 10.5$		$\emptyset_b M_n = 406.0$	
	P_u	Required/ Available (%)	V_u	Required/ Available (%)	M_u	Required/ Available (%)
Roof Weight: 5.0 psf (Basic Model) Max. Required Strength	3.5	49	5.4	52	142.1	35
Roof Weight: 8.0 psf (Add. Weight: 3.0 psf) Max. Required Strength	4.0	57	6.6	63	254.5	63
Roof Weight: 11.0 psf (Add. Weight: 6.0 psf) Max. Required Strength	5.1	72	8.8	83	358.5	88
Roof Weight: 14.0 psf (Add. Weight: 9.0 psf) Max. Required Strength	5.8	82	9.0	86	388.4	96
Roof Weight: 17.0 psf (Add. Weight: 12.0 psf) Max. Required Strength	6.3	89	11.0	<u>105</u>	488.5	<u>120</u>

* LRFD $\emptyset_c = 0.9$, $\emptyset_v = 0.7$, $\emptyset_b = 0.9$

CHAPTER 4
DESIGN AND EVALUATION OF FRAME'S ROOF TESTING MOTION

Qualification testing of suspended ceiling systems is usually done using earthquake like excitations produced by shake table motions generated using spectrum-matching procedures or with suites of motions recorded in past earthquakes. The motion should be representative of the location of the ceiling in the structure. As previously indicated, the motion is amplified by the structural system in which the suspended system is located. Instead of reinventing the testing motion with each new test, standards and recommendations were developed. This chapter revisits the requirements of the standards and suggests ways to improve on the motions which should be used for testing.

4.1 Standard Requirement - Current and Proposed

4.1.1 AC-156 Required Response Spectrum

In the last ten years (Reinhorn, 2000) the qualification testing of suspended ceiling systems has usually been done using earthquake-like excitations produced by shake table motions generated using spectrum-matching procedures recommended by ICC-AC-156 "Acceptance Criteria for Seismic Qualification Testing of Nonstructural Components" (ICC, 2007). The first step in such a procedure is to define a target spectrum or Required Response Spectrum (RRS), which is calculated as a function of the short-period spectral acceleration, S_s, provided by USGS maps for various locations in the US. The AC-156 RRS for horizontal and vertical shaking is presented in Figure 4-1.

The values of the parameters of the spectral acceleration A_{RIG} of a rigid component (assumed to have a frequency, $f \geq 33$ Hz) and that of a flexible component A_{FLX} define the ordinates of the horizontal motion spectra. They are calculated by Equation (1-7) and Equation (1-8). The two equations are repeated here:

$$A_{FLX} = S_{DS} \left(1 + 2\frac{z}{h}\right) \leq 1.6\, S_{DS} \tag{4-1}$$

$$A_{RIG}=0.4\ S_{DS}\ (1+2\frac{z}{h})\leq 1.2\ S_{DS} \tag{4-2}$$

where z is the height above the building base where suspended components are to be installed, and h is the height of the building. The formulation is compatible with the dynamic amplifications explained in the introduction of this study. S_{DS} is the design spectral acceleration at short periods and is determined using Section 1613 of the International Building Code (ICC, 2006) as in Equation (4-3):

$$S_{DS} = \frac{2}{3} F_a S_S \tag{4-3}$$

where F_a is a site soil coefficient, and S_S is the mapped maximum earthquake spectral acceleration at short periods.

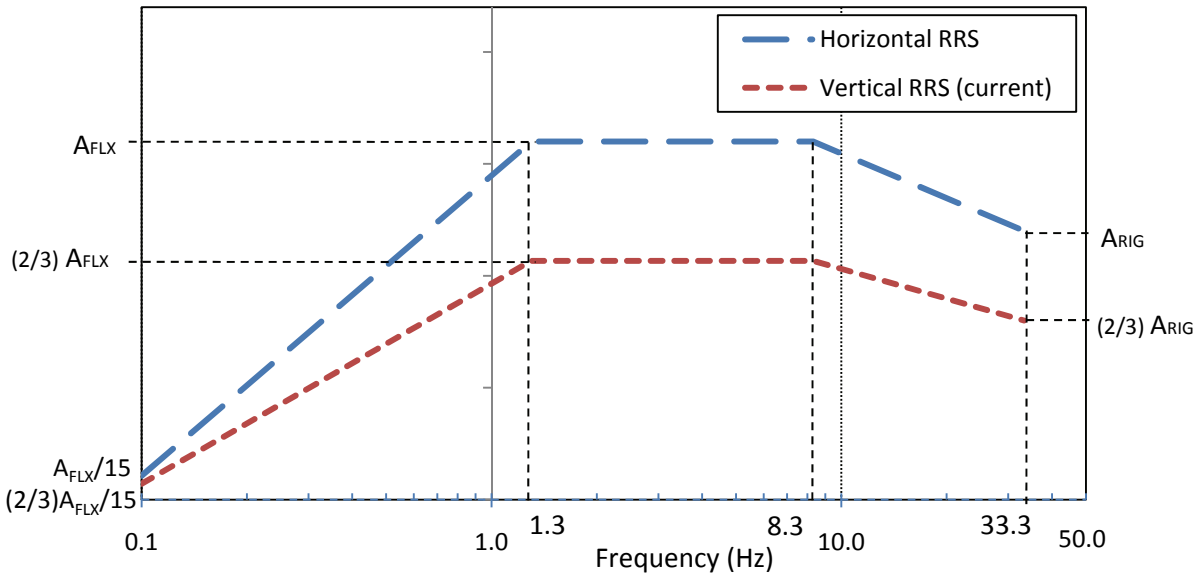

Figure 4-1 AC-156 RRS for Horizontal and Vertical Shaking

The ordinates of the vertical RRS are determined by ICC AC-156 as two-thirds (2/3) of the horizontal RRS as shown in Figure 4-1. Section 6.5.1.2.1 of ICC AC-156 indicates that the parameter z in Equations (4-1) and (4-2) may be taken as zero for the vertical RRS without much elaboration (i.e. assuming no vertical amplification along the height of the building).

4.1.2 Proposed Vertical Motion for AC-156 Required Response Spectrum

Per ICC-AC-156, the vertical required response spectrum (RRS), which is representative of the floor in the building where the ceiling is suspended, is determined as two-thirds (2/3) of those of the horizontal RRS, as indicated above. However, this requirement should be modified, since the vertical acceleration is not amplified as the horizontal motion. The horizontal acceleration applied at the base is amplified by the function $(1+2z/h)$ in Equation (4-1) and (4-2) in order to obtain the required horizontal floor response spectrum as discussed in Chapter 1.1.2.1. At the same time, the vertical motion is not amplified by the "usually" vertically rigid structures. Therefore, this study recommends modifying the required vertical response spectrum (RRS) with no amplification in the vertical direction. Equation (4-1) and Equation (4-2) are modified for the vertical motions eliminating the vertical variation by setting z to zero:

$$A_{FLX,V} = \frac{2}{3} S_{DS} \le 1.6 \left(\frac{2}{3} S_{DS} \right) \tag{4-4}$$

$$A_{RIG,V} = 0.4 \left(\frac{2}{3} S_{DS} \right) \le 1.2 \left(\frac{2}{3} S_{DS} \right) \tag{4-5}$$

where S_{DS} is the design spectral acceleration at short periods for the horizontal direction, and the vertical spectral acceleration is determined as two-thirds (2/3) of the horizontal one per ICC AC-156. The proposed vertical RRS without height amplification should be calculated from the horizontal RRS using a multiplier of 0.42 for A_{FLX} and 0.22 for A_{RIG}, instead of 0.67 (≈ 2/3) for both of them in the current code. For the comparison between the current AC-156 RRS and the proposed RRS, the spectral acceleration demands (represented by A_{FLX} and A_{RIG}) are explained in terms of $\alpha \times S_{DS}$, where α is the maximum coefficient presented in Table 4-1. The differences between the current AC-156 RRS and the proposed RRS are also presented in Figure 4-2, through Figure 4-4. The y axis in each spectrum represents the spectral acceleration demand in a different form: A_{FLX} and A_{RIG} per AC 156 in Figure 4-2, S_{DS} the design spectral acceleration at short periods in Figure 4-3, and S_S the mapped maximum earthquake spectral acceleration at short periods in Figure 4-4, respectively. The relationships between these parameters were presented in the prior section (see Equations (4-1) to (4-5)).

Table 4-1 Spectral Acceleration Demand per AC-156 in Terms of Multiples (α) of S_{DS}

	Horizontal			Vert.(current)			Vert.(proposed)			Ver./Hor.	
	$1+2\frac{z}{h}$	α	limit	$1+2\frac{z}{h}$	α	limit	$1+2\frac{z}{h}$	α	limit	current	proposed
(1)		(2)			(3)			(4)		(3)/(2)	(4)/(2)
$A_{FLX,\ top}$	≤ 3	~~3.0~~ 1.6	1.6	$\leq\frac{2}{3}\cdot 3$	~~2.0~~ 1.07	1.07	$\leq\frac{2}{3}\cdot 1$	0.67	1.07	0.67	0.42
$A_{FLX,\ base}$	1	1.0	1.6	$\frac{2}{3}\cdot 1$	0.67	1.07	$\frac{2}{3}\cdot 1$	0.67	1.07	0.67	0.67
$A_{RIG,\ top}$	≤ 3	1.2	1.2	$\leq\frac{2}{3}\cdot 3$	0.80	0.80	$\leq\frac{2}{3}\cdot 1$	0.27	0.80	0.67	0.22
$A_{RIG,\ base}$	1	0.4	1.2	$\frac{2}{3}\cdot 1$	0.27	0.80	$\frac{2}{3}\cdot 1$	0.27	0.80	0.67	0.67

Spectral Acceleration $= \alpha \times S_{DS}$

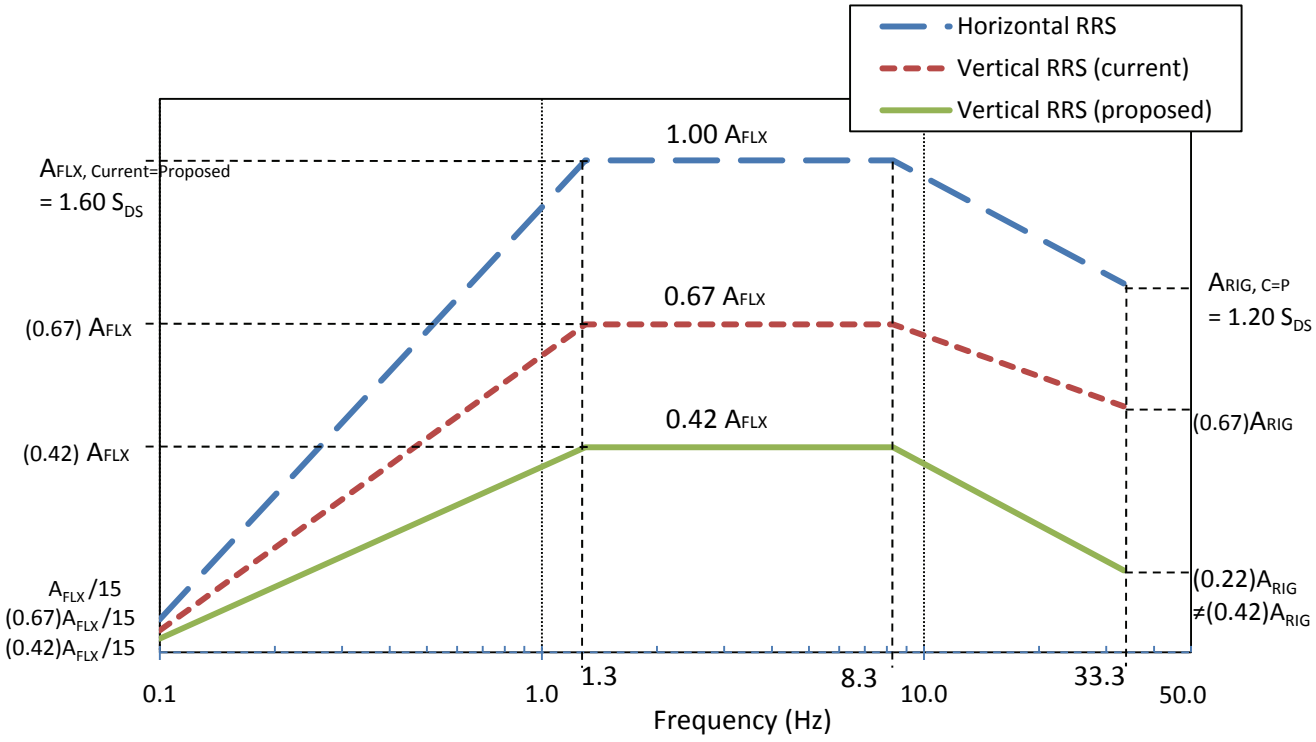

Figure 4-2 AC-156 RRS for Horizontal and Vertical Spectral Acceleration Demand (S_a), A_{FLX} and A_{RIG}

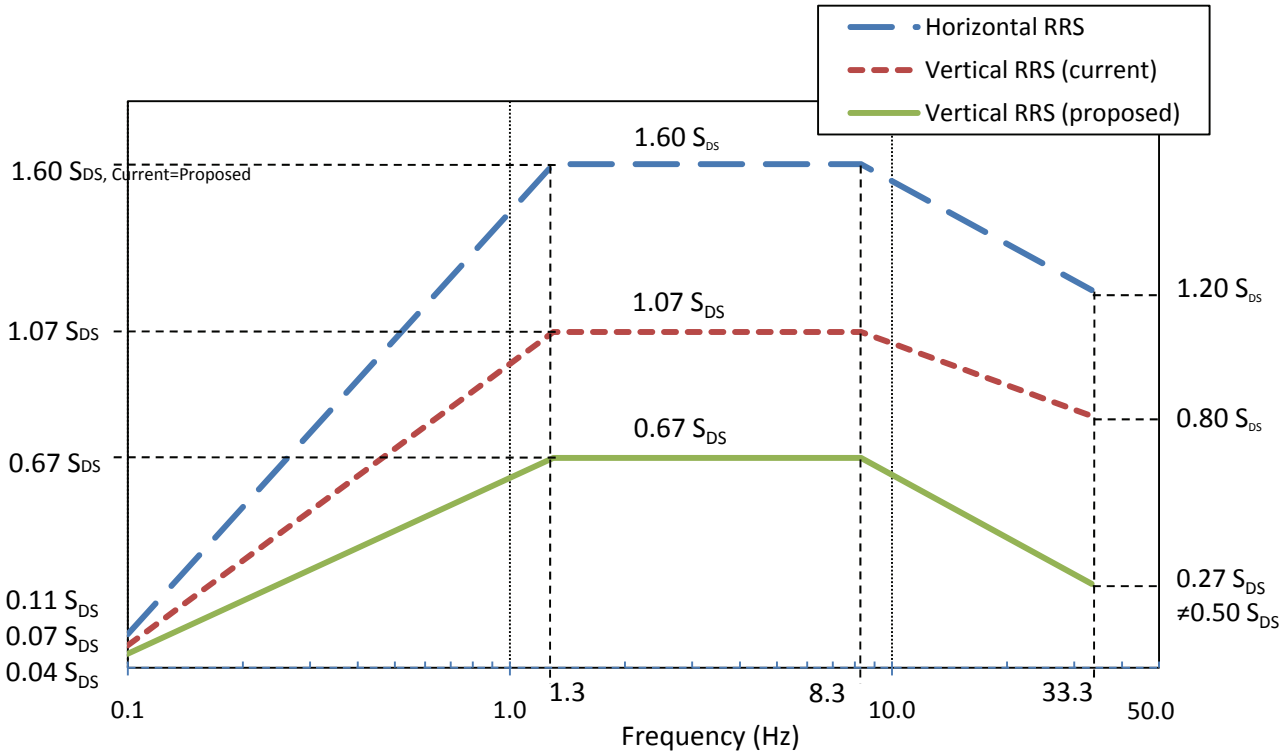

Figure 4-3 AC-156 RRS for Horizontal and Vertical Demand in Terms of S_{DS}

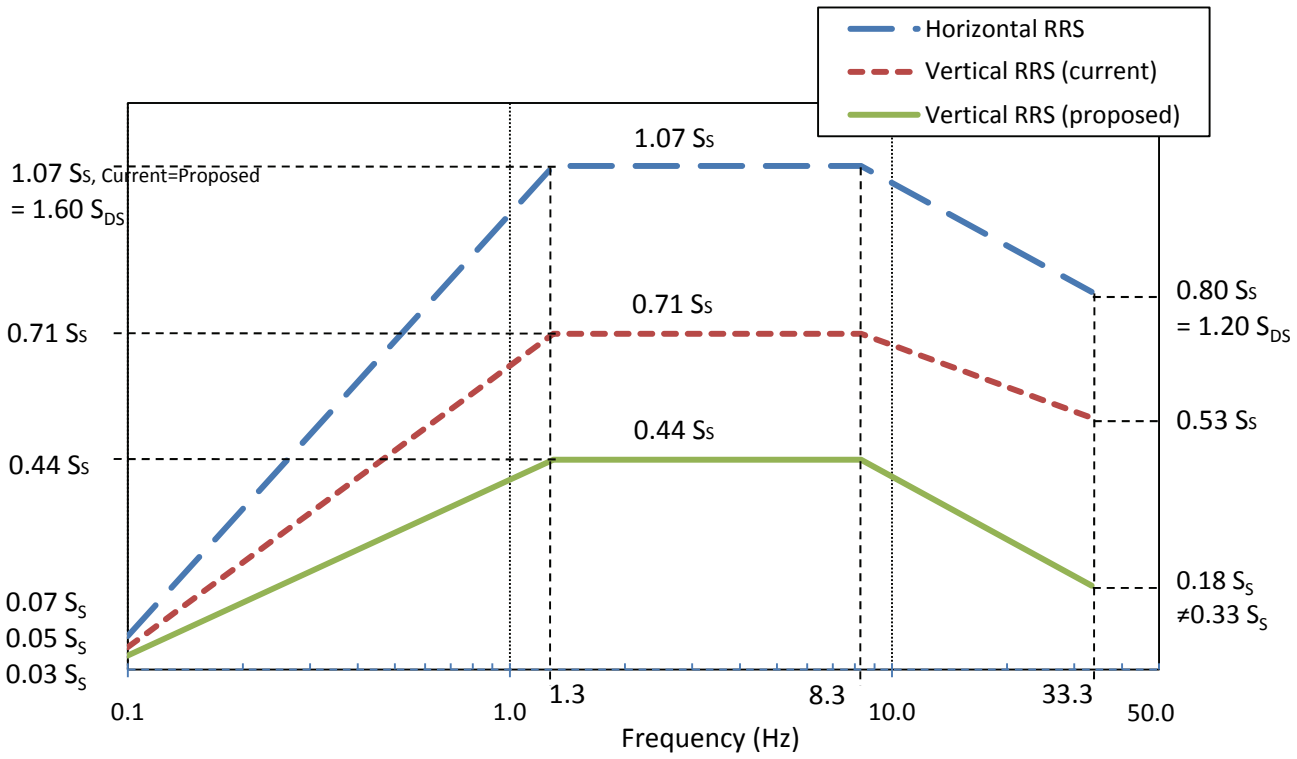

Figure 4-4 AC-156 RRS for Horizontal and Vertical Demand in Terms of S_S

It should be noted that the current code Section 6.5.1.2.1 of ICC AC-156 indicates that the parameter *z* in Equations (4-1) and (4-2) may be taken as zero for the vertical amplification. The statement should not be connected to z, which is a measure of the modal shape (as indicated in Chapter 1.1.2.1). Moreover a specific formulation for the vertical motion should be specified, independent of z and moreover, for suspended ceilings it must include the local amplification of the horizontal floors diaphragms out-of-plane vibrations (in the vertical direction).

4.1.3 Experimental Evaluation on the Proposed Vertical Motion

4.1.3.1 Shake Table Simulated Motions

Full scale testing was conducted to observe the effects of proposed vertical motions on a test frame and suspended ceiling systems. The series of testing was performed using the existing test frame (16 × 16 ft.) on which a ceiling system was installed. The random multi-frequency seismic simulation tests included tri-axial floor motions that were established using scaled RRS as recommended by ICC AC-156 (ICC, 2007). Table 4-2 lists the full series of tests used for the test specimen.

Table 4-2 Test Sequence for a Complete Set of Experiments

Test No.	Target S_S (g)	Description of Required Response Spectrum (RRS)
1	1.50	AC-156 Horizontal RRS (E-W and N-S) and a ***current*** vertical RRS
2	1.50	AC-156 Horizontal RRS (E-W and N-S) and a ***proposed*** vertical RRS
3	1.75	AC-156 Horizontal RRS (E-W and N-S) and a ***current*** vertical RRS
4	1.75	AC-156 Horizontal RRS (E-W and N-S) and a ***proposed*** vertical RRS

The earthquake excitations used for the qualification of the ceiling system were generated according to the guideline of ICC-AC-156 using a spectrum-matching procedure, namely, the "Inverse Response Spectrum Procedure" routine from the program software STEX (MTS, 2004). STEX utilizes industry-standard algorithms for calculation of shock response spectra and inverse shock response spectra. Independent records were generated for each excited degree of freedom: horizontal East-West direction (x), horizontal North-South direction (y), and vertical direction

(z). ICC-AC-156 requires the Test Response Spectrum (TRS) associated with the earthquake histories used for qualification must envelope the required (or target) response spectrum (RRS) based on a maximum-one-sixth octave bandwidth resolution over the range from 1.3 to 33.3 Hz, or up to the shake table limits.

Figure 4-5 through Figure 4-8 present the horizontal and vertical simulator input acceleration histories created by the spectrum matching procedure and their corresponding TRS for the series of this testing. A damping ratio of 5% and a resolution of 50 lines per octave (8.3 times greater than that required by ICC-AC-156) were used to generate the TRS.

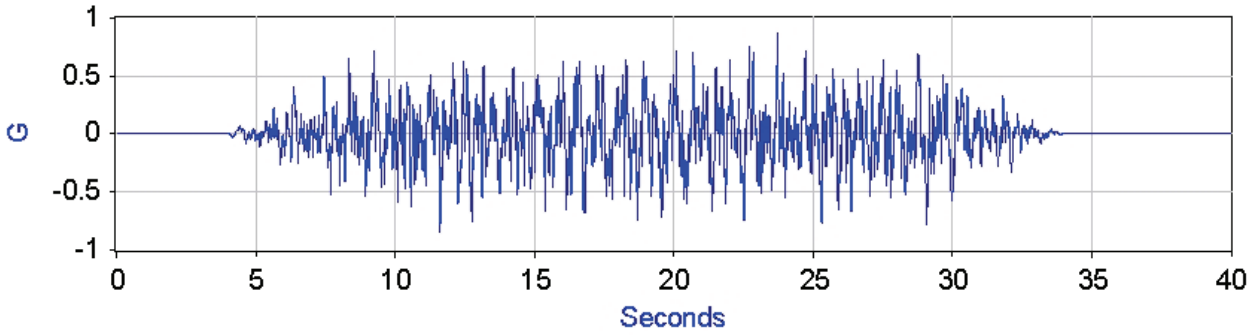

a) Horizontal acceleration history in the X direction (East – West)

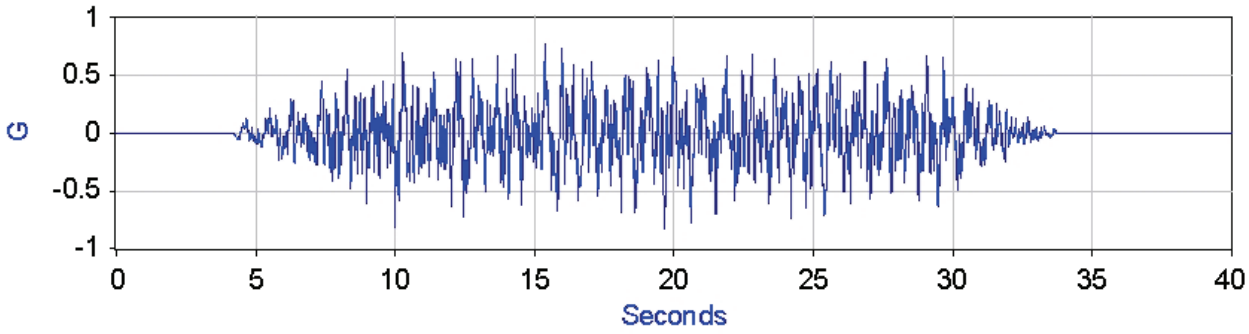

b) Horizontal acceleration history in the Y direction (North – South)

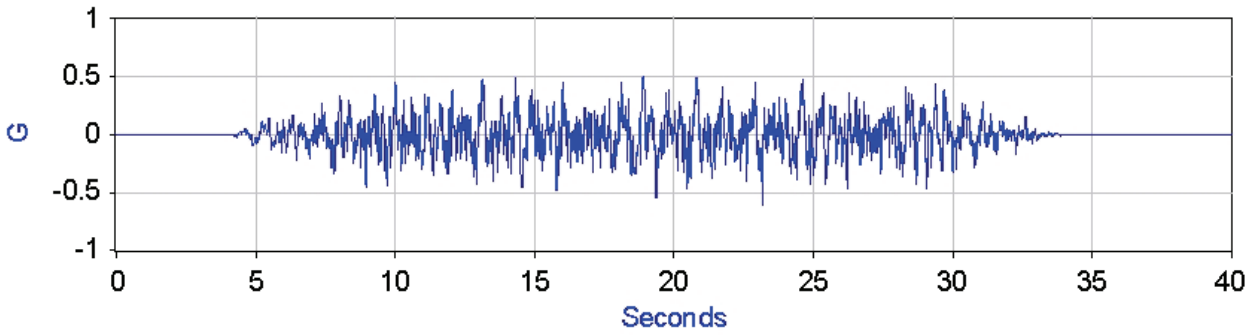

c) Vertical acceleration history in the Z direction

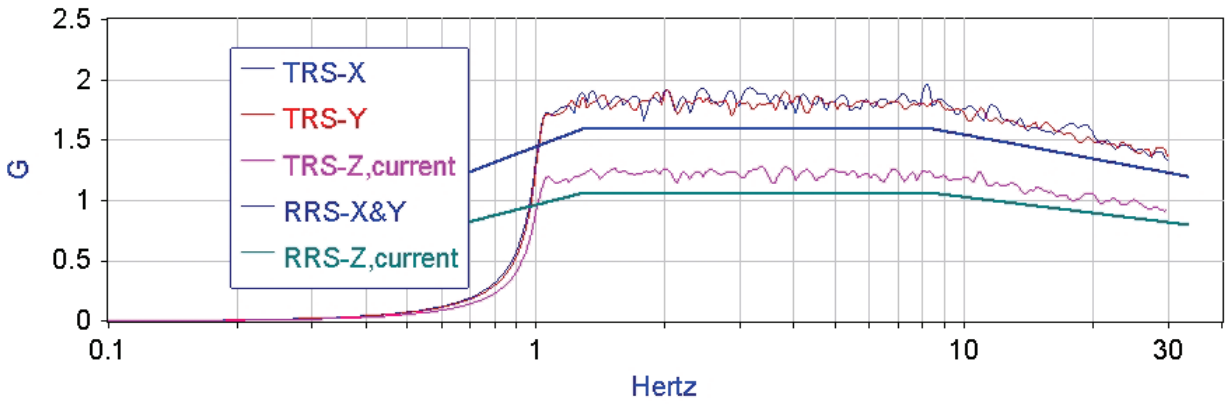

d) Test response spectrum (TRS) and the RRS per ICC-AC-156

Figure 4-5 Test Input Motions and Response Spectra for No.1 (current AC-156, S_S =1.50g)

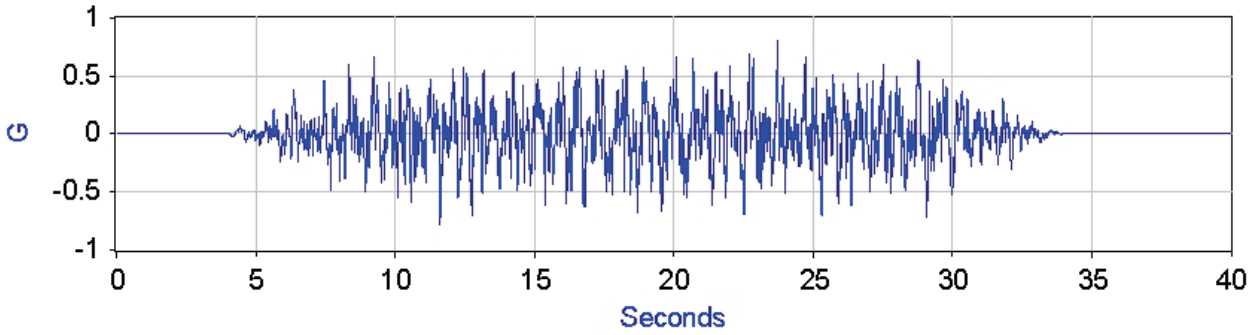

a) Horizontal acceleration history in the X direction (East – West)

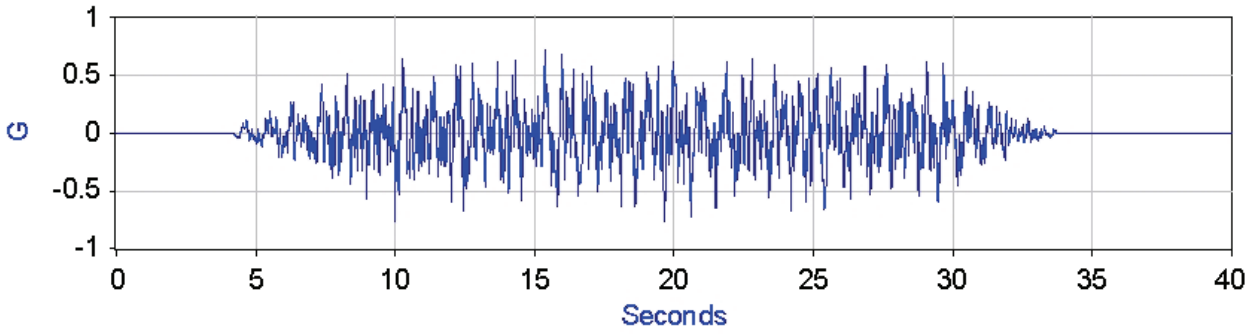

b) Horizontal acceleration history in the Y direction (North – South)

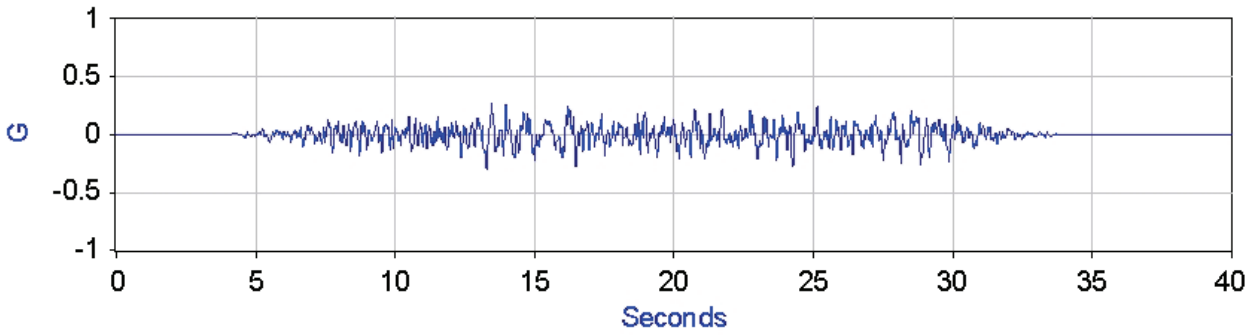

c) Vertical acceleration history in the Z direction

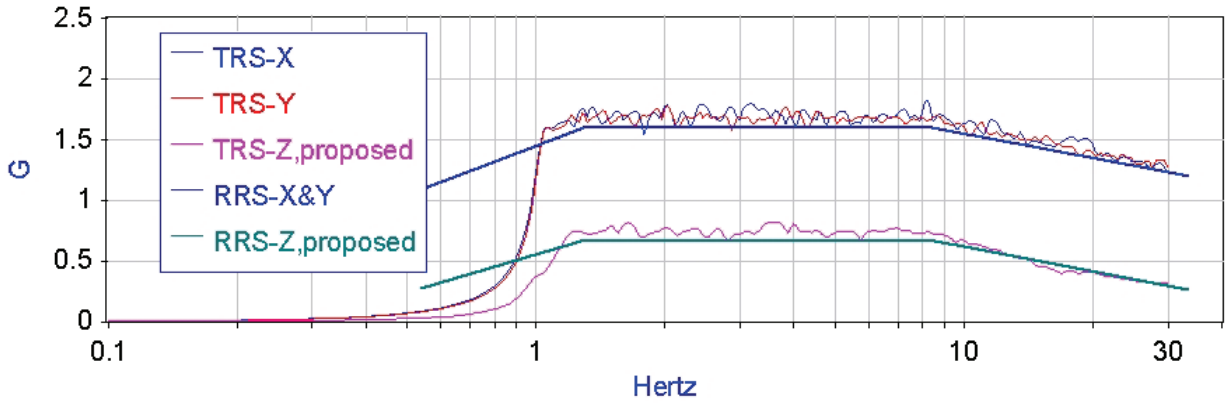

d) Test response spectrum (TRS) and the RRS per ICC-AC-156

Figure 4-6 Test Input Motions and Response Spectra for No.2 (Proposed AC-156, S_S =1.50g)

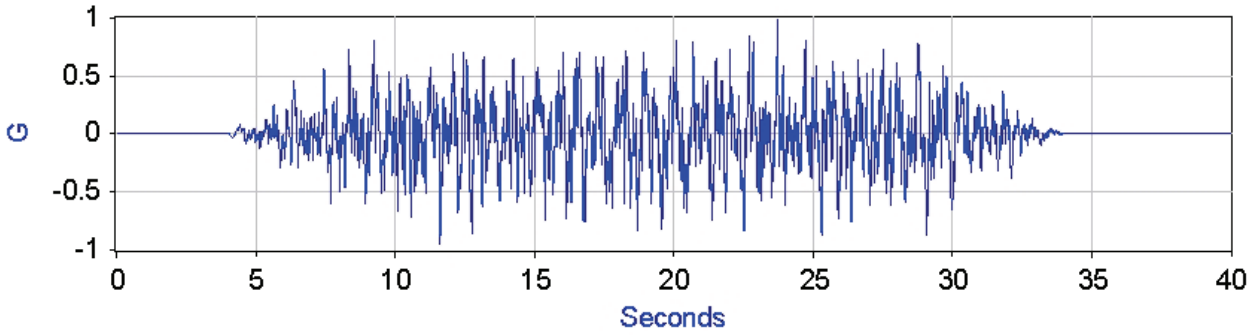

a) Horizontal acceleration history in the X direction (East – West)

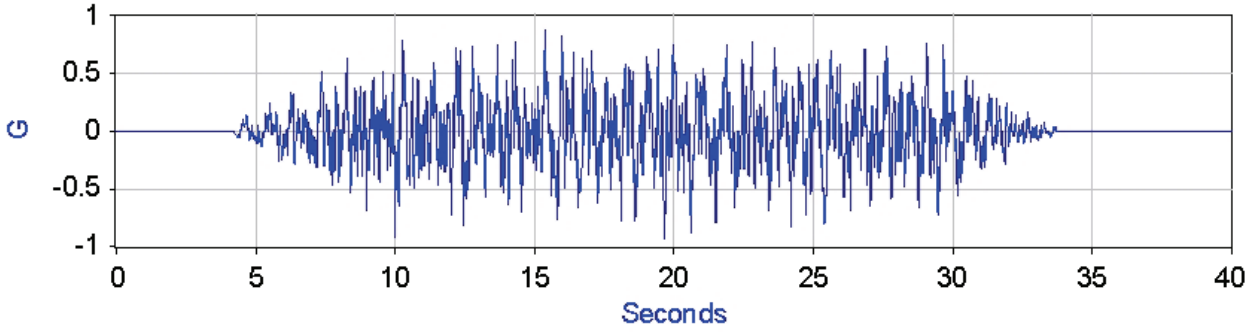

b) Horizontal acceleration history in the Y direction (North – South)

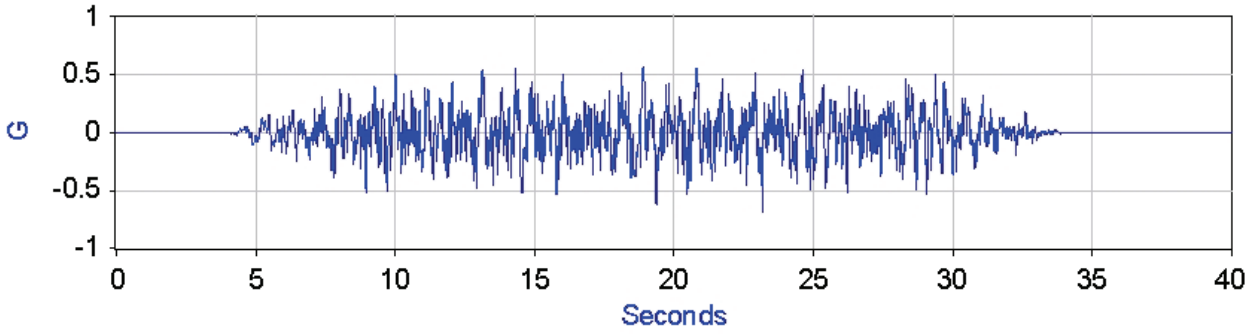

c) Vertical acceleration history in the Z direction

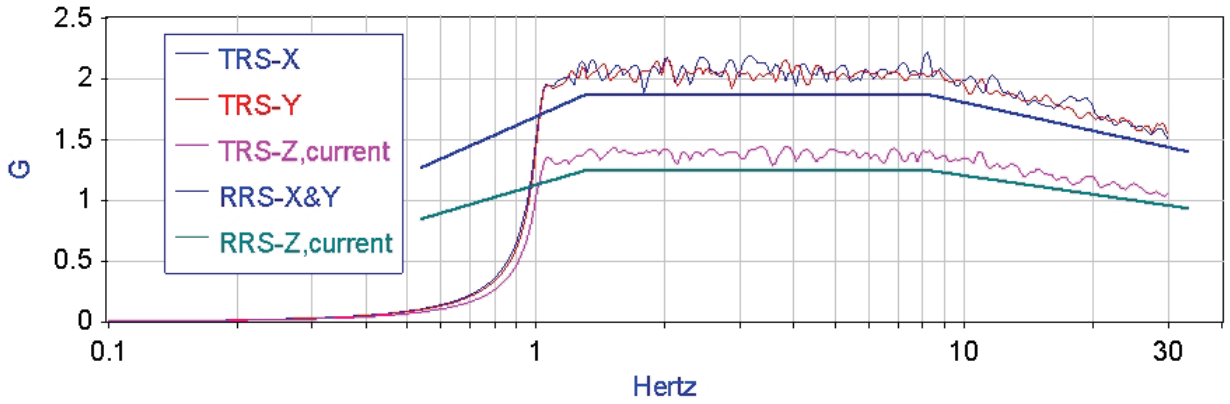

d) Test response spectrum (TRS) and the RRS per ICC-AC-156

Figure 4-7 Test Input Motions and Response Spectra for No.3 (Current AC-156, S_S =1.75g)

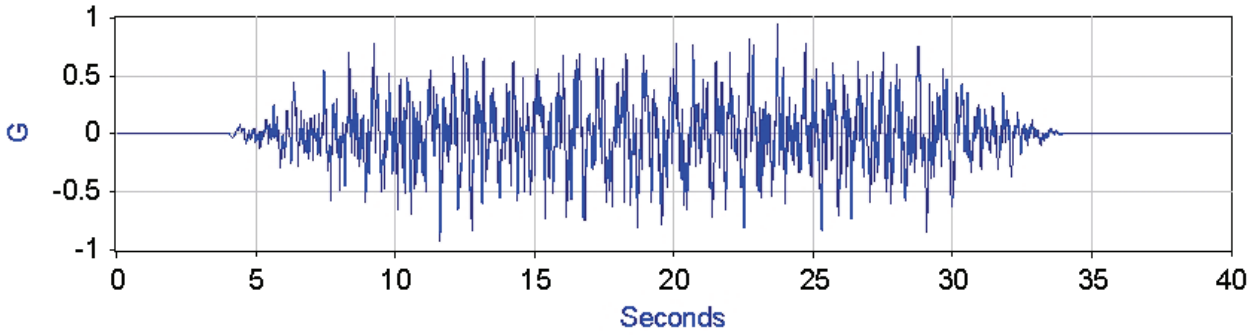

a) Horizontal acceleration history in the X direction (East – West)

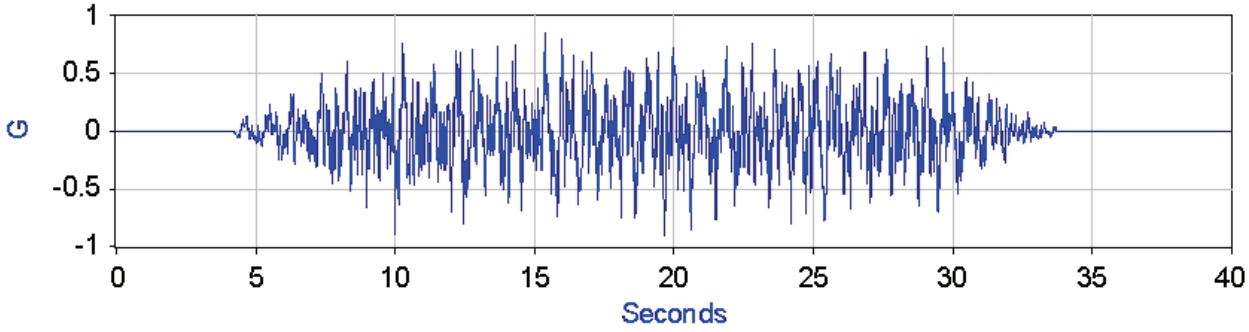

b) Horizontal acceleration history in the Y direction (North – South)

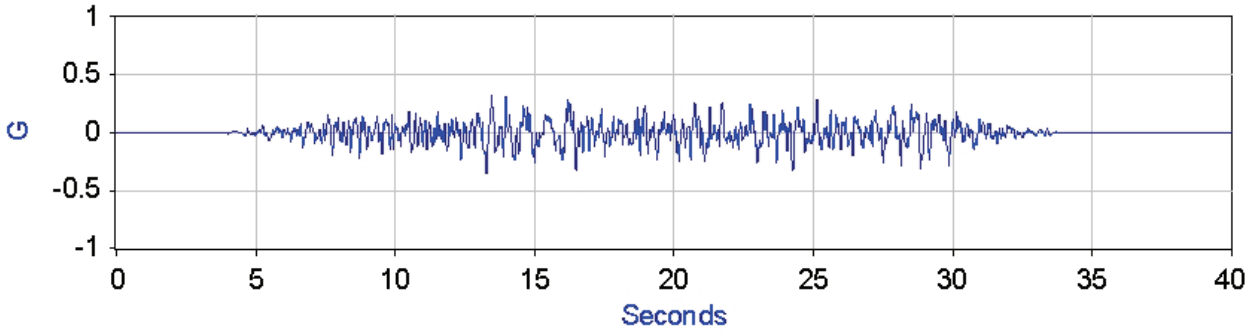

c) Vertical acceleration history in the Z direction

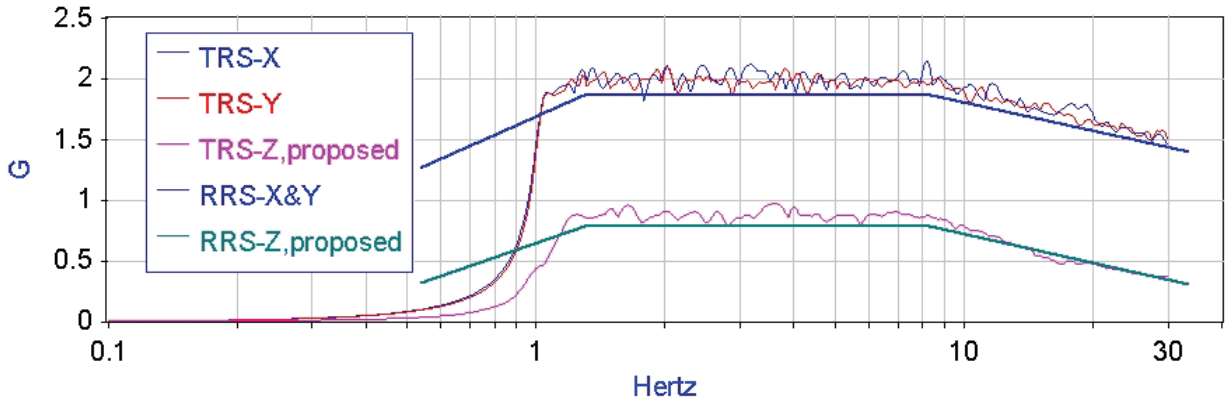

d) Test response spectrum (TRS) and the RRS per ICC-AC-156

Figure 4-8 Test Input Motions and Response Spectra for No.4 (Proposed AC-156, S_S =1.75g)

4.1.3.2 Comparison of Simulated Floor (Roof) Motions

The floor motion histories generated using the procedure described in Chapter 4.1.3.1 were used as the input to a shaking table. The horizontal and vertical responses of the shaking table and the test frame were recorded with accelerometers. These responses were recorded for the purpose of comparing the effects of the proposed ICC-AC-156 vertical motion to the ones of the current vertical motion per ICC-AC-156. Accelerometers were placed on the center of the shaking table extension (AEXT), the center of the roof of the frame (AGRD), and the center of the suspension ceiling system (ATIL).

For Test No.1 and No.2 (using the *current* vertical motion and *proposed* vertical motion, respectively, for a target spectrum with S_S = 1.50g), Figure 4-9 and Figure 4-11 present the tri-axial response motions at the specific locations indicated above (AEXT, AGRD, and ATIL). The response spectra for 5% damping were calculated from the acceleration histories achieved at each location. The response motions at the three locations are also presented in each direction in order to show the amplification of the response when the input motion travels the structure through the path of the motion (AEXT → AGRD → ATIL) in Figure 4-10 and Figure 4-12 for Test No.1 and No.2, respectively.

For Test No.3 and No.4 (using the *current* vertical motion and *proposed* vertical motion, respectively, for a target spectrum with S_S = 1.75g), Figure 4-13 and Figure 4-15 present the tri-axial response motions at the specific locations. The response motions at the three locations are also presented in each direction in Figure 4-14 and Figure 4-16 for Test No.3 and No.4, respectively.

For the purpose of comparison between the responses of the current vertical motion and proposed vertical motion, the peak spectral accelerations of each motion are estimated and listed in Table 4-3. The results indicate that the proposed vertical motion generates the roof response smaller by 0.6g (approximately 11% of the current RRS response) and the suspended ceiling grid response smaller by 1.1g (approximately 16% of the current RRS response) for a target spectrum with S_S = 1.50g, and the roof response smaller by 0.9g (approximately 16% of the current RRS

response) and the suspended ceiling grid response smaller by 0.8g (approximately 11% of the current RRS response) for a target spectrum with S_S = 1.75g.

Table 4-3 Response Peak Spectral Accelerations

Test No.	Target S_S (g)	Direction	FLOOR[1], S_a[2] (g)	ROOF[3], S_a (g)	GRID[4], S_a (g)
1	1.50 (Current Vert.)	X	1.9	5.8	8.9
		Y	2.1	3.6	4.5
		Z	1.3	6.0	6.7
2	1.50 (Proposed Vert.)	X	1.8	5.3	6.7
		Y	1.9	3.6	4.6
		Z	0.8	5.4	5.6
3	1.75 (Current Vert.)	X	2.2	7.0	9.8
		Y	2.3	3.3	5.4
		Z	1.5	6.8	6.8
4	1.75 (Proposed Vert.)	X	2.2	6.3	7.1
		Y	2.3	3.9	5.4
		Z	1.0	5.7	6.0

[1] FLOOR = floor acceleration (center of the shaking table extension, AEXT)

[2] S_a = peak spectral acceleration in the response spectrum in the range of 0.1Hz. to 20Hz

3 ROOF = Roof acceleration (center of the roof of the frame, AGRD)

[4] GRID = Grid acceleration (center of the grid system, ATIL)

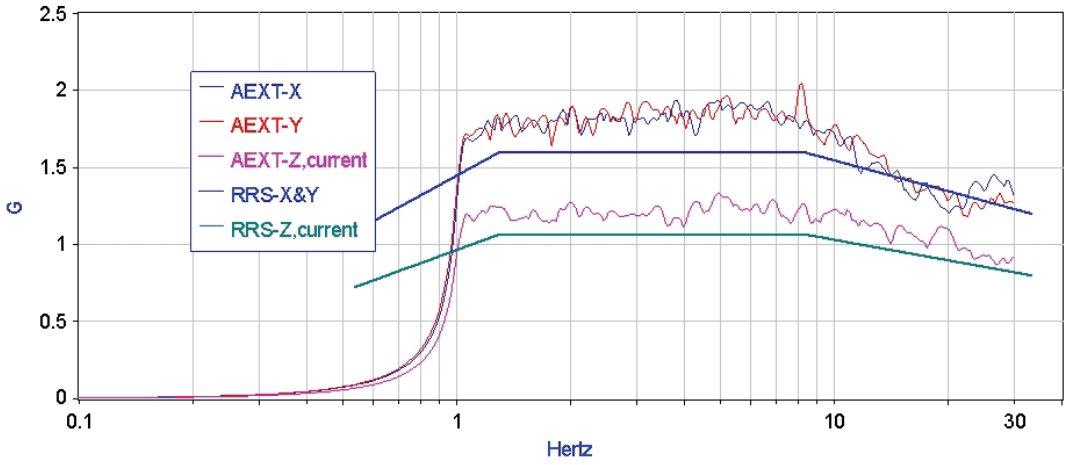

a) Response spectra obtained on the shaking table extension (AEXT)

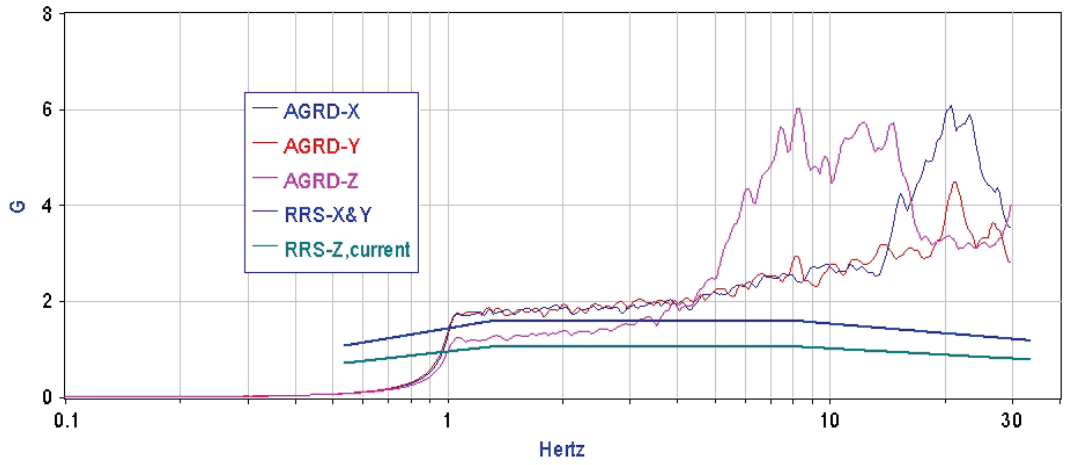

b) Response spectra obtained on the roof of the frame (AGRD)

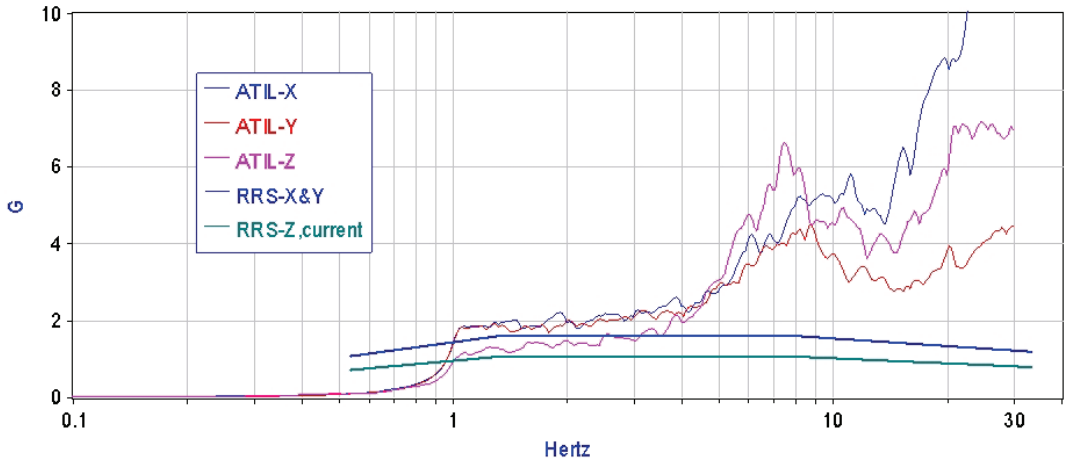

c) Response spectra obtained on the suspension system (ATIL)

Figure 4-9 Response Spectra Obtained from the Accelerometers Located on the Three Locations for Test No. 1 (Current AC-156, S_S =1.50g)

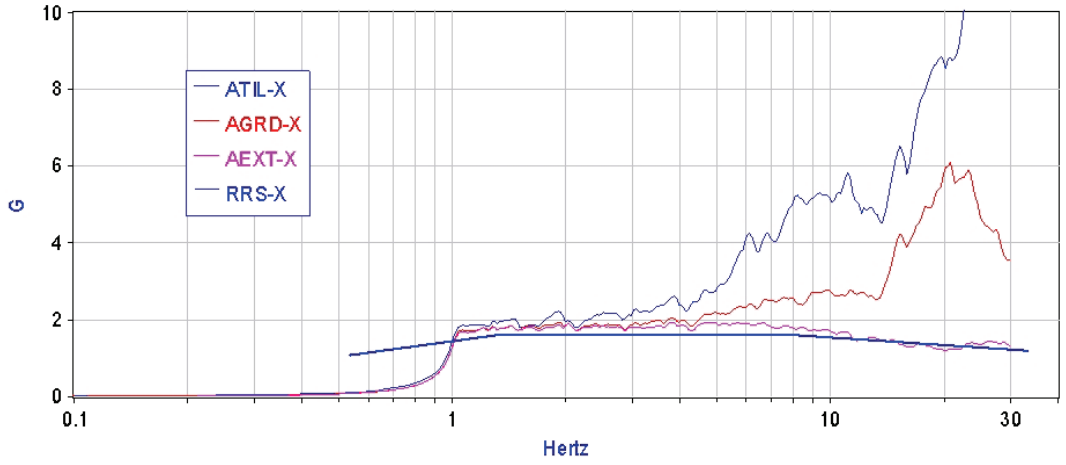

a) Horizontal direction (X)

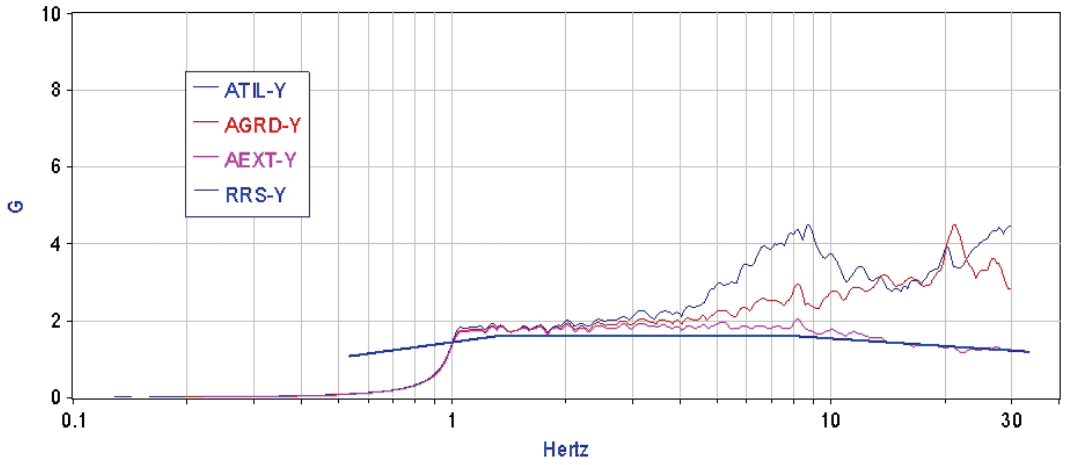

b) Horizontal direction (Y)

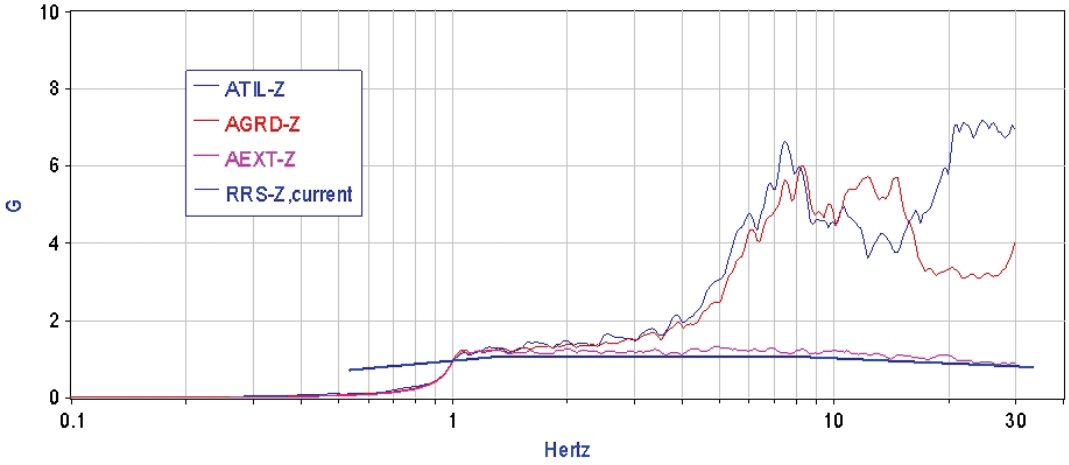

c) Vertical direction (Z)

Figure 4-10 Response Spectra for Each Direction for Test No.1 (Current AC-156, S_S =1.50g)

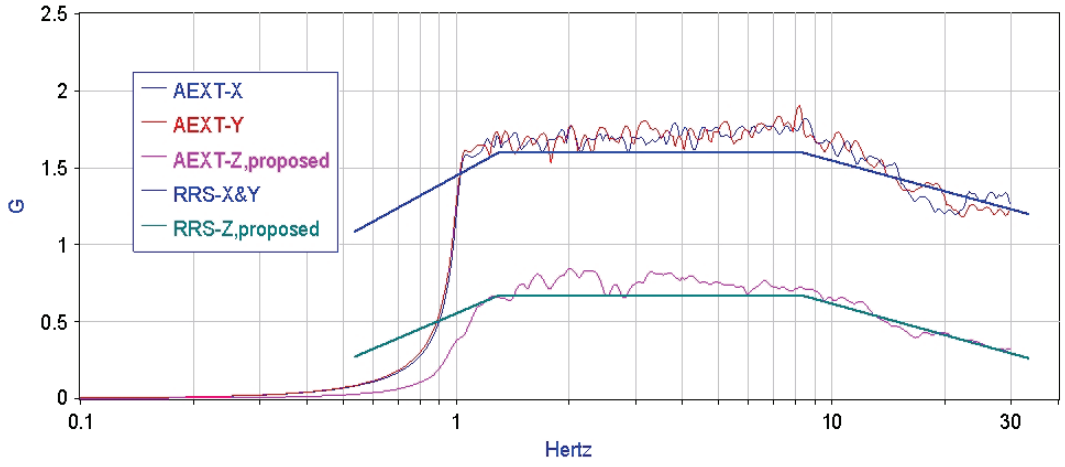

a) Response spectra obtained on the shaking table extension (AEXT)

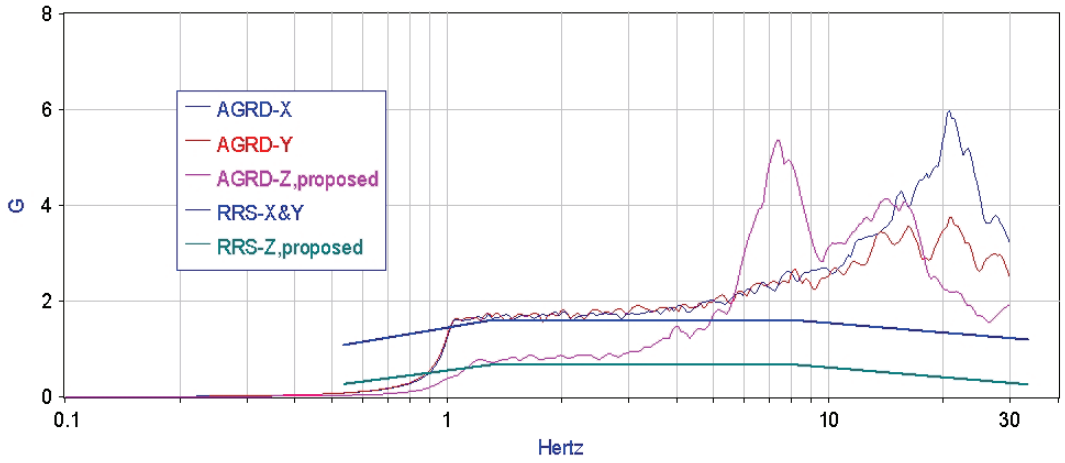

b) Response spectra obtained on the roof of the frame (AGRD)

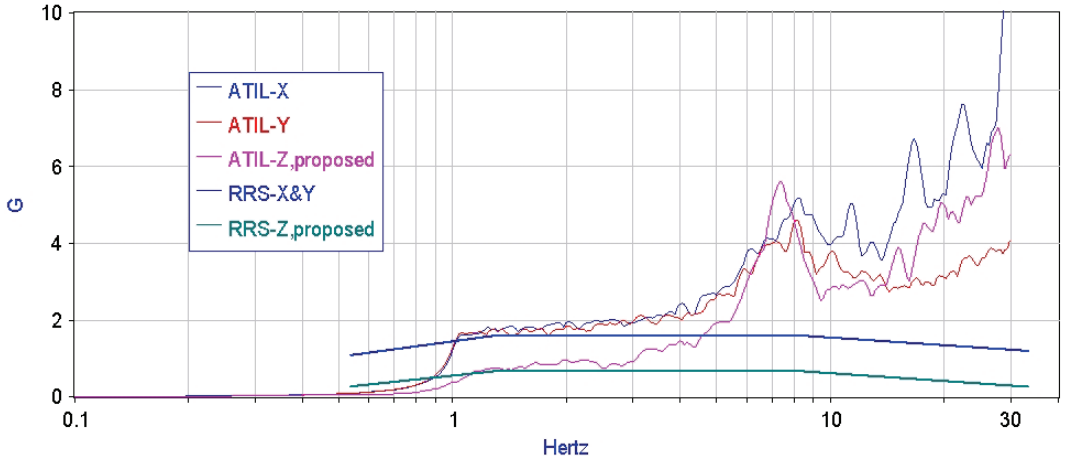

c) Response spectra obtained on the suspension system (ATIL)

Figure 4-11 Response Spectra Obtained from the Accelerometers Located on the Three Locations for Test No.2 (Proposed AC-156, S_S =1.50g)

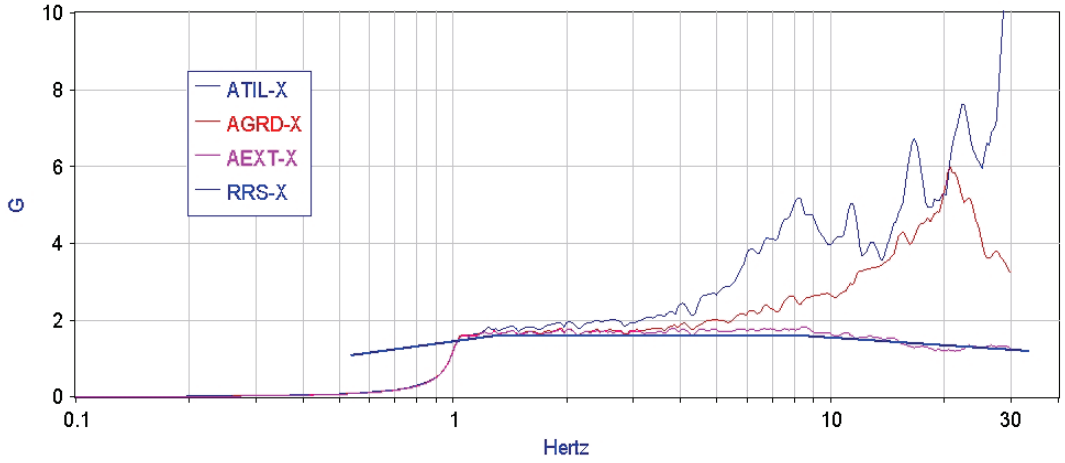

a) Horizontal direction (X)

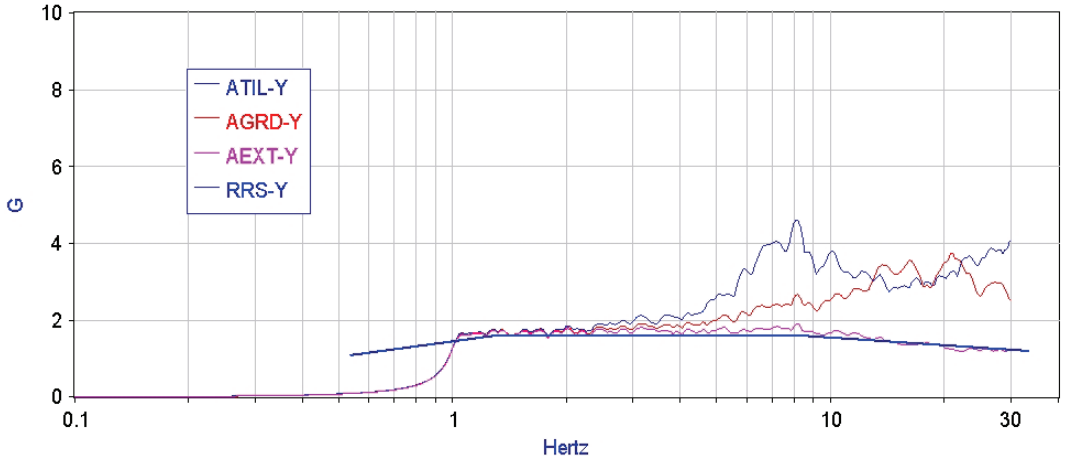

b) Horizontal direction (Y)

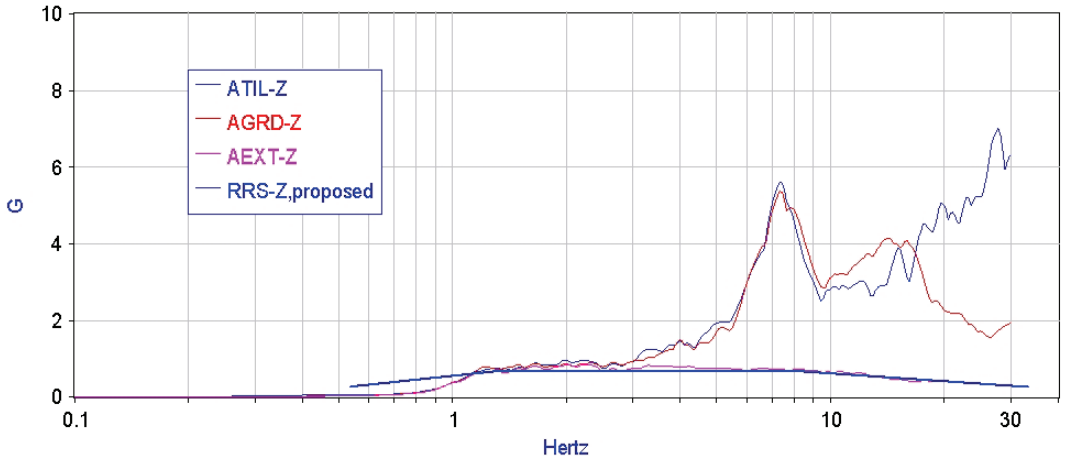

c) Vertical direction (Z)

Figure 4-12 Response Spectra for Each Direction for Test No.2 (Proposed AC-156, S_S =1.50g)

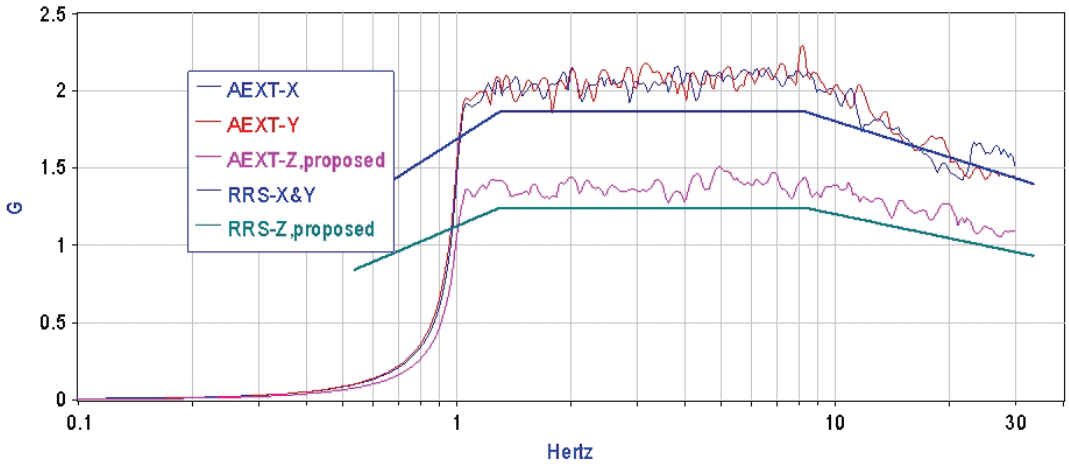

a) Response spectra obtained on the shaking table extension (AEXT)

b) Response spectra obtained on the roof of the frame (AGRD)

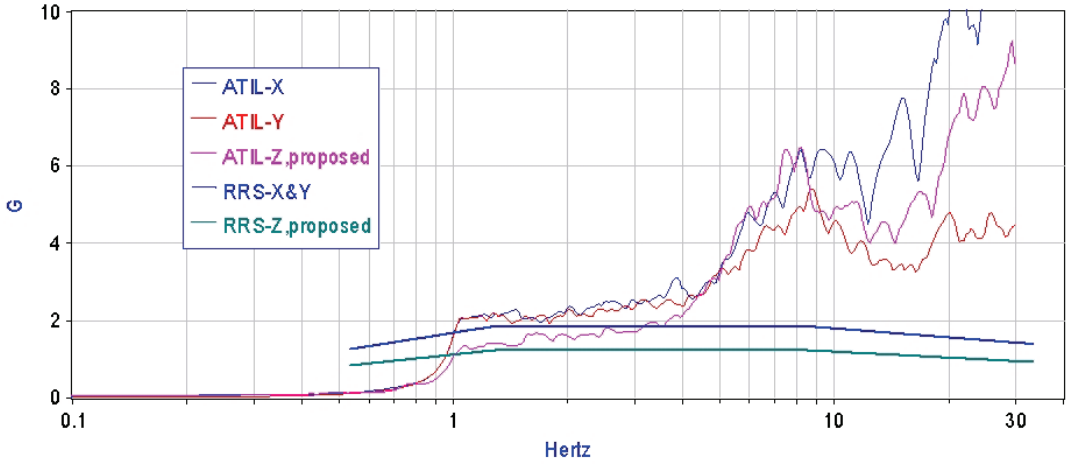

c) Response spectra obtained on the suspension system (ATIL)

Figure 4-13 Response Spectra Obtained from the Accelerometers Located on the Three Locations for Test No.3 (Current AC-156, S_S =1.75g)

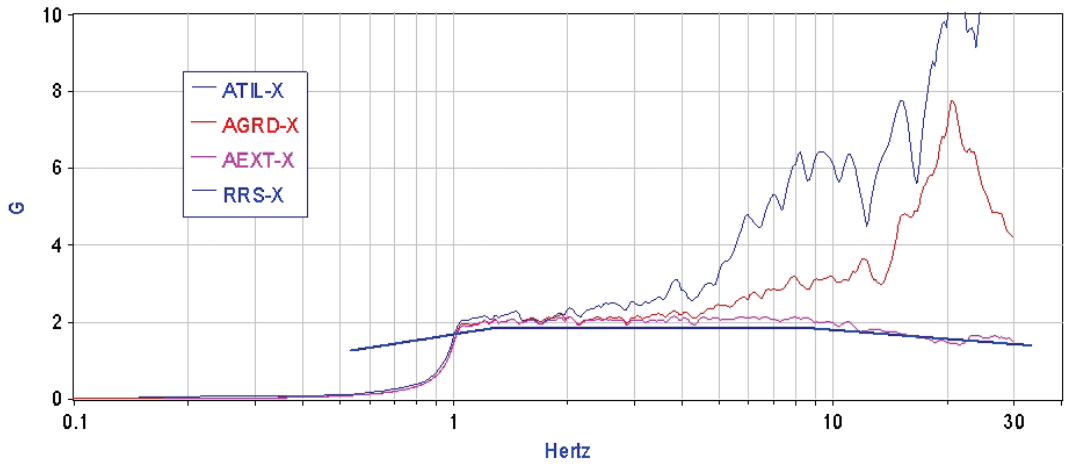

a) Horizontal direction (X)

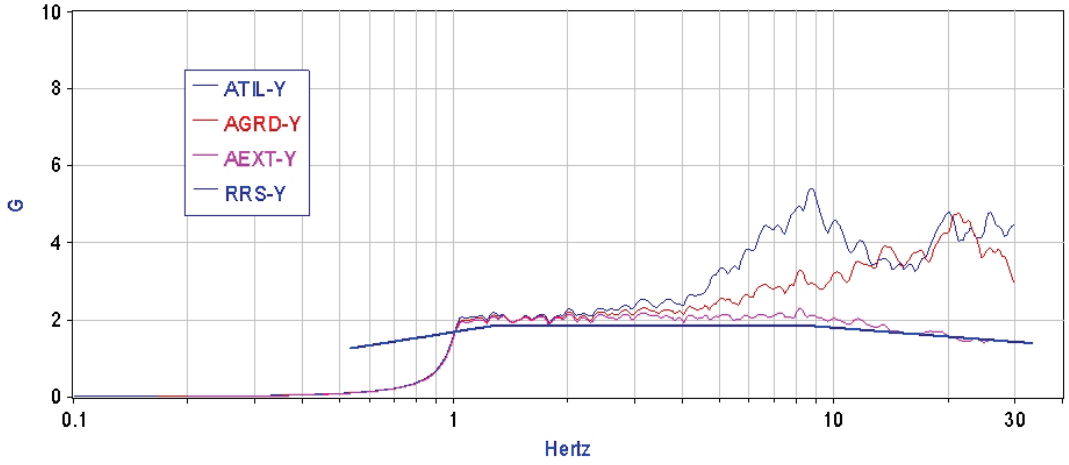

b) Horizontal direction (Y)

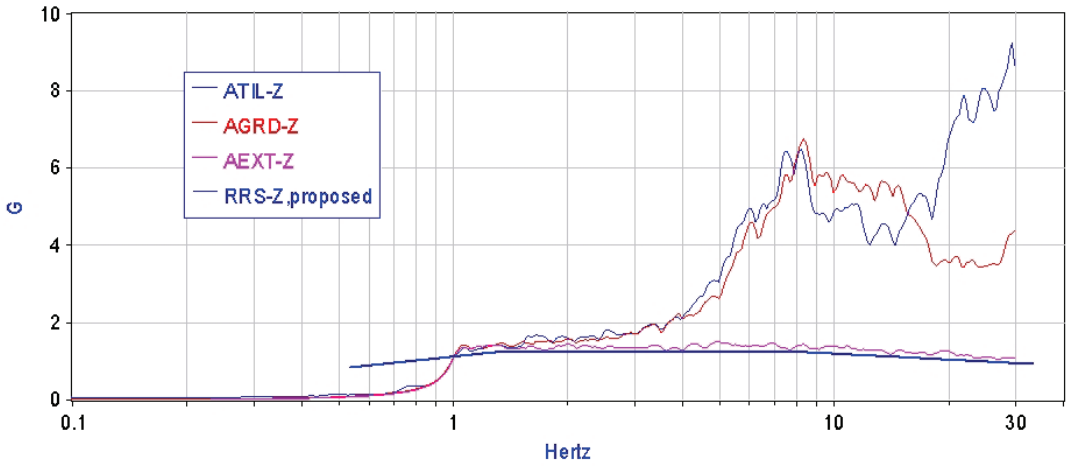

c) Vertical direction (Z)

Figure 4-14 Response Spectra for Each Direction for Test No.3 (Current AC-156, S_S =1.75g)

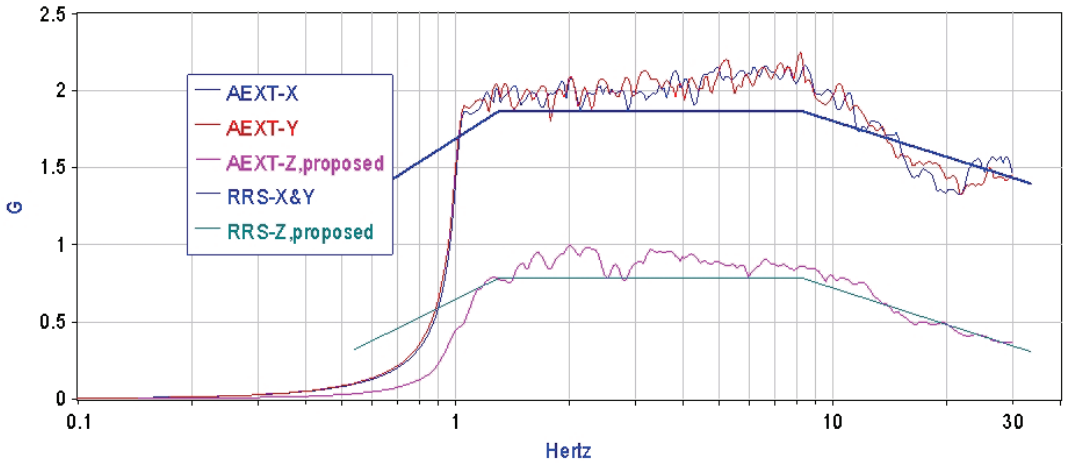

a) Response spectra obtained on the shaking table extension (AEXT)

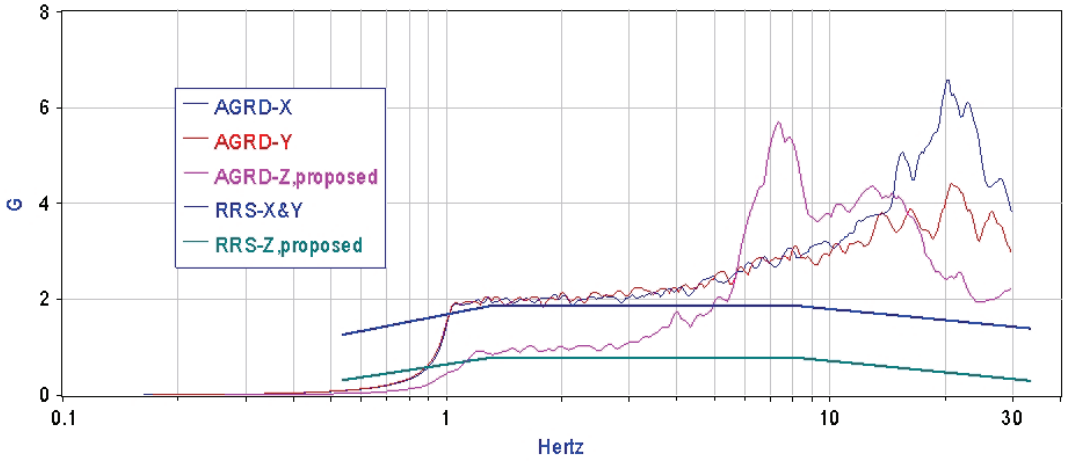

b) Response spectra obtained on the roof of the frame (AGRD)

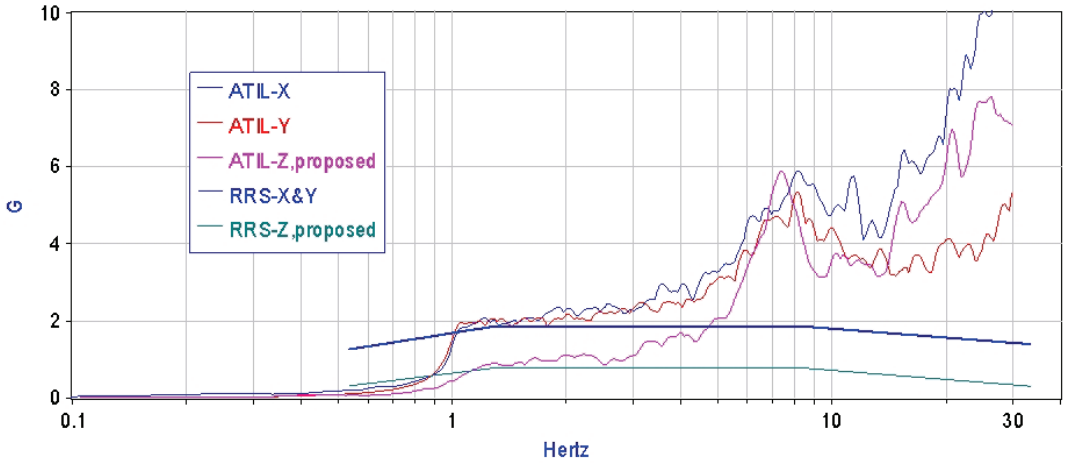

c) Response spectra obtained on the suspension system (ATIL)

Figure 4-15 Response Spectra Obtained from the Accelerometers Located on the Three Locations for Test No.4 (Proposed AC-156, S_S =1.75g)

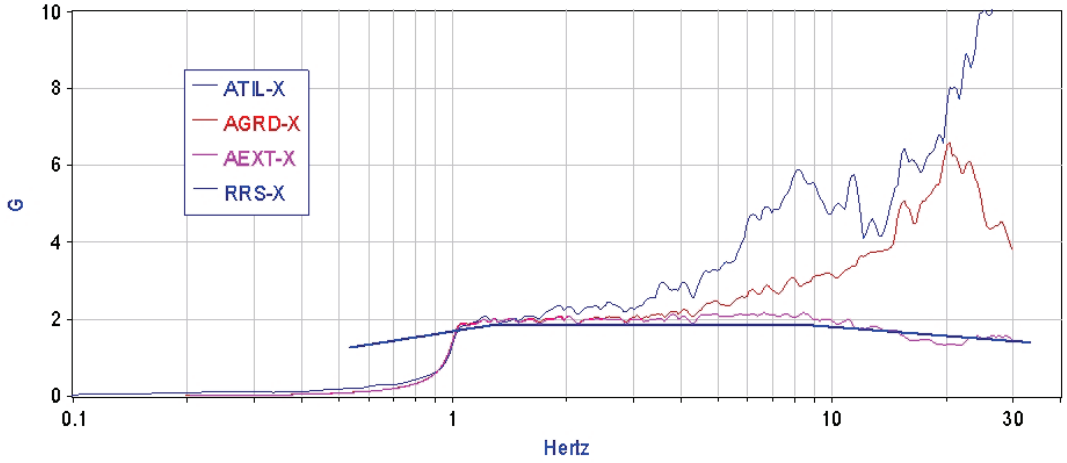

a) Horizontal direction (X)

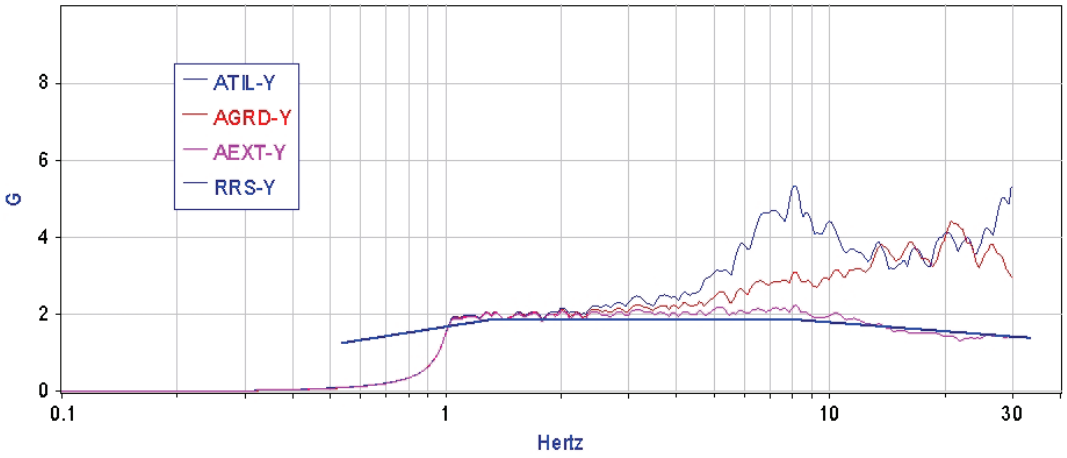

b) Horizontal direction (Y)

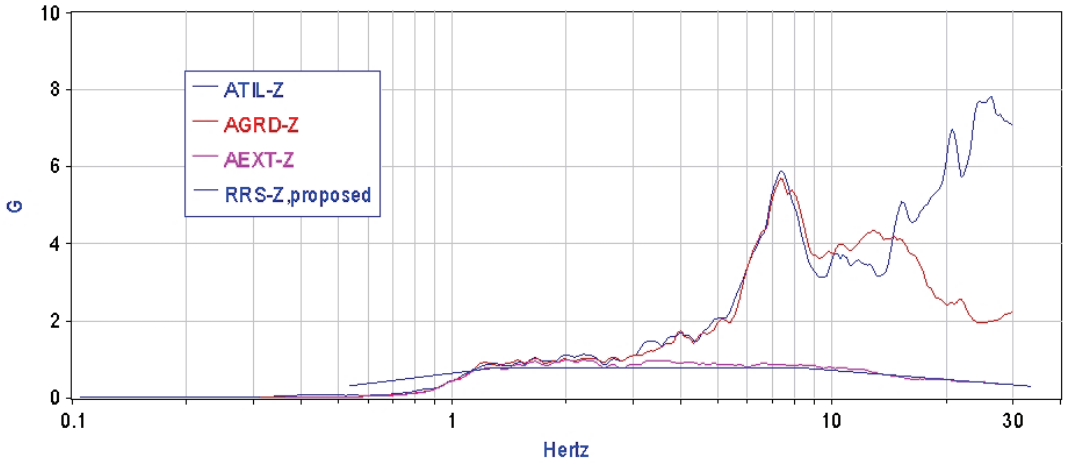

c) Vertical direction (Z)

Figure 4-16 Response Spectra for Each Direction for Test No.4

(proposed AC-156, S_S =1.75g)

4.2 Alternative Floor (Roof) Motion

The earthquake excitations for shake table motions, generated by using the recommendations of ICC-AC-156 (ICC, 2007), were originally developed for seismic evaluation testing of nonstructural components connected at a single point. However, suspended ceiling systems have multiple attachment points to a main structure (e.g., floor or roof). An innovative testing protocol, which accommodates this issue, was suggested by Retamales et al. (2009) and is intended to be used for seismic performance tests of suspended ceiling systems.

This section presents a summary of the proposed test protocol. Retamales et al. (2009) designed a testing protocol for assessing the seismic performance of nonstructural components, systems and equipment, sensitive to the accelerations and/or interstory drifts expected within multistory buildings during seismic shaking. The protocol was mainly developed for use with the University at Buffalo Nonstructural Component Simulator (UB-NCS) and other equipment with similar capabilities. However, the methodology to develop the protocol can be used for experimental seismic qualification of acceleration-sensitive nonstructural components such as suspended ceiling systems, performed using conventional shaking tables. The summary herein focuses on the methodology of the development of the protocol for acceleration sensitive nonstructural components.

A distribution of seismic demands along building height is determined based on the analysis of the continuous beam model (Retamales et al., 2009) shown in Figure 4-17. A multistory building is modeled as a continuous elastic cantilever beam combining flexural and shear beams connected by an infinite number of axially rigid links distributed along its height. This method allows for modeling generic buildings, whose seismic resistant systems consist of either shear walls or moment resistant frames, or a combination of both.

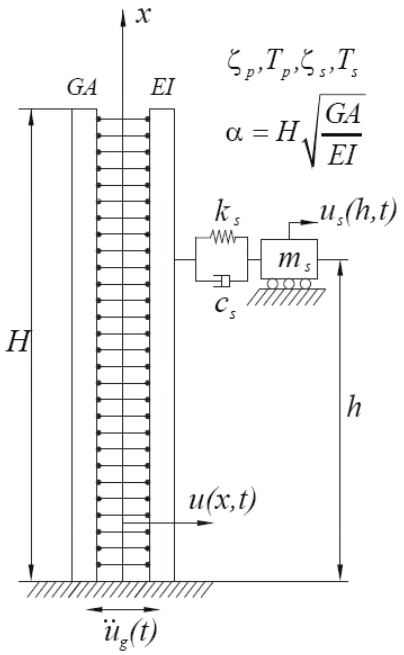

Figure 4-17 Building Model (reproduced from Retamales et al., 2009)

The parameter α, accounting for the relative stiffness of the shear and flexural beams, is calculated as Equation (4-6):

$$\alpha = H\sqrt{\frac{GA}{EI}} \tag{4-6}$$

where *GA* and *EI* denote the shear and flexural rigidities at the base of the structure, respectively, and *H* is the total height of the system. The damping ratios for primary (all modes) and secondary systems, ζ_p and ζ_s, respectively, were assumed equal to 5% of critical. Floor Response Spectra (FRS), which depend on parameters T_p, T_s, h/H and α, are estimated for acceleration demands of floors using this model where T_p and T_s are fundamental periods of primary structure systems and secondary nonstructural systems, respectively. In order to make a generalized testing protocol independent of structural system (associated to the parameter α) and the period of the structure (given by T_p), a statistical acceleration demand analysis was performed. The results of the analysis were used to obtain the FRS as function of normalized building height. A function $FRS_{Factor}\ (h/H)$, calculated as the ratio between the peak value (typically observed at T_s = 0.3 sec) of the resulting FRS's along the height of the building and the peak spectral amplitude

of the Probabilistic Local Seismic Hazard (Gupta and Trifunac, 1998) Ground Response Spectrum, is used to amplify the platform motions and to obtain the target FRS for the protocol. The best fit curve for the FRS_{Factor} (h/H) is given by Equation (4-7):

$$FRS_{Factor}\left(\frac{h}{H}\right) = 1 + 10\left(\frac{h}{H}\right) - 19.4\left(\frac{h}{H}\right)^2 + 12.4\left(\frac{h}{H}\right)^3 \qquad (4-7)$$

This function is analogous to the empirical triangular amplification function of floor accelerations (1+2 h/H) included in IBC code (ICC, 2006) and ICC-AC-156 (2007) standard as indicated in Chapter 1.1.2.1.

A proposed qualification testing protocol is developed considering the spectral acceleration amplification factor FRS_{Factor} (h/H), given by Equation (4-6) and is calibrated to induce the same number of "Rainflow" cycles (ASTM, 1997) on acceleration sensitive nonstructural components as would be experienced during real seismic floor motions (Retamales et al., 2008).

Further evaluations and comparisons of the proposed protocol and the AC-156 should be made before the alternative protocol could be adopted.

4.3 Roof Motion Amplification During Testing

The test frame amplifies the roof motion when it is excited by a base (ground) motion due to system flexibility (see Figure 4-18). If T_V and T_L are response spectra of the command drive (ground) motion of a shake table, then $RM_{V,L}$ and $RC_{V,L}$ are response spectra at the middle and corner of the roof, respectively, which are calculated using the acceleration history achieved at those locations. The RM_V, the vertical response spectrum in the middle of a roof grid, represents response of single degree of freedom components that can be mounted on or hanged from the roof grid.

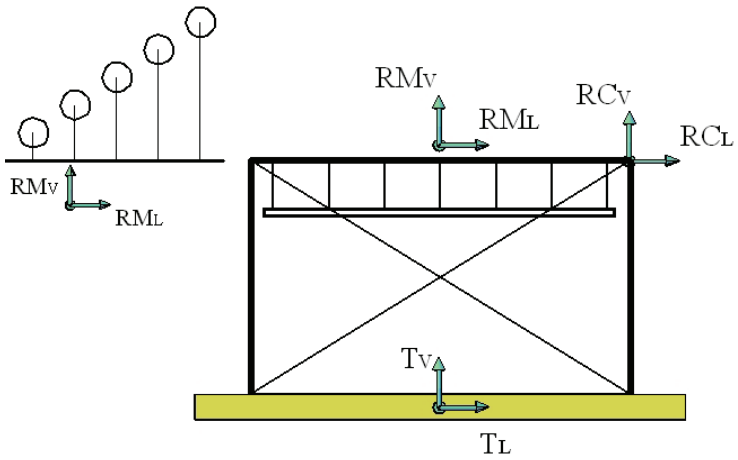

where

RM : Roof Middle *R.S.*,

RC : Roof Corner *R.S.*,

T : Table *R.S.*,

R.S.: Response Spectrum,

$_V$: Vertical, and

$_L$: Longitudinal.

Figure 4-18 Schematic Model for Describing the Roof Motion Amplification

The response spectra of the roof motion in the horizontal and vertical directions are expressed as Equation (4-8) and Equation (4-9). RM_L is assumed to be equal to RC_L since the roof of the testing frame is "usually" rigid horizontally.

$$RM_L = \alpha_{RC_L T_L} \cdot T_L \qquad (4-8)$$

$$RM_V = \alpha_{RM_V RC_V} \cdot RC_V = \alpha_{RM_V RC_V} \cdot \alpha_{RC_V T_V} \cdot T_V \qquad (4-9)$$

where $\alpha_{RC_L T_L}$ and $\alpha_{RC_V T_V}$ denote the amplification factors between the roof corner and the table in the horizontal and vertical directions, respectively. $\alpha_{RM_V RC_V}$ is the amplification factor between the roof middle and corner in the vertical direction. If the columns are rigid vertically, $\alpha_{RC_V T_V} = 1.0$, and if the columns are flexible, $\alpha_{RC_V T_V} \geq 1.0$. Also, if a floor (roof) is rigid vertically, $\alpha_{RM_V RC_V} = 1.0$, and if a floor (roof) is flexible, $\alpha_{RM_V RC_V} \geq 1.0$.

Vertical Acceleration Response Spectrum (RM_V) was developed using the achieved acceleration history at the center point of a roof grid from SAP2000 with random motions (AC-156 spectrum compatible for Ss = 3.0g). The developed analytical model of 20ft. by 20ft. (see Chapter 3) was used for this analysis.

The results indicate that vertical input table motions, generating the RRS, have major influence on roof motions and suspended systems to the roof (see Figure 4-19, Figure 4-20, and Figure 4-21). The proposed vertical RRS recommended in this work (see Chapter 4.1.2) generates roof response smaller by 5.7g, approximately 38% of that obtained by the current motion per AC-156.

Figure 4-19 shows the variation of RM_V by different input motions (current input motions and proposed input motions). The difference between the average peak spectral accelerations obtained for various weights of roofs is 5.7g. Figure 4-20 and Figure 4-21 present the variation of RM_V due to several additional suspended ceiling masses marked as a weight of roof (1 psf (CE1), 2 psf (CE2), 3 psf (CE3), 4 psf (CE4), and 5 psf (CE5)), using the current and the proposed AC-156 simulated input motions. The variation of the peak spectral acceleration using the additional ceiling mass is approximately ± 5% for the both input motions.

The Vertical Acceleration Response Spectra (RM_V) have strong amplification if the frame has vertical fundamental frequency, f_z, in the range of 10.0-11.0 Hz (i.e. the basic frame, having the fundamental frequency of 10.2 Hz). The peak amplitude of the RM_V for the basic frame is 20% greater than the average peak spectral accelerations of the various weight additions, CE1-CE5, as Figure 4-19 indicates. The authors consider that this amplification is a result of the unmatched "desired" input motions. The future tests however, will be designed to compensate for this error through control with the signal compensation procedure developed by the authors (see also Maddaloni et al., 2009b).

To observe further the variation of RM_V using different input motions, another dynamic analysis to the test frame from SAP2000 was performed using FEMA 461/ATC58 shake table testing protocol (FEMA, 2007), having the vertical peak spectral acceleration (S_a) ≈ 1.0g (this peak S_a is equivalent to the one of the proposed AC-156 vertical RRS for S_s ≈ 2.25g), as shown in Figure 4-22. The results are shown in Figure 4-23, indicating the peak amplitude of the RM_V of a basic frame is 12% less than the average peak S_a of the CE1-CE5 (in contrast to the result above for the proposed AC-156 RRS of 20% greater RM_V of a basic frame). These results present that variation of RM_V is mainly influenced by floor "input motions."

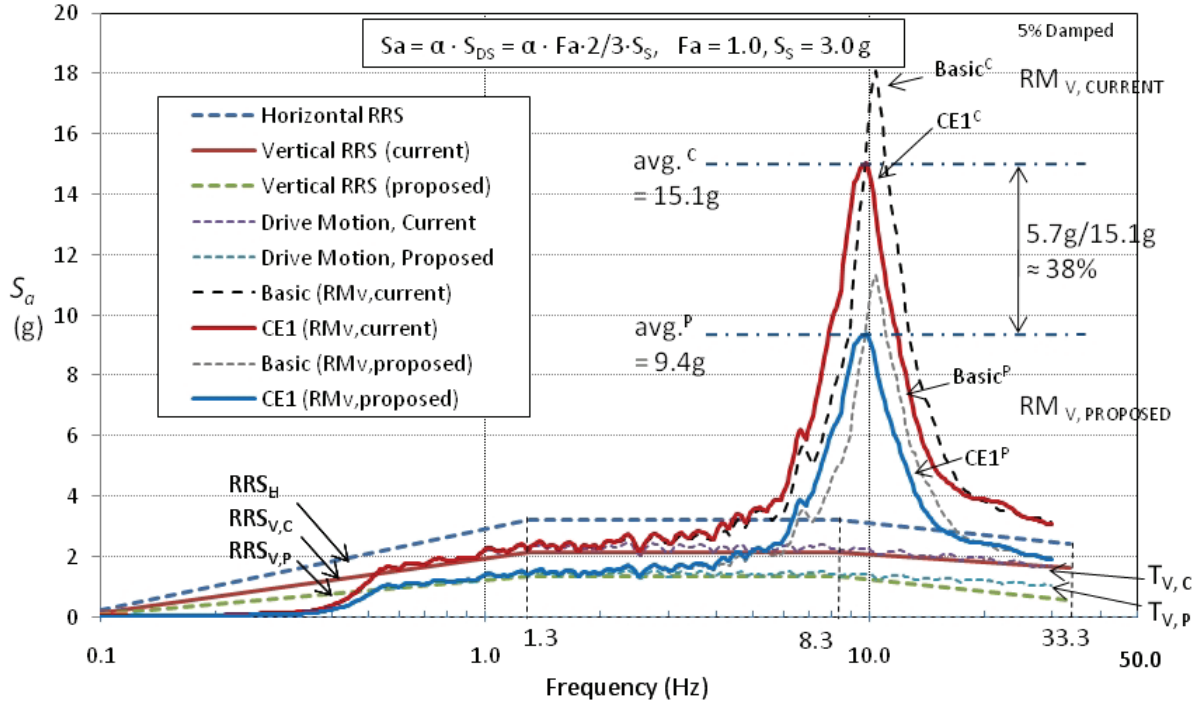

*c**: denotes the current input motion or the corresponding response,
*p**: denotes the proposed input motion or the corresponding response.

Figure 4-19 Variation of Vertical Acceleration Response Spectra (R.S.) using Different Input Motions: Effects of the Proposed Input Motion

Figure 4-19 presents the variation of vertical acceleration response spectra (RM_V) due to two different vertical input motions ($T_{v,c}$ driven to simulate the current AC-156 $RRS_{v,c}$ and $T_{v,p}$ driven to simulate the proposed $RRS_{v,p}$). The responses obtained using the two input motions are presented: *ave.*^{c} and *ave.*^{p} represent the average of the responses obtained from five cases having different weight of ceilings, *Basic*^{c} and *Basic*^{p} represent the response obtained from the basic frame (explained in Chapter 2.4).

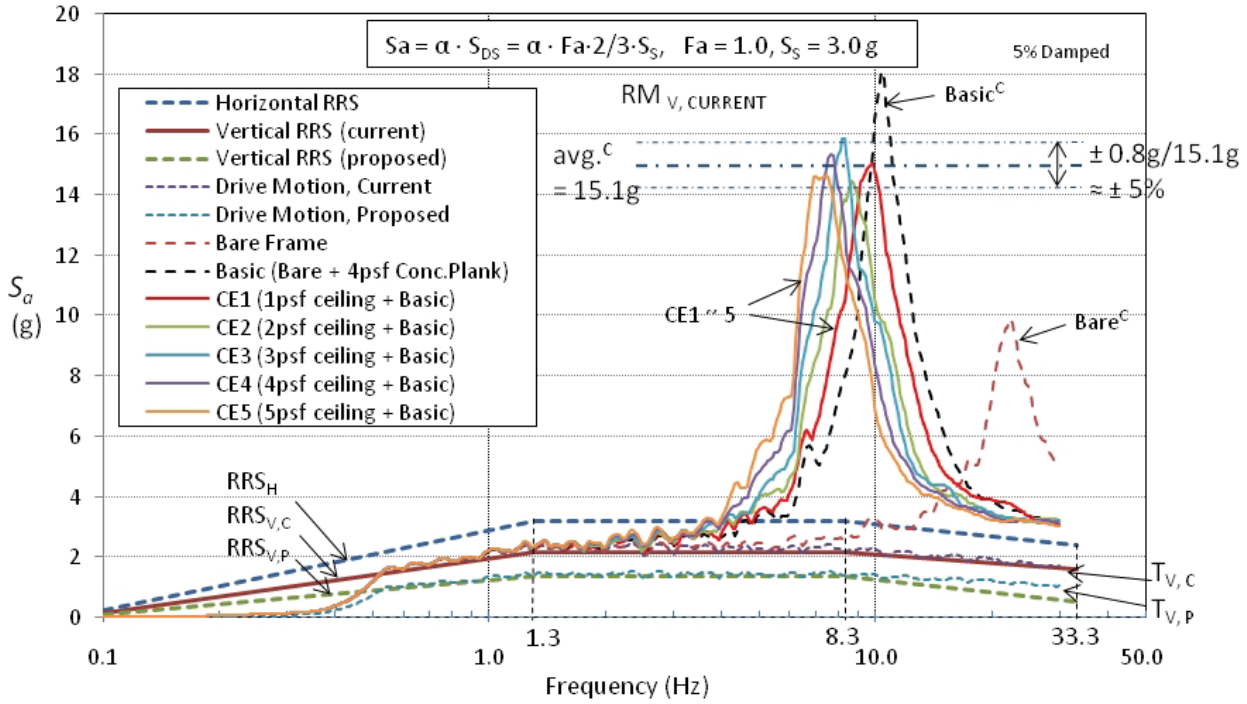

*c**: denotes the current input motion or the corresponding response,
*p**: denotes the proposed input motion or the corresponding response.

Figure 4-20 Variation of Vertical R.S. Acceleration Using the Current AC-156 Simulated Input Motion: Effects of Various Ceilings

Figure 4-20 presents the variation of vertical acceleration response spectra (RM_V) due to various weight of a roof. $T_{v,c}$ driven to simulate the current AC 156 $RRS_{v,c}$ was used as the input motion. The responses for five different ceiling weights - 1 psf (CE1), 2 psf (CE2), 3 psf (CE3), 4 psf (CE4), and 5 psf (CE5) - and their average, $ave.^c$ are presented in addition to the responses of the bare frame $bare^c$ and the basic frame $Basic^c$ (explained in Chapter 2.4).

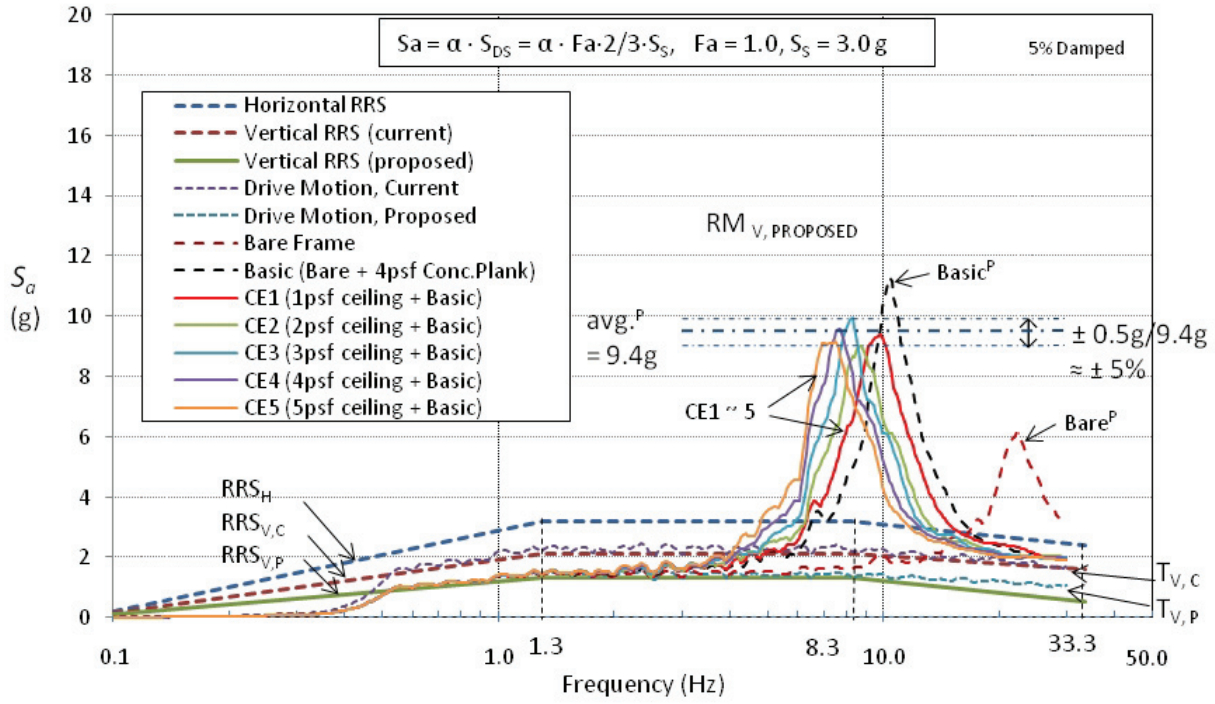

*c**: denotes the current input motion or the corresponding response,
*p**: denotes the proposed input motion or the corresponding response.

Figure 4-21 Variation of Vertical R.S. Acceleration Using the Proposed AC-156 Simulated Input Motion: Effects of Various Ceilings

Figure 4-21 presents the variation of vertical acceleration response spectra (RM_V) due to various weights of a roof. The "drive signal" $T_{v,p}$ to simulate the proposed $RRS_{v,p}$ was used as the input motion. The responses from the five different ceiling weights - 1 psf (CE1), 2 psf (CE2), 3 psf (CE3), 4 psf (CE4), and 5 psf (CE5) and their average $ave.^p$ are presented in addition to the responses of the bare frame $Bare^p$ and the basic frame $Basic^p$ (explained in Chapter 2.4).

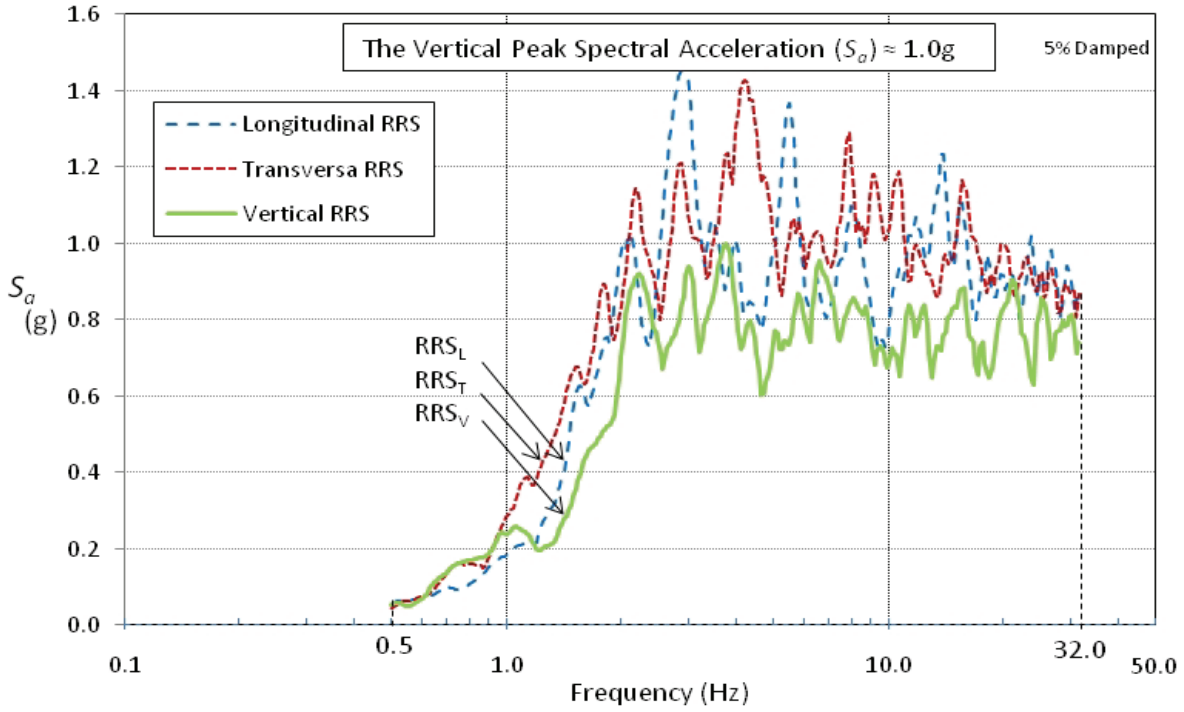

Figure 4-22 Acceleration Response Spectra (R.S.) for Recommended Input Motions in Three Directions: FEMA461/ATC58

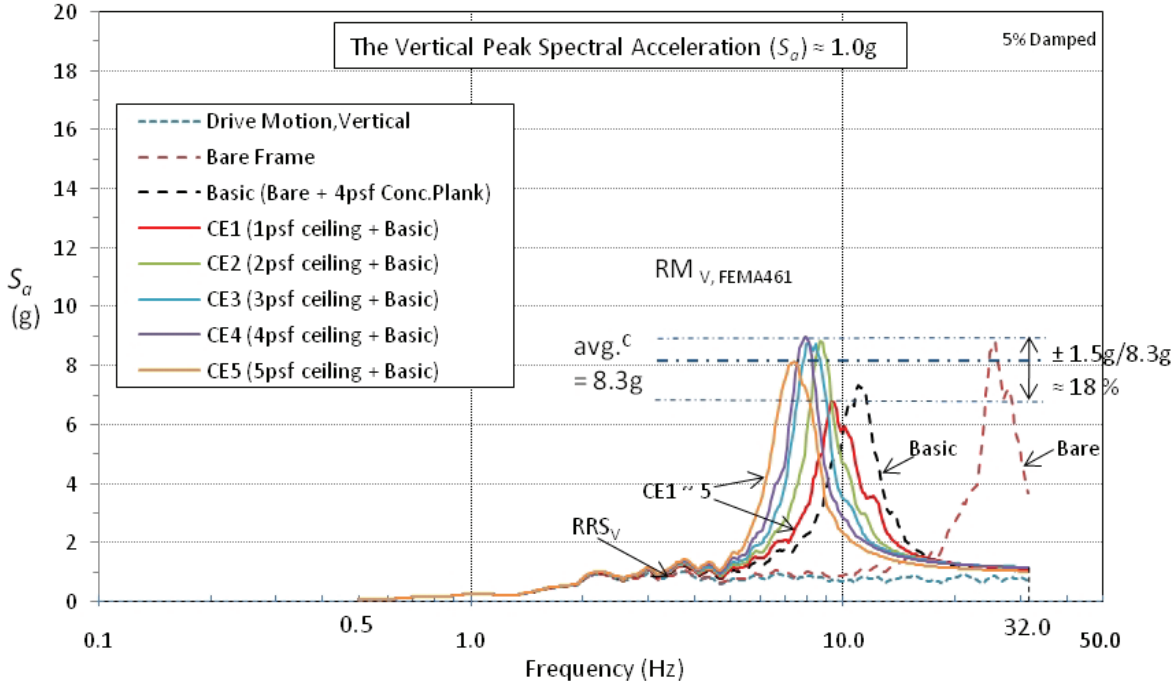

Figure 4-23 Variation of Vertical R.S. using FEMA461/ATC58 Recommended Input Motions: Effects of Input Motions

4.4 Design of Test Roof Motion

The test frame is designed to be used with shake table motions programmed to deliver desired "floor motions" at the roof level. The "shake table command drive" in three directions is modified by a compensation procedure developed by the authors in order to generate and adjust the response of the roof, based on dynamic properties of the frame (Maddaloni et al., 2009b).

A shake table "command drive" can be designed to deliver alternatively damped motions as desired by the testing criteria. There is no need to add damping to the test frame. The "command drive," compensated for the frame characteristics, is designed to reject higher modes effects of the frame structure (see Chapter 5).

CHAPTER 5
COMPENSATION PROCEDURE FOR SHAKE TABLE SIMULATION

As shown in the previous chapter, the response spectrum delivered at the roof level of the frame is distorted by the dynamics of the frame. Moreover, some of the distortions are a result of the imperfect behavior of the shake tables themselves. This chapter describes a "Compensation Procedure" to produce the Required Response Spectrum (RRS) corresponding to input acceleration histories at any desired location of a test frame unaffected by the dynamics of the shake table and the test frame. The chapter consists of two main parts: the first part (Section 5.1 through 5.4) presents the mathematical formulation of the compensation procedure, and the second part (Section 5.5) presents an experimental verification for the compensation procedure. The first part of this chapter is largely based on the team developments originally presented by Maddaloni et al. (2009b). The developments are repeated here for the sake of completeness.

5.1 Introduction

Shake table systems are essential tools in experimental earthquake engineering. They provide effective ways to subject structural components, substructures, or entire structural systems to dynamic excitations similar to those induced by real earthquakes, as well as to test nonstructural elements. In general, components of shake tables can be grouped into three sub-systems: mechanical, hydraulic, and electronic categories. Typically, platform and actuators are included in the mechanical category; pumps, accumulators and servo-valves are included in the hydraulic category; controller and feedback sensors are included in the electronic category (Ozcelik et al., 2008).

The table (or platform) supports the specimen during the test. It is constructed to provide high stiffness with minimum weight and typically consists of a rectangular or square platform able to reproduce up to six degrees of freedom (6-DOF) motions by servo-hydraulic actuators.

The actuators apply the force necessary to create the desired table movement during seismic testing. Linear Differential Transducers (LDT), or the equivalent, are usually mounted in each

actuator to provide an electrical feedback signal and to indicate the actuator piston rod position. The actuators are equipped with servo-valves that control the direction and the amount of fluid flow to the actuators. The servo-valve ports the fluid provided by the hydraulic power system, into the appropriate side of the actuator chambers. This causes the piston to move the actuator arm in the desired direction.

The control system monitors and generates program command and feedback signals for control of the test system. Generally, the control is the key element of the whole system and one of the most difficult technical challenges for mechanical engineers (Clark, 1992). The controller provides the servo-valve command in order to obtain a specific position of the actuator and finally the motion of the platform to reproduce earthquake accelerograms.

However, reproduction of a dynamic signal is known to remain imperfect (Rinawi and Clough, 1991). The degree of distortion in signal reproduction depends on several factors such as physical system parameters (e.g., compressibility of oil column in the actuator chamber, oil leakage through the actuator seals, servo-valve time delay, etc.) and dynamic characteristics of the test structure (Conte and Trombetti, 2000). To obtain the best fidelity reproduction, a compensation closed-loop control is used. In general, a closed-loop control consists of comparing a command signal (generated by a program source) with a feedback signal. The difference between the feedback measurement and the set-point of the command signal is the error "e." The polarity and magnitude of the error signal, causes the servo-valve spool to open in a direction leading to the desired actuator response. As the command input changes, the command-feedback comparison continuously generates error signals that drive the servo-valve to create the desired actuator response. When the command and the feedback are equal, the error is reduced to zero, the servo-valve spool closes, and the actuator does not move (MTS, 2004).

Starting from these concepts, this chapter focuses on shake table simulations using an "open loop" compensation model based on transfer functions (i.e. the frequency domain ratios of the output structural response to the input base motion). In particular, in the first part, the analytical model and the compensation system of a uni-axial shake table is presented considering an equivalent single degree of freedom (SDOF). In this case the compensation transfer function is determined

between the desired (or target) motion and the achieved table motion. Subsequently, a similar input-output mathematical model for a multi degree of freedom (MDOF) system is presented. Finally, the concept of open-loop compensation was implemented and verified in an experiment at the Structural Engineering and Earthquake Simulation Laboratory (SEESL) - http://seesl.buffalo.edu/ - at University at Buffalo using a six degrees-of-freedom (6-DOF) shake table. As a first step, a well known global procedure was reformulated for the compensation of the table motion's distortions due to the servo-hydraulic system. Subsequently the same concept was extended to the table-structure system (i.e. with the testing frame in this study) to adjust the shake table input in order to achieve a desired response spectrum at any floor of the specimen. Such implementation is presented further in this paper.

5.2 Ground Motion for Required Response Spectrum

The primary use of a shake table is to simulate the motion of the ground or location in a structure. However, the reproduction of a dynamic signal, due to several factors (e.g., time delay in the servovalve response, compressibility of the actuator fluid, oil leakage through the actuator seals, influence of the test specimen) can be imperfect. High fidelity response can be obtained using compensated motion as described below.

For this purpose, the development from basic principles of a transfer function able to capture the principal dynamic characteristics of uni-axial shake table system is presented. The objective of this analytical model is to mathematically represent the input-output relationship between desired (or commanded) and achieved absolutes table motions. While the analytical model is presented for a uni-axial system, the same procedure can be easily reformulated to multi-axial systems. The model presented herein can be interpreted by visualizing the shake table system as a single degree of freedom (SDOF) system (as shown in Figure 5-1).

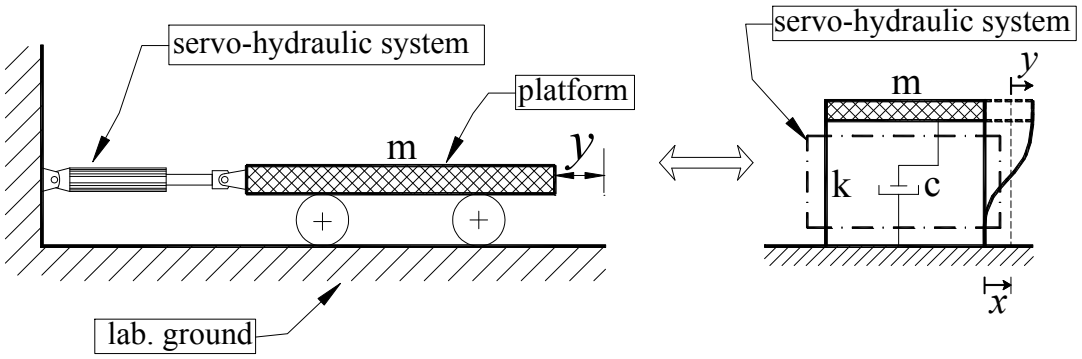

Figure 5-1 Shake Table System: Equivalent SDOF (after Maddaloni et al., 2009b)

Equation (5-1) below shows the dynamic equilibrium for the motion of a SDOF system [6], excited by horizontal base acceleration $\ddot{x}$, expressed in the complex frequency domain by using Fourier Transform*.

$$-m\omega^2 y(\omega) + i\omega c\, y(\omega) + k\, y(\omega) = -m\ddot{x}(\omega) \tag{5-1}$$

In the above equation, *m* and *y(ω)* represent the mass and the corresponding complex displacement of the platform; *k* and *c* are the equivalent stiffness and viscous damping of the servo-hydraulic system, and *i* is $\sqrt{-1}$.

Solving Equation (5-1) for the displacement $y(\omega)$, it results in:

$$y(\omega) = \frac{-m\ddot{x}(\omega)}{-m\omega^2 + i\omega c + k} \tag{5-2}$$

As shown in Figure 5-1, for the equivalent SDOF system and in the time domain, the absolute acceleration $\ddot{a}(t)$ with respect to an inertial reference system (laboratory ground) is simply obtained as the sum of two accelerations:

$$\ddot{a}(t) = \ddot{y}(t) + \ddot{x}(t) \tag{5-3}$$

* Fourier Transform is an operation that converts one function of a real variable into a complex function. The new function, often called the frequency domain *representation* of the original function, describes which frequencies are included in the original function; ω=2π*f* is the circular frequency (in rad/sec) and *f* is the cyclic frequency (in hertz); $i = \sqrt{-1}$

Converting Equation (5-3) in the frequency domain, it results in:

$$\ddot{a}(\omega) = -\omega^2 y(\omega) + \ddot{x}(\omega) \tag{5-4}$$

Substituting Equation (5-2) into Equation (5-4) and performing some adjustments, the absolute acceleration $\ddot{a}(\omega)$ can be represented as follows:

$$\ddot{a}(\omega) = \left(\frac{i\omega c + k}{-m\omega^2 + i\omega c + k} \right) \ddot{x}(\omega) \tag{5-5}$$

The transfer function (*H*) is defined as the ratio of the structural response to an input base motion in the frequency domain:

$$\frac{\ddot{a}(\omega)}{\ddot{x}(\omega)} = H = \left(\frac{i\omega c + k}{-m\omega^2 + i\omega c + k} \right) \tag{5-6}$$

In a shaking table test, the input base motion $\ddot{x}$ and the structural response $\ddot{a}$ are, respectively, called *"drive"* table motion (x_{drive}) and *"achieved"* table motion ($\bar{y}$):

$$\frac{achieved\ table\ motion}{drive\ table\ motion} = \frac{\bar{y}(\omega)}{x_{drive}(\omega)} = H_t = \left(\frac{i\omega c + k}{-m\omega^2 + i\omega c + k} \right) \tag{5-7}$$

The transfer function of the table "H_t" represents the degree of distortion in signal reproduction of a desired motion due to the mechanical and servo-hydraulic system. As indicated above, it depends on many factors such as the oil compressibility, oil leakage, servovalve time delay, etc. (Ozcelik, 2008 and Conte, 2000) that can be obtained from identifications. To obtain the best fidelity reproduction of desired motion, a compensated drive motion can be applied.

In Figure 5-2 this concept is shown as a schematic diagram. The *"desired,"* or often called the *"target,* motion $\bar{x}$, represents the start point of the compensation while the *"achieved"* motion

$\bar{y}$ is the end point. The command signal applied to the table for the shaking is indicated as *"drive"* motion, x_{drive}.

According to this scheme and Equation (5-7), a different command signal (x_{drive}) should be applied in order to achieve a response motion equal to the *desired* motion $\bar{x}$ as shown in the following equation:

$$if \quad x_{drive} = H_t^{-1}\bar{x} \quad then \quad \bar{y} = H_t x_{drive} = H_t H_t^{-1}\bar{x} \cong \bar{x} \tag{5-8}$$

where H_t and H_t^{-1} are the transfer and the inverse transfer functions of the table, respectively. Therefore, the *"drive"* motion is calculated multiplying the *"desired"* or *"target"* motion $\bar{x}$ by the inverse transfer function of the table. In practical applications using the compensated *drive* as input command for the shake table, the achieved motion ($\bar{y}$) could not perfectly match the desired motion ($\bar{x}$) due to non linearity of the servo-hydraulic system (Conte and Trombetti, 2000). As shown in Figure 5-2, an error $\varepsilon = \bar{y} - \bar{x}$ is calculated and an iteration procedure (dashed line) is used to improve the compensation. The block diagram shows that the iterations are stopped when the error is smaller than a predefined tolerance ($\varepsilon < \tau$): it means that this is an acceptable reproduction of the desired motion. In the same figure, in case of compensation without iterations, $\bar{x}^*$ is same as $\bar{x}$; in case of iterations $\bar{x}^*$ includes the desired motion $\bar{x}$ and the error ε ($\bar{x}^* = \bar{x} + \varepsilon$).

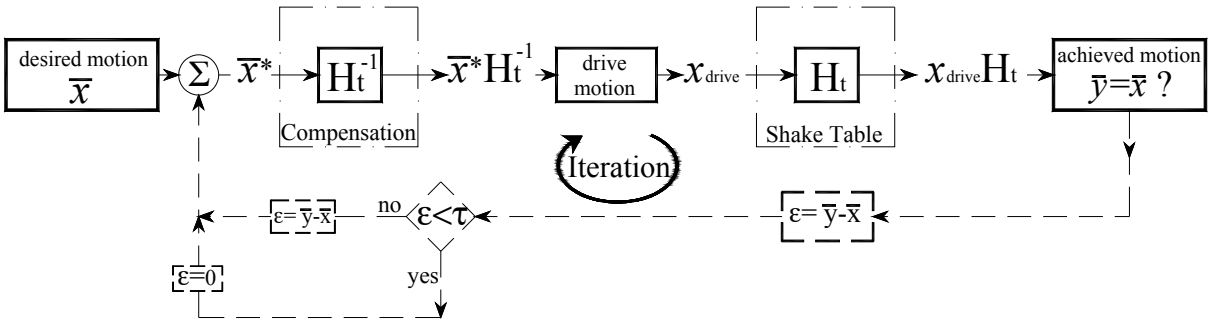

Figure 5-2 Schematic Diagram of Shake Table Simulation of Ground Motion (Dashed Line Indicates Possible Iterations) (reproduced from Maddaloni et al., 2009b)

5.3 Required Response Spectrum in Structures

In the experimental evaluation of architectural or nonstructural component, it is often necessary to produce a *desired* or *target* spectrum at a specified position in the structure. The previous compensation approach can be generalized for a multi-degree of freedom (MDOF) system (Bracci, 1992), which represents the specimen in a shake table test. For simplicity, the MDOF is represented in this development as a simple plane frame as shown in Figure 5-3.

Equation (5-9) below shows the general equation of motion for a MDOF system excited by a base acceleration $\ddot{x}(t)$:

$$[M]\{\ddot{y}(t)\}+[C]\{\dot{y}(t)\}+[K]\{y(t)\}=-[M]\{r\}\ddot{x}(t) \tag{5-9}$$

where $[M]$, $[K]$, $[C]$ are, respectively, the mass, stiffness, viscous damping matrix of the structure-specimen and $\{y(t)\}$, $\{\dot{y}(t)\}$, $\{\ddot{y}(t)\}$, $\{r\}$ are the relative displacement, velocity, acceleration, and influence vector time history (Chopra, 2007).

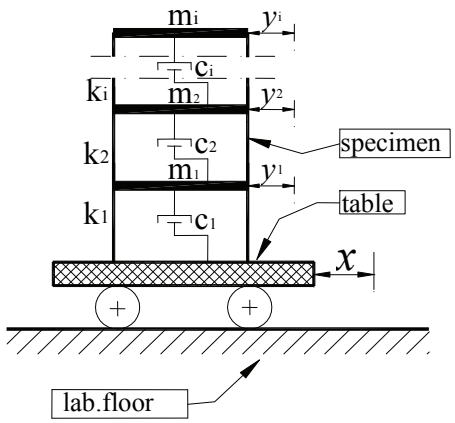

Figure 5-3 Simulation of Structure Motion: Equivalent MDOF (reproduced from Maddaloni et al., 2009b)

The relative displacement vector $\{y(t)\}$ can be expressed in modal form by the product of the modal shape matrix $[\Phi]$ and the modal displacement vector $\{p(t)\}$ of the structure as follows:

$$\{y(t)\} = [\Phi]\{p(t)\} \tag{5-10}$$

Therefore Equation (5-9) can be expressed in modal form as follows:

$$[M][\Phi]\{\ddot{p}(t)\} + [C][\Phi]\{\dot{p}(t)\} + [K][\Phi]\{p(t)\} = -[M]\{r\}\ddot{x}(t) \tag{5-11}$$

Pre-multiplying Equation (5-11) by the transpose of the k-th mode shape ($\{\phi_k\}^T$) and using the modal shape orthogonality properties it is possible to obtain uncoupled equation of motion for the k-th mode of vibration as:

$$M_k^* \cdot \ddot{p}_k(t) + C_k^* \cdot \dot{p}_k(t) + K_k^* \cdot p_k(t) = -\{\phi_k\}^T [M]\{r\}\ddot{x}(t) \tag{5-12}$$

where $M_k^* = \{\phi_k\}^T [M]\{\phi_k\}$ is the k-th modal mass, $C_k^* = \{\phi_k\}^T [C]\{\phi_k\}$ is the k-th modal viscous damping factor and $K_k^* = \{\phi_k\}^T [K]\{\phi_k\}$ is the k-th modal stiffness.

Assuming that $K_k^* / M_k^* = \overline{\omega}_k^2$ ($\overline{\omega}_k$ is the k-th circular frequency) and $C_k^* / M_k^* = 2\xi_k \overline{\omega}_k$ (ξ_k is the k-th damping ratio), Equation (5-12) can be represented as follows:

$$\ddot{p}_k(t) + 2\xi_k \overline{\omega}_k \dot{p}_k(t) + \overline{\omega}_k^2 p_k(t) = -\{\phi_k\}^T [M] / M_k^* \ddot{x}(t) \tag{5-13}$$

Transforming Equation (5-13) to the frequency domain (by Fourier Transform) it results:

$$-\omega^2 p_k(\omega) + 2i\omega\xi_k \overline{\omega}_k p_k(\omega) + \overline{\omega}_k^2 p_k(\omega) = -\{\phi_k\}^T [M] / M_k^* \ddot{x}(\omega) \tag{5-14}$$

Solving in respect to $p_k(\omega)$:

$$p_k(\omega) = \frac{1}{\omega^2 - 2i\omega\xi_k \overline{\omega}_k - \overline{\omega}_k^2} \cdot \frac{\{\phi_k\}^T [M]}{\{\phi_k\}^T [M] \{\phi_k\}} \ddot{x}(\omega) \tag{5-15}$$

The absolute acceleration $\ddot{a}(t)$ can be represented (in time domain) as follows:

$$\{\ddot{a}(t)\} = \{\ddot{y}(t)\} + \ddot{x}(t)\{I\} \tag{5-16}$$

where I is a vector of units. Substituting Equation (5-10) into Equation (5-16) and transforming to the frequency domain, the absolute acceleration becomes:

$$\{\ddot{a}(\omega)\} = -\omega^2 [\Phi] \{p(\omega)\} + \ddot{x}(t)\{I\} \tag{5-17}$$

Pre-multiplying Equation (5-17) by $\{\phi_k\}^T [M]$ and using the modal orthogonality properties it results:

$$\{\phi_k\}^T [M] \{\ddot{a}(\omega)\} = -\omega^2 \underbrace{\{\phi_k\}^T [M] [\Phi] \{p(\omega)\}}_{M_k^* \cdot p_k(\omega)} + \{\phi_k\}^T [M] \{r\} \ddot{x}(\omega) \tag{5-18}$$

$$\zeta_k(\omega) = \{\phi_k\}^T [M] \{\ddot{a}(\omega)\} = -\omega^2 M_k^* \cdot p_k(\omega) + \{\phi_k\}^T [M] \{r\} \ddot{x}(\omega) \tag{5-19}$$

where $\zeta_k(\omega)$ is the k-th modal absolute acceleration. Therefore Equation (5-14) can be rewritten as:

$$\zeta_k(\omega)+p_k(\omega)M_k^*\left(2i\omega\xi_k\bar{\omega}_k+\bar{\omega}_k^2\right)=0 \tag{5-20}$$

or:

$$\zeta_k(\omega)=-p_k(\omega)M_k^*\left(2i\omega\xi_k\bar{\omega}_k+\bar{\omega}_k^2\right) \tag{5-21}$$

Substituting Equation (5-15) into Equation (5-21), the $\zeta_k(\omega)$ absolute k-th modal acceleration can be represented as follows:

$$\zeta_k(\omega)=\frac{\left(2i\omega\xi_k\bar{\omega}_k+\bar{\omega}_k^2\right)}{\left(-\omega^2+2i\omega\xi_k\bar{\omega}_k+\bar{\omega}_k^2\right)}\{\phi_k\}^T[M]\{r\}\ddot{x}(\omega) \tag{5-22}$$

Considering the modal superposition, the absolute j-th acceleration can be expressed as follows:

$$\ddot{a}_j(\omega)=\sum_{k=1}^{n}\left[\phi_k^j\zeta_k(\omega)\right]=\sum_{k=1}^{n}\left[\phi_k^j\frac{\left(2i\omega\xi_k\bar{\omega}_k+\bar{\omega}_k^2\right)}{\left(-\omega^2+2i\omega\xi_k\bar{\omega}_k+\bar{\omega}_k^2\right)}\{\phi_k\}^T[M]\{r\}\right]\cdot\ddot{x}(\omega) \tag{5-23}$$

where k is the k-th vibration mode; j is the j-th degree of freedom; $\bar{\omega}_k$ and ξ_k are the circular frequency and damping ratio relative to the k-th vibration modes.

The acceleration transfer function, defined by the ratio of the output structural response to an input base motion in the frequency domain is therefore:

$$H_{s,j}(\omega)=\frac{\ddot{a}_j(\omega)}{\ddot{x}(\omega)}=\sum_{k=1}^{n}\left[\phi_k^j\frac{\left(2i\omega\xi_k\bar{\omega}_k+\bar{\omega}_k^2\right)}{\left(-\omega^2+2i\omega\xi_k\bar{\omega}_k+\bar{\omega}_k^2\right)}\{\phi_k\}^T[M]\right] \tag{5-24}$$

In a shaking table test, the input base motion to the structure $\ddot{x}$ and the structural response $\ddot{a}_j$ represent the *achieved* shake table motion discussed in the previous section and the *achieved* structure response at the j-th floor. The transfer function "$H_{s,j}$" indicates the degree of amplification of the base motion due to the dynamic characteristics of the system for the j-th floor of the structure.

In a similar fashion described in the previous section, the concept of signal compensation can be applied in order to match the response to a target motion in the structure. As shown in Figure 5-4, the *desired* motion at j-th floor ($\overline{x}$) represents the start point of the compensation model while the *achieved* motion ($\overline{y}$) is the end point. The base motion (x_{base}) represents the effective movement of the shake table and it can be much different than the *desired* motion.

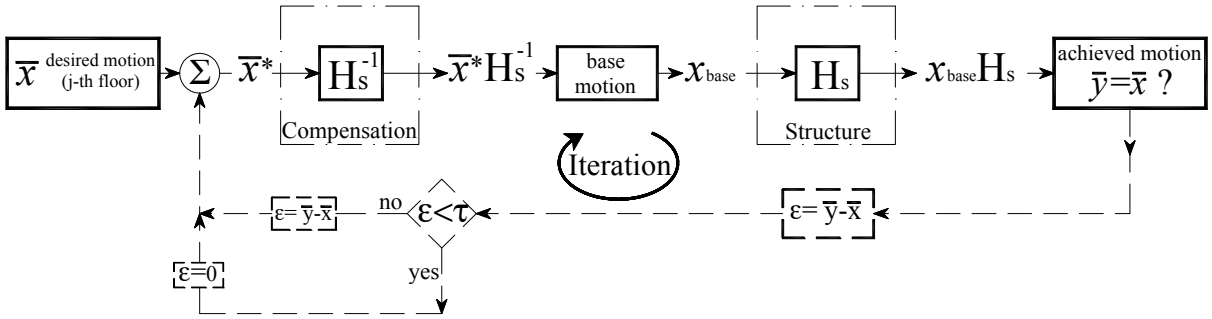

Figure 5-4 Schematic Diagram of Compensated Simulation Motion for the Structure (Dashed Line Indicates Possible Iterations) (reproduced from Maddaloni et al., 2009b)

According to this scheme and Equation (5-24), if the target is determining the desired base motion (x_{base}) in order to achieve a response motion equal to the desired $\overline{x}$, at the j-th floor of the structure ($\overline{y_j}$), the following is required:

$$if \quad x_{base} = H^{-1}{}_{s,j}\,\overline{x} \qquad then \qquad \overline{y_j} = H_{s,j} \cdot x_{base} = H_{s,j} \cdot H^{-1}{}_{s,j} \cdot \overline{x} \cong \overline{x} \tag{5-25}$$

where $H_{s,j}$ and $H^{-1}_{s,j}$ are the transfer and inverse transfer function referred to the j-th floor of the structure. In practical applications the inverse transfer function is determined from identification

with associated uncertainties due to nonlinearities in the structure and imperfections in the identification process. Therefore, the *achieved* motion ($\bar{y}$) cannot match perfectly the *desired* motion ($\bar{x}$). In this case, as shown in Figure 5-4, an error $\varepsilon = \bar{y} - \bar{x}$ is calculated and an iteration (dashed line) can be performed until the error is smaller than an acceptable tolerance ($\varepsilon < \tau$). In the same figure, in case of compensation without iterations, $\bar{x}^*$ is identical to $\bar{x}$; in case of iterations $\bar{x}^*$ includes the *desired* motion $\bar{x}$ and the error ε ($\bar{x}^* = \bar{x} + \varepsilon$).

5.4 Required Floor Response Spectrum

The concepts mentioned above were implemented in a physical experiment performed in the Structural Engineering and Earthquake Simulation Laboratory (SEESL) at the University at Buffalo using a 7m x 7m - 6DOFs shake table (Figure 5-5-left) and a test frame structure used for qualification tests of suspended ceilings (Badillo et al., 2007). The target is to simulate the *required* (or *target)* floor response spectrum (FL-RRS) at the top corner of a test frame.

In this case the compensation concerns both the table and the steel frame above it (i.e. the structure). The longitudinal (East-West), the lateral (North-South) and the vertical displacements at the south-west corner are assumed as degrees of freedom for compensation (Figure 5-5-right). The position of the accelerometers, used to record the accelerations in the tri-axial directions during the shaking, is indicated in Figure 5-5 (red circle).

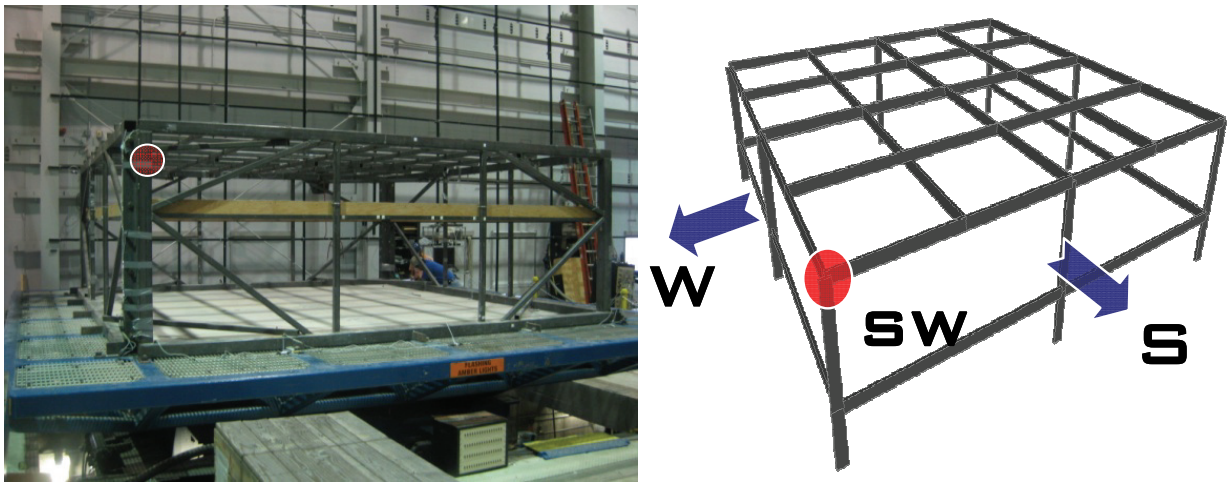

Figure 5-5 Experimental Implementation: Compensation for a Test Frame (reproduced from Maddaloni et al., 2009b)

The concept of open loop compensation for the system table-structure is extended from previous formulations and shown as schematic diagram in Figure 5-6.

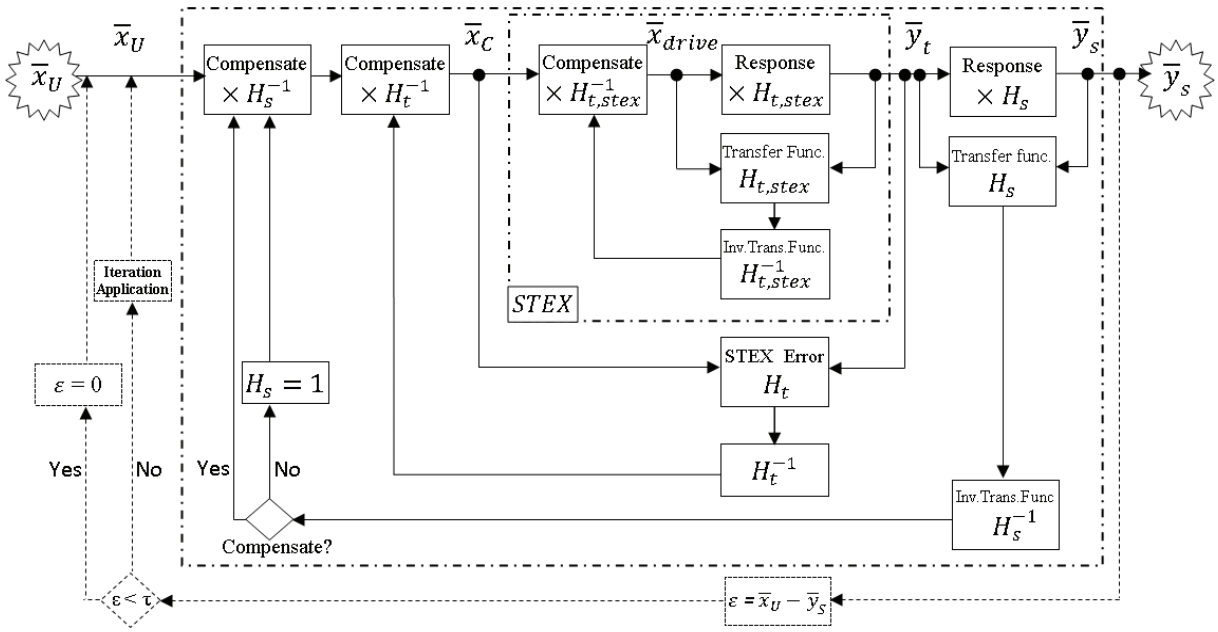

Figure 5-6 Schematic Diagram of Shake Table Simulation of a Required Floor Response Spectrum (Dashed Line Indicates Possible Iterations)

The *desired* floor (or roof) motion (*target* $\overline{x}_U$) is the start point of the compensation model, while the *achieved* structure motion ($\overline{y}_s$) is at the end point.

For the purpose of this study a *desired* motion is derived from the AC-156 testing standard for qualification testing of nonstructural components using shake tables (ICC, 2007). According to this standard, the shape and the levels of required response spectra (RRS, S_s = 1.75g) have been assigned*. The required response spectrum for the vertical direction (RRS, vert) is obtained as two-thirds of the horizontal component amplitude (RRS, hor).

Three time dependent functions have been generated subsequently using an accelerogram simulation program, STEX (MTS, 2004), able to match a specified required response spectrum for each direction of shaking. These acceleration functions represent the uncompensated desired table motions (*target* $\overline{x}_U$). The table transfer function ($H_{t,stex}$) between the *achieved* and *desired* table motions is derived also by STEX (shown in the internal box in the Figure 5-6). The *drive* table motion (x_{drive}) is calculated by multiplying the *desired* table motion by the inverse table transfer function ($H_{t,stex}^{-1}$). Additionally, the table transfer function (H_t) was derived to generate the compensated desired table motion, representing the imperfection of the internal compensation system produced by STEX.

The plot of the RRS and the response spectra of the *desired* (*target* $\overline{x}_U$) and the *achieved* (ACHTBL $\overline{y}_t$) table motions as recorded on the platform are shown in Figure 5-7.

* Shape and magnitude of a RRS is based on the normalized response spectra shown in Figure 1 of section 6.5 of the AC-156 and on the parameters specified in section 4.3 of the same code.

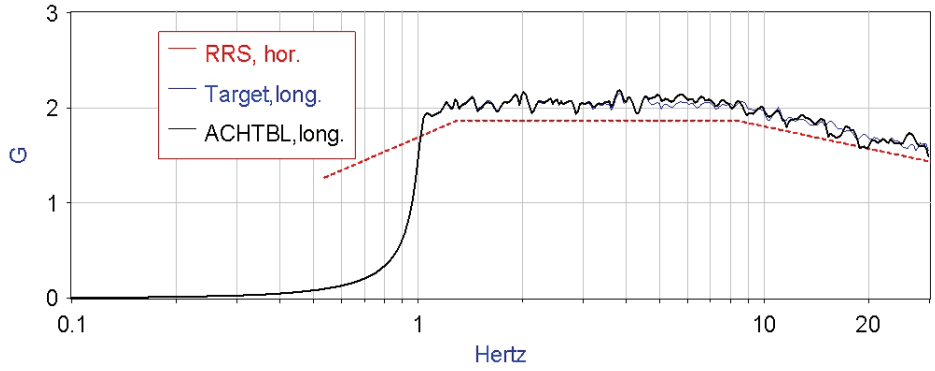

(a) longitudinal (x)

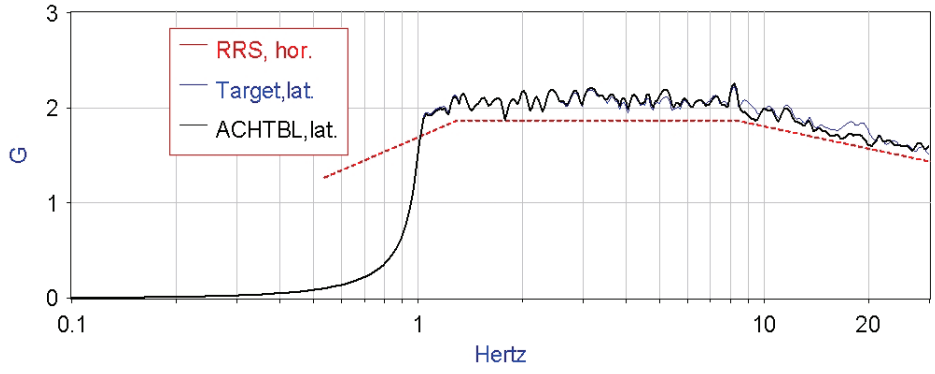

(b) lateral (y)

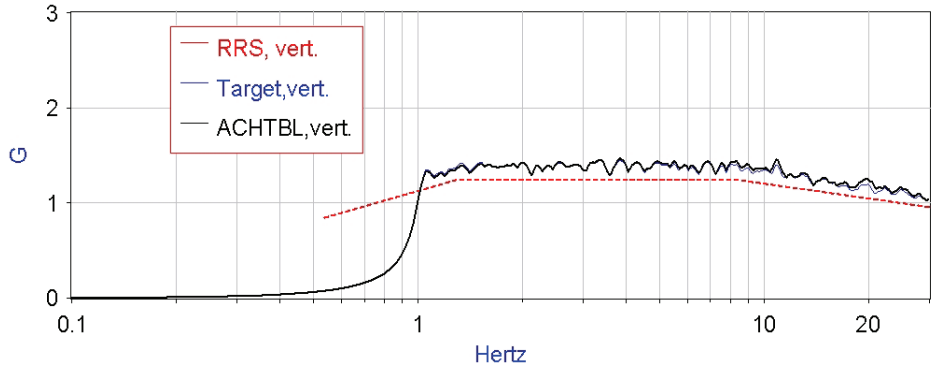

(c) vertical (z)

Figure 5-7 Required Response Spectrum (RRS, S_s = 1.75g) vs. Response Spectra of the Desired (Target) and Achieved (ACHTBL) Table Motions

The difference between the spectrum of the *achieved* and *target* table motions is an indicator of the degree of distortion in signal reproduction. As a measure of distortion of the response spectra of the achieved table signals from the required standard spectrum, a δ factor has been calculated (Table 5-1). The definition of δ (Iervolino et al., 2008) is given in Equation (5-26)

below, where RRS(f_i) is the ordinate of required response spectrum corresponding to the frequency f_i; RS(f_i) is the ordinate of the response spectrum obtained from the achieved table motion at the same frequency; and N is the number of values within the band of frequency assumed as base of analyses (1-30 Hz).

A response spectrum with a low δ value means an *achieved* motion which is well approximating the *desired*.

$$\delta = \sqrt{\frac{1}{N}\sum_{i=1}^{N}\left[\frac{RRS(f_i) - RS(f_i)}{RRS(f_i)}\right]^2} \tag{5-26}$$

The degree of distortion in signal reproduction assumes, for the achieved motions, similar values for the three directions of shaking with an average of 11%, as shown in Table 1. In the same table, the values of δ for the spectra obtained from the *target* table motions are also indicated with an average of 10.6% for sake of comparison.

Table 5-1 δ Values of Desired and Achieved Table Motions

δ	*Target* table motion	*Achieved* table motion
(1)	(2)	(3)
Longitudinal	0.096	0.102
Lateral	0.110	0.109
Vertical	0.112	0.119
Average	0.106	0.110

To fit better the RRS, a compensated *target* motion should be applied. According to Equation (5-8), a new *target* table motion can be obtained by the compensation procedure described above. As schematically illustrated in Figure 5-8, the transfer function for the shake table (H_t) is obtained from the ratio of the *achieved* motion recorded on the table (achieved table motion) to the *drive* table motion in the frequency domain:

$$H_t = \frac{achieved\ table\ motion}{drive\ table\ motion} \tag{5-27}$$

The degree of distortion in signal reproduction can be represented in graphical way as shown in Figure 5-9. The transfer functions in the three directions of shaking are shown with their magnitude and phase. The figures show a good correlation between *target* and *achieved* signals after compensation in terms of magnitude (values approximately equal to 1) for a wide range of frequency. A lower correlation appears in terms of phase.

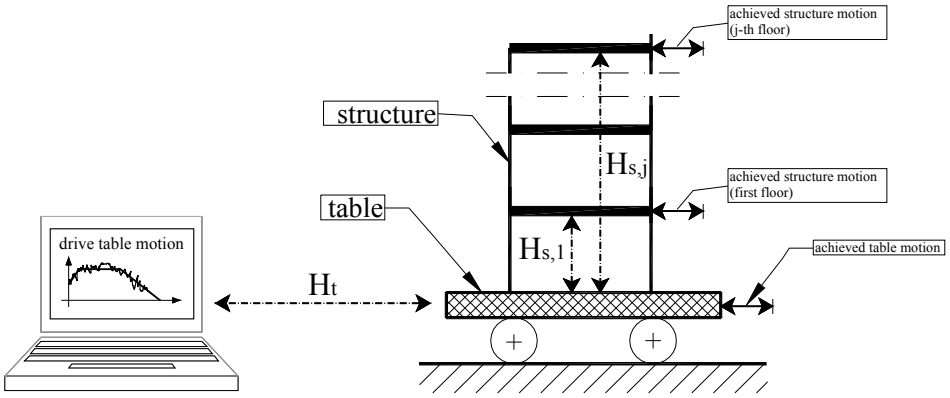

Figure 5-8 Schematic Representation of the Transfer Function Concept for the Table (H_t) and Structure (Hs) (reproduced From Maddaloni et al., 2009b)

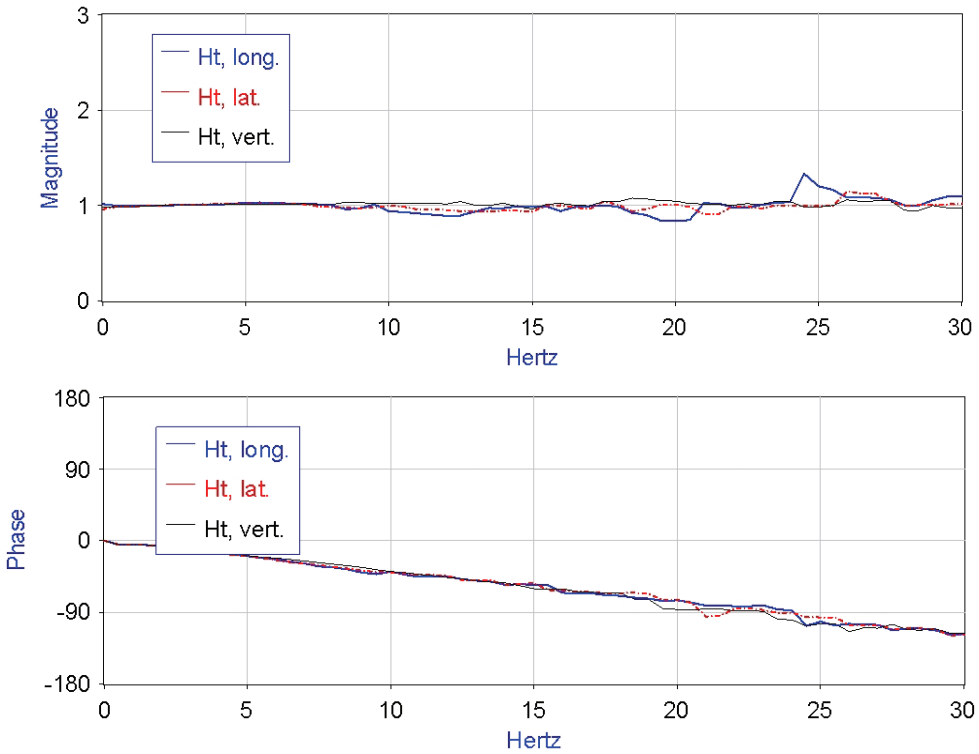

Figure 5-9 Magnitude (top) and Phase (bottom) of Table Transfer Functions

The same concept of transfer function can be applied for the structure (H_s). The structure transfer function defined by the ratio of the *achieved* motion recorded at a specific point in the tested specimen (structure) to the *achieved* table motion providing the input to the structure (Figure 5-8):

$$H_s = \frac{achieved\ structure\ motion}{achieved\ table\ motion} \tag{5-28}$$

The transfer functions at the roof level of the steel structure used during the test performed at SEESL at University at Buffalo (Figure 5-5) are shown in Figure 5-10. The degree of dynamic amplification of the signal in respect to the one recorded at the base, on the table, is shown for all directions of motion. No considerable amplification is present for frequencies below ~5 Hz,. At a frequency of ~20 Hz, the magnitude of H_s reaches largest values (more than 4) for longitudinal and lateral directions of shaking (Figure 5-10 left). The same degree of distortion appears in terms of phase.

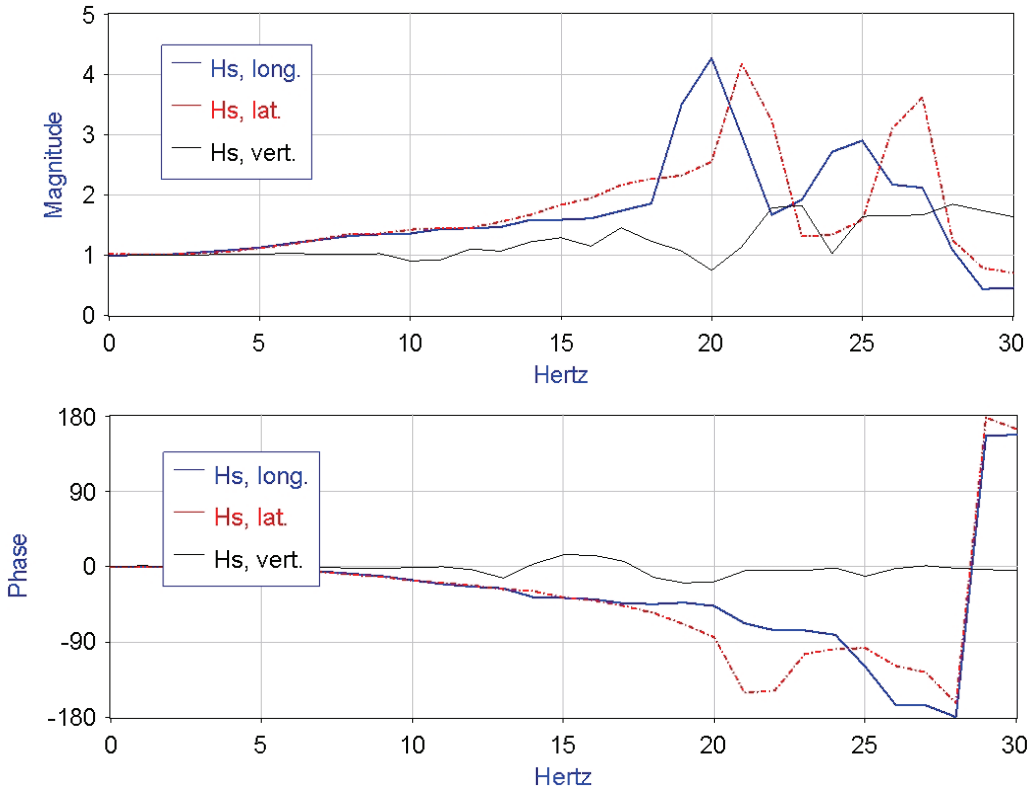

Figure 5-10 Magnitude and Phase of the Structure Transfer Functions

If the target is the best fit of the response spectrum of desired signal at the roof level, a shake table compensated simulation of the required floor response spectrum can be implemented. According to the block diagram of Figure 5-6, it means to modify the *desired* motion by multiplying it with the inverse transfer function of table (H_t^{-1}) and structure (H_s^{-1}), to produce the *drive* command. Due to nonlinearity of the system table-structure, the achieved motion ($\bar{y}$) could not perfectly match the desired ($\bar{x}$). In this case, as shown in Figure 5-6, an error $\varepsilon = \bar{y} - \bar{x}$ was calculated and the iteration (dashed line) became necessary. The block diagram shows that when the error is smaller than the tolerance ($\varepsilon < \tau$) then the iterations are stopped, which means that an acceptable reproduction of the *desired* motion was obtained. For the iteration, a new transfer function $H_{s,\varepsilon}$ between the initial compensated *achieved* roof motion and the *desired* table motion is derived. The new compensated *drive* motion ($\bar{x}_{C,1}$) is calculated by the multiplication of the initial compensated *drive* motion ($\bar{x}_{C,0}$) by the inverse transfer function ($H_{s,\varepsilon}^{-1}$).

The response spectra of the uncompensated desired (Target) and achieved roof motion (ACHFRM-U), and the compensated desired (DESTBL-C) and achieved roof motion (ACHFRM-C) with the required response spectra (RRS) are shown in Figure 5-11. It is clear that the achieved motion at the top of the frame matches quite well the target motion obtained from the desired Required Response Spectrum.

The degrees of distortion of the uncompensated achieved roof motions and compensated achieved roof motions from the test results are calculated using Equation (5-26) in the range of 1 to 30 Hz and shown in Table 5-2. For purpose of comparison, the degree of distortion (δ_{TRS}) in signal reproduction between the RRS and target table motions (TRS) shown in Table 5-1 is repeated in Table 5-2b. The results of compensation clearly show its benefits. However, the remaining distortions are almost same as for the targeted table motions (TRS). The results indicate that in order to reduce the distortion of achieved compensated roof motions to the RRS, it is required to generate better fitted "target table motions," since compensated achieved motions match very well with "target table motions" through the compensation procedure. Moreover, the compensation is not sensitive to the scale of the motion, producing always closest

compensation to the "target table motion." Therefore, to improve the simulation the "target table motion" must be better simulated for the various spectra amplitudes.

Table 5-2a δ Values of *TRS* and Achieved Table Motions vs. *RRS* (S_s = 1.50g)

δ	δ_{TRS}	$\delta_{Uncomp.}$	$\delta_{Comp.}$
(1)	(2)	(3)	(4)
Longitudinal	0.080	0.329	0.070
Lateral	0.073	0.370	0.064
Vertical	0.071	0.092	0.075
Average	**0.075**	**0.264**	**0.070**

Table 5-2b δ Values of *TRS* and Achieved Table Motions vs. *RRS* (S_s = 1.75g)

δ	δ_{TRS}	$\delta_{Uncomp.}$	$\delta_{Comp.}$
(1)	(2)	(3)	(4)
Longitudinal	0.097	0.484	0.105
Lateral	0.110	0.507	0.121
Vertical	0.112	0.195	0.136
Average	**0.106**	**0.395**	**0.121**

Table 5-2c δ Values of *TRS* and Achieved Table Motions vs. *RRS* (S_s = 2.00g)

δ	δ_{TRS}	$\delta_{Uncomp.}$	$\delta_{Comp.}$
(1)	(2)	(3)	(4)
Longitudinal	0.246	0.656	0.247
Lateral	0.261	0.661	0.261
Vertical	0.264	0.353	0.291
Average	**0.257**	**0.557**	**0.266**

Table 5-2d δ Values of *TRS* and Achieved Table Motions vs. *RRS*

S_s (g)	δ_{TRS}	$\delta_{Uncomp.}$	$\delta_{Comp.}$
1.50	0.075	0.264	0.070
1.75	0.106	0.395	0.121
2.00	0.257	0.557	0.266

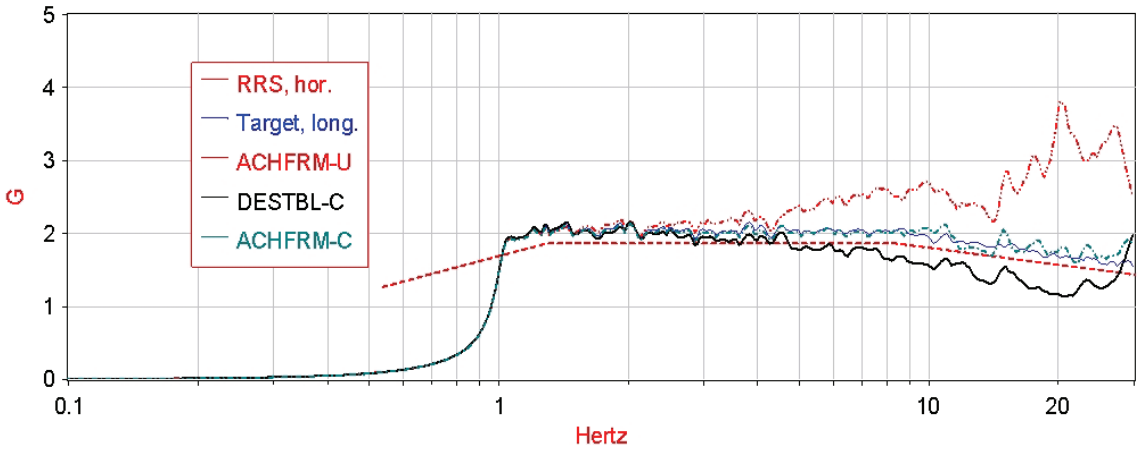

(a) longitudinal (x)

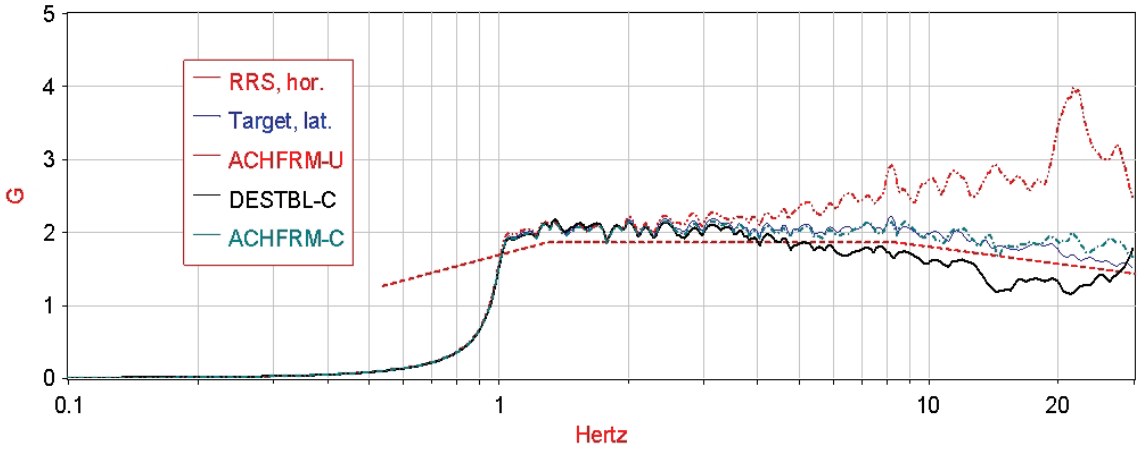

(b) lateral (y)

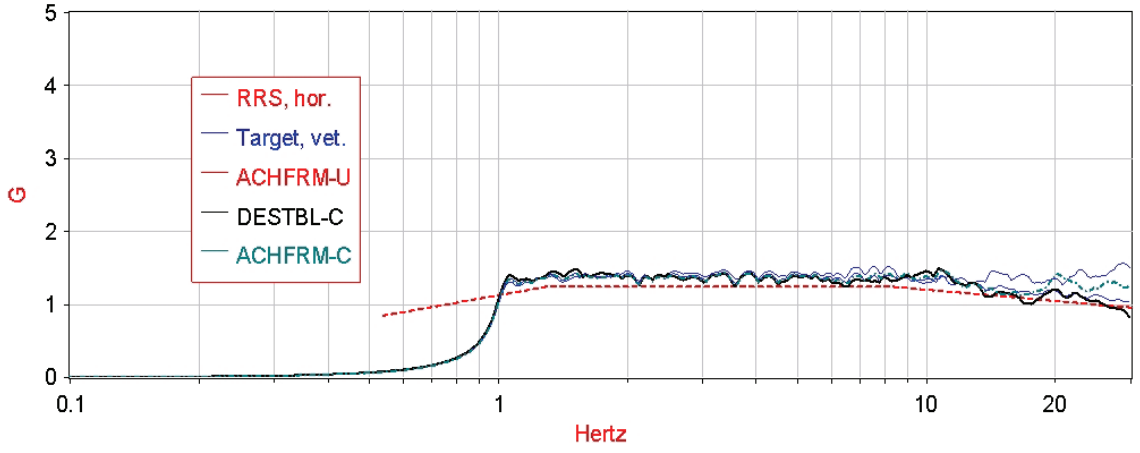

(c) vertical (z)

Figure 5-11 Test Required Response Spectrum (RRS, S_s = 1.75g) and Response Spectra of the Frame in the Longitudinal (X), Lateral (Y) and Vertical (Z) Directions

5.5 Experimental Verification

In order to verify the mathematical formulation of the "Compensation Procedure" presented in this chapter previously, experimental tests were performed using the 16 ft. by 16 ft. test frame at SEESL at University at Buffalo (Figure 5-5). The results and analysis were summarized in Chapter 5.4. In this subchapter, the results of a full series of tests and observations are presented. The properties and dynamic characteristics of the test frame were described briefly in Chapter 2 and more in detail in Badillo et al. (2006). The list of the performed test series is present in Table 5-3.

Table 5-3 Test Series of Compensation Procedure

No.	Title	Description of test excitations
1	Uncompensated White noise test	Unidirectional white noise excitation in the horizontal (x) direction
2		Unidirectional white noise excitation in the horizontal (y) direction
3		Unidirectional white noise excitation in the vertical (z) direction
4	Uncompensated AC-156 test	Triaxial uncompensated input motions per AC-156 RRS (S_S = 1.75g) in the x, y, and z directions
5	Compensated White noise test	Triaxial compensated input motions, per AC-156 RRS (S_S = 1.75g) in the x, y, and z directions, using transfer functions developed from the results of the Uncompensated White noise test
6	Compensated AC-156 test	Triaxial compensated input motions, per AC-156 RRS (S_S = 1.75g) in the x, y, and z directions, using transfer functions developed from the results of the Uncompensated AC-156 test
7	New compensated AC-156 test	Triaxial new compensated input motions, per AC-156 RRS (S_S = 1.75g) in the x, y, and z directions, developed by iteration

5.5.1 Uncompensated Input and Achieved Motions

The test frame was subjected to two sets of uncompensated excitations (target) in order to measure distortion between a target motion and an achieved motion. The first set consisted of three tests using unidirectional white noise excitations along orthogonal axis of the simulation platform in the x (East-West), y (North-South), and z (vertical) directions, respectively, as shown in Figure 5-12. The responses were recorded at the center of the shaking table extension (ATBL) and three top corners of the test frame (AFRNW, AFRNE, and AFRSW). The response spectra corresponding to the achieved motions for each direction are shown in Figure 5-13.

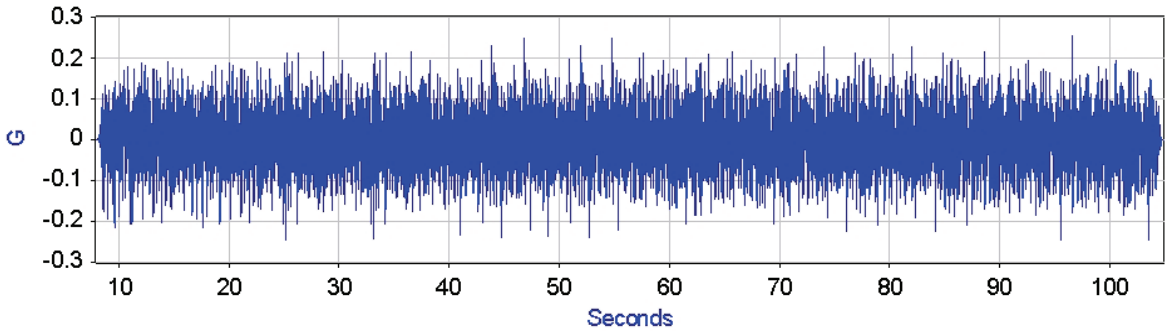

a) Horizontal acceleration history in the X direction (East – West)

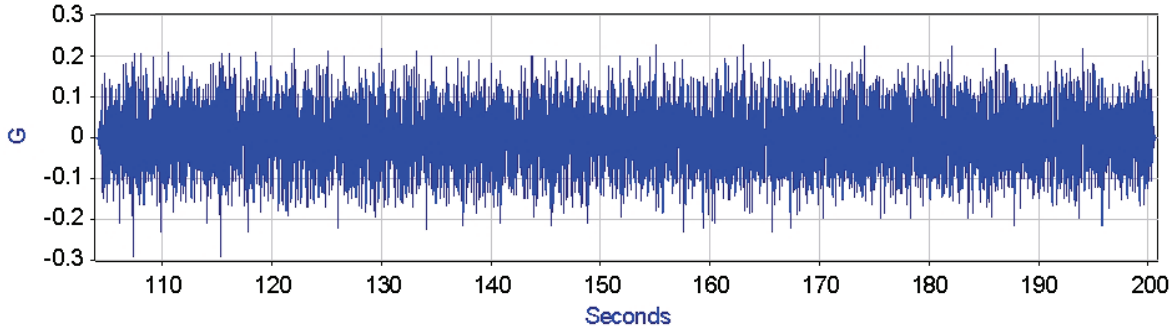

b) Horizontal acceleration history in the Y direction (North – South)

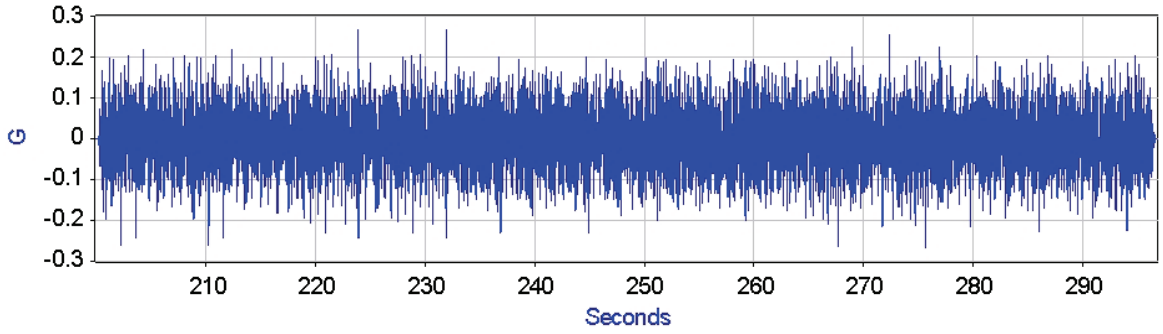

c) Vertical acceleration history in the Z direction

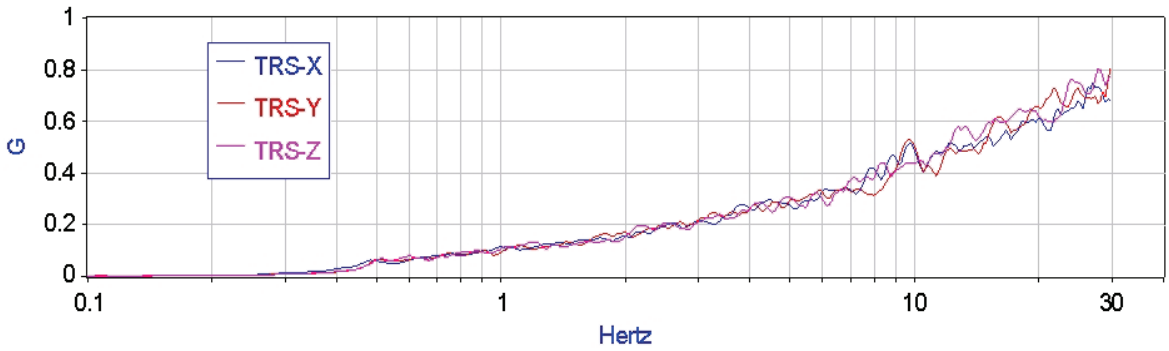

d) Test response spectrum (TRS)

Figure 5-12 White Noise Excitations and Corresponding Response Spectra for Uncompensated White Noise Tests (No. 1~3)

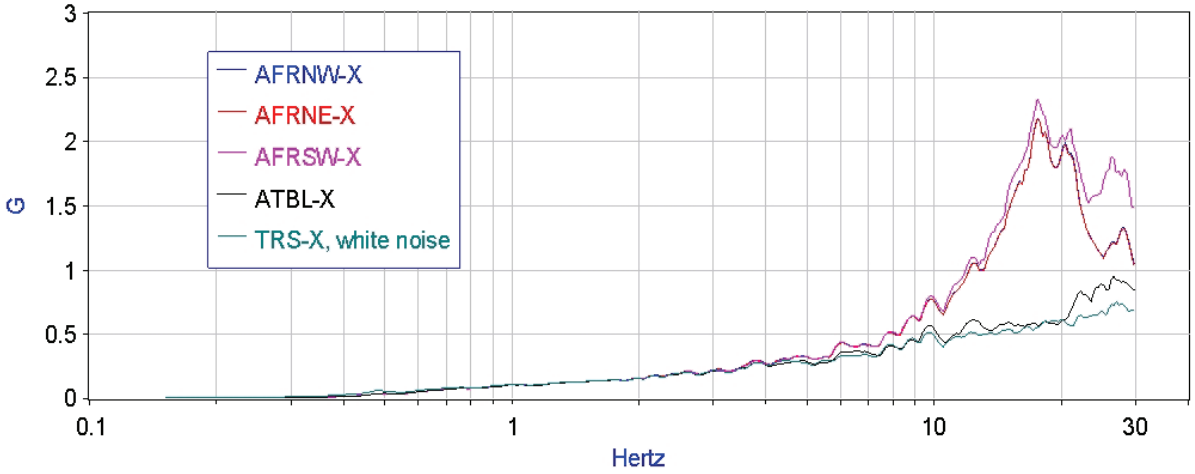

a) Horizontal direction (X)

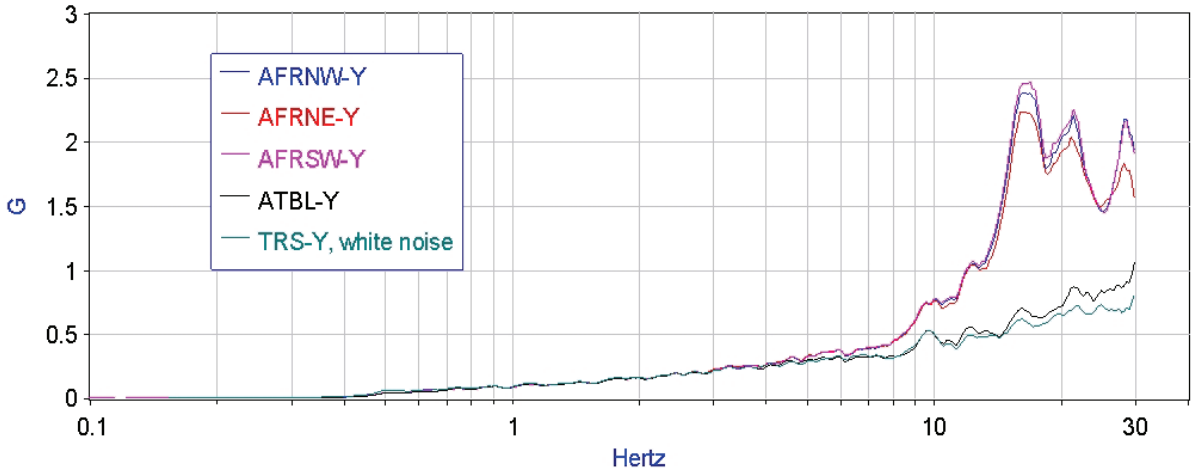

b) Horizontal direction (Y)

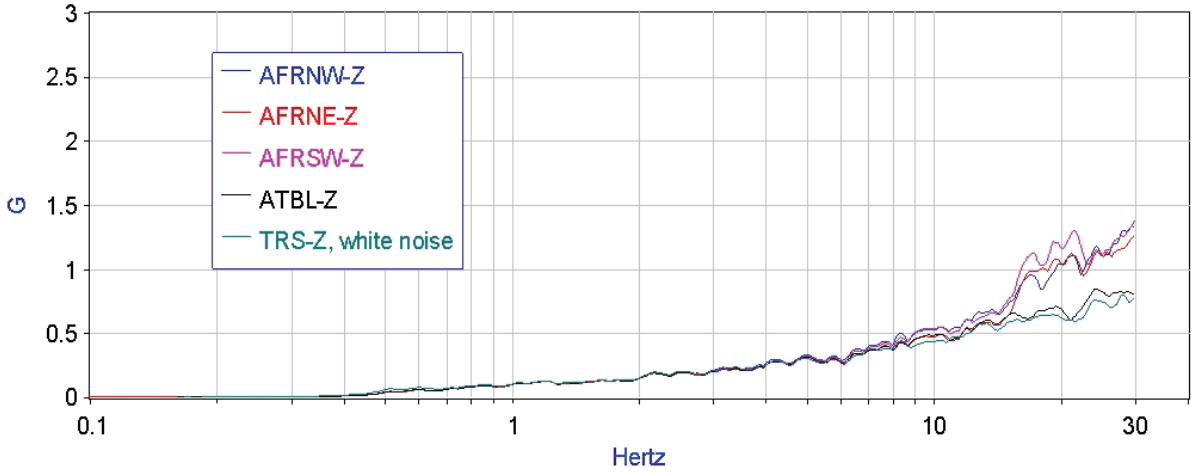

c) Vertical direction (Z)

Figure 5-13 Response Spectra for Each Direction from Uncompensated White Noise Tests (No. 1~3)

The input motions of the second set were tri-axial random motions per AC-156 RRS compatible for S_S = 1.75g in the x, y, and z directions as presented in Figure 5-14. The test frame was subjected to the excitations simultaneously. The response spectra calculated by the achieved motions at the center of the shaking table extension (ATBL) and three top corners of the test frame (AFRNW, AFRNE, and AFRSW) are shown in Figure 5-15 for each direction.

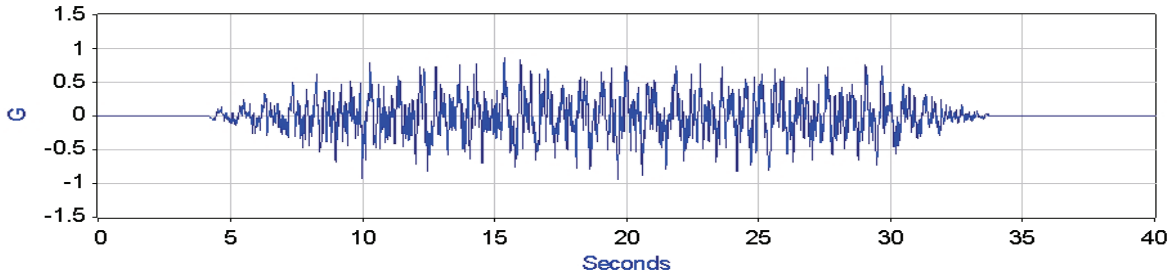

a) Horizontal acceleration history in the X direction (East – West)

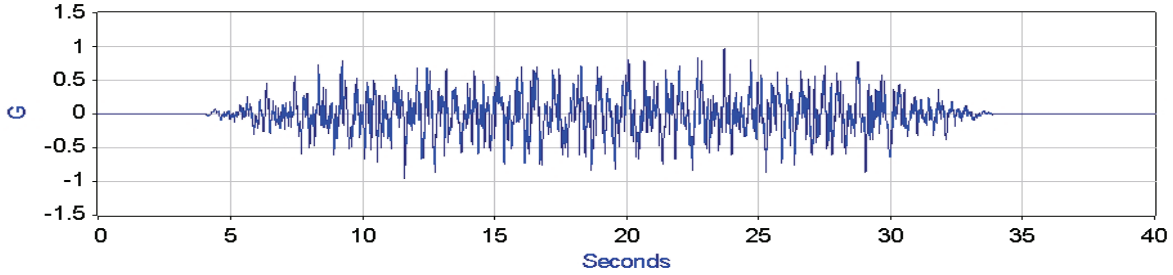

b) Horizontal acceleration history in the Y direction (North – South)

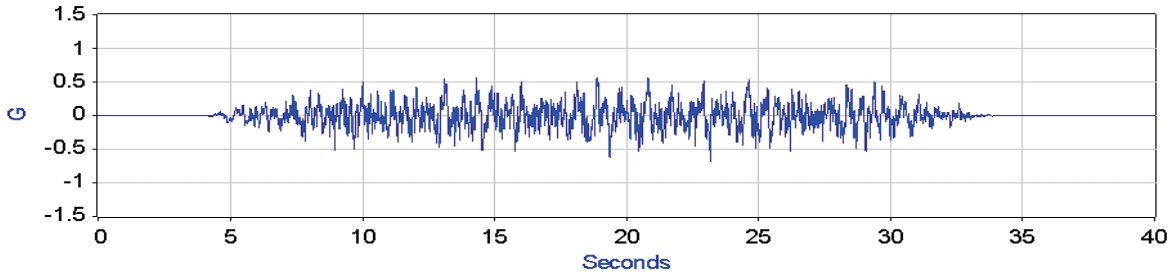

c) Vertical acceleration history in the Z direction

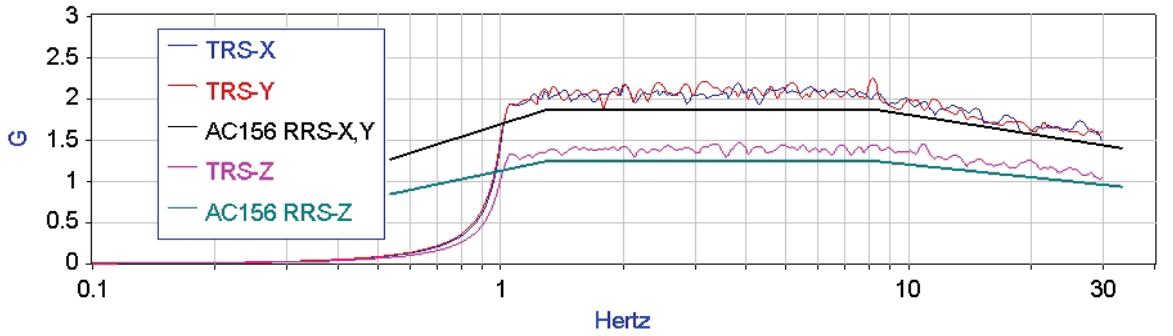

d) Test response spectrum (TRS)

Figure 5-14 Random Input Motions and Corresponding Response Spectra for Uncompensated AC-156 RRS (Ss = 1.75g) Test (No. 4)

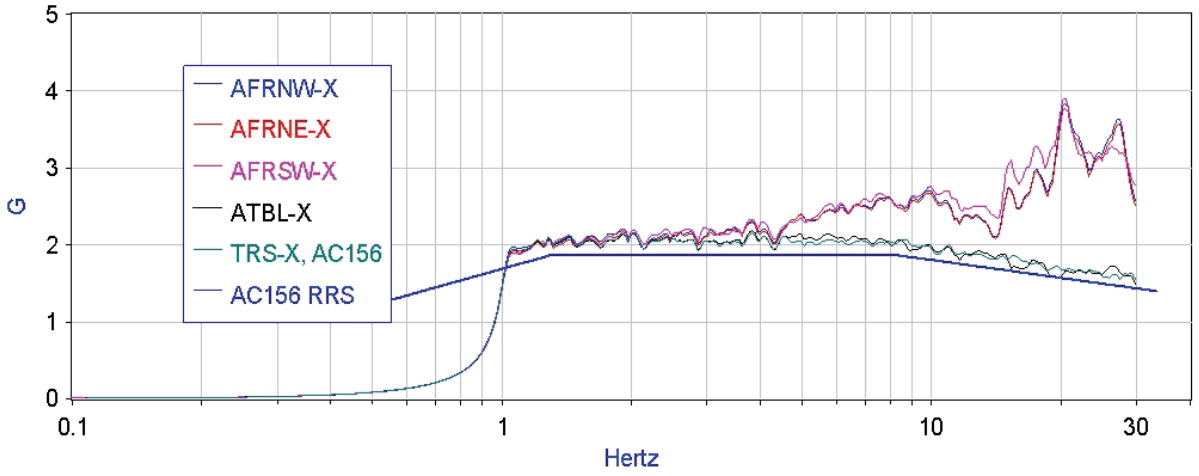

a) Horizontal direction (X)

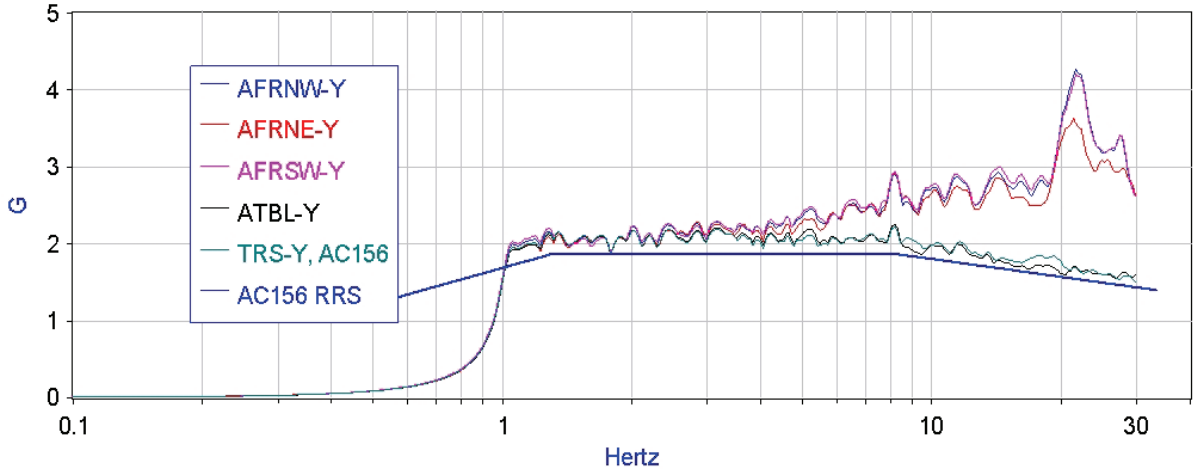

b) Horizontal direction (Y)

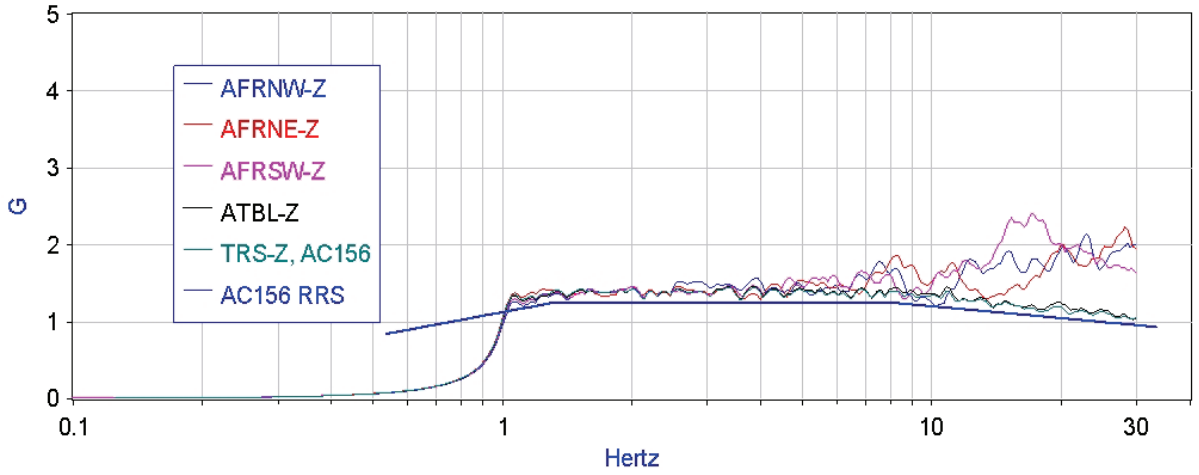

c) Vertical direction (Z)

Figure 5-15 Response Spectra for Each Direction from Uncompensated AC-156 RRS (Ss = 1.75g) Test (No. 4)

5.5.2 Development of Transfer Functions

Using the achieved motions from the Uncompensated White noise test and the AC-156 RRS test, respectively, in Chapter 5.5.1, transfer functions are calculated to develop compensated input motions. The table transfer function (H_t) and structure transfer function (H_s) are calculated in the frequency domain by using Equation (5-27) and (5-28), repeated here:

$$H_t = \frac{achieved\ table\ motion, \bar{y}_t}{uncompensated\ input\ motion, \bar{x}_u} \tag{5-29}$$

$$H_s = \frac{achieved\ structure\ motion, \bar{y}_s}{achieved\ table\ motion, \bar{y}_t} \tag{5-30}$$

where the input motion and the achieved table motion (ATBL = $\bar{y}_t$) and structure motions (the average of AFRNW , AFRNE, and AFRSW = $\bar{y}_s$) in the time domain are transformed into the frequency domain by using Fourier Transform.

5.5.3 Compensated Input and Achieved Motions

Compensated input motions ($\bar{x}_c$) are calculated by multiplying the uncompensated input motion ($\bar{x}_u$) by the two inverse transfer functions as in Equation (5-31) according to the procedure scheme introduced in Chapter 5.3:

$$\bar{x}_c = H_s^{-1} \times H_t^{-1} \times \bar{x}_u \tag{5-31}$$

The two sets of the compensated input motions in the x, y, and z directions were developed using the results of Uncompensated White noise tests and AC-156 RRS tests, respectively, as shown in Figure 5-16 and Figure 5-17.

The test frame was subjected to the two sets of the input motions. The responses were recorded at the center of the shaking table extension (ATBL) and three top corners of the test frame (AFRNW, AFRNE, and AFRSW). The response spectra corresponding to the achieved and compensated input motions for the first set of excitations (developed from the Uncompensated White noise test) and for the second set of excitations (developed from the Uncompensated AC-156 RRS tests) are shown in Figure 5-18 and Figure 5-19, respectively.

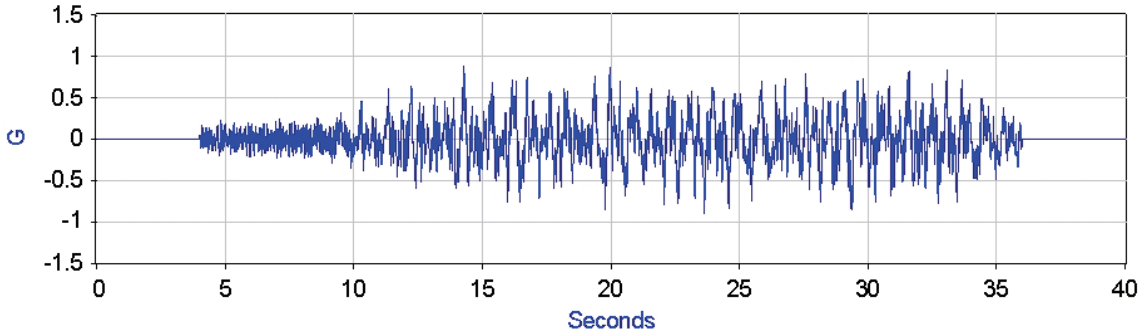

a) Horizontal acceleration history in the X direction (East – West)

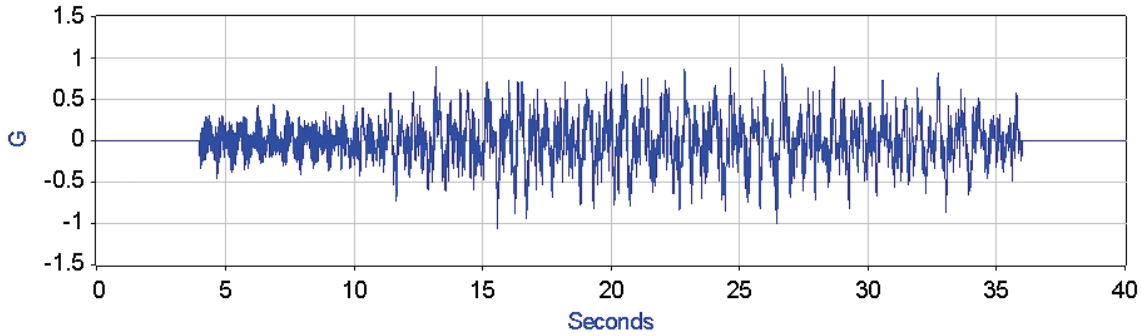

b) Horizontal acceleration history in the Y direction (North – South)

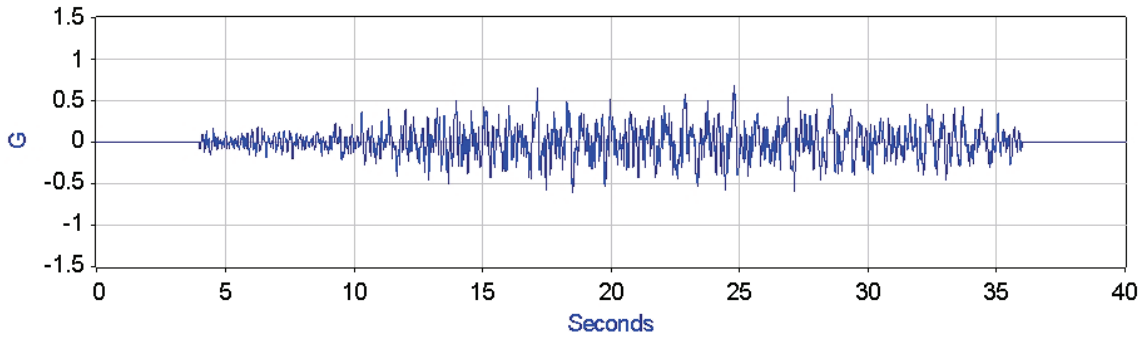

c) Vertical acceleration history in the Z direction

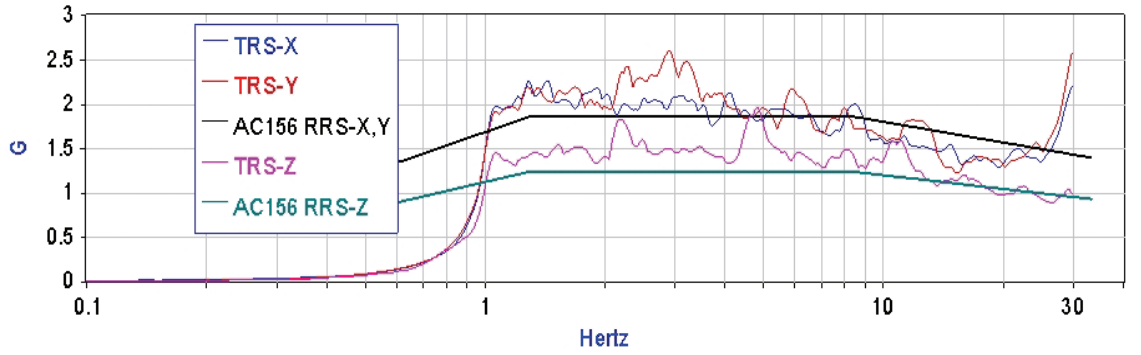

d) Test response spectrum (TRS)

Figure 5-16 Compensated Input Motions and Corresponding Response Spectra for Compensated White Noise Test (No. 5)

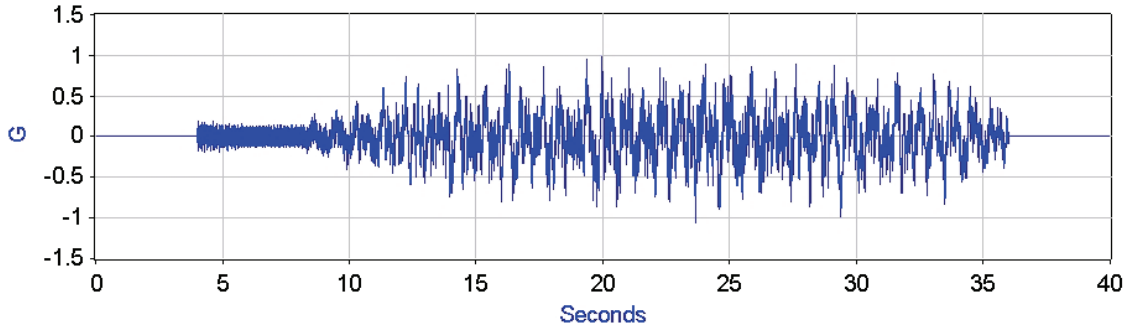

a) Horizontal acceleration history in the X direction (East – West)

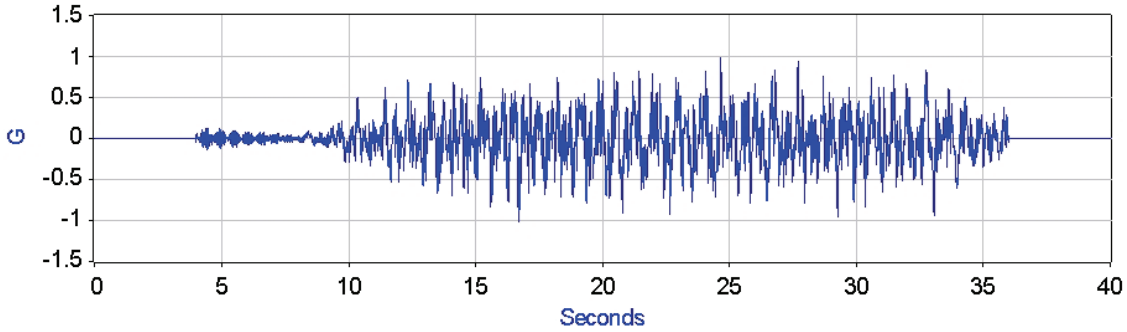

b) Horizontal acceleration history in the Y direction (North – South)

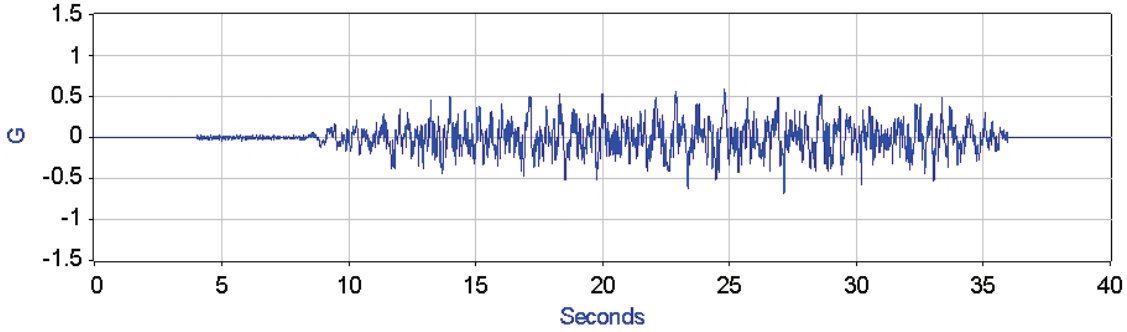

c) Vertical acceleration history in the Z direction

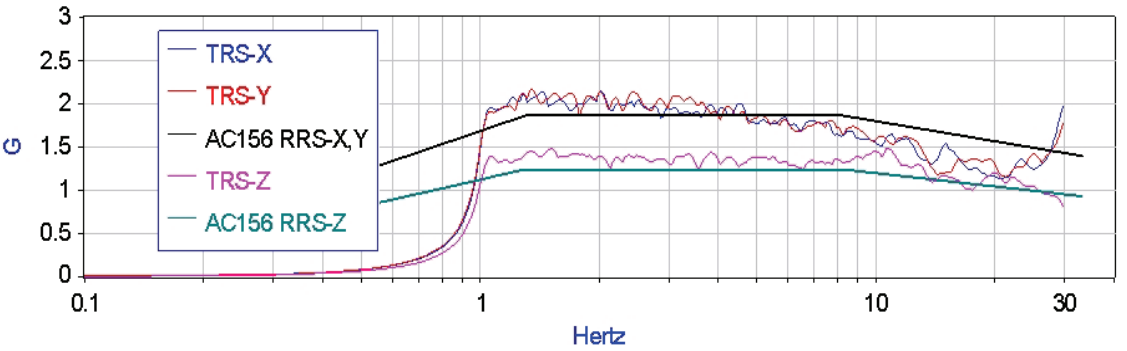

d) Test response spectrum (TRS)

Figure 5-17 Compensated Input Motions and Corresponding Response Spectra for Compensated AC-156 RRS Test (No. 6)

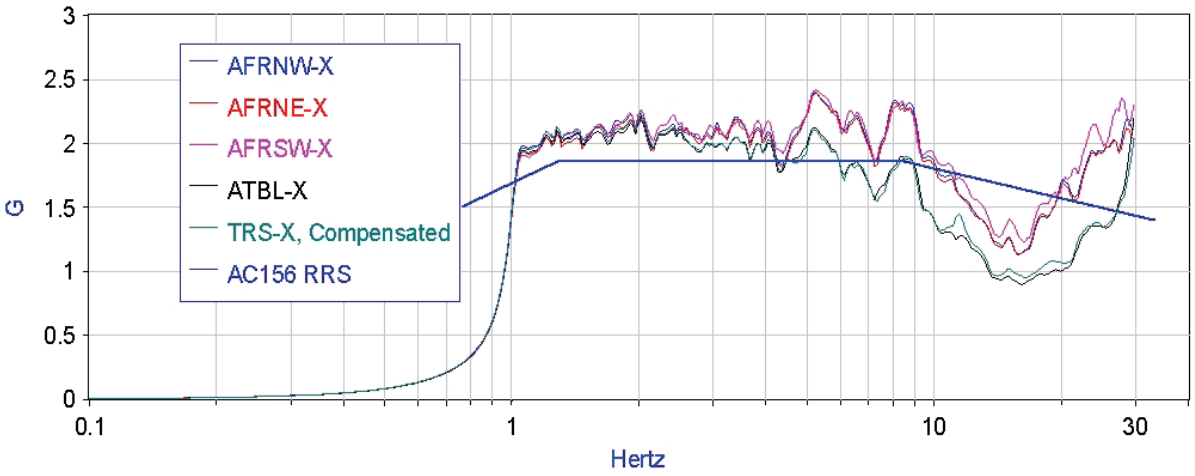

a) Horizontal direction (X)

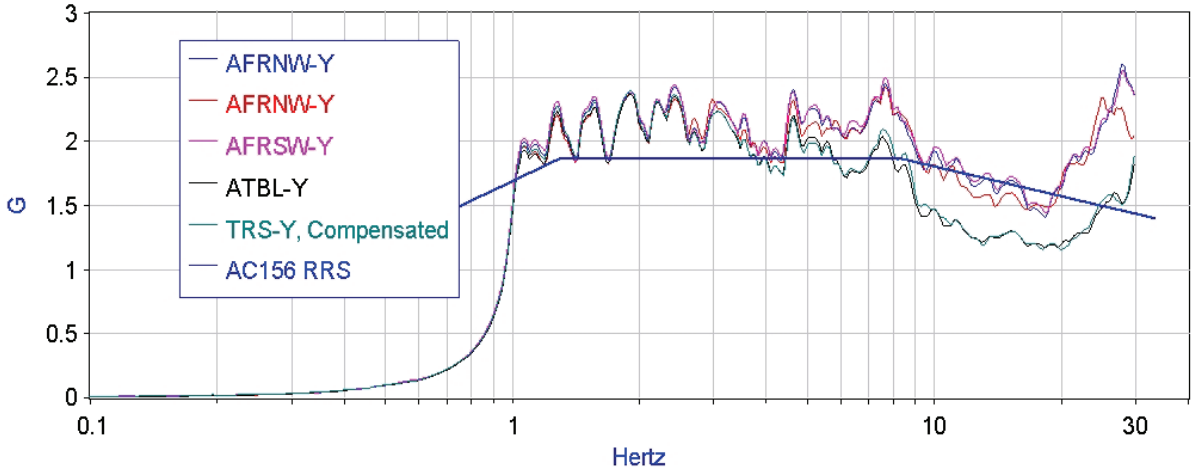

b) Horizontal direction (Y)

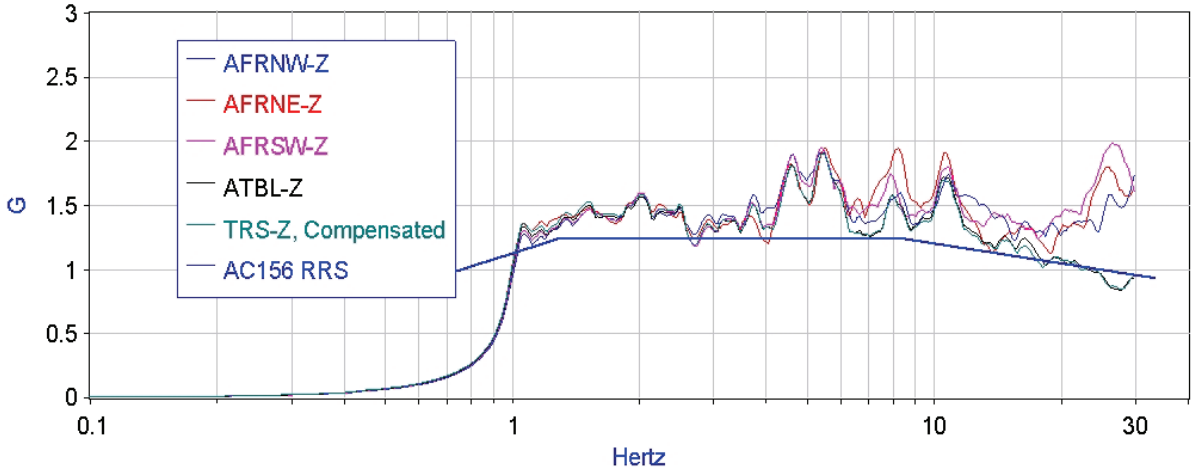

c) Vertical direction (Z)

Figure 5-18 Response Spectra for Each Direction from Compensated White Noise Test (No. 5)

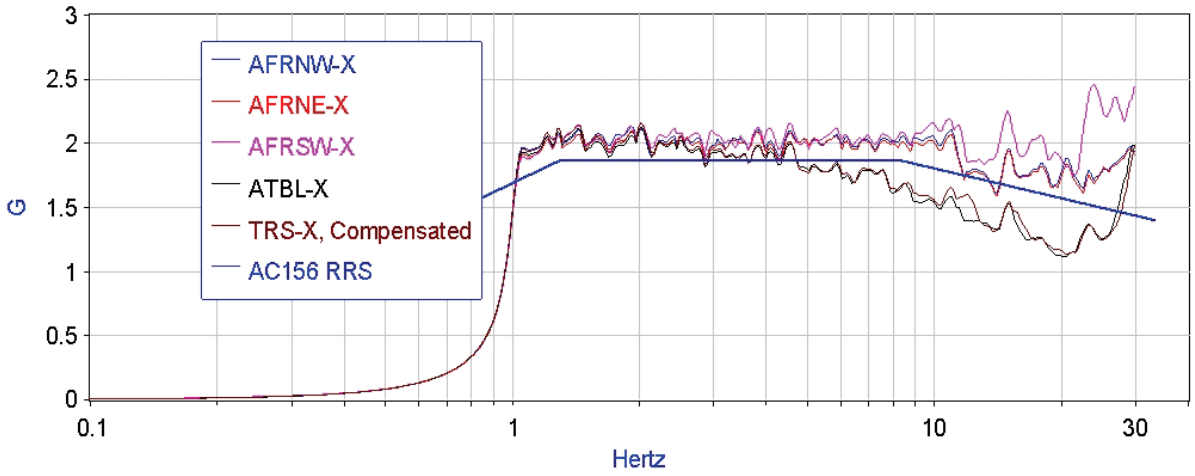

a) Horizontal direction (X)

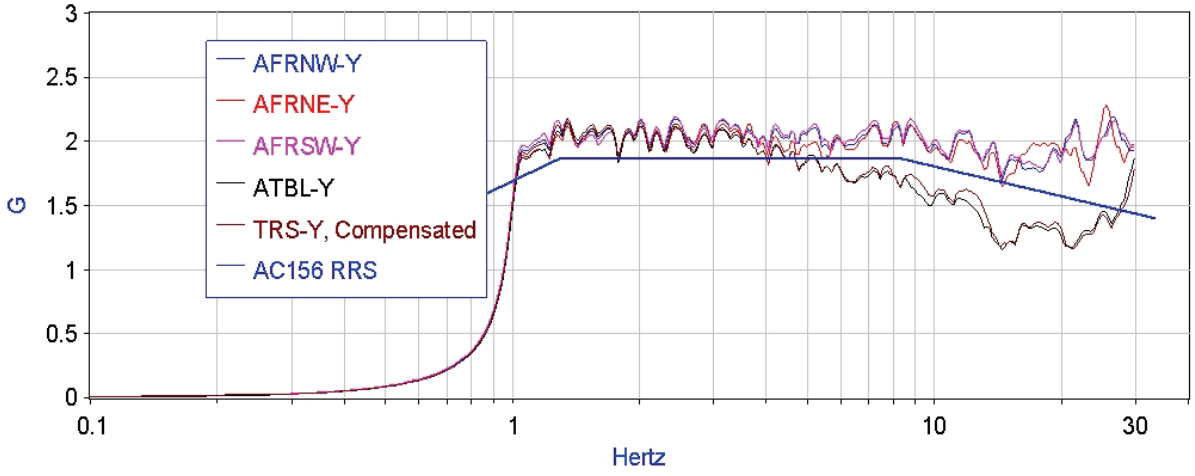

b) Horizontal direction (Y)

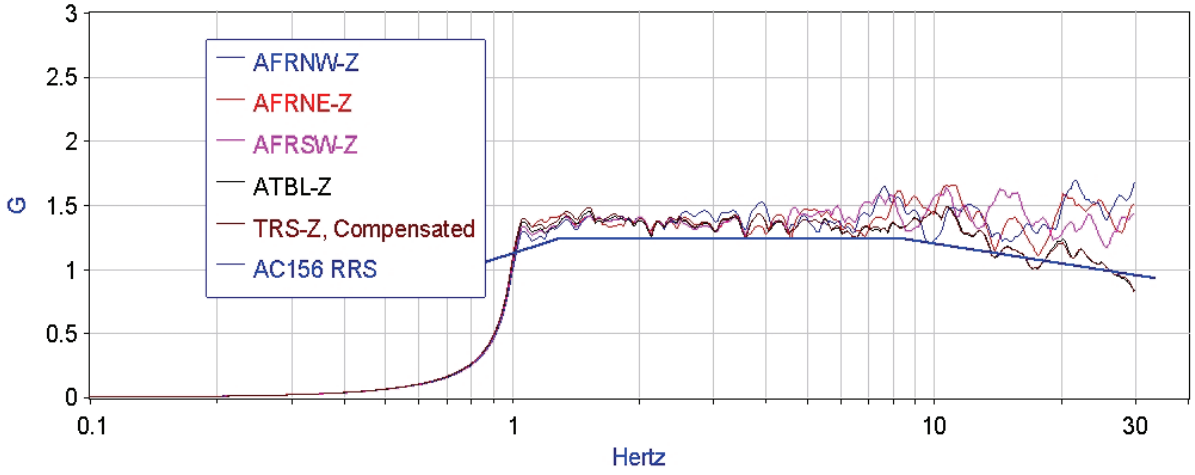

c) Vertical direction (Z)

Figure 5-19 Response Spectra for Each Direction from Compensated AC-156 RRS Test (No. 6)

The degree of distortion (δ) in signal reproduction is calculated using Equation (5-26), repeated here:

$$\delta = \sqrt{\frac{1}{N}\sum_{i=1}^{N}\left[\frac{TRS(f_i) - RS(f_i)}{TRS(f_i)}\right]^2} \tag{5-32}$$

where $TRS(f_i)$ is the ordinate of test response spectrum (target) corresponding to the frequency f_i; $RS(f_i)$ is the ordinate of the response spectrum calculated by the average of achieved accelerations at the three top corners of the frame at the same frequency; and N is the number of values within the band of frequency assumed as base of analyses (1-30 Hz). A response spectrum with a low δ value means an *achieved* motion which is well approximating the *desired* (target) motion.

The degree of distortion for the achieved motions using the compensated input excitations developed by the results of white noise tests and AC-156 RRS tests are presented in Table 5-4. As this table indicates, the transfer functions developed using AC-156 RRS provides better compensated response in terms of having the smaller degree of distortion. It is considered that the transfer functions developed from the AC-156 tests are more accurate to represent "actual" transfer functions as coupled motions in the x, y, and z directions since they were developed using tri-axial input motions while the transfer functions developed from white noise tests are uncoupled motions generated using a unidirectional motion for each direction.

Table 5-4 δ Values of Achieved Table Motions Using Compensated Input Motions

δ	White noise tests	AC-156 RRS tests
(1)	(2)	(3)
Longitudinal	0.124	0.042
Lateral	0.139	0.054
Vertical	0.117	0.066
Average	0.127	0.054

5.5.4 New Compensation Procedure (1st Iteration)

As the degree of distortion (δ values) in Table 5.4 indicates, the compensated input motion does not provide the *desired* (target) motion perfectly at the desired location due to nonlinearity of the system table-structure and imperfection of identification process. To reduce an error, which is calculated by subtracting the *desired* (target) motion ($\overline{x}_u$) from the compensated *achieved* roof motion ($\overline{y}_s$), the iteration procedure is proposed (see Chapter 5.3). The initial compensated input motions ($\overline{x}_{c,0}$) using AC-156 RRS tests are used to develop "new compensated input motions ($\overline{x}_{c,1}$)" as in Equation (5-33):

$$\overline{x}_{c,1} = \overline{x}_{c,0} \times H_{s,\varepsilon}{}^{-1} \tag{5-33}$$

where a new transfer function $H_{s,\varepsilon}$ is defined as the ratio between the initial compensated *achieved* roof motion ($\overline{y}_s$) and the *desired* (target) motion ($\overline{x}_u$). The new compensated input motions are presented in Figure 5-20.

The test frame was subjected to the new compensated input motions. The responses were recorded at the center of the shaking table extension (ATBL) and three top corners of the test frame (AFRNW, AFRNE, and AFRSW). The response spectra corresponding to the achieved motions are shown in Figure 5-21.

For comparison of the achieved motion to the *desired* (target) motion, the degree of distortion (δ values) is calculated and shown in Table 5-5. The average δ value is 0.102, which is larger than that of the no iteration, 0.054 (see Table 5-4). The iteration procedure does not provide better responses fit to the *desired* (target) motion since the used transfer functions for the tests were determined with nonlinearity of the system table-structure and imperfection in identification process. It is expected that the results will be improved when the iteration procedure is continued.

Table 5-5 δ Values of Achieved Table Motions Using the New Compensated Input Motion

δ	New compensated input motion (AC-156 RRS, S_s = 1.75g)
Longitudinal	0.079
Lateral	0.111
Vertical	0.117
Average	0.102

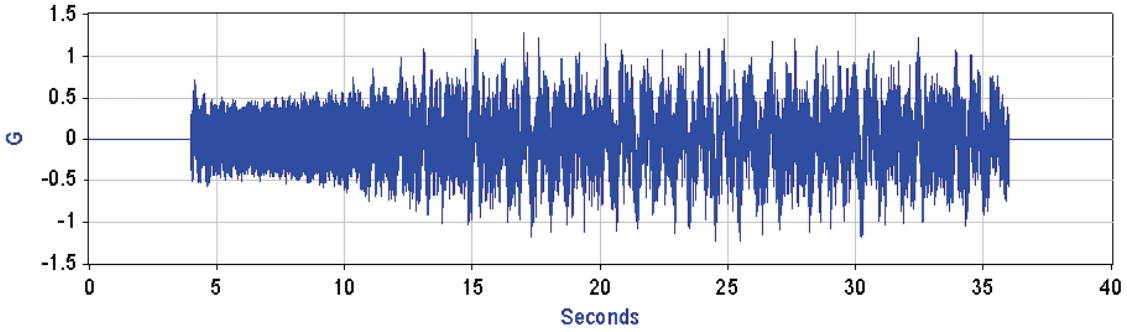

a) Horizontal acceleration history in the X direction (East – West)

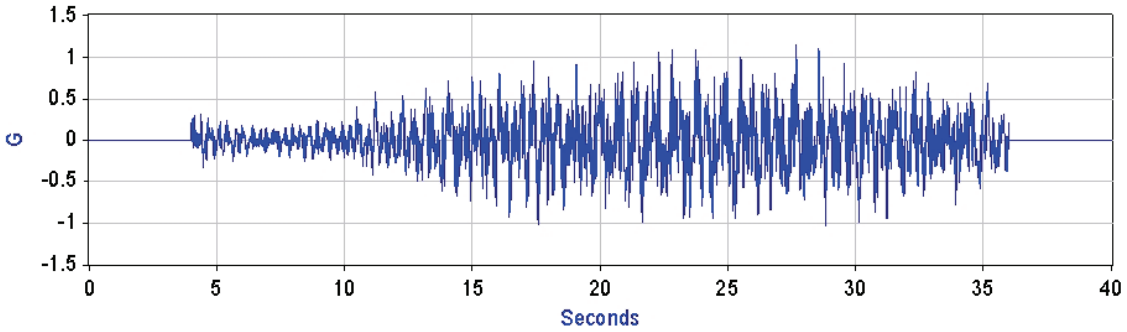

b) Horizontal acceleration history in the Y direction (North – South)

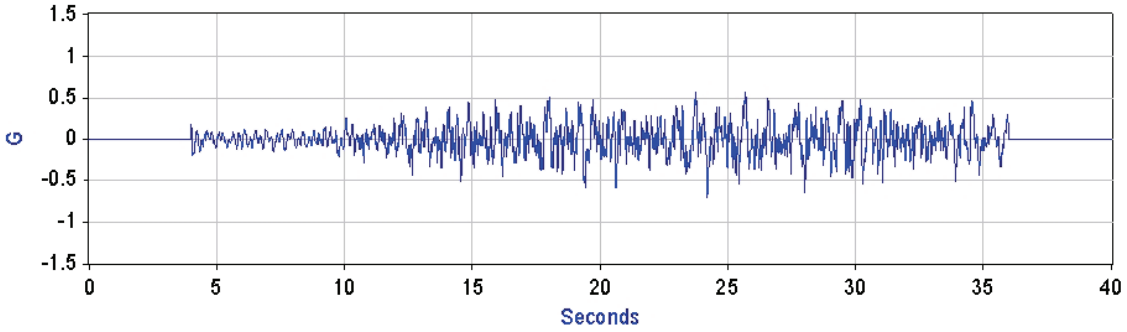

c) Vertical acceleration history in the Z direction

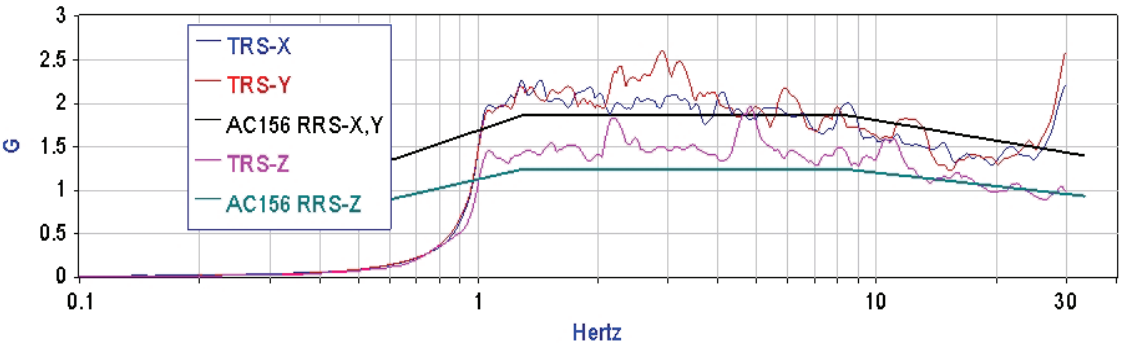

d) Test response spectrum (TRS)

Figure 5-20 New Compensated Input Motions (Developed By Iteration) and Corresponding Response Spectra for New Compensated AC-156 RRS Test (No. 7)

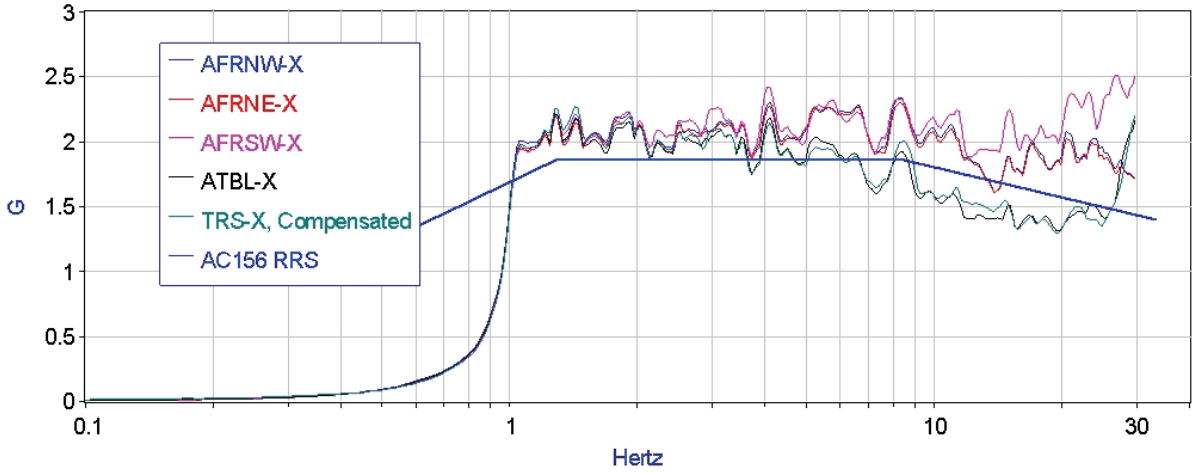

a) Horizontal direction (X)

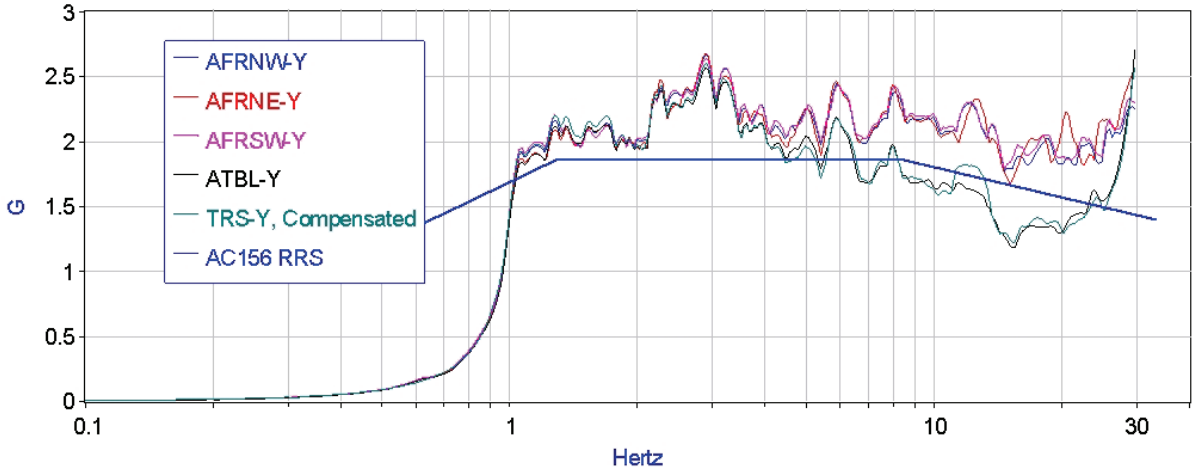

b) Horizontal direction (Y)

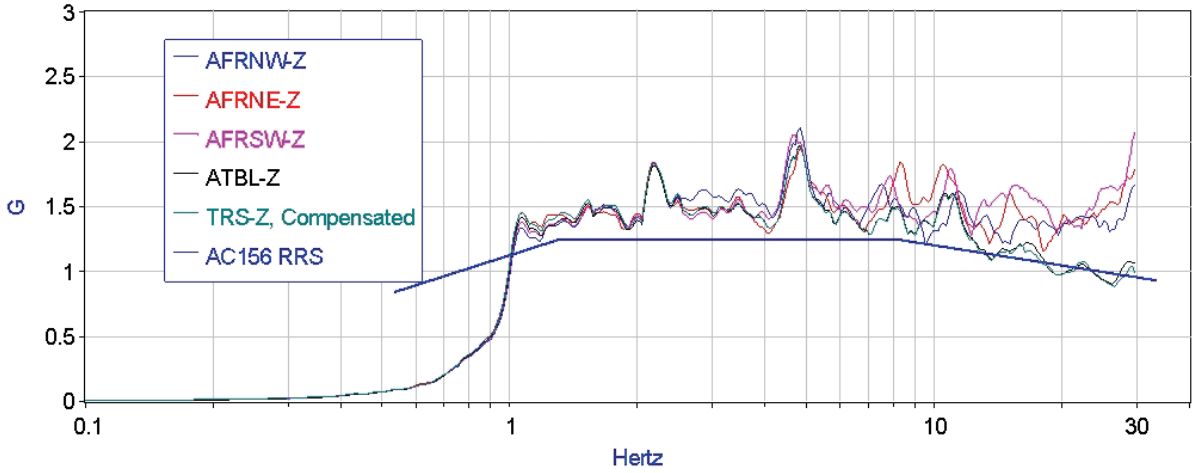

c) Vertical direction (Z)

Figure 5-21 Response Spectra for Each Direction from New Compensated AC-156 RRS Test (No. 7)

5.6 Summary

The compensated shake table simulation for floor response spectrum is developed from basic principles using transfer functions to create compensated signals.

In the first part, the analytical model of a uni-axial shake table considered as an equivalent single-degree-of-freedom system was presented. The transfer functions between desired (or target) and achieved absolute table motion was derived. This represents the degree of distortion in signal reproduction of a desired motion due to the mechanical and servo-hydraulic system. A new compensated drive signal was calculated by multiplying the desired motion with the inverse transfer function. However, using the compensated drive motion as input command for the shake table, the achieved motion could not perfectly match the desired, due to nonlinearity of the servo-hydraulic system. An iterative procedure was suggested to improve the performance.

In the second part, the compensated simulation concept for shake tables was applied to tests performed at the SEESL at the University at Buffalo using one of the two 7m x 7m 6-DOF shake table. A desired motion was selected, derived from the AC-156 testing standard for qualifications of nonstructural components (ICC, 2007). The shape and the levels of required response spectra for horizontal and vertical directions have been assigned according to AC-156 standard. Subsequently, a series of accelerograms were generated to match the specified required response spectrum for each direction of shaking using STEX (MTS, 2004), a simulation package for shake table operations. The three generated acceleration histories represent the "desired" table motions (target). These were initially used as "first input commands" applied to the table. The compensation procedure followed the solution developed in this paper. The structure transfer function along with the table transfer function were simultaneously used to compensate the desired command to the shake table in order to achieve the desired motion at the roof level of the structure using the technique described in the body of this paper. Results achieved from testing in terms of response spectra showed that it is feasible to obtain a much better response using the compensation technique.

Although the presentation herein was made for a planar motion or for independent motions, the formulation can be applied to coupled movement in various directions replacing the transfer functions by a transfer function matrix working simultaneously to all degrees of freedom.

CHAPTER 6
SUMMARY, CONCLUDING REMARKS AND RECOMMENDATIONS

6.1 Summary and Concluding Remarks

The purpose of this study was to design a new extended test frame for seismic qualification tests of suspended ceiling systems and their accessories. Realizing that current practice for suspended ceiling qualifications does not suitably address the vertical motion of the suspended floor/roof caused by seismic motions, a study of the horizontal and vertical motions was conducted. After establishing the importance of the out-of-plane vibrations of the suspended floor/roof, a frame for testing the suspended equipment and architectural-functional components was developed.

A 20 × 50 ft. test frame was designed to realistically simulate ceiling performance correlated with the response observed during real earthquakes. In order to challenge the suspended ceiling systems to maximum (i.e. realistic) motions, the roof of the frame was designed to have "actual floor" dynamic characteristics. The dynamic characteristics of typical floors (or roofs) in buildings were surveyed, and the roof of the test frame was designed to have frequencies of approximately 10 Hz in the vertical direction compatible with the values from the survey. The walls of the frame were designed to be relatively rigid in comparison to the roof system, which is also compatible with structural walls and claddings, having approximately 17 Hz. The frame was also designed to accommodate various construction conditions in terms of structure materials and different framing layouts by changing of the roof properties (frequency) using additional masses. The frame was designed to have modular components to allow smaller frames, such as 20 ft. × 20 ft., to be assembled.

Analytical models were developed using SAP2000 to estimate the dynamic characteristics and the response of the test frame and to evaluate capabilities of the frame, while providing the models for simulation of future experiments. The analytical models developed for 20 × 20 ft. and 20 × 50 ft. frames indicate that the fundamental frequencies of the proposed frames show good agreement with the design criteria.

Test input motions (protocol) were studied, and a new vertical formulation alternative to the AC-156 standard's Required (target) Response Spectrum (RRS), is proposed, without vertical (height) amplification, since structures are typically rigid in the vertical direction. In addition, an alternative protocol (Retamales et al., 2009, summarized in Chapter 4.2), allowing for the assessment of the seismic performance of distributed nonstructural systems with multiple attachment points (i.e. suspended ceiling systems), is also proposed for future considerations.

In order to better simulate the RRS (target) at the top corner of the frame, a "compensation procedure" is introduced in Chapter 5, with its experimental verification at the Structural Engineering and Earthquake Simulation Laboratory (SEESL) at the University at Buffalo using a six degrees-of-freedom (6-DOF) shake table.

Some remarks derived from this study are as follows:

1. In order to realistically simulate earthquake response of typical buildings, a test frame for seismic qualification of suspended ceiling systems and their accessories should have realistic dynamic characteristics, in particular for the vertical direction where the design codes do not have suitable specifications.

2. Through research it was concluded that the fundamental out-of-plane frequencies of most constructed floors were in the range of 2.6 Hz ~ 18.4 Hz. The frequency of the roof of the frame was suggested to be in the range of 2.6 ~ 8.0 Hz to challenge the ceilings to the maximum demand for all possible cases. To accommodate these design criteria, the fundamental frequency of the roof of the frame was designed to have approximately 10 Hz, which was at the right edge of the "plateau" of the required response spectra (AC-156 RRS), so that the fundamental frequency of the roof will be placed in the plateau having maximum input demand after installing a ceiling system.

3. Floor (roof) motions have amplification in the horizontal direction from the ground motion due to the flexibilities of the frame. This amplification will be adjusted by the "compensation procedure" to generate a required response at the top corner of the frame.

4. The vertical amplification for the frame in the vertical direction should be negligible since columns are typically rigid in the vertical direction. Thus, this study proposes a new alternative vertical RRS without height amplification in the vertical direction to be considered by a revised AC-156 and other standards.

5. Using the analytical model developed for the new test frame (20 × 50 ft.) in SAP2000, the capabilities of the frame were estimated by dynamic analyses using the AC-156 RRS simulated motions. The results indicated that the designed frame was safe up to the target of S_s = 4.5g as the roof weight of the frame was 8.0 psf. For various roof weights, the frame with the shaking intensity of S_s = 3.0g was safe up to the weight of 17 psf.

6. Using the analytical model developed for the new test frame (20 × 20 ft.) in SAP2000, the variation of the response of the frame roof was evaluated. Peak spectral accelerations were estimated using different input motions and different roof properties (frequencies). The results indicate that the variation of the roof response was mainly influenced by floor "input motions" rather than change of the roof properties with different additional weights.

7. With the proposed "compensation procedure" it is feasible to obtain a much better simulation of the roof motion of the frame using adjusted shake table command drive motions in the three directions, based on the actual dynamic properties of the frame. The compensation procedure can be applied at other laboratories and for other applications.

6.2 Recommendations for Future Developments

1. Both the large test frame, 20 × 50 ft., and square test frame, 20 × 20 ft., will be used for qualification tests for suspended ceiling systems. The experimental test results using the two frames could be compared. If the results are comparable, the design of the 20 × 20 ft. square test frame can be used for future tests also in other laboratories with smaller shaking platforms.

2. Further evaluation and comparisons of the alternative protocol (Retamales et al., 2009) and the AC-156 should be made before an alternative protocol is adopted for future tests.

3. Since the test frame has flexibilities and the shake table system is not perfect, the input motions have distortions. Although the "compensation procedure" significantly reduces these errors during tests, the results can be improved by an "iterative compensation procedure," discussed in Chapter 5.5.4. In order to obtain better response in terms of matching the achieved response spectrum to the required response spectrum at the desired location of the test frame, the "iterative compensation procedure" is recommended.

4. The transfer functions developed for the "compensation procedure" were made for independent motions in the x, y, and z directions, respectively. However, the transfer functions can be replaced by a full transfer function matrix including the cross-correlated transfer functions, working simultaneously to all degrees of freedom for coupled movement in various directions.

CHAPTER 7
REFERENCES

AISC (2007). "Steel Construction Manual," *American Institute of Steel Construction*, 13th Edition, Chicago, IL.

Allen, D. E. and Pernica, G. (1998). "Control of Floor Vibration," *Construction Technology Update*, No. 22, NRC Institute for Research in Construction, National Research Council Canada.

Allen, D. E., and Rainer, J. H. (1976). "Vibration Criteria for Long Span Floors," *Canadian Journal of Civil Engineering*, Vol. 3, No. 2, The National Research Council of Canada, June, pp.165-173.

ANCO (1983). "Seismic Hazard Assessment of Nonstructural Ceiling Components," *NSF Rep*. No. CEE-8114155.

ASTM E1049-85. (1997). "Standard Practices for Cycle Counting in Fatigue Analysis," *American Society for Testing and Materials,* now ASTM International.

ASTM - A 588. (2005). "Standard Specification for High-Strength Low-Alloy Structural Steel, up to 50 ksi [345 MPa] Minimum Yield Point, with Atmospheric Corrosion Resistance," *ASTM International*, West Conshohocken, PA .

ASTM - E 580. (2008). "Standard Practice for Installation of Ceiling Suspension Systems for Acoustical Tile and Lay-in Panels in Areas Subject to Earthquake Ground Motions," *ASTM International*, West Conshohocken, PA..

Badillo, H., Kusumastuti, D., Reinhorn, A.M., and Whittaker, A.S. (2002). "Seismic qualification of suspended ceiling systems," *Technical Report UB CSEE/SEESL-2002-01*, Vol. 1. Department of Civil, Structural, and Environmental Engineering, University at Buffalo, Buffalo, New York.

Badillo, H., Whittaker, A.S., and Reinhorn, A.M. (2003a). "Seismic qualification of suspended ceiling systems," *Technical Report UB CSEE/SEESL-2003-01*, Vol. 3. Department of Civil, Structural, and Environmental Engineering, University at Buffalo, Buffalo, New York.

Badillo, H., Whittaker, A.S., and Reinhorn, A.M. (2003b). "Testing for seismic qualification of suspended ceiling systems, Part 3," *Technical Report UB CSEE/SEESL-2003-01*, Department of Civil, Structural, and Environmental Engineering, University at Buffalo, Buffalo, New York.

Badillo, H., Whittaker, A.S., and Reinhorn, A.M. (2003c). "Testing for seismic qualification of suspended ceiling systems, Part 4," *Technical Report UB CSEE/SEESL-2003-02*, Department of Civil, Structural, and Environmental Engineering, University at Buffalo, Buffalo, New York.

Badillo, H., Whittaker, A.S., and Reinhorn, A.M. (2003d). "Performance Characterization of Suspended Ceiling Systems," *Proceedings, ATC-29-2 Seminar on the Seismic Design*, Performance and Retrofit of Nonstructural Components in Critical Facilities, Irvine, CA.

Badillo, H., Whittaker, A.S. Reinhorn, A.M. and Cimellaro, G.P. (2006). "Seismic Fragility of Suspended Ceiling Systems," *Technical Report MCEER-06-0001*, MCEER, University at Buffalo-the State University of New York, Buffalo, NY.

Badillo, H., Whittaker, A.S. and Reinhorn, A.M. (2007). "Seismic Fragility of Suspended Ceiling Systems," *Earthquake Spectra*, 23(1), 21-40.

Blevins, R.D. (1983). "Formulas for Natural Frequency and Mode Shape," Van Nostrand Reinhold, NY.

Boice, M.D. (2003). "Study to Improve the Predicted Response of Floor Systems due to Walking," *M.S. Thesis*, Department of Civil Engineering, Virginia Polytechnic Institute and State University, Blacksburg, Virginia.

Bracci, J.M., Reinhorn, A.M., and Mander, J.B. (1992). "Seismic resistance of Reinforced Concrete frame structures designed only for gravity loads: part 1- design and properties of a one-third scale model structure," *Technical report NCEER 92-0027*, University at Buffalo-the State University of New York, Buffalo, NY.

BSSC. (1997). "FEMA 303: NEHRP Recommended Provisions for Seismic Regulations for New Buildings and Other Structures. Part 2: Commentary," *Building Seismic Safety Council*, Washington, D.C.

Chopra, A.K. (2007). "Dynamics of Structures: Theory and Application to Earthquake Engineering," Prentice Hall, 3rd Ed., Upper Saddle River, NJ.

Christovasilis, I.P., Filiatrault, A., and Wanitkorkul, A. (2007). "Seismic Testing of a Full-Scale Two-Story Light-Frame Wood Building : NEESWood Benchmark Test," *NEESWood Report No. NW-01*, University at Buffalo, the State University of New York, Buffalo, NY.

CISCA. (2004a). "Recommendations for Direct-hung Acoustical Tile and Lay-in Panel Ceilings – Seismic Zones 0-2," *Ceilings & Interior Systems Construction Association*, St. Charles, IL.

CISCA. (2004b). “Guidelines for Seismic Restraint for Direct Hung Suspended Ceiling Assemblies – Seismic Zones 3 & 4,” *Ceilings & Interior Systems Construction Association*, St. Charles, IL.

Clark, A. (1992). “Dynamic characteristics of large multiple degrees of freedom shaking tables,” *Proceedings of the 10th World Conference on Earthquake Engineering*, 2823–2828, Madrid, Spain.

Conte, J.P. and Trombetti, T.L. (2000). “Linear dynamic modeling of a uni-axial servo-hydraulic shaking table system,” *Earthquake Engineering and Structural Dynamic*, 29, 1375-1404.

FEMA. (2007). “Interim Testing protocols for Determining Seismic Performance Characteristics of Structural and Nonstructural Components,” *FEMA 461*, Federal Emergency Management Agency, Washington DC.

Gilani, A.S., Glasgow, R.B., Ingratta, T., Reinhorn A,M., and Lavan, O. (2007a). “Seismic Qualification, Fragility, and Evaluation of Suspended Ceilings: Earthquake Simulator Testing and Application to Structural Engineering,” *SEAOC Convention*, September 26-29, 2007, Olympic Valley, CA.

Gilani, A.S., Reinhorn, A.M. and Glasgow, R.B. (2007b). “Earthquake Simulator Testing and Evaluation of Suspended Ceiling System,” *Proceedings 12th US-Japan Workshop / ATC-15-11 Seminar* (Invited paper), Kauai, HI.

Gilani, A.S., Reinhorn, A.M., Ingratta, T., Glasgow, R.B. and Lavan, O. (2008). “Earthquake Simulator Testing and Evaluation of Suspended Ceilings: Standard and Alternate Perimeter Installations,” *Proceedings of 2008 ASCE Structures Congress*, May 16-19, 2008, Vancouver, BC, Canada.

Gupta, I.D. and Trifunac, M.D. (1998). “Defining Equivalent Stationary PSDF to Account for Nonstationarity of Earthquake Ground Motion,” *Soil Dynamics and Earthquake Engineering* 17(2), 89-99.

ICC. (2006). “International Building Code,” International Code Council, Whittier, CA.

ICC. (2007). “ICC ES-AC 156, Acceptance Criteria for Seismic Qualification by Shake-table Testing of Nonstructural Components and Systems,” *International Code Council*, Whittier, CA.

Iervolino I, Maddaloni G and Cosenza E. (2008). “Eurocode 8: compliant real record sets for seismic analysis of structures,” *Journal of Earthquake Engineering*, 12(1), 54-90.

Kusumastuti, D., Badillo, H., Reinhorn, A.M., and Whittaker, A.S. (2002). "Seismic qualification of suspended ceiling systems," *Technical Report UB CSEE/SEESL-2002-01*, Vol. 2., Department of Civil, Structural, and Environmental Engineering, University at Buffalo, Buffalo, NY.

Lavan, O., Reinhorn, A.M., Shao, X., and Pitman, M. (2006). "Seismic qualification test of suspended ceiling systems: System H, a study for Chicago Metallic Corporation," *Report No. UB CSEE/SEESL-2006-15*, Department of Civil, Structural and Environmental Engineering, University at Buffalo-the State University of New York, Buffalo, NY. (private distribution only)

Maddaloni G, Syed AM, Naser A, and Reinhorn AM. (2009a). "User manual for 6 DOFs shake table," *Report No. UB CSEE/SEESL-2009-XX*, Department of Civil, Structural and Environmental Engineering, University at Buffalo-the State University of New York, Buffalo, NY. (in press).

Maddaloni, G., Ryu, K.P. and Reinhorn, A.M. (2009b). "Shake Table Simulation of Models Floor Response Spectrum," Department of Civil, Structural and Environmental Engineering, University at Buffalo-the State University of New York, Buffalo, NY (also submitted for review to *International Journal of earthquake Engineering and Structural Dynamics* (EESD).

Maragakis et al. (2007). "NEESR-GC: Simulation of the Seismic Performance of Non-structural Systems," *Proposal for NEESR-GC project* funded by the US National Science Foundation in 2007.

Mosqueda, G., Retamales, R., Filiatrault, A., and Reinhorn, A. (2008). "Testing Facility for Experimental Evaluation of Non-Structural Components under Full-Scale Floor Motions," *Journal of the Structural Design of Tall and Special Buildings*, DOI: 10.1002/tal.441.

MTS-RTHSTS (2004). "Real Time Hybrid Seismic Test System-User's Manual," MTS System Corporation, USA.

Murray, T.M., Allen, D.E., and Ungar, E.E. (1997). "Floor Vibrations Due to Human Activity," *Steel Design Guide* Series 11, AISC.

NEHRP. (2008). "NEHRP Provisions update - *PROPOSAL 8-113R1* (2009)," 3rd Member Organization Ballot.

Niousha, A. (1999). "Investigation on the Vertical Vibration Characteristics of Actual Structure for Earthquake Observation Records and Impactor Test," *Architectural Institute of Japan*, 62, 463-466.

Ozcelik, O., Luco, J.E., Conte, J.P., Trombetti, T.L., and Restrepo, J.I. (2008). "Experimental characterization, modeling and identification of the NEES-UCSD shake table mechanical system," *Earthquake Engineering and Structural Dynamics*, 37, 243–264.

Reinhorn (2000). "Design and development of testing frame for suspended ceilings," *Internal report and private communication*.

Repp, J., Badillo, H., Whittaker, A.S., and Reinhorn, A.M. (2003a). "Seismic qualification of suspended ceiling systems, Part 5," *Technical Report UB CSEE/SEESL-2003-03*, Department of Civil, Structural, and Environmental Engineering, University at Buffalo, Buffalo, New York.

Repp, J., Badillo, H., Whittaker, A.S., and Reinhorn, A.M. (2003b). "Seismic qualification of suspended ceiling systems, Part 6," *Technical Report UB CSEE/SEESL-2003-03*, Department of Civil, Structural, and Environmental Engineering, University at Buffalo, Buffalo, New York.

Retamales, R., Mosqueda, G., Filiatrault, A., and Reinhorn, A.M. (2008). "New Experimental Capabilities and Loading Protocols for Seismic Qualification and Fragility Assessment of Nonstructural Components," *Technical Report MCEER-08-0026,* MCEER, University at Buffalo-the State University of New York, Buffalo, NY.

Retamales, R., Mosqueda, G., Filiatrault, A., and Reinhorn, A.M. (2009). "Testing Protocol for Experimental Seismic Qualification of Distributed Nonstructural Systems," in *Earthquake Spectra* (in press)

Rihal, S. and Granneman, G. (1984). "Experimental Investigation of the Dynamic Behavior of Building Partitions and Suspended Ceilings during Earthquakes," *Report No. ARCE R84-1*, California Polytechnic State University, Pomona, California.

Rinawi, A.M. and Clough, R.W. (1991). "Shaking table–structure interaction," *EERC Report No. 91/13*, Earthquake Engineering Research Center, University of California at Berkeley, CA.

Roh, H.S., Reinhorn, A.M., and Pitman, M. (2008). "Seismic qualification test of suspended ceiling systems: System F8 of Chicago Metallic Corporation," *Report No UB CSEE/SEESL-2008-08*, Department of Civil, Structural and Environmental Engineering, University at Buffalo-the State University of New York, Buffalo, NY.

Whittaker, A.S., Soong, T.T. (2003). "An Overview of Nonstructural Components Research at Three U.S. Earthquake Engineering Research Centers," *Proc. ATC 29-2 Seminar on Seismic Design, Performance, and Retrofit of Nonstructural Components in Critical Facilities*, October 23-24, 2003. Newport Beach, CA.

Whittaker A.S., Hough P.A., Reinhorn A.M. and Bachman R.E. (2007). "Interpretation of Seismic Qualification and Fragility Data for Suspended Ceiling Systems," *Proceedings of 2007 ASCE Structures Congress*, May 16-19, 2007, Long Beach, CA.

Williams, M.S. and Waldron, P. (1994). "Evaluation of Methods for Predicting Occupant-induced Vibrations in Concrete Floors," *The Structural Engineer*, 72(20), 334-340.

Yao, G. C. (2000). "Seismic Performance of Direct Hung Suspended Ceiling Systems," *ASCE/Journal of Architectural Engineering*, 6(1), 6-11.

Appendix A
DESIGN & MODELING FEEDBACK-1

Response to Issues raised by the advisory group to Draft 1 of the Suggested Design

Comments to the geometric design of a new test frame were requested from the industry partners of SEESL and NEES *Simulation of the Seismic Performance of Nonstructural Systems* project, research management team (of NEES *Simulation of the Seismic Performance of Nonstructural Systems* project), and SEESL technical staff. The feedback was obtained during the period from January 30, 2009 to February 19, 2009. The frame design was developed, incorporating the feedback. The comments and the issues addressed in the reply are summarized Table A-1.

Table A-1 Feedback on the Draft 1 for the Period from 1/30/09 to 2/19/2009

Reader	Comments & Questions	Initial Reply	How Issued is Addressed in Actual Design
Dennis Alvarez	1. What is the proposed size of the joists?	The joists were picked from a list provided by a manufacturer of "open web floor joists." However, the joist could be made in-house to be slightly more flexible, compatible with the design frequencies (see answers below.)	Suggested use of commercial joist type: 10K1: Depth: 10 in. Spacing: 4 ft. (Joists start 2 ft. from the frame edge.)
	2. Has anyone estimated the fundamental frequencies of the proposed new frame? I realize this may be difficult given the required, flexible connection. Of most concern is the Z direction, as that was too flexible in the first table causing some undesirable test phenomena that seemed at odds with observed ceiling damage.	We are using the floor considerations based on Murray et al. (1997) and similar information. The design is conceived to have basic frequency (stiffness) of 20 Hz with the possibility to adjust it downwards by adding masses. This is in line with the suggestion above.	Estimated frequency in the vertical direction of the 20 ft. x 50 ft. frame is 10.01 Hz from SAP2000; this is compatible with the upper limit suggested by Murray et al. (1997). As designed, the new roof's lower frequencies ($\geq$ 4Hz) can be achieved by addition of weight in center of roof.

Dennis Alvarez	3. The description stated that the ceiling height could be lowered. Is that proposed to be something that could be changed after the frame is constructed? Another variable I think should be examined is plenum depth. I would expect a larger "plenum depth" would affect the horizontal forces experienced by the ceiling.	See the answer about the #6 question.	The dimensions of the frame were established as: Frame Height: 10 ft.-0 in. Ceiling Height: 7 ft.-6 in. Plenum depth: 1 ft.-9 in. (Plenum depth can be increased. Ceiling system can be installed lower.)
	4. The new frame is designed to have a fundamental frequency in the Z-direction of 20-40 Hz with no added mass. When loaded to the maximum recommended by the manufacturer, the result is expected to be approximately 5 Hz. This will allow the fundamental frequency to be adjusted between these two values by varying the mass and can be used to achieve results more in line with observed earthquake damage.	We are using the floor considerations based on Murray et al. (1997) and similar information. The design is conceived to have basic frequency (stiffness) of 20 Hz with the possibility to adjust it downwards by adding masses. This is in line with the suggestion above.	See the issue addressed in #2 above.
	5. As was discussed extensively at ASTM, setting the z/h=1 causes amplification of the vertical motion not experienced in actual structures. Setting z/h=0, as in the current state of the proposed ASTM standard, will help eliminate overly conservative, vertical failure modes.	This proposal was made previously by the UB team and support documentation is being developed. The design team is preparing shake table motions compatible with the delivery of real roof motions at the roof level of the frame (Maddaloni et al. 2009b). This includes compensated shake table motions horizontally and un-amplified motions vertically.	See considerations in the left column.

Dennis Alvarez	6. I suggested we start with the plenum depth (the distance from the bottom of the trusses to the suspended ceiling) that has been used for previous testing (18"?), so as to not introduce an unnecessary variable. At some point in the future, I think we should examine the effect of plenum depth. The design of the frame will allow for the ceiling height to be easily altered.	This point is well taken. The position of the "wall angle" would be made variable (screwed to the frame walls) such that it will accommodate various plenum heights.	See the issue addressed in #3 above.
	7. At this point, Dr. Reinhorn is seeking technical comments. An official request for industry funding will follow the finalized design of the frame.	-	-
Bob Bachman	8. The height of the test frame seems rather restrictive. I would think we would want more height. The height range between the bottom of the suspended ceiling and the above floor should be at least 6 feet. perhaps 8 feet plus minimum of 4 feet below the ceiling and the deck. I would say the minimum height should be at least 12 feet and maybe it should be 14 feet. Speed of installation is nice but covering the height range of importance is far more important. I think we are only to have one chance to get this right.	It is unclear to the designers why the overall height is important. Although IBC (ICC, 2006) requirements are 7'-6" above floor level for architectural reasons, this height is not important for structural considerations. The horizontal and transversal stiffness can be controlled by structural changes in the "wall" frames. The height above the suspended ceiling (plenum) seems to be defined by the minimum required for non-structural components, light fixture, piping, grid suspension system. All current documents indicate 2 ft. below the open web trusses. We would like more details from the commenter.	The dimensions of the frame were slightly modified See reply at item #3 above. The height of a structural frame was designed to be the minimum required by standard IBC (ICC, 2006), to allow efficient space for assembling the "ceiling" systems, while accommodating requirements of standards.

Bob Bachman	9. The design parameter for the floor above is extremely important. I would prefer the floor were rigid but that is not likely doable so next best thing is that it should simulate the vertical response of a real floor. In other words, when tested the vertical response should have the same frequency and damping characteristics of a typical floor and the mass of the floor should have sufficient weight so that the response of the ceiling system should have no influence on the response of the floor above. To do this, perhaps the floor above should be simulated with metal deck and cast in place concrete pieces or concrete planks. I recognize this will add a lot more weight to the frame and will cause the frame to increase in size. But the vertical response must be properly simulated or else we may be causing unreal responses, which I think we are doing with the current frame. And the resulting diaphragm of the floor above should be torsionally stiff.	We are using the floor considerations based on Murray et al. (1997) and similar information. The design is conceived to have basic frequency (stiffness) of 20 Hz with the possibility to adjust it downwards by adding masses. This is in line with the suggestion above.	See the issue addressed in #2 above.

Bob Bachman	10. Unfortunately, the vertical earthquake response of floors systems is virtually never studied (It is studied for floor vibrations, so for small amplitudes, the range of frequencies and damping are readily available). However, I know of one building, the LA county 911 building, where vertical responses at the center of a floor have been measured along with the vertical accelerations of the columns since 1990. This should be looked at to determine the effective damping of an actual floor during real earthquakes. For some stupid reason, the committee that decides on CSMIP instrumentation never instruments the center of a floor vertically. The only reason it's measured in the LA county 911 is because I personally caused it to happen.	This is a good suggestion. Combined with the recommendations of Murray et al. (1997), prior information about floor response data from various earthquakes will be considered in the detailed design	Additional modifications of vertical properties might be done upon completion of survey.
	11. The horizontal framing should either be very stiff and not introduce unreal vibration horizontally, or if spurious high frequency vibrations are introduced, they should be damped in some way so that the horizontal response actually simulates building response.	This is a good suggestion also. The walls of the frame are made to be very stiff to prevent any differential motion of the roof corners and boundaries to the shaking platform. Frequencies of 20 to 30 Hz will be implemented for this purpose.	Estimated fundamental frequencies of the walls are 19.29 Hz and 19.02 Hz in the horizontal directions, X and Y, respectively, for the 20 ft. × 50 ft. frame. The frequencies are compatible with typical walls in structures. The higher frequencies have very low participation mass and should not contribute to the overall set. Adjustments of damping if necessary could be done during qualification testing.

Shakhzod Takhirov	12. What is an estimated frequency of the frame in all three directions?	20->30 Hz horizontally; 40->50 Hz vertically	Modified design in Draft 2 has estimated frequencies of the 20 ft. × 50 ft. frame.: 19.29 Hz in X, 19.02 Hz in Y, 10.01 Hz in Z.
	13. What is an estimated frequency of the frame's top from which the ceiling system is going to be suspended	20->10 Hz vertically (starting at 20 Hz, adjustable by adding masses)	See the issue addressed in #2 above.
	14. Since the frame will be fused to avoid the frame's failure and/or equipment failure, it is doubtful that the experimental setup is suitable for testing a continuous suspended ceiling system. The members of the suspended ceiling are significantly weaker than the frame members, so failure of the ceiling system most likely will happen along the line connecting the fuses	The interpretation of the reader is incorrect. The lower level fuse is set to allow continuous structural behavior of the frame at small coupling errors in the shake table motions (such as realized in the Woodframe House testing) without any differential movement. The fuse will be activated only when the frame may reach one of its limits, which are set higher than the failure of ceilings or any other equipment. The higher level fuse will be set to damage the frame without damaging the tables.	See considerations in the left column and in the main document's descriptions.
	15. Most likely the test setup would represent an ordinary testing of two regular-sized suspended ceilings on two separate shaking tables connected to each other with some nonlinear extension.	See considerations explained in #14 above.	See considerations explained in #14.

Shakhzod Takhirov	16. Based on the two first bullets the reviewer would recommend to use the same setup that was used in the NEESWood project at the NEES's experimental site in Buffalo. According to the website of the project, the two tables were rigidly connected to each other to expand the footprint of the joined tables to 54' x 23' which would accommodate the 50'x20' frame	See considerations explained in #14 above.	See considerations explained in #14.
	17. It is not clear how the frame design reflects actual properties (frequency and stiffness) of a suspended ceiling's installation in real buildings. If the study on this matter had been conducted, the reference and main findings should be provided to backup the frame design.	We are using the floor considerations based on Murray et al. (1997), and assembly standards described in CISCA (2004a and 2004b), ASTM-580 (2008). Moreover, estimates of structural and nonstructural connections are being considered. While this is work in progress, the first draft was focused on geometric design. The properties of the frame are still in development. If the commenter has some additional information this can be used now.	See note on left column and in the issue addressed in #2.
Paul A Hough	18. Can the open web joists start 2' from the frame edge rather than 4'? This would greatly add installation of a ceiling.	Sure, we can manage that.	The new draft accommodates this requirement. The joists start now 2' from the frame edge.

Paul A Hough	19. Can the anchors or attachments of the frame go on the outside of the frame rather than the inside? (safety reasons)	NO, since there are no suitable anchoring holes on the outside. However, I shall check what can be done.	The anchor extensions (attachments) of the frame were eliminated. Frames are now connected directly to shake tables (extensions).
	20. Are the diagonal corner braces at the base of the frame needed after the frame is installed? Safety could be improved if they are not there but can be worked around if they are needed for stiffening.	We shall try to eliminate them in the detailed design	The diagonal bottom braces have been eliminated.
	21. Move initial ceiling height to just over 6'.	This is what I was hoping since the speed of test execution is very important (personnel time, safety, equipment usage, as well efficiency of industry testing).	See considerations explained in #8 (plenum depth) above.
	22. Side wall timbers should be expanded to at least 12 inches in width. They should be made of laminated 3/4" plywood and the inside walls of the frame squared. (Again installation help.)	Sure this can be done.	See considerations in the left column. (Details are being developed for the final draft.)
	23. Am I correct is assuming that z/h has nothing to do with the actual frame but does impact the way the table motions are developed?	Yes, you are correct.	See the initial answer in #5

Paul A Hough	24. I am also assuming that the ceilings & all suspension wire, etc will be fastened to the joists which will have the same stiffness as the frame. If this is not the case we need another surface with the same properties to attach to. It would be nice to make provisions that a case in place steel/concrete deck can be added at some future time, which could accommodate anchors into concrete.	We think along these lines, but more on using precast planks for adjustment of frequency.	See considerations in the left column. See also the issue addressed in #2.
	25. Some thought has to be given to a bridge or working surface that is safe to work from for the transitional piece between the two tables. I know you have thoughts but there was nothing detailed.	Indeed we are looking to extend the bridge used for the "wood-frame" structure testing as base for the transition between tables	An additional 10'-6" by 23'-0" bridge is planned between the two tables as a workspace and base plat-form See Draft 2 of frame assembly.

Appendix B
DESIGN & MODELING FEEDBACK-2

Response to Issues raised by the advisory group to Draft 2 of the Suggested Design

Comments to the design of an extended test frame were requested from the industry partners of SEESL and NEES *Simulation of the Seismic Performance of Nonstructural Systems* project, research management team (of NEES *Simulation of the Seismic Performance of Nonstructural Systems* project), and SEESL technical staff. The feedback was obtained for the period from May 10, 2009 to May 27, 2009. The frame design has been developed, incorporating the feedback. The comments and the issues addressed in the reply are summarized in Table B-1.

Table B-1 Feedback on the Draft 2 for the Period from 5/10/2009 to 5/27/2009

Reader	Comments & Questions	Reply
Bob Bachman	1. "The height of the test frame is 10 feet. with current assumed plenum depth being 1 ft. 9 inches. I have no clue where that number came from. We should have a range of plenum depths. As indicated, the minimum should be 1 ft. – 9 inches with the maximum being either 6 feet or 8 feet which raise the height of the test frame to either 12 feet or 14 feet. Remember the primary reason for this test frame in the first place is to determine the seismic vulnerabilities (and capacities) of ceiling systems and their interactions with other ceiling nonstructural components. There is some belief based on observations that ceilings with greater plenum depths are much more vulnerable and have lower capacity. Plenum depths of 6 or 8 feet are common in some building applications. It is important to have this capability built into the test frame."	#1. Height of frame (a) The height of frame was selected such that could allow rapid assembly and disassembly of components, therefore allowing a greater utilization of shake tables. (b) The plenum can be built of different heights by placing the "perimeter angles" at various elevations in increments of 4 ft. below the joists, therefore allowing plenum heights of 12 ft. to 72 ft. (c) Adverse effects for extreme plenum heights can be eliminated by designing the "table drive" – see the reply #2.

Bob Bachman	2. "I am still very concerned about the weight of the test frame roof. Actual typical floor/roof weights are in the range of 30 to 60 psf. While suspended ceiling weights are in the range of 2 to 4 psft. So the ratio between typical roof/flooring weights is in the range of 15 to 25 and therefore dynamic interaction between the two is not expected. However, it appears the test frame roof has weight is in the range of 5 - 8 psft and there the ratio is only 2 to 4 and dynamic interaction appears much more problematic vertically. There is some mention of concrete planks but they are not currently included in the design. I would feel very much more comfortable if the concrete planks were included in the design and the test frame roof weight was at least 30 psf."	#2. Roof weight and frequency range of frame (a) The roof was designed to have a vertical frequency above 20 Hz without additional mass (bare frame) having weight of roof ≤ 1 psf. (b) The roof will support an additional "floor weight" made of four planks of 4'×4'×2" placed above the center bays. This accounts for a distributed weight of 4 psf. This is the basic configuration having a vertical frequency of approximately 10 Hz which is characteristic to structural floors. (c) When extremely heavy ceiling tiles are added (having a weight of 3 psf), the frequency reduces to approximately 8 Hz, where further addition of tiles will create same effects as the original. Therefore the added mass of the roof would affect the floor frequency, but will keep it limited above 8 Hz, well within the range of regularity constructed floors. The response variations are limited to +/- 5% as shown in this document. Increase of weight of frame to values indicated in the comment is not feasible with shake tables (in the opinion of the design team).

Bob Bachman	3. "I am still very concerned about the damping of the test frame especially the test frame roof. Actual floor/ceilings are expected to have damping in the range of 5% for earthquake level vibrations. I expect the current bare steel test frame will have damping in the range of 1% or less. This will greatly overly amplify floor motions especially in the vertical direction particularly at the natural frequency of the roof ceiling. This may be reduced by concrete planks. It would good if the planks were not pre-tensioned. Pre-tensioned planks will have much less damping than non-pre-tensioned planks. I would like to see the damping of the roof/ceiling have damping the 5 % range."	#3. Roof Motion The frame was designed to be used with shake table motions programmed to deliver a desired "floor motion" at the roof level: (a) The "shake table command drive," in three directions, is modified by a procedure developed by the designers of the frame to generate a response of the roof based on dynamic properties of the frame (Maddaloni et al., 2009b). (b) The "command drive" can be designed to deliver alternatively damped motions as desired by the testing criteria. There is no need in the constructed frame to add damping. (c) The "command drive," compensated for the frame characteristics, is designed to reject higher modes effect in the frame structure. (d) The compensation procedure was already developed and a journal paper was written and is awaiting review. The information will be released to public as soon as the paper is approved. The procedure is suitable for applications to other types of shake tables, testing equipment, nonstructural components or substructures.
Dennis Alvarez	4. "I'm assuming the 1 ft. 9 in. is the plenum depth used for previous tests. I agree with Bob that the frame needs to be able to test larger plenums to evaluate the effect of plenum depth of ceiling performance. Plenum depths of up to 30 ft. are not uncommon, but I would agree with Bob to limit the depth to 6 ft. to 8 ft. as this should be sufficient to evaluate the effect of plenum depth on ceiling performance and 30' ft. plenums would not be practical."	See the issue addressed in the reply #1 above.

Dennis Alvarez	5. "I'll have to defer to Bob's greater expertise with regard to ceiling/structure interaction. I would like to see the vertical stiffness of the top of the frame increased to also avoid amplification of the vertical motion. Deeper/stiffer/additional joists would also increase the mass, although not nearly as much as concrete slabs."	See the issue addressed in the reply #2 above.
	6. "As Bob states, increased damping will also decrease over amplification of motion. Because of either stiffness concerns, weight concerns, or a combination of both, this will be a larger problem in the vertical direction."	See the issue addressed in the reply #3 above.
	7. "There are several positive changes to the frame and test program that I believe will enable a more accurate evaluation of ceiling performance. Currently, most tests show failure from vertical displacement of ceiling panels while most observed damage in ceilings is lateral damage at the perimeter. Previous tests were run with the acceleration set to z/h=1 for all three directions [Aflx=Sds*(1+(2*z/h)]. Vertically, z/h should have been set to zero. This will lessen the tendency for ceiling panels to be dislodged."	#4. Design of roof motion (a) The design of the roof motion is based on Mosqueda, Retamales, Filiatrault, and Reinhorn (2008), which could replace the AC-156 spectra (ICC, 2007). The primary change will have great effects on the vertical motion. (b) If AC-156 is not changed as indicated in (a) above, then the vertical motion should be determined from the horizontal using a function of 0.42 for A_{FLX} and 0.22 for A_{RIG}, not 0.67 as indicated today. The reason for such design is that motion in vertical direction developed at ground level is not amplified by the "usually" vertically rigid structure. (c) Command drive motion design (see the reply #3) is described in a journal paper (awaiting review).

Amir S.J. Gilani	**Test frame (#8 ~ #15)** 8. "Please clarify if the test frame intended to represent a typical story of a building or a generic frame used to envelope the response of many types of the construction. In the former case, the goal would be to survey a number of buildings and obtain their dynamic properties. While in the latter, the goal is try to design the frame dynamic properties to maximize the AC-156 (or other standard) input accelerations. I am not sure if the stated frequencies are representative of typical construction. The horizontal frequency is 20 Hz (0.05 sec) and could represent a very stiff walled or braced but not framed building. Most of our buildings are more flexible. The vertical frequency also appears high for typical construction."	#5. Wall Frequencies in and out-of-plane: (a) The in plane motion characteristics were designed considering flexibility (rigidity) of typical walls, having a natural frequency, approximately 17.7 Hz. (b) The shake table "floor motion" is designed (see the reply #3) to compensate for any excessive flexibility of walls.
	9. "The 10 ft. height might be Ok for testing but again it is not a typical building height. Would it be feasible to have a range for the heights for ceiling installations?"	See the issue addressed in the reply #1 above.
	10. "Is the roof design intended to be a rigid diaphragm?"	#6. The roof design is "rigid" in plane, i.e. frequencies larger than ten times of any service frequency.
	11. "The frame roof framing consists of HSS sections in one direction and open joists in the orthogonal direction. In typical floor construction, W sections are usually used with joists."	#7. It is correct that W sections are usually used with joists, however due to fabrication and instrumentation needs square tube bars were selected. The mechanical properties are equivalent in the relevant direction.
	12. "Would the typical floor inertial mass be included in tests? The existing bare metal frame is likely too light and does not include typical floor mass (60 or so psf) in design."	See the issue addressed in the reply #2 above.

Amir S.J. Gilani	13. "Could you elaborate on why a rigid connection (rather than the fuse) is not used between the two sub-frames? I believe the rigid type of arrangement was previously used in NEESWood project."	#8. The tandem shake table synchronization: The designed frame system has a middle component built to: (i) allow synchronized motion and suppress "minor discrepancies" between shake tables. Differential movement of up to 0.10" could be suppressed. This is a rigid brittle connection as used in the NEES wood project. (ii) larger differential motions "larger than 0.60" will break a "fuse" that will allow independent motion of shake tables without damaging any of the tables (controllers, connections, etc.).
	14. "The frame schematics show that the columns are not fixed at the base. The fixity location is offset from column longitudinal axis. The concern is that the column will uplift and induce addition flexibility to the system."	#9. The columns are supported by a base beam connected every 4 ft. to the shaking platform. The flexibility of the beam influences the vertical vibrations characteristics by 0.1 Hz (within the error of calculation) and 2 Hz in horizontal (which is compensated through the motion design). The designers shall explore a higher rigidity for the base beam.
	15. "Will you be able to adjust both the horizontal and vertical frame frequencies to mimic different type of construction?"	See the issue addressed in the reply #2 above.
	SAP model (#16 ~ #19) 16. "Could you describe the modeling used for the open web joist members and whether the shear deformation was included?"	#10. Used the joist element available in SAP2000. It is not clear how SAP2000 is considering shear. However, the stress analysis performed by hand calculations does not raise a flag. The shear stiffness and deformations are negligible here.

Amir S.J. Gilani	17. "I am not sure if you have used the SAP model for response history analysis. If so, do you have an analytical estimate on the level of seismic force transmitted by the frame to the grid components at a given input intensity?"	#11. See Figure 4-19 for analysis of the frame with random motions (AC-156 spectrum compatible for S_s = 3.0g) with peak ground acceleration of 1.28g horizontally and 0.53g vertically. Results are comparable to "Badillo et al. (2006)."
	18. "Would it be possible to obtain a copy of your analytical model of the test frame?"	#12. The current model is available upon request by e-mail.
	Input histories (#19 ~ #22) 19. "Will z/h be set to zero for vertical motion? If so, would the vertical RSS of the AC-156 should be modified for testing."	See the issue addressed in the reply #4 above. #13. Note: when z/h = 0, the vertical motion becomes approximately 0.42 (for A_{FLX}) and 0.22 (for A_{RIG}) of the horizontal motion (see AC-156 for guidance (ICC, 2007)), as well as the results.
	20. "The AC-156 response spectrum already includes all amplification for frame flexibility; I believe the intent is to apply the target motions to the roof (by applying the inverse transfer function at the base). This is a very good approach and we had previously discussed such method. <u>The question I have is whether you plan to use data from the corners or middle of the roof or a combination of the two.</u>"	#14. The motion is designed for the corner movement. The roof will amplify the motion depending on its dynamics. A user (lab engineer) may design the delivery of a center roof motion, or a combination of corner and center.
	21. "During the past tests, the input motions were filtered and the zero period accelerations were reduced. Will the same type of filtering be used in the upcoming tests?"	#15. (a) The accelerations at low frequencies are reduced to fit table max displacements. (b) The testing is done using incremental peak motions. (c) Filtering will be applied to meet equipment limits at max displacements.
	22. "Would it be possible to obtain a draft copy of reference 4 in the document?"	#16. A draft will be available with the completion of design. The paper is awaiting review.

Amir S.J. Gilani	**Test methodology** 23. "I have a question that is not directly related to the current project status but would like your input on. Currently, an ASTM test committee (comprised on many of us in the email list) is developing a standard regarding the earthquake simulator testing of suspended ceilings. The primary objective of the standard would be to serve as a reference document that provides guidelines and recommendations for future tests. Will the project team be inclined to consider using such document for the upcoming tests?"	#17. We are already studying the final draft of ASTM standard and we shall include it in the NEES program.
Tony Ingratta	24. "Since the ceiling height is +7 ft., ladders and or rolling scaffolds will be necessary to install the ceiling. A unitized smooth & level floor covering will be necessary over the existing grated floor on the shaker tables and link frame. The covering should to be tied to the shaker table to prevent shifting during the test. This will prevent tripping hazards and facilitate the use of rolling scaffolds etc. The slate sheets used previously continually shifted out of place causing a tripping hazard."	-
	25. "The 2'-4" deep built up trusses on the East and West ends of the link frame will set the plenum depth of the ceiling. Also, if one wanted to test concealed or direct attached drywall ceilings to the open web joists these deep members would not permit this type of installation. It is preferable to have all bottom cords of the joists and trusses in the same plane."	#18. While it is desirable to have all trusses and joists of same height, this is not possible. The vision is that all ceilings will be suspended from the upper surface of the roof which has all components in the same plane. In such case the plenum can be measured from the top surface.

Tony Ingratta	26. "It is preferable to maintain a 4- ft. or even better a 2- ft. on center spacing of the open web joists along the entire length of the frame. Ceiling hanger wires usually span 4- ft. on center. Compression posts and seismic bracing wires are usually located 12- ft. on center."	The new frame accommodates this within limits of the geometric design.
	27. "Should the perimeter angle be connected to a wood 1 x 6 as was done in previous shaker table testing? Or should consideration be given to a drywall and stud (steel or wood) perimeter to evaluate perimeter angle attachments to this common type of wall structure?"	#19. Both alternatives can be accommodated in the current design. Perhaps a suggested detail (from the commenter) would allow adequate provisions for both solutions.
	28. "If an ASTM standard could be promulgated before the tests begin, would you consider using that standard as the test methodology for the NSF -NEES Grand Challenge for Suspended Ceilings and Associated Fixtures?"	See comment in the reply #17 above.
Shakhzod Takhirov	**Which RRS to use? Industry needs new spectrum. (#29 ~ #32)** 29. "Coming back to the history of development of AC-156 document, it was originally developed by Square D / Scheider Electric Co and was primarily intended for testing electrical equipment which has limited number attachment points usually located close to each other."	#20. We are starting with the RRS from the AC-156, but have developed suggestions for new motions as published by Mosqueda et al. (2009b) for nonstructural components. Moreover we suggest developing new suit of ground motions compatible with the desired RS, which preserve the energy and velocity field. This will be part of the research in NEES project
	30. "In opposite to equipment, the suspended ceiling system represents a complex system with many and many attachment points while mass of the system is distributed over large area."	See comment in the reply #20 above.
	31. "Therefore, the current practice of using AC-156 spectra in seismic testing of suspended ceilings raises concern about validity of the approach."	See comment in the reply #20 above.

Shakhzod Takhirov	32. "Ideally, the primary goal of the NEES project should be to develop a solid approach for seismic testing of the suspended ceiling systems, which is easy to implement at various labs nationwide. As one of the examples of such solid approach would be to have 1) a relatively rigid frame in all three directions (size of which to be determined) that passes shaking table's impact with no or minimal amplification and 2) a spectrum that takes into account flexibility of the floor and horizontal amplification, as it is done in current AC-156. Once again, this new spectrum should take into account the majority of possible variations of the floor natural frequencies and their modes of vibration. In this case the main features of suspended ceilings systems such as large number of attachment points and distributed mass will be taken into account."	#21. Applicability of design to other installations: (a) The system is custom designed for the shake tables at SEESL. (b) However, the basic design (components) of 20 ft. × 20 ft. can be used in other large installations (Berkeley, CERL, UCSD, Reno, etc). (c) The procedure for roof motion generation developed in this research can be used at other installations with proper adjustment for local dynamics. (d) The design team can provide training to users and lab operators for similar developments
	Transfer Function Approach. (#33 ~ #36) 33. "The utilization of transfer function to achieve the required response spectra at the attachment points of the ceiling is a good approach to overcome some flexibility of the frame."	No comment necessary here.
	34. "In case of the NEES project it is not clear how the project will benefit from this approach. The amplification of the frame due its flexibility will be forced down by the transfer function to achieve matching criteria to the RRS."	See comment in the reply #3.
	35. "So, let's assume that we reduced the natural frequency of the floor and generated a transfer function for this setup. For the new natural frequency of the frame the transfer function will eliminate that amplification if are still trying to match to the same spectra."	No comment is necessary here.

Shakhzod Takhirov	36. "Another concern is a about transfer function itself which is usually based on prerecorded data. The suspended ceiling systems will perform non-linearly from level to level; therefore, the transfer function generated for certain level of testing most likely will not work for the next one up. If the transfer function can be generated on-fly, there is a concern about stability of shaking table control."	#22. Indeed the transfer function is generated prior to the testing. However during the testing this function will remain approximately the same. The qualification is done for ton level (the most challenging) therefore there is no need to look at variability with the level. However, if a future protocol will require that, then we suggest to use different amplification method (see Mosqueda et al. (2009b))
	Floor flexibility and its natural frequencies. (#37 ~ 38) 37. "There are many actual measurements of resonant frequencies of the floors. For instance, one of them studied composite 31m x 18.5m (93 ft. x 55 ft., so more than 5000 ft^2) steel deck floors and measured actual resonant frequency as low as 6.25 Hz. The other research studied 32 buildings and found that frequencies can vary from 3.5 Hz to 9.5 Hz."	#23. The designers shall appreciate getting the references for further cross checking. The current design is based on the information from Murray et al. (1997) and from his sources. The range goes from 2.8-12 Hz. We developed a system with frequencies between 8 and 10 Hz primarily but may be varied downwards.
	38. "So it looks that we have a quite a bit of variation of resonant frequencies. The other complication is a mode of vibration: one of the panels of the floor might be at its upside peak and another one can be at its downside peak as it is shown in SAP model of your frame. I would recommend conducting a detailed research on this issue. I support the majority of concerns raised by the community. Some of my comments described herein are similar to the concerns raised by others."	#24. It is the intent of work to develop the base motion such that will not excite the unwanted modes. But this will remain to be verified during the "shakedown" testing.

Dennis Alvarez	39. “While I'm sure Dr. Takhirov's comments are well taken, I'm concerned that some of his objectives are outside of the proposed objectives for the NEES study. I think there is a general consensus in the ceiling industry that further testing, using the same table as the NEES study, would be more appropriate for topics such as examining the suitability of the transfer function.”	#25. While one of the intentions is to verify the compensations using transfer functions, we are aware to the needs of industry, and try to reconcile some of the conflicting effects.

MCEER Technical Reports

MCEER publishes technical reports on a variety of subjects written by authors funded through MCEER. These reports are available from both MCEER Publications and the National Technical Information Service (NTIS). Requests for reports should be directed to MCEER Publications, MCEER, University at Buffalo, State University of New York, 133A Ketter Hall, Buffalo, New York 14260. Reports can also be requested through NTIS, P.O. Box 1425, Springfield, Virginia 22151. NTIS accession numbers are shown in parenthesis, if available.

NCEER-87-0001 "First-Year Program in Research, Education and Technology Transfer," 3/5/87, (PB88-134275, A04, MF-A01).

NCEER-87-0002 "Experimental Evaluation of Instantaneous Optimal Algorithms for Structural Control," by R.C. Lin, T.T. Soong and A.M. Reinhorn, 4/20/87, (PB88-134341, A04, MF-A01).

NCEER-87-0003 "Experimentation Using the Earthquake Simulation Facilities at University at Buffalo," by A.M. Reinhorn and R.L. Ketter, to be published.

NCEER-87-0004 "The System Characteristics and Performance of a Shaking Table," by J.S. Hwang, K.C. Chang and G.C. Lee, 6/1/87, (PB88-134259, A03, MF-A01). This report is available only through NTIS (see address given above).

NCEER-87-0005 "A Finite Element Formulation for Nonlinear Viscoplastic Material Using a Q Model," by O. Gyebi and G. Dasgupta, 11/2/87, (PB88-213764, A08, MF-A01).

NCEER-87-0006 "Symbolic Manipulation Program (SMP) - Algebraic Codes for Two and Three Dimensional Finite Element Formulations," by X. Lee and G. Dasgupta, 11/9/87, (PB88-218522, A05, MF-A01).

NCEER-87-0007 "Instantaneous Optimal Control Laws for Tall Buildings Under Seismic Excitations," by J.N. Yang, A. Akbarpour and P. Ghaemmaghami, 6/10/87, (PB88-134333, A06, MF-A01). This report is only available through NTIS (see address given above).

NCEER-87-0008 "IDARC: Inelastic Damage Analysis of Reinforced Concrete Frame - Shear-Wall Structures," by Y.J. Park, A.M. Reinhorn and S.K. Kunnath, 7/20/87, (PB88-134325, A09, MF-A01). This report is only available through NTIS (see address given above).

NCEER-87-0009 "Liquefaction Potential for New York State: A Preliminary Report on Sites in Manhattan and Buffalo," by M. Budhu, V. Vijayakumar, R.F. Giese and L. Baumgras, 8/31/87, (PB88-163704, A03, MF-A01). This report is available only through NTIS (see address given above).

NCEER-87-0010 "Vertical and Torsional Vibration of Foundations in Inhomogeneous Media," by A.S. Veletsos and K.W. Dotson, 6/1/87, (PB88-134291, A03, MF-A01). This report is only available through NTIS (see address given above).

NCEER-87-0011 "Seismic Probabilistic Risk Assessment and Seismic Margins Studies for Nuclear Power Plants," by Howard H.M. Hwang, 6/15/87, (PB88-134267, A03, MF-A01). This report is only available through NTIS (see address given above).

NCEER-87-0012 "Parametric Studies of Frequency Response of Secondary Systems Under Ground-Acceleration Excitations," by Y. Yong and Y.K. Lin, 6/10/87, (PB88-134309, A03, MF-A01). This report is only available through NTIS (see address given above).

NCEER-87-0013 "Frequency Response of Secondary Systems Under Seismic Excitation," by J.A. HoLung, J. Cai and Y.K. Lin, 7/31/87, (PB88-134317, A05, MF-A01). This report is only available through NTIS (see address given above).

NCEER-87-0014 "Modelling Earthquake Ground Motions in Seismically Active Regions Using Parametric Time Series Methods," by G.W. Ellis and A.S. Cakmak, 8/25/87, (PB88-134283, A08, MF-A01). This report is only available through NTIS (see address given above).

NCEER-87-0015 "Detection and Assessment of Seismic Structural Damage," by E. DiPasquale and A.S. Cakmak, 8/25/87, (PB88-163712, A05, MF-A01). This report is only available through NTIS (see address given above).

NCEER-87-0016 "Pipeline Experiment at Parkfield, California," by J. Isenberg and E. Richardson, 9/15/87, (PB88-163720, A03, MF-A01). This report is available only through NTIS (see address given above).

NCEER-87-0017 "Digital Simulation of Seismic Ground Motion," by M. Shinozuka, G. Deodatis and T. Harada, 8/31/87, (PB88-155197, A04, MF-A01). This report is available only through NTIS (see address given above).

NCEER-87-0018 "Practical Considerations for Structural Control: System Uncertainty, System Time Delay and Truncation of Small Control Forces," J.N. Yang and A. Akbarpour, 8/10/87, (PB88-163738, A08, MF-A01). This report is only available through NTIS (see address given above).

NCEER-87-0019 "Modal Analysis of Nonclassically Damped Structural Systems Using Canonical Transformation," by J.N. Yang, S. Sarkani and F.X. Long, 9/27/87, (PB88-187851, A04, MF-A01).

NCEER-87-0020 "A Nonstationary Solution in Random Vibration Theory," by J.R. Red-Horse and P.D. Spanos, 11/3/87, (PB88-163746, A03, MF-A01).

NCEER-87-0021 "Horizontal Impedances for Radially Inhomogeneous Viscoelastic Soil Layers," by A.S. Veletsos and K.W. Dotson, 10/15/87, (PB88-150859, A04, MF-A01).

NCEER-87-0022 "Seismic Damage Assessment of Reinforced Concrete Members," by Y.S. Chung, C. Meyer and M. Shinozuka, 10/9/87, (PB88-150867, A05, MF-A01). This report is available only through NTIS (see address given above).

NCEER-87-0023 "Active Structural Control in Civil Engineering," by T.T. Soong, 11/11/87, (PB88-187778, A03, MF-A01).

NCEER-87-0024 "Vertical and Torsional Impedances for Radially Inhomogeneous Viscoelastic Soil Layers," by K.W. Dotson and A.S. Veletsos, 12/87, (PB88-187786, A03, MF-A01).

NCEER-87-0025 "Proceedings from the Symposium on Seismic Hazards, Ground Motions, Soil-Liquefaction and Engineering Practice in Eastern North America," October 20-22, 1987, edited by K.H. Jacob, 12/87, (PB88-188115, A23, MF-A01). This report is available only through NTIS (see address given above).

NCEER-87-0026 "Report on the Whittier-Narrows, California, Earthquake of October 1, 1987," by J. Pantelic and A. Reinhorn, 11/87, (PB88-187752, A03, MF-A01). This report is available only through NTIS (see address given above).

NCEER-87-0027 "Design of a Modular Program for Transient Nonlinear Analysis of Large 3-D Building Structures," by S. Srivastav and J.F. Abel, 12/30/87, (PB88-187950, A05, MF-A01). This report is only available through NTIS (see address given above).

NCEER-87-0028 "Second-Year Program in Research, Education and Technology Transfer," 3/8/88, (PB88-219480, A04, MF-A01).

NCEER-88-0001 "Workshop on Seismic Computer Analysis and Design of Buildings With Interactive Graphics," by W. McGuire, J.F. Abel and C.H. Conley, 1/18/88, (PB88-187760, A03, MF-A01). This report is only available through NTIS (see address given above).

NCEER-88-0002 "Optimal Control of Nonlinear Flexible Structures," by J.N. Yang, F.X. Long and D. Wong, 1/22/88, (PB88-213772, A06, MF-A01).

NCEER-88-0003 "Substructuring Techniques in the Time Domain for Primary-Secondary Structural Systems," by G.D. Manolis and G. Juhn, 2/10/88, (PB88-213780, A04, MF-A01).

NCEER-88-0004 "Iterative Seismic Analysis of Primary-Secondary Systems," by A. Singhal, L.D. Lutes and P.D. Spanos, 2/23/88, (PB88-213798, A04, MF-A01).

NCEER-88-0005 "Stochastic Finite Element Expansion for Random Media," by P.D. Spanos and R. Ghanem, 3/14/88, (PB88-213806, A03, MF-A01).

NCEER-88-0006 "Combining Structural Optimization and Structural Control," by F.Y. Cheng and C.P. Pantelides, 1/10/88, (PB88-213814, A05, MF-A01).

NCEER-88-0007 "Seismic Performance Assessment of Code-Designed Structures," by H.H-M. Hwang, J-W. Jaw and H-J. Shau, 3/20/88, (PB88-219423, A04, MF-A01). This report is only available through NTIS (see address given above).

NCEER-88-0008 "Reliability Analysis of Code-Designed Structures Under Natural Hazards," by H.H-M. Hwang, H. Ushiba and M. Shinozuka, 2/29/88, (PB88-229471, A07, MF-A01). This report is only available through NTIS (see address given above).

NCEER-88-0009 "Seismic Fragility Analysis of Shear Wall Structures," by J-W Jaw and H.H-M. Hwang, 4/30/88, (PB89-102867, A04, MF-A01).

NCEER-88-0010 "Base Isolation of a Multi-Story Building Under a Harmonic Ground Motion - A Comparison of Performances of Various Systems," by F-G Fan, G. Ahmadi and I.G. Tadjbakhsh, 5/18/88, (PB89-122238, A06, MF-A01). This report is only available through NTIS (see address given above).

NCEER-88-0011 "Seismic Floor Response Spectra for a Combined System by Green's Functions," by F.M. Lavelle, L.A. Bergman and P.D. Spanos, 5/1/88, (PB89-102875, A03, MF-A01).

NCEER-88-0012 "A New Solution Technique for Randomly Excited Hysteretic Structures," by G.Q. Cai and Y.K. Lin, 5/16/88, (PB89-102883, A03, MF-A01).

NCEER-88-0013 "A Study of Radiation Damping and Soil-Structure Interaction Effects in the Centrifuge," by K. Weissman, supervised by J.H. Prevost, 5/24/88, (PB89-144703, A06, MF-A01).

NCEER-88-0014 "Parameter Identification and Implementation of a Kinematic Plasticity Model for Frictional Soils," by J.H. Prevost and D.V. Griffiths, to be published.

NCEER-88-0015 "Two- and Three- Dimensional Dynamic Finite Element Analyses of the Long Valley Dam," by D.V. Griffiths and J.H. Prevost, 6/17/88, (PB89-144711, A04, MF-A01).

NCEER-88-0016 "Damage Assessment of Reinforced Concrete Structures in Eastern United States," by A.M. Reinhorn, M.J. Seidel, S.K. Kunnath and Y.J. Park, 6/15/88, (PB89-122220, A04, MF-A01). This report is only available through NTIS (see address given above).

NCEER-88-0017 "Dynamic Compliance of Vertically Loaded Strip Foundations in Multilayered Viscoelastic Soils," by S. Ahmad and A.S.M. Israil, 6/17/88, (PB89-102891, A04, MF-A01).

NCEER-88-0018 "An Experimental Study of Seismic Structural Response With Added Viscoelastic Dampers," by R.C. Lin, Z. Liang, T.T. Soong and R.H. Zhang, 6/30/88, (PB89-122212, A05, MF-A01). This report is available only through NTIS (see address given above).

NCEER-88-0019 "Experimental Investigation of Primary - Secondary System Interaction," by G.D. Manolis, G. Juhn and A.M. Reinhorn, 5/27/88, (PB89-122204, A04, MF-A01).

NCEER-88-0020 "A Response Spectrum Approach For Analysis of Nonclassically Damped Structures," by J.N. Yang, S. Sarkani and F.X. Long, 4/22/88, (PB89-102909, A04, MF-A01).

NCEER-88-0021 "Seismic Interaction of Structures and Soils: Stochastic Approach," by A.S. Veletsos and A.M. Prasad, 7/21/88, (PB89-122196, A04, MF-A01). This report is only available through NTIS (see address given above).

NCEER-88-0022 "Identification of the Serviceability Limit State and Detection of Seismic Structural Damage," by E. DiPasquale and A.S. Cakmak, 6/15/88, (PB89-122188, A05, MF-A01). This report is available only through NTIS (see address given above).

NCEER-88-0023 "Multi-Hazard Risk Analysis: Case of a Simple Offshore Structure," by B.K. Bhartia and E.H. Vanmarcke, 7/21/88, (PB89-145213, A05, MF-A01).

NCEER-88-0024 "Automated Seismic Design of Reinforced Concrete Buildings," by Y.S. Chung, C. Meyer and M. Shinozuka, 7/5/88, (PB89-122170, A06, MF-A01). This report is available only through NTIS (see address given above).

NCEER-88-0025 "Experimental Study of Active Control of MDOF Structures Under Seismic Excitations," by L.L. Chung, R.C. Lin, T.T. Soong and A.M. Reinhorn, 7/10/88, (PB89-122600, A04, MF-A01).

NCEER-88-0026 "Earthquake Simulation Tests of a Low-Rise Metal Structure," by J.S. Hwang, K.C. Chang, G.C. Lee and R.L. Ketter, 8/1/88, (PB89-102917, A04, MF-A01).

NCEER-88-0027 "Systems Study of Urban Response and Reconstruction Due to Catastrophic Earthquakes," by F. Kozin and H.K. Zhou, 9/22/88, (PB90-162348, A04, MF-A01).

NCEER-88-0028 "Seismic Fragility Analysis of Plane Frame Structures," by H.H-M. Hwang and Y.K. Low, 7/31/88, (PB89-131445, A06, MF-A01).

NCEER-88-0029 "Response Analysis of Stochastic Structures," by A. Kardara, C. Bucher and M. Shinozuka, 9/22/88, (PB89-174429, A04, MF-A01).

NCEER-88-0030 "Nonnormal Accelerations Due to Yielding in a Primary Structure," by D.C.K. Chen and L.D. Lutes, 9/19/88, (PB89-131437, A04, MF-A01).

NCEER-88-0031 "Design Approaches for Soil-Structure Interaction," by A.S. Veletsos, A.M. Prasad and Y. Tang, 12/30/88, (PB89-174437, A03, MF-A01). This report is available only through NTIS (see address given above).

NCEER-88-0032 "A Re-evaluation of Design Spectra for Seismic Damage Control," by C.J. Turkstra and A.G. Tallin, 11/7/88, (PB89-145221, A05, MF-A01).

NCEER-88-0033 "The Behavior and Design of Noncontact Lap Splices Subjected to Repeated Inelastic Tensile Loading," by V.E. Sagan, P. Gergely and R.N. White, 12/8/88, (PB89-163737, A08, MF-A01).

NCEER-88-0034 "Seismic Response of Pile Foundations," by S.M. Mamoon, P.K. Banerjee and S. Ahmad, 11/1/88, (PB89-145239, A04, MF-A01).

NCEER-88-0035 "Modeling of R/C Building Structures With Flexible Floor Diaphragms (IDARC2)," by A.M. Reinhorn, S.K. Kunnath and N. Panahshahi, 9/7/88, (PB89-207153, A07, MF-A01).

NCEER-88-0036 "Solution of the Dam-Reservoir Interaction Problem Using a Combination of FEM, BEM with Particular Integrals, Modal Analysis, and Substructuring," by C-S. Tsai, G.C. Lee and R.L. Ketter, 12/31/88, (PB89-207146, A04, MF-A01).

NCEER-88-0037 "Optimal Placement of Actuators for Structural Control," by F.Y. Cheng and C.P. Pantelides, 8/15/88, (PB89-162846, A05, MF-A01).

NCEER-88-0038 "Teflon Bearings in Aseismic Base Isolation: Experimental Studies and Mathematical Modeling," by A. Mokha, M.C. Constantinou and A.M. Reinhorn, 12/5/88, (PB89-218457, A10, MF-A01). This report is available only through NTIS (see address given above).

NCEER-88-0039 "Seismic Behavior of Flat Slab High-Rise Buildings in the New York City Area," by P. Weidlinger and M. Ettouney, 10/15/88, (PB90-145681, A04, MF-A01).

NCEER-88-0040 "Evaluation of the Earthquake Resistance of Existing Buildings in New York City," by P. Weidlinger and M. Ettouney, 10/15/88, to be published.

NCEER-88-0041 "Small-Scale Modeling Techniques for Reinforced Concrete Structures Subjected to Seismic Loads," by W. Kim, A. El-Attar and R.N. White, 11/22/88, (PB89-189625, A05, MF-A01).

NCEER-88-0042 "Modeling Strong Ground Motion from Multiple Event Earthquakes," by G.W. Ellis and A.S. Cakmak, 10/15/88, (PB89-174445, A03, MF-A01).

NCEER-88-0043 "Nonstationary Models of Seismic Ground Acceleration," by M. Grigoriu, S.E. Ruiz and E. Rosenblueth, 7/15/88, (PB89-189617, A04, MF-A01).

NCEER-88-0044 "SARCF User's Guide: Seismic Analysis of Reinforced Concrete Frames," by Y.S. Chung, C. Meyer and M. Shinozuka, 11/9/88, (PB89-174452, A08, MF-A01).

NCEER-88-0045 "First Expert Panel Meeting on Disaster Research and Planning," edited by J. Pantelic and J. Stoyle, 9/15/88, (PB89-174460, A05, MF-A01).

NCEER-88-0046 "Preliminary Studies of the Effect of Degrading Infill Walls on the Nonlinear Seismic Response of Steel Frames," by C.Z. Chrysostomou, P. Gergely and J.F. Abel, 12/19/88, (PB89-208383, A05, MF-A01).

NCEER-88-0047 "Reinforced Concrete Frame Component Testing Facility - Design, Construction, Instrumentation and Operation," by S.P. Pessiki, C. Conley, T. Bond, P. Gergely and R.N. White, 12/16/88, (PB89-174478, A04, MF-A01).

NCEER-89-0001 "Effects of Protective Cushion and Soil Compliancy on the Response of Equipment Within a Seismically Excited Building," by J.A. HoLung, 2/16/89, (PB89-207179, A04, MF-A01).

NCEER-89-0002 "Statistical Evaluation of Response Modification Factors for Reinforced Concrete Structures," by H.H-M. Hwang and J-W. Jaw, 2/17/89, (PB89-207187, A05, MF-A01).

NCEER-89-0003 "Hysteretic Columns Under Random Excitation," by G-Q. Cai and Y.K. Lin, 1/9/89, (PB89-196513, A03, MF-A01).

NCEER-89-0004 "Experimental Study of `Elephant Foot Bulge' Instability of Thin-Walled Metal Tanks," by Z-H. Jia and R.L. Ketter, 2/22/89, (PB89-207195, A03, MF-A01).

NCEER-89-0005 "Experiment on Performance of Buried Pipelines Across San Andreas Fault," by J. Isenberg, E. Richardson and T.D. O'Rourke, 3/10/89, (PB89-218440, A04, MF-A01). This report is available only through NTIS (see address given above).

NCEER-89-0006 "A Knowledge-Based Approach to Structural Design of Earthquake-Resistant Buildings," by M. Subramani, P. Gergely, C.H. Conley, J.F. Abel and A.H. Zaghw, 1/15/89, (PB89-218465, A06, MF-A01).

NCEER-89-0007 "Liquefaction Hazards and Their Effects on Buried Pipelines," by T.D. O'Rourke and P.A. Lane, 2/1/89, (PB89-218481, A09, MF-A01).

NCEER-89-0008 "Fundamentals of System Identification in Structural Dynamics," by H. Imai, C-B. Yun, O. Maruyama and M. Shinozuka, 1/26/89, (PB89-207211, A04, MF-A01).

NCEER-89-0009 "Effects of the 1985 Michoacan Earthquake on Water Systems and Other Buried Lifelines in Mexico," by A.G. Ayala and M.J. O'Rourke, 3/8/89, (PB89-207229, A06, MF-A01).

NCEER-89-R010 "NCEER Bibliography of Earthquake Education Materials," by K.E.K. Ross, Second Revision, 9/1/89, (PB90-125352, A05, MF-A01). This report is replaced by NCEER-92-0018.

NCEER-89-0011 "Inelastic Three-Dimensional Response Analysis of Reinforced Concrete Building Structures (IDARC-3D), Part I - Modeling," by S.K. Kunnath and A.M. Reinhorn, 4/17/89, (PB90-114612, A07, MF-A01). This report is available only through NTIS (see address given above).

NCEER-89-0012 "Recommended Modifications to ATC-14," by C.D. Poland and J.O. Malley, 4/12/89, (PB90-108648, A15, MF-A01).

NCEER-89-0013 "Repair and Strengthening of Beam-to-Column Connections Subjected to Earthquake Loading," by M. Corazao and A.J. Durrani, 2/28/89, (PB90-109885, A06, MF-A01).

NCEER-89-0014 "Program EXKAL2 for Identification of Structural Dynamic Systems," by O. Maruyama, C-B. Yun, M. Hoshiya and M. Shinozuka, 5/19/89, (PB90-109877, A09, MF-A01).

NCEER-89-0015 "Response of Frames With Bolted Semi-Rigid Connections, Part I - Experimental Study and Analytical Predictions," by P.J. DiCorso, A.M. Reinhorn, J.R. Dickerson, J.B. Radziminski and W.L. Harper, 6/1/89, to be published.

NCEER-89-0016 "ARMA Monte Carlo Simulation in Probabilistic Structural Analysis," by P.D. Spanos and M.P. Mignolet, 7/10/89, (PB90-109893, A03, MF-A01).

NCEER-89-P017 "Preliminary Proceedings from the Conference on Disaster Preparedness - The Place of Earthquake Education in Our Schools," Edited by K.E.K. Ross, 6/23/89, (PB90-108606, A03, MF-A01).

NCEER-89-0017 "Proceedings from the Conference on Disaster Preparedness - The Place of Earthquake Education in Our Schools," Edited by K.E.K. Ross, 12/31/89, (PB90-207895, A012, MF-A02). This report is available only through NTIS (see address given above).

NCEER-89-0018 "Multidimensional Models of Hysteretic Material Behavior for Vibration Analysis of Shape Memory Energy Absorbing Devices, by E.J. Graesser and F.A. Cozzarelli, 6/7/89, (PB90-164146, A04, MF-A01).

NCEER-89-0019 "Nonlinear Dynamic Analysis of Three-Dimensional Base Isolated Structures (3D-BASIS)," by S. Nagarajaiah, A.M. Reinhorn and M.C. Constantinou, 8/3/89, (PB90-161936, A06, MF-A01). This report has been replaced by NCEER-93-0011.

NCEER-89-0020 "Structural Control Considering Time-Rate of Control Forces and Control Rate Constraints," by F.Y. Cheng and C.P. Pantelides, 8/3/89, (PB90-120445, A04, MF-A01).

NCEER-89-0021 "Subsurface Conditions of Memphis and Shelby County," by K.W. Ng, T-S. Chang and H-H.M. Hwang, 7/26/89, (PB90-120437, A03, MF-A01).

NCEER-89-0022 "Seismic Wave Propagation Effects on Straight Jointed Buried Pipelines," by K. Elhmadi and M.J. O'Rourke, 8/24/89, (PB90-162322, A10, MF-A02).

NCEER-89-0023 "Workshop on Serviceability Analysis of Water Delivery Systems," edited by M. Grigoriu, 3/6/89, (PB90-127424, A03, MF-A01).

NCEER-89-0024 "Shaking Table Study of a 1/5 Scale Steel Frame Composed of Tapered Members," by K.C. Chang, J.S. Hwang and G.C. Lee, 9/18/89, (PB90-160169, A04, MF-A01).

NCEER-89-0025 "DYNA1D: A Computer Program for Nonlinear Seismic Site Response Analysis - Technical Documentation," by Jean H. Prevost, 9/14/89, (PB90-161944, A07, MF-A01). This report is available only through NTIS (see address given above).

NCEER-89-0026 "1:4 Scale Model Studies of Active Tendon Systems and Active Mass Dampers for Aseismic Protection," by A.M. Reinhorn, T.T. Soong, R.C. Lin, Y.P. Yang, Y. Fukao, H. Abe and M. Nakai, 9/15/89, (PB90-173246, A10, MF-A02). This report is available only through NTIS (see address given above).

NCEER-89-0027 "Scattering of Waves by Inclusions in a Nonhomogeneous Elastic Half Space Solved by Boundary Element Methods," by P.K. Hadley, A. Askar and A.S. Cakmak, 6/15/89, (PB90-145699, A07, MF-A01).

NCEER-89-0028 "Statistical Evaluation of Deflection Amplification Factors for Reinforced Concrete Structures," by H.H.M. Hwang, J-W. Jaw and A.L. Ch'ng, 8/31/89, (PB90-164633, A05, MF-A01).

NCEER-89-0029 "Bedrock Accelerations in Memphis Area Due to Large New Madrid Earthquakes," by H.H.M. Hwang, C.H.S. Chen and G. Yu, 11/7/89, (PB90-162330, A04, MF-A01).

NCEER-89-0030 "Seismic Behavior and Response Sensitivity of Secondary Structural Systems," by Y.Q. Chen and T.T. Soong, 10/23/89, (PB90-164658, A08, MF-A01).

NCEER-89-0031 "Random Vibration and Reliability Analysis of Primary-Secondary Structural Systems," by Y. Ibrahim, M. Grigoriu and T.T. Soong, 11/10/89, (PB90-161951, A04, MF-A01).

NCEER-89-0032 "Proceedings from the Second U.S. - Japan Workshop on Liquefaction, Large Ground Deformation and Their Effects on Lifelines, September 26-29, 1989," Edited by T.D. O'Rourke and M. Hamada, 12/1/89, (PB90-209388, A22, MF-A03).

NCEER-89-0033 "Deterministic Model for Seismic Damage Evaluation of Reinforced Concrete Structures," by J.M. Bracci, A.M. Reinhorn, J.B. Mander and S.K. Kunnath, 9/27/89, (PB91-108803, A06, MF-A01).

NCEER-89-0034 "On the Relation Between Local and Global Damage Indices," by E. DiPasquale and A.S. Cakmak, 8/15/89, (PB90-173865, A05, MF-A01).

NCEER-89-0035 "Cyclic Undrained Behavior of Nonplastic and Low Plasticity Silts," by A.J. Walker and H.E. Stewart, 7/26/89, (PB90-183518, A10, MF-A01).

NCEER-89-0036 "Liquefaction Potential of Surficial Deposits in the City of Buffalo, New York," by M. Budhu, R. Giese and L. Baumgrass, 1/17/89, (PB90-208455, A04, MF-A01).

NCEER-89-0037 "A Deterministic Assessment of Effects of Ground Motion Incoherence," by A.S. Veletsos and Y. Tang, 7/15/89, (PB90-164294, A03, MF-A01).

NCEER-89-0038 "Workshop on Ground Motion Parameters for Seismic Hazard Mapping," July 17-18, 1989, edited by R.V. Whitman, 12/1/89, (PB90-173923, A04, MF-A01).

NCEER-89-0039 "Seismic Effects on Elevated Transit Lines of the New York City Transit Authority," by C.J. Costantino, C.A. Miller and E. Heymsfield, 12/26/89, (PB90-207887, A06, MF-A01).

NCEER-89-0040 "Centrifugal Modeling of Dynamic Soil-Structure Interaction," by K. Weissman, Supervised by J.H. Prevost, 5/10/89, (PB90-207879, A07, MF-A01).

NCEER-89-0041 "Linearized Identification of Buildings With Cores for Seismic Vulnerability Assessment," by I-K. Ho and A.E. Aktan, 11/1/89, (PB90-251943, A07, MF-A01).

NCEER-90-0001 "Geotechnical and Lifeline Aspects of the October 17, 1989 Loma Prieta Earthquake in San Francisco," by T.D. O'Rourke, H.E. Stewart, F.T. Blackburn and T.S. Dickerman, 1/90, (PB90-208596, A05, MF-A01).

NCEER-90-0002 "Nonnormal Secondary Response Due to Yielding in a Primary Structure," by D.C.K. Chen and L.D. Lutes, 2/28/90, (PB90-251976, A07, MF-A01).

NCEER-90-0003 "Earthquake Education Materials for Grades K-12," by K.E.K. Ross, 4/16/90, (PB91-251984, A05, MF-A05). This report has been replaced by NCEER-92-0018.

NCEER-90-0004 "Catalog of Strong Motion Stations in Eastern North America," by R.W. Busby, 4/3/90, (PB90-251984, A05, MF-A01).

NCEER-90-0005 "NCEER Strong-Motion Data Base: A User Manual for the GeoBase Release (Version 1.0 for the Sun3)," by P. Friberg and K. Jacob, 3/31/90 (PB90-258062, A04, MF-A01).

NCEER-90-0006 "Seismic Hazard Along a Crude Oil Pipeline in the Event of an 1811-1812 Type New Madrid Earthquake," by H.H.M. Hwang and C-H.S. Chen, 4/16/90, (PB90-258054, A04, MF-A01).

NCEER-90-0007 "Site-Specific Response Spectra for Memphis Sheahan Pumping Station," by H.H.M. Hwang and C.S. Lee, 5/15/90, (PB91-108811, A05, MF-A01).

NCEER-90-0008 "Pilot Study on Seismic Vulnerability of Crude Oil Transmission Systems," by T. Ariman, R. Dobry, M. Grigoriu, F. Kozin, M. O'Rourke, T. O'Rourke and M. Shinozuka, 5/25/90, (PB91-108837, A06, MF-A01).

NCEER-90-0009 "A Program to Generate Site Dependent Time Histories: EQGEN," by G.W. Ellis, M. Srinivasan and A.S. Cakmak, 1/30/90, (PB91-108829, A04, MF-A01).

NCEER-90-0010 "Active Isolation for Seismic Protection of Operating Rooms," by M.E. Talbott, Supervised by M. Shinozuka, 6/8/9, (PB91-110205, A05, MF-A01).

NCEER-90-0011 "Program LINEARID for Identification of Linear Structural Dynamic Systems," by C-B. Yun and M. Shinozuka, 6/25/90, (PB91-110312, A08, MF-A01).

NCEER-90-0012 "Two-Dimensional Two-Phase Elasto-Plastic Seismic Response of Earth Dams," by A.N. Yiagos, Supervised by J.H. Prevost, 6/20/90, (PB91-110197, A13, MF-A02).

NCEER-90-0013 "Secondary Systems in Base-Isolated Structures: Experimental Investigation, Stochastic Response and Stochastic Sensitivity," by G.D. Manolis, G. Juhn, M.C. Constantinou and A.M. Reinhorn, 7/1/90, (PB91-110320, A08, MF-A01).

NCEER-90-0014 "Seismic Behavior of Lightly-Reinforced Concrete Column and Beam-Column Joint Details," by S.P. Pessiki, C.H. Conley, P. Gergely and R.N. White, 8/22/90, (PB91-108795, A11, MF-A02).

NCEER-90-0015 "Two Hybrid Control Systems for Building Structures Under Strong Earthquakes," by J.N. Yang and A. Danielians, 6/29/90, (PB91-125393, A04, MF-A01).

NCEER-90-0016 "Instantaneous Optimal Control with Acceleration and Velocity Feedback," by J.N. Yang and Z. Li, 6/29/90, (PB91-125401, A03, MF-A01).

NCEER-90-0017 "Reconnaissance Report on the Northern Iran Earthquake of June 21, 1990," by M. Mehrain, 10/4/90, (PB91-125377, A03, MF-A01).

NCEER-90-0018 "Evaluation of Liquefaction Potential in Memphis and Shelby County," by T.S. Chang, P.S. Tang, C.S. Lee and H. Hwang, 8/10/90, (PB91-125427, A09, MF-A01).

NCEER-90-0019 "Experimental and Analytical Study of a Combined Sliding Disc Bearing and Helical Steel Spring Isolation System," by M.C. Constantinou, A.S. Mokha and A.M. Reinhorn, 10/4/90, (PB91-125385, A06, MF-A01). This report is available only through NTIS (see address given above).

NCEER-90-0020 "Experimental Study and Analytical Prediction of Earthquake Response of a Sliding Isolation System with a Spherical Surface," by A.S. Mokha, M.C. Constantinou and A.M. Reinhorn, 10/11/90, (PB91-125419, A05, MF-A01).

NCEER-90-0021 "Dynamic Interaction Factors for Floating Pile Groups," by G. Gazetas, K. Fan, A. Kaynia and E. Kausel, 9/10/90, (PB91-170381, A05, MF-A01).

NCEER-90-0022 "Evaluation of Seismic Damage Indices for Reinforced Concrete Structures," by S. Rodriguez-Gomez and A.S. Cakmak, 9/30/90, PB91-171322, A06, MF-A01).

NCEER-90-0023 "Study of Site Response at a Selected Memphis Site," by H. Desai, S. Ahmad, E.S. Gazetas and M.R. Oh, 10/11/90, (PB91-196857, A03, MF-A01).

NCEER-90-0024 "A User's Guide to Strongmo: Version 1.0 of NCEER's Strong-Motion Data Access Tool for PCs and Terminals," by P.A. Friberg and C.A.T. Susch, 11/15/90, (PB91-171272, A03, MF-A01).

NCEER-90-0025 "A Three-Dimensional Analytical Study of Spatial Variability of Seismic Ground Motions," by L-L. Hong and A.H.-S. Ang, 10/30/90, (PB91-170399, A09, MF-A01).

NCEER-90-0026 "MUMOID User's Guide - A Program for the Identification of Modal Parameters," by S. Rodriguez-Gomez and E. DiPasquale, 9/30/90, (PB91-171298, A04, MF-A01).

NCEER-90-0027 "SARCF-II User's Guide - Seismic Analysis of Reinforced Concrete Frames," by S. Rodriguez-Gomez, Y.S. Chung and C. Meyer, 9/30/90, (PB91-171280, A05, MF-A01).

NCEER-90-0028 "Viscous Dampers: Testing, Modeling and Application in Vibration and Seismic Isolation," by N. Makris and M.C. Constantinou, 12/20/90 (PB91-190561, A06, MF-A01).

NCEER-90-0029 "Soil Effects on Earthquake Ground Motions in the Memphis Area," by H. Hwang, C.S. Lee, K.W. Ng and T.S. Chang, 8/2/90, (PB91-190751, A05, MF-A01).

NCEER-91-0001 "Proceedings from the Third Japan-U.S. Workshop on Earthquake Resistant Design of Lifeline Facilities and Countermeasures for Soil Liquefaction, December 17-19, 1990," edited by T.D. O'Rourke and M. Hamada, 2/1/91, (PB91-179259, A99, MF-A04).

NCEER-91-0002 "Physical Space Solutions of Non-Proportionally Damped Systems," by M. Tong, Z. Liang and G.C. Lee, 1/15/91, (PB91-179242, A04, MF-A01).

NCEER-91-0003 "Seismic Response of Single Piles and Pile Groups," by K. Fan and G. Gazetas, 1/10/91, (PB92-174994, A04, MF-A01).

NCEER-91-0004 "Damping of Structures: Part 1 - Theory of Complex Damping," by Z. Liang and G. Lee, 10/10/91, (PB92-197235, A12, MF-A03).

NCEER-91-0005 "3D-BASIS - Nonlinear Dynamic Analysis of Three Dimensional Base Isolated Structures: Part II," by S. Nagarajaiah, A.M. Reinhorn and M.C. Constantinou, 2/28/91, (PB91-190553, A07, MF-A01). This report has been replaced by NCEER-93-0011.

NCEER-91-0006 "A Multidimensional Hysteretic Model for Plasticity Deforming Metals in Energy Absorbing Devices," by E.J. Graesser and F.A. Cozzarelli, 4/9/91, (PB92-108364, A04, MF-A01).

NCEER-91-0007 "A Framework for Customizable Knowledge-Based Expert Systems with an Application to a KBES for Evaluating the Seismic Resistance of Existing Buildings," by E.G. Ibarra-Anaya and S.J. Fenves, 4/9/91, (PB91-210930, A08, MF-A01).

NCEER-91-0008 "Nonlinear Analysis of Steel Frames with Semi-Rigid Connections Using the Capacity Spectrum Method," by G.G. Deierlein, S-H. Hsieh, Y-J. Shen and J.F. Abel, 7/2/91, (PB92-113828, A05, MF-A01).

NCEER-91-0009 "Earthquake Education Materials for Grades K-12," by K.E.K. Ross, 4/30/91, (PB91-212142, A06, MF-A01). This report has been replaced by NCEER-92-0018.

NCEER-91-0010 "Phase Wave Velocities and Displacement Phase Differences in a Harmonically Oscillating Pile," by N. Makris and G. Gazetas, 7/8/91, (PB92-108356, A04, MF-A01).

NCEER-91-0011 "Dynamic Characteristics of a Full-Size Five-Story Steel Structure and a 2/5 Scale Model," by K.C. Chang, G.C. Yao, G.C. Lee, D.S. Hao and Y.C. Yeh," 7/2/91, (PB93-116648, A06, MF-A02).

NCEER-91-0012 "Seismic Response of a 2/5 Scale Steel Structure with Added Viscoelastic Dampers," by K.C. Chang, T.T. Soong, S-T. Oh and M.L. Lai, 5/17/91, (PB92-110816, A05, MF-A01).

NCEER-91-0013 "Earthquake Response of Retaining Walls; Full-Scale Testing and Computational Modeling," by S. Alampalli and A-W.M. Elgamal, 6/20/91, to be published.

NCEER-91-0014 "3D-BASIS-M: Nonlinear Dynamic Analysis of Multiple Building Base Isolated Structures," by P.C. Tsopelas, S. Nagarajaiah, M.C. Constantinou and A.M. Reinhorn, 5/28/91, (PB92-113885, A09, MF-A02).

NCEER-91-0015 "Evaluation of SEAOC Design Requirements for Sliding Isolated Structures," by D. Theodossiou and M.C. Constantinou, 6/10/91, (PB92-114602, A11, MF-A03).

NCEER-91-0016 "Closed-Loop Modal Testing of a 27-Story Reinforced Concrete Flat Plate-Core Building," by H.R. Somaprasad, T. Toksoy, H. Yoshiyuki and A.E. Aktan, 7/15/91, (PB92-129980, A07, MF-A02).

NCEER-91-0017 "Shake Table Test of a 1/6 Scale Two-Story Lightly Reinforced Concrete Building," by A.G. El-Attar, R.N. White and P. Gergely, 2/28/91, (PB92-222447, A06, MF-A02).

NCEER-91-0018 "Shake Table Test of a 1/8 Scale Three-Story Lightly Reinforced Concrete Building," by A.G. El-Attar, R.N. White and P. Gergely, 2/28/91, (PB93-116630, A08, MF-A02).

NCEER-91-0019 "Transfer Functions for Rigid Rectangular Foundations," by A.S. Veletsos, A.M. Prasad and W.H. Wu, 7/31/91, to be published.

NCEER-91-0020 "Hybrid Control of Seismic-Excited Nonlinear and Inelastic Structural Systems," by J.N. Yang, Z. Li and A. Danielians, 8/1/91, (PB92-143171, A06, MF-A02).

NCEER-91-0021 "The NCEER-91 Earthquake Catalog: Improved Intensity-Based Magnitudes and Recurrence Relations for U.S. Earthquakes East of New Madrid," by L. Seeber and J.G. Armbruster, 8/28/91, (PB92-176742, A06, MF-A02).

NCEER-91-0022 "Proceedings from the Implementation of Earthquake Planning and Education in Schools: The Need for Change - The Roles of the Changemakers," by K.E.K. Ross and F. Winslow, 7/23/91, (PB92-129998, A12, MF-A03).

NCEER-91-0023 "A Study of Reliability-Based Criteria for Seismic Design of Reinforced Concrete Frame Buildings," by H.H.M. Hwang and H-M. Hsu, 8/10/91, (PB92-140235, A09, MF-A02).

NCEER-91-0024 "Experimental Verification of a Number of Structural System Identification Algorithms," by R.G. Ghanem, H. Gavin and M. Shinozuka, 9/18/91, (PB92-176577, A18, MF-A04).

NCEER-91-0025 "Probabilistic Evaluation of Liquefaction Potential," by H.H.M. Hwang and C.S. Lee," 11/25/91, (PB92-143429, A05, MF-A01).

NCEER-91-0026 "Instantaneous Optimal Control for Linear, Nonlinear and Hysteretic Structures - Stable Controllers," by J.N. Yang and Z. Li, 11/15/91, (PB92-163807, A04, MF-A01).

NCEER-91-0027 "Experimental and Theoretical Study of a Sliding Isolation System for Bridges," by M.C. Constantinou, A. Kartoum, A.M. Reinhorn and P. Bradford, 11/15/91, (PB92-176973, A10, MF-A03).

NCEER-92-0001 "Case Studies of Liquefaction and Lifeline Performance During Past Earthquakes, Volume 1: Japanese Case Studies," Edited by M. Hamada and T. O'Rourke, 2/17/92, (PB92-197243, A18, MF-A04).

NCEER-92-0002 "Case Studies of Liquefaction and Lifeline Performance During Past Earthquakes, Volume 2: United States Case Studies," Edited by T. O'Rourke and M. Hamada, 2/17/92, (PB92-197250, A20, MF-A04).

NCEER-92-0003 "Issues in Earthquake Education," Edited by K. Ross, 2/3/92, (PB92-222389, A07, MF-A02).

NCEER-92-0004 "Proceedings from the First U.S. - Japan Workshop on Earthquake Protective Systems for Bridges," Edited by I.G. Buckle, 2/4/92, (PB94-142239, A99, MF-A06).

NCEER-92-0005 "Seismic Ground Motion from a Haskell-Type Source in a Multiple-Layered Half-Space," A.P. Theoharis, G. Deodatis and M. Shinozuka, 1/2/92, to be published.

NCEER-92-0006 "Proceedings from the Site Effects Workshop," Edited by R. Whitman, 2/29/92, (PB92-197201, A04, MF-A01).

NCEER-92-0007 "Engineering Evaluation of Permanent Ground Deformations Due to Seismically-Induced Liquefaction," by M.H. Baziar, R. Dobry and A-W.M. Elgamal, 3/24/92, (PB92-222421, A13, MF-A03).

NCEER-92-0008 "A Procedure for the Seismic Evaluation of Buildings in the Central and Eastern United States," by C.D. Poland and J.O. Malley, 4/2/92, (PB92-222439, A20, MF-A04).

NCEER-92-0009 "Experimental and Analytical Study of a Hybrid Isolation System Using Friction Controllable Sliding Bearings," by M.Q. Feng, S. Fujii and M. Shinozuka, 5/15/92, (PB93-150282, A06, MF-A02).

NCEER-92-0010 "Seismic Resistance of Slab-Column Connections in Existing Non-Ductile Flat-Plate Buildings," by A.J. Durrani and Y. Du, 5/18/92, (PB93-116812, A06, MF-A02).

NCEER-92-0011 "The Hysteretic and Dynamic Behavior of Brick Masonry Walls Upgraded by Ferrocement Coatings Under Cyclic Loading and Strong Simulated Ground Motion," by H. Lee and S.P. Prawel, 5/11/92, to be published.

NCEER-92-0012 "Study of Wire Rope Systems for Seismic Protection of Equipment in Buildings," by G.F. Demetriades, M.C. Constantinou and A.M. Reinhorn, 5/20/92, (PB93-116655, A08, MF-A02).

NCEER-92-0013 "Shape Memory Structural Dampers: Material Properties, Design and Seismic Testing," by P.R. Witting and F.A. Cozzarelli, 5/26/92, (PB93-116663, A05, MF-A01).

NCEER-92-0014 "Longitudinal Permanent Ground Deformation Effects on Buried Continuous Pipelines," by M.J. O'Rourke, and C. Nordberg, 6/15/92, (PB93-116671, A08, MF-A02).

NCEER-92-0015 "A Simulation Method for Stationary Gaussian Random Functions Based on the Sampling Theorem," by M. Grigoriu and S. Balopoulou, 6/11/92, (PB93-127496, A05, MF-A01).

NCEER-92-0016 "Gravity-Load-Designed Reinforced Concrete Buildings: Seismic Evaluation of Existing Construction and Detailing Strategies for Improved Seismic Resistance," by G.W. Hoffmann, S.K. Kunnath, A.M. Reinhorn and J.B. Mander, 7/15/92, (PB94-142007, A08, MF-A02).

NCEER-92-0017 "Observations on Water System and Pipeline Performance in the Limón Area of Costa Rica Due to the April 22, 1991 Earthquake," by M. O'Rourke and D. Ballantyne, 6/30/92, (PB93-126811, A06, MF-A02).

NCEER-92-0018 "Fourth Edition of Earthquake Education Materials for Grades K-12," Edited by K.E.K. Ross, 8/10/92, (PB93-114023, A07, MF-A02).

NCEER-92-0019 "Proceedings from the Fourth Japan-U.S. Workshop on Earthquake Resistant Design of Lifeline Facilities and Countermeasures for Soil Liquefaction," Edited by M. Hamada and T.D. O'Rourke, 8/12/92, (PB93-163939, A99, MF-E11).

NCEER-92-0020 "Active Bracing System: A Full Scale Implementation of Active Control," by A.M. Reinhorn, T.T. Soong, R.C. Lin, M.A. Riley, Y.P. Wang, S. Aizawa and M. Higashino, 8/14/92, (PB93-127512, A06, MF-A02).

NCEER-92-0021 "Empirical Analysis of Horizontal Ground Displacement Generated by Liquefaction-Induced Lateral Spreads," by S.F. Bartlett and T.L. Youd, 8/17/92, (PB93-188241, A06, MF-A02).

NCEER-92-0022 "IDARC Version 3.0: Inelastic Damage Analysis of Reinforced Concrete Structures," by S.K. Kunnath, A.M. Reinhorn and R.F. Lobo, 8/31/92, (PB93-227502, A07, MF-A02).

NCEER-92-0023 "A Semi-Empirical Analysis of Strong-Motion Peaks in Terms of Seismic Source, Propagation Path and Local Site Conditions, by M. Kamiyama, M.J. O'Rourke and R. Flores-Berrones, 9/9/92, (PB93-150266, A08, MF-A02).

NCEER-92-0024 "Seismic Behavior of Reinforced Concrete Frame Structures with Nonductile Details, Part I: Summary of Experimental Findings of Full Scale Beam-Column Joint Tests," by A. Beres, R.N. White and P. Gergely, 9/30/92, (PB93-227783, A05, MF-A01).

NCEER-92-0025 "Experimental Results of Repaired and Retrofitted Beam-Column Joint Tests in Lightly Reinforced Concrete Frame Buildings," by A. Beres, S. El-Borgi, R.N. White and P. Gergely, 10/29/92, (PB93-227791, A05, MF-A01).

NCEER-92-0026 "A Generalization of Optimal Control Theory: Linear and Nonlinear Structures," by J.N. Yang, Z. Li and S. Vongchavalitkul, 11/2/92, (PB93-188621, A05, MF-A01).

NCEER-92-0027 "Seismic Resistance of Reinforced Concrete Frame Structures Designed Only for Gravity Loads: Part I - Design and Properties of a One-Third Scale Model Structure," by J.M. Bracci, A.M. Reinhorn and J.B. Mander, 12/1/92, (PB94-104502, A08, MF-A02).

NCEER-92-0028 "Seismic Resistance of Reinforced Concrete Frame Structures Designed Only for Gravity Loads: Part II - Experimental Performance of Subassemblages," by L.E. Aycardi, J.B. Mander and A.M. Reinhorn, 12/1/92, (PB94-104510, A08, MF-A02).

NCEER-92-0029 "Seismic Resistance of Reinforced Concrete Frame Structures Designed Only for Gravity Loads: Part III - Experimental Performance and Analytical Study of a Structural Model," by J.M. Bracci, A.M. Reinhorn and J.B. Mander, 12/1/92, (PB93-227528, A09, MF-A01).

NCEER-92-0030 "Evaluation of Seismic Retrofit of Reinforced Concrete Frame Structures: Part I - Experimental Performance of Retrofitted Subassemblages," by D. Choudhuri, J.B. Mander and A.M. Reinhorn, 12/8/92, (PB93-198307, A07, MF-A02).

NCEER-92-0031 "Evaluation of Seismic Retrofit of Reinforced Concrete Frame Structures: Part II - Experimental Performance and Analytical Study of a Retrofitted Structural Model," by J.M. Bracci, A.M. Reinhorn and J.B. Mander, 12/8/92, (PB93-198315, A09, MF-A03).

NCEER-92-0032 "Experimental and Analytical Investigation of Seismic Response of Structures with Supplemental Fluid Viscous Dampers," by M.C. Constantinou and M.D. Symans, 12/21/92, (PB93-191435, A10, MF-A03). This report is available only through NTIS (see address given above).

NCEER-92-0033 "Reconnaissance Report on the Cairo, Egypt Earthquake of October 12, 1992," by M. Khater, 12/23/92, (PB93-188621, A03, MF-A01).

NCEER-92-0034 "Low-Level Dynamic Characteristics of Four Tall Flat-Plate Buildings in New York City," by H. Gavin, S. Yuan, J. Grossman, E. Pekelis and K. Jacob, 12/28/92, (PB93-188217, A07, MF-A02).

NCEER-93-0001 "An Experimental Study on the Seismic Performance of Brick-Infilled Steel Frames With and Without Retrofit," by J.B. Mander, B. Nair, K. Wojtkowski and J. Ma, 1/29/93, (PB93-227510, A07, MF-A02).

NCEER-93-0002 "Social Accounting for Disaster Preparedness and Recovery Planning," by S. Cole, E. Pantoja and V. Razak, 2/22/93, (PB94-142114, A12, MF-A03).

NCEER-93-0003 "Assessment of 1991 NEHRP Provisions for Nonstructural Components and Recommended Revisions," by T.T. Soong, G. Chen, Z. Wu, R-H. Zhang and M. Grigoriu, 3/1/93, (PB93-188639, A06, MF-A02).

NCEER-93-0004 "Evaluation of Static and Response Spectrum Analysis Procedures of SEAOC/UBC for Seismic Isolated Structures," by C.W. Winters and M.C. Constantinou, 3/23/93, (PB93-198299, A10, MF-A03).

NCEER-93-0005 "Earthquakes in the Northeast - Are We Ignoring the Hazard? A Workshop on Earthquake Science and Safety for Educators," edited by K.E.K. Ross, 4/2/93, (PB94-103066, A09, MF-A02).

NCEER-93-0006 "Inelastic Response of Reinforced Concrete Structures with Viscoelastic Braces," by R.F. Lobo, J.M. Bracci, K.L. Shen, A.M. Reinhorn and T.T. Soong, 4/5/93, (PB93-227486, A05, MF-A02).

NCEER-93-0007 "Seismic Testing of Installation Methods for Computers and Data Processing Equipment," by K. Kosar, T.T. Soong, K.L. Shen, J.A. HoLung and Y.K. Lin, 4/12/93, (PB93-198299, A07, MF-A02).

NCEER-93-0008 "Retrofit of Reinforced Concrete Frames Using Added Dampers," by A. Reinhorn, M. Constantinou and C. Li, to be published.

NCEER-93-0009 "Seismic Behavior and Design Guidelines for Steel Frame Structures with Added Viscoelastic Dampers," by K.C. Chang, M.L. Lai, T.T. Soong, D.S. Hao and Y.C. Yeh, 5/1/93, (PB94-141959, A07, MF-A02).

NCEER-93-0010 "Seismic Performance of Shear-Critical Reinforced Concrete Bridge Piers," by J.B. Mander, S.M. Waheed, M.T.A. Chaudhary and S.S. Chen, 5/12/93, (PB93-227494, A08, MF-A02).

NCEER-93-0011 "3D-BASIS-TABS: Computer Program for Nonlinear Dynamic Analysis of Three Dimensional Base Isolated Structures," by S. Nagarajaiah, C. Li, A.M. Reinhorn and M.C. Constantinou, 8/2/93, (PB94-141819, A09, MF-A02).

NCEER-93-0012 "Effects of Hydrocarbon Spills from an Oil Pipeline Break on Ground Water," by O.J. Helweg and H.H.M. Hwang, 8/3/93, (PB94-141942, A06, MF-A02).

NCEER-93-0013 "Simplified Procedures for Seismic Design of Nonstructural Components and Assessment of Current Code Provisions," by M.P. Singh, L.E. Suarez, E.E. Matheu and G.O. Maldonado, 8/4/93, (PB94-141827, A09, MF-A02).

NCEER-93-0014 "An Energy Approach to Seismic Analysis and Design of Secondary Systems," by G. Chen and T.T. Soong, 8/6/93, (PB94-142767, A11, MF-A03).

NCEER-93-0015 "Proceedings from School Sites: Becoming Prepared for Earthquakes - Commemorating the Third Anniversary of the Loma Prieta Earthquake," Edited by F.E. Winslow and K.E.K. Ross, 8/16/93, (PB94-154275, A16, MF-A02).

NCEER-93-0016 "Reconnaissance Report of Damage to Historic Monuments in Cairo, Egypt Following the October 12, 1992 Dahshur Earthquake," by D. Sykora, D. Look, G. Croci, E. Karaesmen and E. Karaesmen, 8/19/93, (PB94-142221, A08, MF-A02).

NCEER-93-0017 "The Island of Guam Earthquake of August 8, 1993," by S.W. Swan and S.K. Harris, 9/30/93, (PB94-141843, A04, MF-A01).

NCEER-93-0018 "Engineering Aspects of the October 12, 1992 Egyptian Earthquake," by A.W. Elgamal, M. Amer, K. Adalier and A. Abul-Fadl, 10/7/93, (PB94-141983, A05, MF-A01).

NCEER-93-0019 "Development of an Earthquake Motion Simulator and its Application in Dynamic Centrifuge Testing," by I. Krstelj, Supervised by J.H. Prevost, 10/23/93, (PB94-181773, A-10, MF-A03).

NCEER-93-0020 "NCEER-Taisei Corporation Research Program on Sliding Seismic Isolation Systems for Bridges: Experimental and Analytical Study of a Friction Pendulum System (FPS)," by M.C. Constantinou, P. Tsopelas, Y-S. Kim and S. Okamoto, 11/1/93, (PB94-142775, A08, MF-A02).

NCEER-93-0021 "Finite Element Modeling of Elastomeric Seismic Isolation Bearings," by L.J. Billings, Supervised by R. Shepherd, 11/8/93, to be published.

NCEER-93-0022 "Seismic Vulnerability of Equipment in Critical Facilities: Life-Safety and Operational Consequences," by K. Porter, G.S. Johnson, M.M. Zadeh, C. Scawthorn and S. Eder, 11/24/93, (PB94-181765, A16, MF-A03).

NCEER-93-0023 "Hokkaido Nansei-oki, Japan Earthquake of July 12, 1993, by P.I. Yanev and C.R. Scawthorn, 12/23/93, (PB94-181500, A07, MF-A01).

NCEER-94-0001 "An Evaluation of Seismic Serviceability of Water Supply Networks with Application to the San Francisco Auxiliary Water Supply System," by I. Markov, Supervised by M. Grigoriu and T. O'Rourke, 1/21/94, (PB94-204013, A07, MF-A02).

NCEER-94-0002 "NCEER-Taisei Corporation Research Program on Sliding Seismic Isolation Systems for Bridges: Experimental and Analytical Study of Systems Consisting of Sliding Bearings, Rubber Restoring Force Devices and Fluid Dampers," Volumes I and II, by P. Tsopelas, S. Okamoto, M.C. Constantinou, D. Ozaki and S. Fujii, 2/4/94, (PB94-181740, A09, MF-A02 and PB94-181757, A12, MF-A03).

NCEER-94-0003 "A Markov Model for Local and Global Damage Indices in Seismic Analysis," by S. Rahman and M. Grigoriu, 2/18/94, (PB94-206000, A12, MF-A03).

NCEER-94-0004 "Proceedings from the NCEER Workshop on Seismic Response of Masonry Infills," edited by D.P. Abrams, 3/1/94, (PB94-180783, A07, MF-A02).

NCEER-94-0005 "The Northridge, California Earthquake of January 17, 1994: General Reconnaissance Report," edited by J.D. Goltz, 3/11/94, (PB94-193943, A10, MF-A03).

NCEER-94-0006 "Seismic Energy Based Fatigue Damage Analysis of Bridge Columns: Part I - Evaluation of Seismic Capacity," by G.A. Chang and J.B. Mander, 3/14/94, (PB94-219185, A11, MF-A03).

NCEER-94-0007 "Seismic Isolation of Multi-Story Frame Structures Using Spherical Sliding Isolation Systems," by T.M. Al-Hussaini, V.A. Zayas and M.C. Constantinou, 3/17/94, (PB94-193745, A09, MF-A02).

NCEER-94-0008 "The Northridge, California Earthquake of January 17, 1994: Performance of Highway Bridges," edited by I.G. Buckle, 3/24/94, (PB94-193851, A06, MF-A02).

NCEER-94-0009 "Proceedings of the Third U.S.-Japan Workshop on Earthquake Protective Systems for Bridges," edited by I.G. Buckle and I. Friedland, 3/31/94, (PB94-195815, A99, MF-A06).

NCEER-94-0010 "3D-BASIS-ME: Computer Program for Nonlinear Dynamic Analysis of Seismically Isolated Single and Multiple Structures and Liquid Storage Tanks," by P.C. Tsopelas, M.C. Constantinou and A.M. Reinhorn, 4/12/94, (PB94-204922, A09, MF-A02).

NCEER-94-0011 "The Northridge, California Earthquake of January 17, 1994: Performance of Gas Transmission Pipelines," by T.D. O'Rourke and M.C. Palmer, 5/16/94, (PB94-204989, A05, MF-A01).

NCEER-94-0012 "Feasibility Study of Replacement Procedures and Earthquake Performance Related to Gas Transmission Pipelines," by T.D. O'Rourke and M.C. Palmer, 5/25/94, (PB94-206638, A09, MF-A02).

NCEER-94-0013 "Seismic Energy Based Fatigue Damage Analysis of Bridge Columns: Part II - Evaluation of Seismic Demand," by G.A. Chang and J.B. Mander, 6/1/94, (PB95-18106, A08, MF-A02).

NCEER-94-0014 "NCEER-Taisei Corporation Research Program on Sliding Seismic Isolation Systems for Bridges: Experimental and Analytical Study of a System Consisting of Sliding Bearings and Fluid Restoring Force/Damping Devices," by P. Tsopelas and M.C. Constantinou, 6/13/94, (PB94-219144, A10, MF-A03).

NCEER-94-0015 "Generation of Hazard-Consistent Fragility Curves for Seismic Loss Estimation Studies," by H. Hwang and J-R. Huo, 6/14/94, (PB95-181996, A09, MF-A02).

NCEER-94-0016 "Seismic Study of Building Frames with Added Energy-Absorbing Devices," by W.S. Pong, C.S. Tsai and G.C. Lee, 6/20/94, (PB94-219136, A10, A03).

NCEER-94-0017 "Sliding Mode Control for Seismic-Excited Linear and Nonlinear Civil Engineering Structures," by J. Yang, J. Wu, A. Agrawal and Z. Li, 6/21/94, (PB95-138483, A06, MF-A02).

NCEER-94-0018 "3D-BASIS-TABS Version 2.0: Computer Program for Nonlinear Dynamic Analysis of Three Dimensional Base Isolated Structures," by A.M. Reinhorn, S. Nagarajaiah, M.C. Constantinou, P. Tsopelas and R. Li, 6/22/94, (PB95-182176, A08, MF-A02).

NCEER-94-0019 "Proceedings of the International Workshop on Civil Infrastructure Systems: Application of Intelligent Systems and Advanced Materials on Bridge Systems," Edited by G.C. Lee and K.C. Chang, 7/18/94, (PB95-252474, A20, MF-A04).

NCEER-94-0020 "Study of Seismic Isolation Systems for Computer Floors," by V. Lambrou and M.C. Constantinou, 7/19/94, (PB95-138533, A10, MF-A03).

NCEER-94-0021 "Proceedings of the U.S.-Italian Workshop on Guidelines for Seismic Evaluation and Rehabilitation of Unreinforced Masonry Buildings," Edited by D.P. Abrams and G.M. Calvi, 7/20/94, (PB95-138749, A13, MF-A03).

NCEER-94-0022 "NCEER-Taisei Corporation Research Program on Sliding Seismic Isolation Systems for Bridges: Experimental and Analytical Study of a System Consisting of Lubricated PTFE Sliding Bearings and Mild Steel Dampers," by P. Tsopelas and M.C. Constantinou, 7/22/94, (PB95-182184, A08, MF-A02).

NCEER-94-0023 “Development of Reliability-Based Design Criteria for Buildings Under Seismic Load,” by Y.K. Wen, H. Hwang and M. Shinozuka, 8/1/94, (PB95-211934, A08, MF-A02).

NCEER-94-0024 “Experimental Verification of Acceleration Feedback Control Strategies for an Active Tendon System,” by S.J. Dyke, B.F. Spencer, Jr., P. Quast, M.K. Sain, D.C. Kaspari, Jr. and T.T. Soong, 8/29/94, (PB95-212320, A05, MF-A01).

NCEER-94-0025 “Seismic Retrofitting Manual for Highway Bridges,” Edited by I.G. Buckle and I.F. Friedland, published by the Federal Highway Administration (PB95-212676, A15, MF-A03).

NCEER-94-0026 “Proceedings from the Fifth U.S.-Japan Workshop on Earthquake Resistant Design of Lifeline Facilities and Countermeasures Against Soil Liquefaction,” Edited by T.D. O’Rourke and M. Hamada, 11/7/94, (PB95-220802, A99, MF-E08).

NCEER-95-0001 "Experimental and Analytical Investigation of Seismic Retrofit of Structures with Supplemental Damping: Part 1 - Fluid Viscous Damping Devices," by A.M. Reinhorn, C. Li and M.C. Constantinou, 1/3/95, (PB95-266599, A09, MF-A02).

NCEER-95-0002 "Experimental and Analytical Study of Low-Cycle Fatigue Behavior of Semi-Rigid Top-And-Seat Angle Connections," by G. Pekcan, J.B. Mander and S.S. Chen, 1/5/95, (PB95-220042, A07, MF-A02).

NCEER-95-0003 "NCEER-ATC Joint Study on Fragility of Buildings," by T. Anagnos, C. Rojahn and A.S. Kiremidjian, 1/20/95, (PB95-220026, A06, MF-A02).

NCEER-95-0004 "Nonlinear Control Algorithms for Peak Response Reduction," by Z. Wu, T.T. Soong, V. Gattulli and R.C. Lin, 2/16/95, (PB95-220349, A05, MF-A01).

NCEER-95-0005 "Pipeline Replacement Feasibility Study: A Methodology for Minimizing Seismic and Corrosion Risks to Underground Natural Gas Pipelines," by R.T. Eguchi, H.A. Seligson and D.G. Honegger, 3/2/95, (PB95-252326, A06, MF-A02).

NCEER-95-0006 "Evaluation of Seismic Performance of an 11-Story Frame Building During the 1994 Northridge Earthquake," by F. Naeim, R. DiSulio, K. Benuska, A. Reinhorn and C. Li, to be published.

NCEER-95-0007 "Prioritization of Bridges for Seismic Retrofitting," by N. Basöz and A.S. Kiremidjian, 4/24/95, (PB95-252300, A08, MF-A02).

NCEER-95-0008 "Method for Developing Motion Damage Relationships for Reinforced Concrete Frames," by A. Singhal and A.S. Kiremidjian, 5/11/95, (PB95-266607, A06, MF-A02).

NCEER-95-0009 "Experimental and Analytical Investigation of Seismic Retrofit of Structures with Supplemental Damping: Part II - Friction Devices," by C. Li and A.M. Reinhorn, 7/6/95, (PB96-128087, A11, MF-A03).

NCEER-95-0010 "Experimental Performance and Analytical Study of a Non-Ductile Reinforced Concrete Frame Structure Retrofitted with Elastomeric Spring Dampers," by G. Pekcan, J.B. Mander and S.S. Chen, 7/14/95, (PB96-137161, A08, MF-A02).

NCEER-95-0011 "Development and Experimental Study of Semi-Active Fluid Damping Devices for Seismic Protection of Structures," by M.D. Symans and M.C. Constantinou, 8/3/95, (PB96-136940, A23, MF-A04).

NCEER-95-0012 "Real-Time Structural Parameter Modification (RSPM): Development of Innervated Structures," by Z. Liang, M. Tong and G.C. Lee, 4/11/95, (PB96-137153, A06, MF-A01).

NCEER-95-0013 "Experimental and Analytical Investigation of Seismic Retrofit of Structures with Supplemental Damping: Part III - Viscous Damping Walls," by A.M. Reinhorn and C. Li, 10/1/95, (PB96-176409, A11, MF-A03).

NCEER-95-0014 "Seismic Fragility Analysis of Equipment and Structures in a Memphis Electric Substation," by J-R. Huo and H.H.M. Hwang, 8/10/95, (PB96-128087, A09, MF-A02).

NCEER-95-0015 "The Hanshin-Awaji Earthquake of January 17, 1995: Performance of Lifelines," Edited by M. Shinozuka, 11/3/95, (PB96-176383, A15, MF-A03).

NCEER-95-0016 "Highway Culvert Performance During Earthquakes," by T.L. Youd and C.J. Beckman, available as NCEER-96-0015.

NCEER-95-0017 "The Hanshin-Awaji Earthquake of January 17, 1995: Performance of Highway Bridges," Edited by I.G. Buckle, 12/1/95, to be published.

NCEER-95-0018 "Modeling of Masonry Infill Panels for Structural Analysis," by A.M. Reinhorn, A. Madan, R.E. Valles, Y. Reichmann and J.B. Mander, 12/8/95, (PB97-110886, MF-A01, A06).

NCEER-95-0019 "Optimal Polynomial Control for Linear and Nonlinear Structures," by A.K. Agrawal and J.N. Yang, 12/11/95, (PB96-168737, A07, MF-A02).

NCEER-95-0020 "Retrofit of Non-Ductile Reinforced Concrete Frames Using Friction Dampers," by R.S. Rao, P. Gergely and R.N. White, 12/22/95, (PB97-133508, A10, MF-A02).

NCEER-95-0021 "Parametric Results for Seismic Response of Pile-Supported Bridge Bents," by G. Mylonakis, A. Nikolaou and G. Gazetas, 12/22/95, (PB97-100242, A12, MF-A03).

NCEER-95-0022 "Kinematic Bending Moments in Seismically Stressed Piles," by A. Nikolaou, G. Mylonakis and G. Gazetas, 12/23/95, (PB97-113914, MF-A03, A13).

NCEER-96-0001 "Dynamic Response of Unreinforced Masonry Buildings with Flexible Diaphragms," by A.C. Costley and D.P. Abrams," 10/10/96, (PB97-133573, MF-A03, A15).

NCEER-96-0002 "State of the Art Review: Foundations and Retaining Structures," by I. Po Lam, to be published.

NCEER-96-0003 "Ductility of Rectangular Reinforced Concrete Bridge Columns with Moderate Confinement," by N. Wehbe, M. Saiidi, D. Sanders and B. Douglas, 11/7/96, (PB97-133557, A06, MF-A02).

NCEER-96-0004 "Proceedings of the Long-Span Bridge Seismic Research Workshop," edited by I.G. Buckle and I.M. Friedland, to be published.

NCEER-96-0005 "Establish Representative Pier Types for Comprehensive Study: Eastern United States," by J. Kulicki and Z. Prucz, 5/28/96, (PB98-119217, A07, MF-A02).

NCEER-96-0006 "Establish Representative Pier Types for Comprehensive Study: Western United States," by R. Imbsen, R.A. Schamber and T.A. Osterkamp, 5/28/96, (PB98-118607, A07, MF-A02).

NCEER-96-0007 "Nonlinear Control Techniques for Dynamical Systems with Uncertain Parameters," by R.G. Ghanem and M.I. Bujakov, 5/27/96, (PB97-100259, A17, MF-A03).

NCEER-96-0008 "Seismic Evaluation of a 30-Year Old Non-Ductile Highway Bridge Pier and Its Retrofit," by J.B. Mander, B. Mahmoodzadegan, S. Bhadra and S.S. Chen, 5/31/96, (PB97-110902, MF-A03, A10).

NCEER-96-0009 "Seismic Performance of a Model Reinforced Concrete Bridge Pier Before and After Retrofit," by J.B. Mander, J.H. Kim and C.A. Ligozio, 5/31/96, (PB97-110910, MF-A02, A10).

NCEER-96-0010 "IDARC2D Version 4.0: A Computer Program for the Inelastic Damage Analysis of Buildings," by R.E. Valles, A.M. Reinhorn, S.K. Kunnath, C. Li and A. Madan, 6/3/96, (PB97-100234, A17, MF-A03).

NCEER-96-0011 "Estimation of the Economic Impact of Multiple Lifeline Disruption: Memphis Light, Gas and Water Division Case Study," by S.E. Chang, H.A. Seligson and R.T. Eguchi, 8/16/96, (PB97-133490, A11, MF-A03).

NCEER-96-0012 "Proceedings from the Sixth Japan-U.S. Workshop on Earthquake Resistant Design of Lifeline Facilities and Countermeasures Against Soil Liquefaction, Edited by M. Hamada and T. O'Rourke, 9/11/96, (PB97-133581, A99, MF-A06).

NCEER-96-0013 "Chemical Hazards, Mitigation and Preparedness in Areas of High Seismic Risk: A Methodology for Estimating the Risk of Post-Earthquake Hazardous Materials Release," by H.A. Seligson, R.T. Eguchi, K.J. Tierney and K. Richmond, 11/7/96, (PB97-133565, MF-A02, A08).

NCEER-96-0014 "Response of Steel Bridge Bearings to Reversed Cyclic Loading," by J.B. Mander, D-K. Kim, S.S. Chen and G.J. Premus, 11/13/96, (PB97-140735, A12, MF-A03).

NCEER-96-0015 "Highway Culvert Performance During Past Earthquakes," by T.L. Youd and C.J. Beckman, 11/25/96, (PB97-133532, A06, MF-A01).

NCEER-97-0001 "Evaluation, Prevention and Mitigation of Pounding Effects in Building Structures," by R.E. Valles and A.M. Reinhorn, 2/20/97, (PB97-159552, A14, MF-A03).

NCEER-97-0002 "Seismic Design Criteria for Bridges and Other Highway Structures," by C. Rojahn, R. Mayes, D.G. Anderson, J. Clark, J.H. Hom, R.V. Nutt and M.J. O'Rourke, 4/30/97, (PB97-194658, A06, MF-A03).

NCEER-97-0003 “Proceedings of the U.S.-Italian Workshop on Seismic Evaluation and Retrofit,” Edited by D.P. Abrams and G.M. Calvi, 3/19/97, (PB97-194666, A13, MF-A03).

NCEER-97-0004 "Investigation of Seismic Response of Buildings with Linear and Nonlinear Fluid Viscous Dampers," by A.A. Seleemah and M.C. Constantinou, 5/21/97, (PB98-109002, A15, MF-A03).

NCEER-97-0005 "Proceedings of the Workshop on Earthquake Engineering Frontiers in Transportation Facilities," edited by G.C. Lee and I.M. Friedland, 8/29/97, (PB98-128911, A25, MR-A04).

NCEER-97-0006 "Cumulative Seismic Damage of Reinforced Concrete Bridge Piers," by S.K. Kunnath, A. El-Bahy, A. Taylor and W. Stone, 9/2/97, (PB98-108814, A11, MF-A03).

NCEER-97-0007 "Structural Details to Accommodate Seismic Movements of Highway Bridges and Retaining Walls," by R.A. Imbsen, R.A. Schamber, E. Thorkildsen, A. Kartoum, B.T. Martin, T.N. Rosser and J.M. Kulicki, 9/3/97, (PB98-108996, A09, MF-A02).

NCEER-97-0008 "A Method for Earthquake Motion-Damage Relationships with Application to Reinforced Concrete Frames," by A. Singhal and A.S. Kiremidjian, 9/10/97, (PB98-108988, A13, MF-A03).

NCEER-97-0009 "Seismic Analysis and Design of Bridge Abutments Considering Sliding and Rotation," by K. Fishman and R. Richards, Jr., 9/15/97, (PB98-108897, A06, MF-A02).

NCEER-97-0010 "Proceedings of the FHWA/NCEER Workshop on the National Representation of Seismic Ground Motion for New and Existing Highway Facilities," edited by I.M. Friedland, M.S. Power and R.L. Mayes, 9/22/97, (PB98-128903, A21, MF-A04).

NCEER-97-0011 "Seismic Analysis for Design or Retrofit of Gravity Bridge Abutments," by K.L. Fishman, R. Richards, Jr. and R.C. Divito, 10/2/97, (PB98-128937, A08, MF-A02).

NCEER-97-0012 "Evaluation of Simplified Methods of Analysis for Yielding Structures," by P. Tsopelas, M.C. Constantinou, C.A. Kircher and A.S. Whittaker, 10/31/97, (PB98-128929, A10, MF-A03).

NCEER-97-0013 "Seismic Design of Bridge Columns Based on Control and Repairability of Damage," by C-T. Cheng and J.B. Mander, 12/8/97, (PB98-144249, A11, MF-A03).

NCEER-97-0014 "Seismic Resistance of Bridge Piers Based on Damage Avoidance Design," by J.B. Mander and C-T. Cheng, 12/10/97, (PB98-144223, A09, MF-A02).

NCEER-97-0015 “Seismic Response of Nominally Symmetric Systems with Strength Uncertainty,” by S. Balopoulou and M. Grigoriu, 12/23/97, (PB98-153422, A11, MF-A03).

NCEER-97-0016 “Evaluation of Seismic Retrofit Methods for Reinforced Concrete Bridge Columns,” by T.J. Wipf, F.W. Klaiber and F.M. Russo, 12/28/97, (PB98-144215, A12, MF-A03).

NCEER-97-0017 “Seismic Fragility of Existing Conventional Reinforced Concrete Highway Bridges,” by C.L. Mullen and A.S. Cakmak, 12/30/97, (PB98-153406, A08, MF-A02).

NCEER-97-0018 “Loss Asssessment of Memphis Buildings,” edited by D.P. Abrams and M. Shinozuka, 12/31/97, (PB98-144231, A13, MF-A03).

NCEER-97-0019 “Seismic Evaluation of Frames with Infill Walls Using Quasi-static Experiments,” by K.M. Mosalam, R.N. White and P. Gergely, 12/31/97, (PB98-153455, A07, MF-A02).

NCEER-97-0020 “Seismic Evaluation of Frames with Infill Walls Using Pseudo-dynamic Experiments,” by K.M. Mosalam, R.N. White and P. Gergely, 12/31/97, (PB98-153430, A07, MF-A02).

NCEER-97-0021 “Computational Strategies for Frames with Infill Walls: Discrete and Smeared Crack Analyses and Seismic Fragility,” by K.M. Mosalam, R.N. White and P. Gergely, 12/31/97, (PB98-153414, A10, MF-A02).

NCEER-97-0022 "Proceedings of the NCEER Workshop on Evaluation of Liquefaction Resistance of Soils," edited by T.L. Youd and I.M. Idriss, 12/31/97, (PB98-155617, A15, MF-A03).

MCEER-98-0001 "Extraction of Nonlinear Hysteretic Properties of Seismically Isolated Bridges from Quick-Release Field Tests," by Q. Chen, B.M. Douglas, E.M. Maragakis and I.G. Buckle, 5/26/98, (PB99-118838, A06, MF-A01).

MCEER-98-0002 "Methodologies for Evaluating the Importance of Highway Bridges," by A. Thomas, S. Eshenaur and J. Kulicki, 5/29/98, (PB99-118846, A10, MF-A02).

MCEER-98-0003 "Capacity Design of Bridge Piers and the Analysis of Overstrength," by J.B. Mander, A. Dutta and P. Goel, 6/1/98, (PB99-118853, A09, MF-A02).

MCEER-98-0004 "Evaluation of Bridge Damage Data from the Loma Prieta and Northridge, California Earthquakes," by N. Basoz and A. Kiremidjian, 6/2/98, (PB99-118861, A15, MF-A03).

MCEER-98-0005 "Screening Guide for Rapid Assessment of Liquefaction Hazard at Highway Bridge Sites," by T. L. Youd, 6/16/98, (PB99-118879, A06, not available on microfiche).

MCEER-98-0006 "Structural Steel and Steel/Concrete Interface Details for Bridges," by P. Ritchie, N. Kauhl and J. Kulicki, 7/13/98, (PB99-118945, A06, MF-A01).

MCEER-98-0007 "Capacity Design and Fatigue Analysis of Confined Concrete Columns," by A. Dutta and J.B. Mander, 7/14/98, (PB99-118960, A14, MF-A03).

MCEER-98-0008 "Proceedings of the Workshop on Performance Criteria for Telecommunication Services Under Earthquake Conditions," edited by A.J. Schiff, 7/15/98, (PB99-118952, A08, MF-A02).

MCEER-98-0009 "Fatigue Analysis of Unconfined Concrete Columns," by J.B. Mander, A. Dutta and J.H. Kim, 9/12/98, (PB99-123655, A10, MF-A02).

MCEER-98-0010 "Centrifuge Modeling of Cyclic Lateral Response of Pile-Cap Systems and Seat-Type Abutments in Dry Sands," by A.D. Gadre and R. Dobry, 10/2/98, (PB99-123606, A13, MF-A03).

MCEER-98-0011 "IDARC-BRIDGE: A Computational Platform for Seismic Damage Assessment of Bridge Structures," by A.M. Reinhorn, V. Simeonov, G. Mylonakis and Y. Reichman, 10/2/98, (PB99-162919, A15, MF-A03).

MCEER-98-0012 "Experimental Investigation of the Dynamic Response of Two Bridges Before and After Retrofitting with Elastomeric Bearings," by D.A. Wendichansky, S.S. Chen and J.B. Mander, 10/2/98, (PB99-162927, A15, MF-A03).

MCEER-98-0013 "Design Procedures for Hinge Restrainers and Hinge Sear Width for Multiple-Frame Bridges," by R. Des Roches and G.L. Fenves, 11/3/98, (PB99-140477, A13, MF-A03).

MCEER-98-0014 "Response Modification Factors for Seismically Isolated Bridges," by M.C. Constantinou and J.K. Quarshie, 11/3/98, (PB99-140485, A14, MF-A03).

MCEER-98-0015 "Proceedings of the U.S.-Italy Workshop on Seismic Protective Systems for Bridges," edited by I.M. Friedland and M.C. Constantinou, 11/3/98, (PB2000-101711, A22, MF-A04).

MCEER-98-0016 "Appropriate Seismic Reliability for Critical Equipment Systems: Recommendations Based on Regional Analysis of Financial and Life Loss," by K. Porter, C. Scawthorn, C. Taylor and N. Blais, 11/10/98, (PB99-157265, A08, MF-A02).

MCEER-98-0017 "Proceedings of the U.S. Japan Joint Seminar on Civil Infrastructure Systems Research," edited by M. Shinozuka and A. Rose, 11/12/98, (PB99-156713, A16, MF-A03).

MCEER-98-0018 "Modeling of Pile Footings and Drilled Shafts for Seismic Design," by I. PoLam, M. Kapuskar and D. Chaudhuri, 12/21/98, (PB99-157257, A09, MF-A02).

MCEER-99-0001 "Seismic Evaluation of a Masonry Infilled Reinforced Concrete Frame by Pseudodynamic Testing," by S.G. Buonopane and R.N. White, 2/16/99, (PB99-162851, A09, MF-A02).

MCEER-99-0002 "Response History Analysis of Structures with Seismic Isolation and Energy Dissipation Systems: Verification Examples for Program SAP2000," by J. Scheller and M.C. Constantinou, 2/22/99, (PB99-162869, A08, MF-A02).

MCEER-99-0003 "Experimental Study on the Seismic Design and Retrofit of Bridge Columns Including Axial Load Effects," by A. Dutta, T. Kokorina and J.B. Mander, 2/22/99, (PB99-162877, A09, MF-A02).

MCEER-99-0004 "Experimental Study of Bridge Elastomeric and Other Isolation and Energy Dissipation Systems with Emphasis on Uplift Prevention and High Velocity Near-source Seismic Excitation," by A. Kasalanati and M. C. Constantinou, 2/26/99, (PB99-162885, A12, MF-A03).

MCEER-99-0005 "Truss Modeling of Reinforced Concrete Shear-flexure Behavior," by J.H. Kim and J.B. Mander, 3/8/99, (PB99-163693, A12, MF-A03).

MCEER-99-0006 "Experimental Investigation and Computational Modeling of Seismic Response of a 1:4 Scale Model Steel Structure with a Load Balancing Supplemental Damping System," by G. Pekcan, J.B. Mander and S.S. Chen, 4/2/99, (PB99-162893, A11, MF-A03).

MCEER-99-0007 "Effect of Vertical Ground Motions on the Structural Response of Highway Bridges," by M.R. Button, C.J. Cronin and R.L. Mayes, 4/10/99, (PB2000-101411, A10, MF-A03).

MCEER-99-0008 "Seismic Reliability Assessment of Critical Facilities: A Handbook, Supporting Documentation, and Model Code Provisions," by G.S. Johnson, R.E. Sheppard, M.D. Quilici, S.J. Eder and C.R. Scawthorn, 4/12/99, (PB2000-101701, A18, MF-A04).

MCEER-99-0009 "Impact Assessment of Selected MCEER Highway Project Research on the Seismic Design of Highway Structures," by C. Rojahn, R. Mayes, D.G. Anderson, J.H. Clark, D'Appolonia Engineering, S. Gloyd and R.V. Nutt, 4/14/99, (PB99-162901, A10, MF-A02).

MCEER-99-0010 "Site Factors and Site Categories in Seismic Codes," by R. Dobry, R. Ramos and M.S. Power, 7/19/99, (PB2000-101705, A08, MF-A02).

MCEER-99-0011 "Restrainer Design Procedures for Multi-Span Simply-Supported Bridges," by M.J. Randall, M. Saiidi, E. Maragakis and T. Isakovic, 7/20/99, (PB2000-101702, A10, MF-A02).

MCEER-99-0012 "Property Modification Factors for Seismic Isolation Bearings," by M.C. Constantinou, P. Tsopelas, A. Kasalanati and E. Wolff, 7/20/99, (PB2000-103387, A11, MF-A03).

MCEER-99-0013 "Critical Seismic Issues for Existing Steel Bridges," by P. Ritchie, N. Kauhl and J. Kulicki, 7/20/99, (PB2000-101697, A09, MF-A02).

MCEER-99-0014 "Nonstructural Damage Database," by A. Kao, T.T. Soong and A. Vender, 7/24/99, (PB2000-101407, A06, MF-A01).

MCEER-99-0015 "Guide to Remedial Measures for Liquefaction Mitigation at Existing Highway Bridge Sites," by H.G. Cooke and J. K. Mitchell, 7/26/99, (PB2000-101703, A11, MF-A03).

MCEER-99-0016 "Proceedings of the MCEER Workshop on Ground Motion Methodologies for the Eastern United States," edited by N. Abrahamson and A. Becker, 8/11/99, (PB2000-103385, A07, MF-A02).

MCEER-99-0017 "Quindío, Colombia Earthquake of January 25, 1999: Reconnaissance Report," by A.P. Asfura and P.J. Flores, 10/4/99, (PB2000-106893, A06, MF-A01).

MCEER-99-0018 "Hysteretic Models for Cyclic Behavior of Deteriorating Inelastic Structures," by M.V. Sivaselvan and A.M. Reinhorn, 11/5/99, (PB2000-103386, A08, MF-A02).

MCEER-99-0019 "Proceedings of the 7th U.S.- Japan Workshop on Earthquake Resistant Design of Lifeline Facilities and Countermeasures Against Soil Liquefaction," edited by T.D. O'Rourke, J.P. Bardet and M. Hamada, 11/19/99, (PB2000-103354, A99, MF-A06).

MCEER-99-0020 "Development of Measurement Capability for Micro-Vibration Evaluations with Application to Chip Fabrication Facilities," by G.C. Lee, Z. Liang, J.W. Song, J.D. Shen and W.C. Liu, 12/1/99, (PB2000-105993, A08, MF-A02).

MCEER-99-0021 "Design and Retrofit Methodology for Building Structures with Supplemental Energy Dissipating Systems," by G. Pekcan, J.B. Mander and S.S. Chen, 12/31/99, (PB2000-105994, A11, MF-A03).

MCEER-00-0001 "The Marmara, Turkey Earthquake of August 17, 1999: Reconnaissance Report," edited by C. Scawthorn; with major contributions by M. Bruneau, R. Eguchi, T. Holzer, G. Johnson, J. Mander, J. Mitchell, W. Mitchell, A. Papageorgiou, C. Scaethorn, and G. Webb, 3/23/00, (PB2000-106200, A11, MF-A03).

MCEER-00-0002 "Proceedings of the MCEER Workshop for Seismic Hazard Mitigation of Health Care Facilities," edited by G.C. Lee, M. Ettouney, M. Grigoriu, J. Hauer and J. Nigg, 3/29/00, (PB2000-106892, A08, MF-A02).

MCEER-00-0003 "The Chi-Chi, Taiwan Earthquake of September 21, 1999: Reconnaissance Report," edited by G.C. Lee and C.H. Loh, with major contributions by G.C. Lee, M. Bruneau, I.G. Buckle, S.E. Chang, P.J. Flores, T.D. O'Rourke, M. Shinozuka, T.T. Soong, C-H. Loh, K-C. Chang, Z-J. Chen, J-S. Hwang, M-L. Lin, G-Y. Liu, K-C. Tsai, G.C. Yao and C-L. Yen, 4/30/00, (PB2001-100980, A10, MF-A02).

MCEER-00-0004 "Seismic Retrofit of End-Sway Frames of Steel Deck-Truss Bridges with a Supplemental Tendon System: Experimental and Analytical Investigation," by G. Pekcan, J.B. Mander and S.S. Chen, 7/1/00, (PB2001-100982, A10, MF-A02).

MCEER-00-0005 "Sliding Fragility of Unrestrained Equipment in Critical Facilities," by W.H. Chong and T.T. Soong, 7/5/00, (PB2001-100983, A08, MF-A02).

MCEER-00-0006 "Seismic Response of Reinforced Concrete Bridge Pier Walls in the Weak Direction," by N. Abo-Shadi, M. Saiidi and D. Sanders, 7/17/00, (PB2001-100981, A17, MF-A03).

MCEER-00-0007 "Low-Cycle Fatigue Behavior of Longitudinal Reinforcement in Reinforced Concrete Bridge Columns," by J. Brown and S.K. Kunnath, 7/23/00, (PB2001-104392, A08, MF-A02).

MCEER-00-0008 "Soil Structure Interaction of Bridges for Seismic Analysis," I. PoLam and H. Law, 9/25/00, (PB2001-105397, A08, MF-A02).

MCEER-00-0009 "Proceedings of the First MCEER Workshop on Mitigation of Earthquake Disaster by Advanced Technologies (MEDAT-1), edited by M. Shinozuka, D.J. Inman and T.D. O'Rourke, 11/10/00, (PB2001-105399, A14, MF-A03).

MCEER-00-0010 "Development and Evaluation of Simplified Procedures for Analysis and Design of Buildings with Passive Energy Dissipation Systems, Revision 01," by O.M. Ramirez, M.C. Constantinou, C.A. Kircher, A.S. Whittaker, M.W. Johnson, J.D. Gomez and C. Chrysostomou, 11/16/01, (PB2001-105523, A23, MF-A04).

MCEER-00-0011 "Dynamic Soil-Foundation-Structure Interaction Analyses of Large Caissons," by C-Y. Chang, C-M. Mok, Z-L. Wang, R. Settgast, F. Waggoner, M.A. Ketchum, H.M. Gonnermann and C-C. Chin, 12/30/00, (PB2001-104373, A07, MF-A02).

MCEER-00-0012 "Experimental Evaluation of Seismic Performance of Bridge Restrainers," by A.G. Vlassis, E.M. Maragakis and M. Saiid Saiidi, 12/30/00, (PB2001-104354, A09, MF-A02).

MCEER-00-0013 "Effect of Spatial Variation of Ground Motion on Highway Structures," by M. Shinozuka, V. Saxena and G. Deodatis, 12/31/00, (PB2001-108755, A13, MF-A03).

MCEER-00-0014 "A Risk-Based Methodology for Assessing the Seismic Performance of Highway Systems," by S.D. Werner, C.E. Taylor, J.E. Moore, II, J.S. Walton and S. Cho, 12/31/00, (PB2001-108756, A14, MF-A03).

MCEER-01-0001 "Experimental Investigation of P-Delta Effects to Collapse During Earthquakes," by D. Vian and M. Bruneau, 6/25/01, (PB2002-100534, A17, MF-A03).

MCEER-01-0002 "Proceedings of the Second MCEER Workshop on Mitigation of Earthquake Disaster by Advanced Technologies (MEDAT-2)," edited by M. Bruneau and D.J. Inman, 7/23/01, (PB2002-100434, A16, MF-A03).

MCEER-01-0003 "Sensitivity Analysis of Dynamic Systems Subjected to Seismic Loads," by C. Roth and M. Grigoriu, 9/18/01, (PB2003-100884, A12, MF-A03).

MCEER-01-0004 "Overcoming Obstacles to Implementing Earthquake Hazard Mitigation Policies: Stage 1 Report," by D.J. Alesch and W.J. Petak, 12/17/01, (PB2002-107949, A07, MF-A02).

MCEER-01-0005 "Updating Real-Time Earthquake Loss Estimates: Methods, Problems and Insights," by C.E. Taylor, S.E. Chang and R.T. Eguchi, 12/17/01, (PB2002-107948, A05, MF-A01).

MCEER-01-0006 "Experimental Investigation and Retrofit of Steel Pile Foundations and Pile Bents Under Cyclic Lateral Loadings," by A. Shama, J. Mander, B. Blabac and S. Chen, 12/31/01, (PB2002-107950, A13, MF-A03).

MCEER-02-0001 "Assessment of Performance of Bolu Viaduct in the 1999 Duzce Earthquake in Turkey" by P.C. Roussis, M.C. Constantinou, M. Erdik, E. Durukal and M. Dicleli, 5/8/02, (PB2003-100883, A08, MF-A02).

MCEER-02-0002 "Seismic Behavior of Rail Counterweight Systems of Elevators in Buildings," by M.P. Singh, Rildova and L.E. Suarez, 5/27/02. (PB2003-100882, A11, MF-A03).

MCEER-02-0003 "Development of Analysis and Design Procedures for Spread Footings," by G. Mylonakis, G. Gazetas, S. Nikolaou and A. Chauncey, 10/02/02, (PB2004-101636, A13, MF-A03, CD-A13).

MCEER-02-0004 "Bare-Earth Algorithms for Use with SAR and LIDAR Digital Elevation Models," by C.K. Huyck, R.T. Eguchi and B. Houshmand, 10/16/02, (PB2004-101637, A07, CD-A07).

MCEER-02-0005 "Review of Energy Dissipation of Compression Members in Concentrically Braced Frames," by K.Lee and M. Bruneau, 10/18/02, (PB2004-101638, A10, CD-A10).

MCEER-03-0001 "Experimental Investigation of Light-Gauge Steel Plate Shear Walls for the Seismic Retrofit of Buildings" by J. Berman and M. Bruneau, 5/2/03, (PB2004-101622, A10, MF-A03, CD-A10).

MCEER-03-0002 "Statistical Analysis of Fragility Curves," by M. Shinozuka, M.Q. Feng, H. Kim, T. Uzawa and T. Ueda, 6/16/03, (PB2004-101849, A09, CD-A09).

MCEER-03-0003 "Proceedings of the Eighth U.S.-Japan Workshop on Earthquake Resistant Design f Lifeline Facilities and Countermeasures Against Liquefaction," edited by M. Hamada, J.P. Bardet and T.D. O'Rourke, 6/30/03, (PB2004-104386, A99, CD-A99).

MCEER-03-0004 "Proceedings of the PRC-US Workshop on Seismic Analysis and Design of Special Bridges," edited by L.C. Fan and G.C. Lee, 7/15/03, (PB2004-104387, A14, CD-A14).

MCEER-03-0005 "Urban Disaster Recovery: A Framework and Simulation Model," by S.B. Miles and S.E. Chang, 7/25/03, (PB2004-104388, A07, CD-A07).

MCEER-03-0006 "Behavior of Underground Piping Joints Due to Static and Dynamic Loading," by R.D. Meis, M. Maragakis and R. Siddharthan, 11/17/03, (PB2005-102194, A13, MF-A03, CD-A00).

MCEER-04-0001 "Experimental Study of Seismic Isolation Systems with Emphasis on Secondary System Response and Verification of Accuracy of Dynamic Response History Analysis Methods," by E. Wolff and M. Constantinou, 1/16/04 (PB2005-102195, A99, MF-E08, CD-A00).

MCEER-04-0002 "Tension, Compression and Cyclic Testing of Engineered Cementitious Composite Materials," by K. Kesner and S.L. Billington, 3/1/04, (PB2005-102196, A08, CD-A08).

MCEER-04-0003 "Cyclic Testing of Braces Laterally Restrained by Steel Studs to Enhance Performance During Earthquakes," by O.C. Celik, J.W. Berman and M. Bruneau, 3/16/04, (PB2005-102197, A13, MF-A03, CD-A00).

MCEER-04-0004 "Methodologies for Post Earthquake Building Damage Detection Using SAR and Optical Remote Sensing: Application to the August 17, 1999 Marmara, Turkey Earthquake," by C.K. Huyck, B.J. Adams, S. Cho, R.T. Eguchi, B. Mansouri and B. Houshmand, 6/15/04, (PB2005-104888, A10, CD-A00).

MCEER-04-0005 "Nonlinear Structural Analysis Towards Collapse Simulation: A Dynamical Systems Approach," by M.V. Sivaselvan and A.M. Reinhorn, 6/16/04, (PB2005-104889, A11, MF-A03, CD-A00).

MCEER-04-0006 "Proceedings of the Second PRC-US Workshop on Seismic Analysis and Design of Special Bridges," edited by G.C. Lee and L.C. Fan, 6/25/04, (PB2005-104890, A16, CD-A00).

MCEER-04-0007 "Seismic Vulnerability Evaluation of Axially Loaded Steel Built-up Laced Members," by K. Lee and M. Bruneau, 6/30/04, (PB2005-104891, A16, CD-A00).

MCEER-04-0008 "Evaluation of Accuracy of Simplified Methods of Analysis and Design of Buildings with Damping Systems for Near-Fault and for Soft-Soil Seismic Motions," by E.A. Pavlou and M.C. Constantinou, 8/16/04, (PB2005-104892, A08, MF-A02, CD-A00).

MCEER-04-0009 "Assessment of Geotechnical Issues in Acute Care Facilities in California," by M. Lew, T.D. O'Rourke, R. Dobry and M. Koch, 9/15/04, (PB2005-104893, A08, CD-A00).

MCEER-04-0010 "Scissor-Jack-Damper Energy Dissipation System," by A.N. Sigaher-Boyle and M.C. Constantinou, 12/1/04 (PB2005-108221).

MCEER-04-0011 "Seismic Retrofit of Bridge Steel Truss Piers Using a Controlled Rocking Approach," by M. Pollino and M. Bruneau, 12/20/04 (PB2006-105795).

MCEER-05-0001 "Experimental and Analytical Studies of Structures Seismically Isolated with an Uplift-Restraint Isolation System," by P.C. Roussis and M.C. Constantinou, 1/10/05 (PB2005-108222).

MCEER-05-0002 "A Versatile Experimentation Model for Study of Structures Near Collapse Applied to Seismic Evaluation of Irregular Structures," by D. Kusumastuti, A.M. Reinhorn and A. Rutenberg, 3/31/05 (PB2006-101523).

MCEER-05-0003 "Proceedings of the Third PRC-US Workshop on Seismic Analysis and Design of Special Bridges," edited by L.C. Fan and G.C. Lee, 4/20/05, (PB2006-105796).

MCEER-05-0004 "Approaches for the Seismic Retrofit of Braced Steel Bridge Piers and Proof-of-Concept Testing of an Eccentrically Braced Frame with Tubular Link," by J.W. Berman and M. Bruneau, 4/21/05 (PB2006-101524).

MCEER-05-0005 "Simulation of Strong Ground Motions for Seismic Fragility Evaluation of Nonstructural Components in Hospitals," by A. Wanitkorkul and A. Filiatrault, 5/26/05 (PB2006-500027).

MCEER-05-0006 "Seismic Safety in California Hospitals: Assessing an Attempt to Accelerate the Replacement or Seismic Retrofit of Older Hospital Facilities," by D.J. Alesch, L.A. Arendt and W.J. Petak, 6/6/05 (PB2006-105794).

MCEER-05-0007 "Development of Seismic Strengthening and Retrofit Strategies for Critical Facilities Using Engineered Cementitious Composite Materials," by K. Kesner and S.L. Billington, 8/29/05 (PB2006-111701).

MCEER-05-0008 "Experimental and Analytical Studies of Base Isolation Systems for Seismic Protection of Power Transformers," by N. Murota, M.Q. Feng and G-Y. Liu, 9/30/05 (PB2006-111702).

MCEER-05-0009 "3D-BASIS-ME-MB: Computer Program for Nonlinear Dynamic Analysis of Seismically Isolated Structures," by P.C. Tsopelas, P.C. Roussis, M.C. Constantinou, R. Buchanan and A.M. Reinhorn, 10/3/05 (PB2006-111703).

MCEER-05-0010 "Steel Plate Shear Walls for Seismic Design and Retrofit of Building Structures," by D. Vian and M. Bruneau, 12/15/05 (PB2006-111704).

MCEER-05-0011 "The Performance-Based Design Paradigm," by M.J. Astrella and A. Whittaker, 12/15/05 (PB2006-111705).

MCEER-06-0001 "Seismic Fragility of Suspended Ceiling Systems," H. Badillo-Almaraz, A.S. Whittaker, A.M. Reinhorn and G.P. Cimellaro, 2/4/06 (PB2006-111706).

MCEER-06-0002 "Multi-Dimensional Fragility of Structures," by G.P. Cimellaro, A.M. Reinhorn and M. Bruneau, 3/1/06 (PB2007-106974, A09, MF-A02, CD A00).

MCEER-06-0003 "Built-Up Shear Links as Energy Dissipators for Seismic Protection of Bridges," by P. Dusicka, A.M. Itani and I.G. Buckle, 3/15/06 (PB2006-111708).

MCEER-06-0004 "Analytical Investigation of the Structural Fuse Concept," by R.E. Vargas and M. Bruneau, 3/16/06 (PB2006-111709).

MCEER-06-0005 "Experimental Investigation of the Structural Fuse Concept," by R.E. Vargas and M. Bruneau, 3/17/06 (PB2006-111710).

MCEER-06-0006 "Further Development of Tubular Eccentrically Braced Frame Links for the Seismic Retrofit of Braced Steel Truss Bridge Piers," by J.W. Berman and M. Bruneau, 3/27/06 (PB2007-105147).

MCEER-06-0007 "REDARS Validation Report," by S. Cho, C.K. Huyck, S. Ghosh and R.T. Eguchi, 8/8/06 (PB2007-106983).

MCEER-06-0008 "Review of Current NDE Technologies for Post-Earthquake Assessment of Retrofitted Bridge Columns," by J.W. Song, Z. Liang and G.C. Lee, 8/21/06 (PB2007-106984).

MCEER-06-0009 "Liquefaction Remediation in Silty Soils Using Dynamic Compaction and Stone Columns," by S. Thevanayagam, G.R. Martin, R. Nashed, T. Shenthan, T. Kanagalingam and N. Ecemis, 8/28/06 (PB2007-106985).

MCEER-06-0010 "Conceptual Design and Experimental Investigation of Polymer Matrix Composite Infill Panels for Seismic Retrofitting," by W. Jung, M. Chiewanichakorn and A.J. Aref, 9/21/06 (PB2007-106986).

MCEER-06-0011 "A Study of the Coupled Horizontal-Vertical Behavior of Elastomeric and Lead-Rubber Seismic Isolation Bearings," by G.P. Warn and A.S. Whittaker, 9/22/06 (PB2007-108679).

MCEER-06-0012 "Proceedings of the Fourth PRC-US Workshop on Seismic Analysis and Design of Special Bridges: Advancing Bridge Technologies in Research, Design, Construction and Preservation," Edited by L.C. Fan, G.C. Lee and L. Ziang, 10/12/06 (PB2007-109042).

MCEER-06-0013 "Cyclic Response and Low Cycle Fatigue Characteristics of Plate Steels," by P. Dusicka, A.M. Itani and I.G. Buckle, 11/1/06 06 (PB2007-106987).

MCEER-06-0014 "Proceedings of the Second US-Taiwan Bridge Engineering Workshop," edited by W.P. Yen, J. Shen, J-Y. Chen and M. Wang, 11/15/06 (PB2008-500041).

MCEER-06-0015 "User Manual and Technical Documentation for the REDARS^{TM} Import Wizard," by S. Cho, S. Ghosh, C.K. Huyck and S.D. Werner, 11/30/06 (PB2007-114766).

MCEER-06-0016 "Hazard Mitigation Strategy and Monitoring Technologies for Urban and Infrastructure Public Buildings: Proceedings of the China-US Workshops," edited by X.Y. Zhou, A.L. Zhang, G.C. Lee and M. Tong, 12/12/06 (PB2008-500018).

MCEER-07-0001 "Static and Kinetic Coefficients of Friction for Rigid Blocks," by C. Kafali, S. Fathali, M. Grigoriu and A.S. Whittaker, 3/20/07 (PB2007-114767).

MCEER-07-0002 "Hazard Mitigation Investment Decision Making: Organizational Response to Legislative Mandate," by L.A. Arendt, D.J. Alesch and W.J. Petak, 4/9/07 (PB2007-114768).

MCEER-07-0003 "Seismic Behavior of Bidirectional-Resistant Ductile End Diaphragms with Unbonded Braces in Straight or Skewed Steel Bridges," by O. Celik and M. Bruneau, 4/11/07 (PB2008-105141).

MCEER-07-0004 "Modeling Pile Behavior in Large Pile Groups Under Lateral Loading," by A.M. Dodds and G.R. Martin, 4/16/07(PB2008-105142).

MCEER-07-0005 "Experimental Investigation of Blast Performance of Seismically Resistant Concrete-Filled Steel Tube Bridge Piers," by S. Fujikura, M. Bruneau and D. Lopez-Garcia, 4/20/07 (PB2008-105143).

MCEER-07-0006 "Seismic Analysis of Conventional and Isolated Liquefied Natural Gas Tanks Using Mechanical Analogs," by I.P. Christovasilis and A.S. Whittaker, 5/1/07.

MCEER-07-0007 "Experimental Seismic Performance Evaluation of Isolation/Restraint Systems for Mechanical Equipment – Part 1: Heavy Equipment Study," by S. Fathali and A. Filiatrault, 6/6/07 (PB2008-105144).

MCEER-07-0008 "Seismic Vulnerability of Timber Bridges and Timber Substructures," by A.A. Sharma, J.B. Mander, I.M. Friedland and D.R. Allicock, 6/7/07 (PB2008-105145).

MCEER-07-0009 "Experimental and Analytical Study of the XY-Friction Pendulum (XY-FP) Bearing for Bridge Applications," by C.C. Marin-Artieda, A.S. Whittaker and M.C. Constantinou, 6/7/07 (PB2008-105191).

MCEER-07-0010 "Proceedings of the PRC-US Earthquake Engineering Forum for Young Researchers," Edited by G.C. Lee and X.Z. Qi, 6/8/07 (PB2008-500058).

MCEER-07-0011 "Design Recommendations for Perforated Steel Plate Shear Walls," by R. Purba and M. Bruneau, 6/18/07, (PB2008-105192).

MCEER-07-0012 "Performance of Seismic Isolation Hardware Under Service and Seismic Loading," by M.C. Constantinou, A.S. Whittaker, Y. Kalpakidis, D.M. Fenz and G.P. Warn, 8/27/07, (PB2008-105193).

MCEER-07-0013 "Experimental Evaluation of the Seismic Performance of Hospital Piping Subassemblies," by E.R. Goodwin, E. Maragakis and A.M. Itani, 9/4/07, (PB2008-105194).

MCEER-07-0014 "A Simulation Model of Urban Disaster Recovery and Resilience: Implementation for the 1994 Northridge Earthquake," by S. Miles and S.E. Chang, 9/7/07, (PB2008-106426).

MCEER-07-0015 "Statistical and Mechanistic Fragility Analysis of Concrete Bridges," by M. Shinozuka, S. Banerjee and S-H. Kim, 9/10/07, (PB2008-106427).

MCEER-07-0016 "Three-Dimensional Modeling of Inelastic Buckling in Frame Structures," by M. Schachter and AM. Reinhorn, 9/13/07, (PB2008-108125).

MCEER-07-0017 "Modeling of Seismic Wave Scattering on Pile Groups and Caissons," by I. Po Lam, H. Law and C.T. Yang, 9/17/07 (PB2008-108150).

MCEER-07-0018 "Bridge Foundations: Modeling Large Pile Groups and Caissons for Seismic Design," by I. Po Lam, H. Law and G.R. Martin (Coordinating Author), 12/1/07 (PB2008-111190).

MCEER-07-0019 "Principles and Performance of Roller Seismic Isolation Bearings for Highway Bridges," by G.C. Lee, Y.C. Ou, Z. Liang, T.C. Niu and J. Song, 12/10/07 (PB2009-110466).

MCEER-07-0020 "Centrifuge Modeling of Permeability and Pinning Reinforcement Effects on Pile Response to Lateral Spreading," by L.L Gonzalez-Lagos, T. Abdoun and R. Dobry, 12/10/07 (PB2008-111191).

MCEER-07-0021 "Damage to the Highway System from the Pisco, Perú Earthquake of August 15, 2007," by J.S. O'Connor, L. Mesa and M. Nykamp, 12/10/07, (PB2008-108126).

MCEER-07-0022 "Experimental Seismic Performance Evaluation of Isolation/Restraint Systems for Mechanical Equipment – Part 2: Light Equipment Study," by S. Fathali and A. Filiatrault, 12/13/07 (PB2008-111192).

MCEER-07-0023 "Fragility Considerations in Highway Bridge Design," by M. Shinozuka, S. Banerjee and S.H. Kim, 12/14/07 (PB2008-111193).

MCEER-07-0024 "Performance Estimates for Seismically Isolated Bridges," by G.P. Warn and A.S. Whittaker, 12/30/07 (PB2008-112230).

MCEER-08-0001 "Seismic Performance of Steel Girder Bridge Superstructures with Conventional Cross Frames," by L.P. Carden, A.M. Itani and I.G. Buckle, 1/7/08, (PB2008-112231).

MCEER-08-0002 "Seismic Performance of Steel Girder Bridge Superstructures with Ductile End Cross Frames with Seismic Isolators," by L.P. Carden, A.M. Itani and I.G. Buckle, 1/7/08 (PB2008-112232).

MCEER-08-0003 "Analytical and Experimental Investigation of a Controlled Rocking Approach for Seismic Protection of Bridge Steel Truss Piers," by M. Pollino and M. Bruneau, 1/21/08 (PB2008-112233).

MCEER-08-0004 "Linking Lifeline Infrastructure Performance and Community Disaster Resilience: Models and Multi-Stakeholder Processes," by S.E. Chang, C. Pasion, K. Tatebe and R. Ahmad, 3/3/08 (PB2008-112234).

MCEER-08-0005 "Modal Analysis of Generally Damped Linear Structures Subjected to Seismic Excitations," by J. Song, Y-L. Chu, Z. Liang and G.C. Lee, 3/4/08 (PB2009-102311).

MCEER-08-0006 "System Performance Under Multi-Hazard Environments," by C. Kafali and M. Grigoriu, 3/4/08 (PB2008-112235).

MCEER-08-0007 "Mechanical Behavior of Multi-Spherical Sliding Bearings," by D.M. Fenz and M.C. Constantinou, 3/6/08 (PB2008-112236).

MCEER-08-0008 "Post-Earthquake Restoration of the Los Angeles Water Supply System," by T.H.P. Tabucchi and R.A. Davidson, 3/7/08 (PB2008-112237).

MCEER-08-0009 "Fragility Analysis of Water Supply Systems," by A. Jacobson and M. Grigoriu, 3/10/08 (PB2009-105545).

MCEER-08-0010 "Experimental Investigation of Full-Scale Two-Story Steel Plate Shear Walls with Reduced Beam Section Connections," by B. Qu, M. Bruneau, C-H. Lin and K-C. Tsai, 3/17/08 (PB2009-106368).

MCEER-08-0011 "Seismic Evaluation and Rehabilitation of Critical Components of Electrical Power Systems," S. Ersoy, B. Feizi, A. Ashrafi and M. Ala Saadeghvaziri, 3/17/08 (PB2009-105546).

MCEER-08-0012 "Seismic Behavior and Design of Boundary Frame Members of Steel Plate Shear Walls," by B. Qu and M. Bruneau, 4/26/08 . (PB2009-106744).

MCEER-08-0013 "Development and Appraisal of a Numerical Cyclic Loading Protocol for Quantifying Building System Performance," by A. Filiatrault, A. Wanitkorkul and M. Constantinou, 4/27/08 (PB2009-107906).

MCEER-08-0014 "Structural and Nonstructural Earthquake Design: The Challenge of Integrating Specialty Areas in Designing Complex, Critical Facilities," by W.J. Petak and D.J. Alesch, 4/30/08 (PB2009-107907).

MCEER-08-0015 "Seismic Performance Evaluation of Water Systems," by Y. Wang and T.D. O'Rourke, 5/5/08 (PB2009-107908).

MCEER-08-0016 "Seismic Response Modeling of Water Supply Systems," by P. Shi and T.D. O'Rourke, 5/5/08 (PB2009-107910).

MCEER-08-0017 "Numerical and Experimental Studies of Self-Centering Post-Tensioned Steel Frames," by D. Wang and A. Filiatrault, 5/12/08 (PB2009-110479).

MCEER-08-0018 "Development, Implementation and Verification of Dynamic Analysis Models for Multi-Spherical Sliding Bearings," by D.M. Fenz and M.C. Constantinou, 8/15/08 (PB2009-107911).

MCEER-08-0019 "Performance Assessment of Conventional and Base Isolated Nuclear Power Plants for Earthquake Blast Loadings," by Y.N. Huang, A.S. Whittaker and N. Luco, 10/28/08 (PB2009-107912).

MCEER-08-0020 "Remote Sensing for Resilient Multi-Hazard Disaster Response – Volume I: Introduction to Damage Assessment Methodologies," by B.J. Adams and R.T. Eguchi, 11/17/08 (PB2010-102695).

MCEER-08-0021 "Remote Sensing for Resilient Multi-Hazard Disaster Response – Volume II: Counting the Number of Collapsed Buildings Using an Object-Oriented Analysis: Case Study of the 2003 Bam Earthquake," by L. Gusella, C.K. Huyck and B.J. Adams, 11/17/08 (PB2010-100925).

MCEER-08-0022 "Remote Sensing for Resilient Multi-Hazard Disaster Response – Volume III: Multi-Sensor Image Fusion Techniques for Robust Neighborhood-Scale Urban Damage Assessment," by B.J. Adams and A. McMillan, 11/17/08 (PB2010-100926).

MCEER-08-0023 "Remote Sensing for Resilient Multi-Hazard Disaster Response – Volume IV: A Study of Multi-Temporal and Multi-Resolution SAR Imagery for Post-Katrina Flood Monitoring in New Orleans," by A. McMillan, J.G. Morley, B.J. Adams and S. Chesworth, 11/17/08 (PB2010-100927).

MCEER-08-0024 "Remote Sensing for Resilient Multi-Hazard Disaster Response – Volume V: Integration of Remote Sensing Imagery and VIEWS^{TM} Field Data for Post-Hurricane Charley Building Damage Assessment," by J.A. Womble, K. Mehta and B.J. Adams, 11/17/08 (PB2009-115532).

MCEER-08-0025 "Building Inventory Compilation for Disaster Management: Application of Remote Sensing and Statistical Modeling," by P. Sarabandi, A.S. Kiremidjian, R.T. Eguchi and B. J. Adams, 11/20/08 (PB2009-110484).

MCEER-08-0026 "New Experimental Capabilities and Loading Protocols for Seismic Qualification and Fragility Assessment of Nonstructural Systems," by R. Retamales, G. Mosqueda, A. Filiatrault and A. Reinhorn, 11/24/08 (PB2009-110485).

MCEER-08-0027 "Effects of Heating and Load History on the Behavior of Lead-Rubber Bearings," by I.V. Kalpakidis and M.C. Constantinou, 12/1/08 (PB2009-115533).

MCEER-08-0028 "Experimental and Analytical Investigation of Blast Performance of Seismically Resistant Bridge Piers," by S.Fujikura and M. Bruneau, 12/8/08 (PB2009-115534).

MCEER-08-0029 "Evolutionary Methodology for Aseismic Decision Support," by Y. Hu and G. Dargush, 12/15/08.

MCEER-08-0030 "Development of a Steel Plate Shear Wall Bridge Pier System Conceived from a Multi-Hazard Perspective," by D. Keller and M. Bruneau, 12/19/08 (PB2010-102696).

MCEER-09-0001 "Modal Analysis of Arbitrarily Damped Three-Dimensional Linear Structures Subjected to Seismic Excitations," by Y.L. Chu, J. Song and G.C. Lee, 1/31/09 (PB2010-100922).

MCEER-09-0002 "Air-Blast Effects on Structural Shapes," by G. Ballantyne, A.S. Whittaker, A.J. Aref and G.F. Dargush, 2/2/09 (PB2010-102697).

MCEER-09-0003 "Water Supply Performance During Earthquakes and Extreme Events," by A.L. Bonneau and T.D. O'Rourke, 2/16/09 (PB2010-100923).

MCEER-09-0004 "Generalized Linear (Mixed) Models of Post-Earthquake Ignitions," by R.A. Davidson, 7/20/09 (PB2010-102698).

MCEER-09-0005 "Seismic Testing of a Full-Scale Two-Story Light-Frame Wood Building: NEESWood Benchmark Test," by I.P. Christovasilis, A. Filiatrault and A. Wanitkorkul, 7/22/09.

MCEER-09-0006 "IDARC2D Version 7.0: A Program for the Inelastic Damage Analysis of Structures," by A.M. Reinhorn, H. Roh, M. Sivaselvan, S.K. Kunnath, R.E. Valles, A. Madan, C. Li, R. Lobo and Y.J. Park, 7/28/09 (PB2010-103199).

MCEER-09-0007 "Enhancements to Hospital Resiliency: Improving Emergency Planning for and Response to Hurricanes," by D.B. Hess and L.A. Arendt, 7/30/09 (PB2010-100924).

MCEER-09-0008 "Assessment of Base-Isolated Nuclear Structures for Design and Beyond-Design Basis Earthquake Shaking," by Y.N. Huang, A.S. Whittaker, R.P. Kennedy and R.L. Mayes, 8/20/09 (PB2010-102699).

MCEER-09-0009 "Quantification of Disaster Resilience of Health Care Facilities," by G.P. Cimellaro, C. Fumo, A.M Reinhorn and M. Bruneau, 9/14/09.

MCEER-09-0010 "Performance-Based Assessment and Design of Squat Reinforced Concrete Shear Walls," by C.K. Gulec and A.S. Whittaker, 9/15/09 (PB2010-102700).

MCEER-09-0011 "Proceedings of the Fourth US-Taiwan Bridge Engineering Workshop," edited by W.P. Yen, J.J. Shen, T.M. Lee and R.B. Zheng, 10/27/09 (PB2010-500009).

MCEER-09-0012 "Proceedings of the Special International Workshop on Seismic Connection Details for Segmental Bridge Construction," edited by W. Phillip Yen and George C. Lee, 12/21/09.

MCEER-10-0001 "Direct Displacement Procedure for Performance-Based Seismic Design of Multistory Woodframe Structures," by W. Pang and D. Rosowsky, 4/26/10.

MCEER-10-0002 "Simplified Direct Displacement Design of Six-Story NEESWood Capstone Building and Pre-Test Seismic Performance Assessment," by W. Pang, D. Rosowsky, J. van de Lindt and S. Pei, 5/28/10.

MCEER-10-0003 "Integration of Seismic Protection Systems in Performance-Based Seismic Design of Woodframed Structures," by J.K. Shinde and M.D. Symans, 6/18/10.

MCEER-10-0004 "Modeling and Seismic Evaluation of Nonstructural Components: Testing Frame for Experimental Evaluation of Suspended Ceiling Systems," by A.M. Reinhorn, K.P. Ryu and G. Maddaloni, 6/30/10.